THESIS

GEOLOGY, MINERALOGY AND GEOCHEMISTRY OF

THE CERRO MATOSO NICKELIFEROUS LATERITE, CORDOBA, COLOMBIA

Submitted by

Jorge E. Lopez-Rendon

Department of Earth Resources

In partial fulfillment of the requirements

for the Degree of Master of Science

Colorado State University

Fort Collins, Colorado

Spring 1986

COLORADO STATE UNIVERSITY

December 9   1985

WE HEREBY RECOMMEND THAT THE THESIS PREPARED UNDER OUR SUPERVISION

BY   Jorge E. Lopez-Rendon

ENTITLED   Geology, Mineralogy and Geochemistry of the Cerro

            Matoso Nickeliferous Laterite, Cordoba, Colombia.

BE ACCEPTED AS FULFILLING IN PART REQUIREMENTS FOR THE DEGREE OF

                    Master of Science

Committee on Graduate Work

Adviser

Department Head

ABSTRACT OF THESIS

GEOLOGY, MINERALOGY AND GEOCHEMISTRY OF

THE CERRO MATOSO NICKELIFEROUS LATERITE, CORDOBA, COLOMBIA.

The Cerro Matoso nickeliferous laterite, located in
northern Colombia near the town of Montelíbano, was
developed in pre-Late Cretaceous ultramafic rocks con-
sisting principally of slightly serpentinized harzburgite.
The peridotite body is flanked by ferruginous sandy sedi-
ments with interbedded coal beds of the Ciénaga de Oro
Formation (early Oligocene-early Miocene) and Recent
alluvial gravels and sands.

The harzburgite consists predominantly of olivine with
lesser amounts of orthopyroxene and secondary serpentine.
Intense serpentinization is primarily confined to areas of
faulting and brecciation particularly along the western and
eastern boundaries of the peridotite body. Development of
the nickel laterite profile was greater in weakly serpen-
tinized peridotite both in vertical extent and in the degree
of enrichment of nickel-rich secondary products than in
strongly serpentinized peridotite.

The Cerro Matoso peridotite was affected by two major
tectonic events. Compressional stresses associated with the
late phases of the Pre-Andean orogeny in middle Eocene-late

iii

Eocene time brought the peridotite to the surface and also generated a major NE trending fault system in the peridotite body and local serpentinization particularly along fault zones. Lateritization of the harzburgite probably began in late Eocene-early Oligocene time and chemical weathering and erosion favoured by a tropical humid and rainy climate with probable alternating wet-relatively dry seasons, continued throughout the Oligocene period. A major NW trending fault system developed in the peridotite body during the late Miocene-Pliocene Andean orogeny and the southwestern part of the weathered peridotite body was uplifted relative to the northeastern part. This uplift apparently was sufficient for intense erosion to remove most of the laterite profile from the uplifted block while the northeastern block was being only slightly modified.

The laterite profile consists of an upper Canga zone underlain respectively by a Limonite zone and Upper and Lower Saprolite zones. The economic silicate-type nickel mineralization at Cerro Matoso is confined to the saprolite zones. Nickel content in parent peridotite ranges from 0.28 to 0.36%, and ore grade cutoff for materials comprising the laterite profile is 1.5%. Ore occurs as massive and fracture filling types, the massive ore constituting the most important part of the deposit economically. Smectite and serpentine are the dominant Ni-bearing minerals in the massive ore and are particularly abundant in the Upper Saprolite zone. Pimelite, nimite and Ni-bearing sepiolite fill fractures in

both the Upper and Lower Saprolite zones. Nickel averages 3% in the massive ore and ranges to as much as 7% locally. Nickel grades in fracture fillings range to as much as 30%.

Variations in pH, and to a lesser extent Eh, of the weathering solutions influenced the selective differential element accumulation and mineral formation throughout the laterite profile. Oxidizing and slightly acidic conditions apparently were present in the Limonite and Canga zones and led to precipitation of Fe as goethite. Slight increase in pH in the Limonite zone as compared to the Canga zone favored Mn precipitation at the lower part of the Limonite zone as Mn oxide. Ni was highly mobile in the Canga and Limonite zones and alkaline conditions present in the saprolite zones promoted its deposition in garnierite. Co was less mobile than Ni and the zone of maximum Co concentration formed near the base of the Limonite zone. Moderate mobility of silica occurred in upper profile levels but mobility decreased rapidly in the Upper Saprolite zone apparently due in part to the presence of higher amounts of dissolved Mg in the weathering solutions. Cr mobility was very low in this weathering environment. Alumina behaved as a highly immobile component and concentrated primarily in the near surface part of the Canga zone.

Jorge E. Lopez-Rendon
Department of Earth Resources
Colorado State University
Fort Collins, Colorado, 80523
Spring 1986

ACKNOWLEDGEMENTS

for help during the course of this research, continued encouragement, valuable assistance and guidance and for their comments on earlier drafts of this thesis, which greatly improved it. Last but not least, I would like to express my profound gratitude to my wife Beatriz, a woman who gave all of her to continuously support me both spiritually and psychologically.

TABLE OF CONTENTS

LIST OF TABLES

LIST OF FIGURES

xvi

xix

LIST OF PLATES

INTRODUCTION

Purpose of study

This study was undertaken to provide a comprehensive geological evaluation of the Cerro Matoso nickeliferous laterite in Colombia. Another major objective was the assessment of geological and geochemical parameters that might be applicable to exploration for other nickeliferous laterite deposits in Colombia and in comparable terrain elsewhere. The study area involves part of a concession for exploration and mining of nickel ores owned by Cerro Matoso S.A., a joint venture between Hanna Mining Company, Billiton International Metals and the Colombian government.

In order to accomplish the above primary objectives, the following approaches were utilized: a) Direct geological examination of outcrops to determine physical characteristics of the laterite profile, relationships between the different units present in the profile and structural elements, b) Mineralogical study of the profile, particularly the mineralized horizons, in order to identify the nickel-bearing minerals, and c) Assessment of the geochemical distribution of selected components, both vertically and laterally, to infer migration and

accumulation characteristics pertinent to the evolution of
the deposit.

Methods of investigation

Field work was conducted from May through August 1984.
Topographic base was established from the following maps:
Regional topography of the Montelíbano area, Plate 82-III-D,
Instituto Geográfico Agustín Codazzi, scale 1:25,000;
topographic map of the Cerro Matoso hill, Compañía de Níquel
Colombiano, scale 1:4,000; and topographic map of benches,
Cerro Matoso S.A., scale 1:1,000. Outcrop sampling was
conducted along a series of benches at 7 m elevation
difference that were excavated for open pit mining pur-
poses. One hundred eighty-seven outcrop samples of the
laterite profile and the different ore types were recovered.

Laboratory work included petrographic examination of
thin sections, Differential Thermal Analysis (D.T.A.),
X-ray powder diffraction analysis, and X-ray fluorescence
analysis. Petrographic examination was directed primarily
to the determination of mineralogical composition and tex-
tures of the peridotite parent rock. Thin sections of nine
samples were prepared at Ingeominas-Medellín and studied in
the laboratories at Colorado State University.

Differential Thermal Analysis of 93 samples selected
from the different units and ores present in the laterite
profile were performed on a Shimadzu model DT-30 differen-
tial thermal analyzer at Suministros de Colombia-Medellín.

Powdered samples (minus 120 mesh) were used and analyses were conducted at a heating rate of $12^{\circ}C$/min from room temperature to $1,000^{\circ}C$. A Pt – Pt+Rh10% thermocouple was used as reference material for determination of exothermic and endothermic reactions occurring in the samples upon heating.

X-ray diffraction patterns of 102 samples were obtained on a Jeol XRD diffractometer at Ingeominas-Medellín utilizing the following instrumental conditions: Cu K-alpha radiation, 40 kV, 20 mA, scanning from 2° to $70^{\circ}2\theta$ at a scanning speed of $2^{\circ}2\theta$/min, and counting rate of 2,000 counts per second. The glass slide mounting technique was used. A first run was accomplished for untreated samples. A second run was carried out, after glycol treatment, to verify the presence of smectitic components. No other treatments were performed on the samples.

X-ray fluorescence analysis was performed on a Phillips XRF model 1400 spectrometer at the laboratories of Cerro Matoso S.A.. Samples from drill holes corresponding to the lines 500 NW, 1200 NW, 1300 NW, and 2000 NW (Plates 1 and 2) and samples recovered from outcrops were analyzed. Approximately 1.0g of powdered, minus 100 mesh sample was fused with a lithium tetraborate flux in the presence of cerium oxide (internal standard). Fusion was made in platinum-gold crucibles onto which 40 mm glass discs were molded. Ni, Co, Fe, MgO, SiO_2, Al_2O_3, Cr_2O_3, CaO, and Mn were determined. Analytical results are presented in

Appendix 1 for drill hole samples and in various tables throughout the text for selected outcrop samples.

Statistical treatment of data, particularly inter-element correlations and linear regressions, was carried out utilizing a CDC Cyber 720 computer at Colorado State University and a version of the Minitab program developed at Pennsylvania State University which corresponds to the March 1981 Reference Manual (Penn. State Univ.). Chemical data processed utilizing this program were those obtained from drill hole samples.

Location, Access, Topography and Climate

The area of detailed study, the Cerro Matoso hill, is approximately 2.7 km (SE-NW) by 1.9 km (SW-NE). It is located at approximately $75°33'W$ longitude and $7°54'N$ latitude southwest of the town of Montelíbano, Department of Córdoba, in northern Colombia (Figures 1 and 2). Access is by gravel road from Montelíbano which in turn is connected by paved road to the main cities of Colombia. Montelíbano also is served by fixed-wing aircraft.

Gently rolling terrain surrounds the moderately to steeply sloping Cerro Matoso hill. Relief between the summit of the hill and the adjacent lowlands is about 200 meters and the maximum elevation above sea level is 254 meters. Mean annual rainfall is about 2,500 mm, average temperature is $29°C$, and relative humidity averages approximately 87%. Alternating wet-relatively dry seasons

Figure 1.   Index map showing localities cited in text
            (1: Montelíbano   2: Planeta Rica
            3: Barranquilla   4: Guayaquil, Ecuador),
            approximate extent of the three cordilleras
            constituting the Andes in Colombia, and
            region depicted in Figures 3 and 4 (area
            enclosed by heavy dashed lines).   Arrow
            points to approximate location of the Cerro
            Matoso nickeliferous laterite deposit.
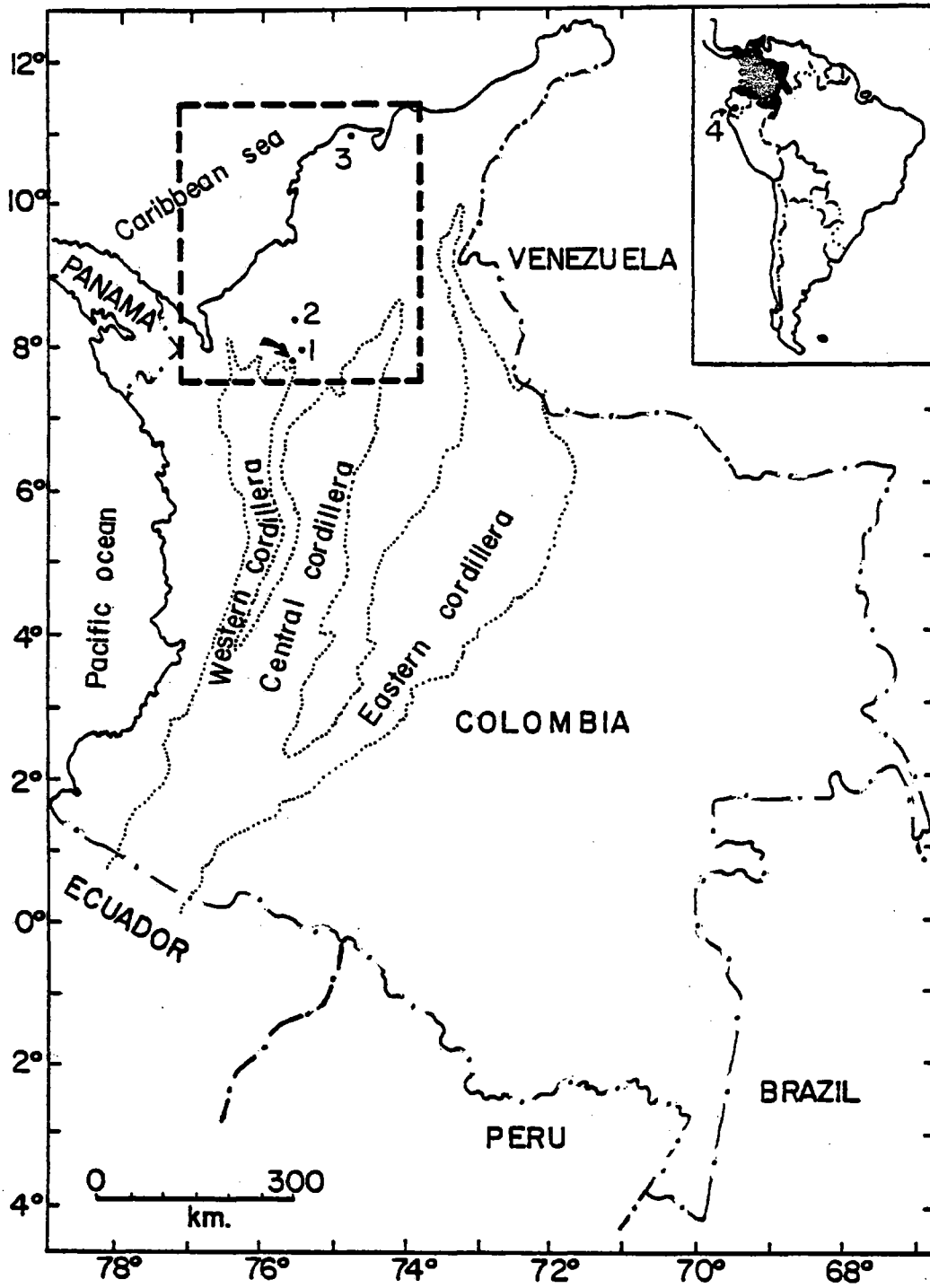
Figure 2. Map showing access route from the town of
           Montelíbano to the study area.
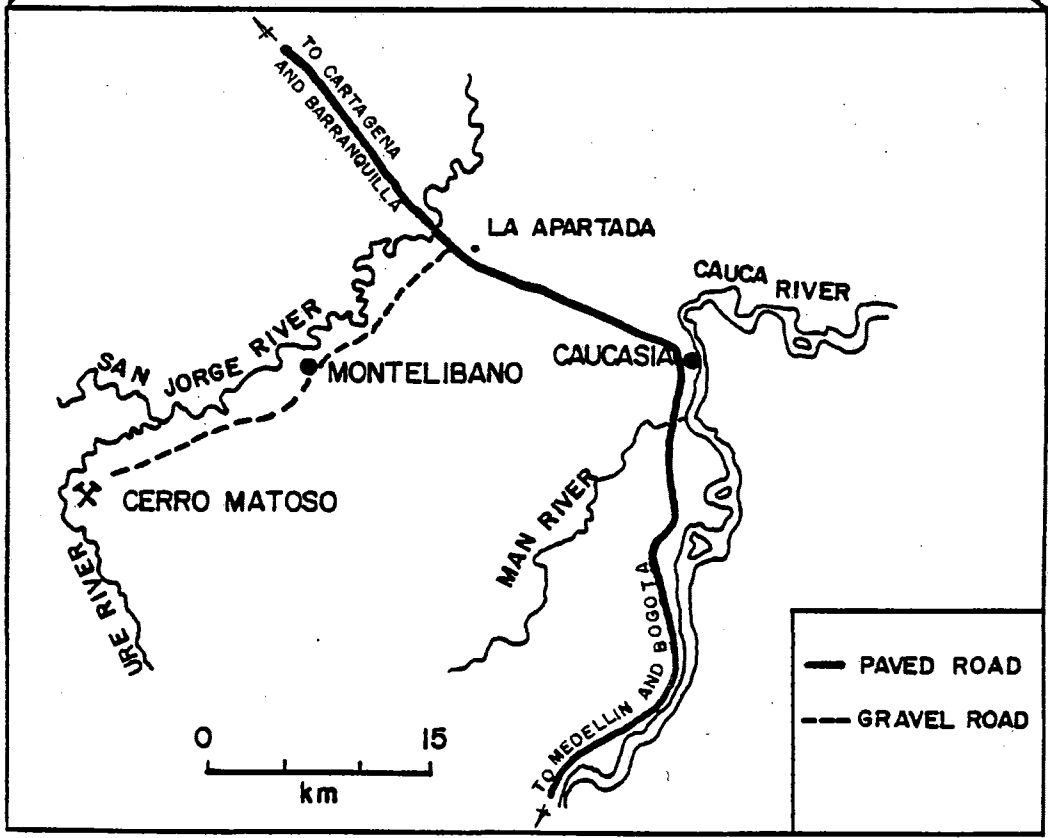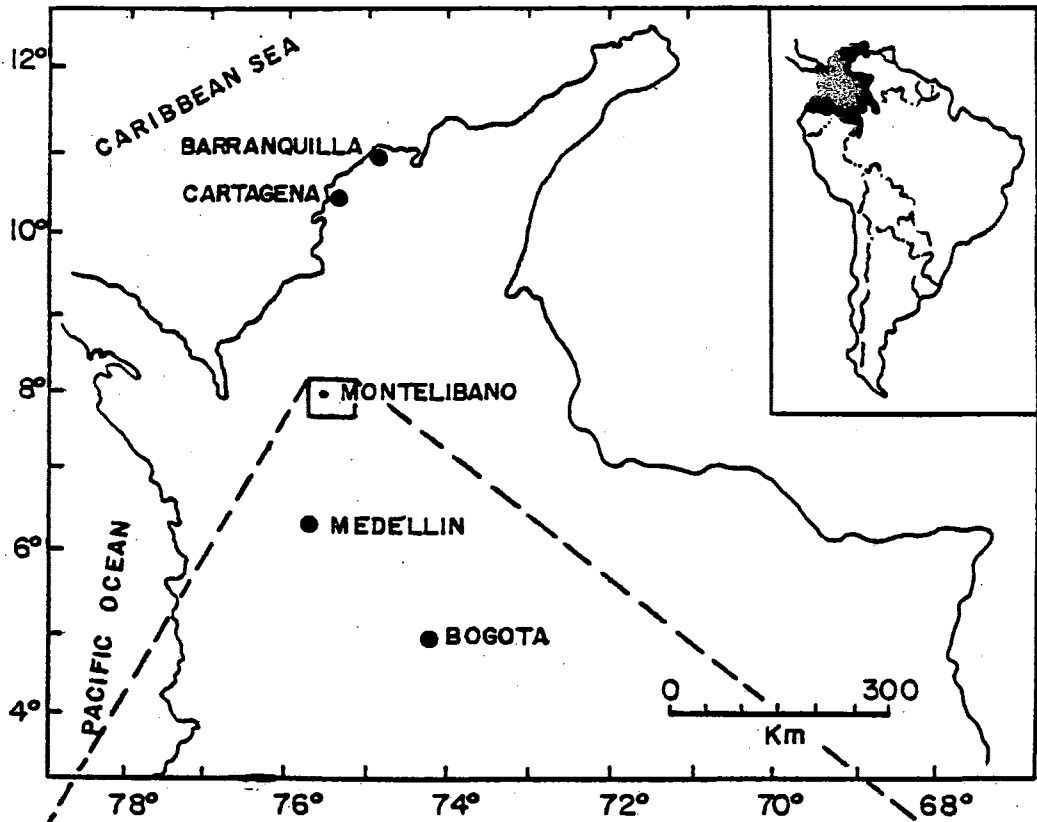
constitute the rain regime. Relatively dry seasons do not always occur during the same period of the year but usually fall in the time periods November–January and May–June.

Previous work

Since the discovery of the Cerro Matoso nickeliferous laterite by geologists of Richmond Oil Company in 1958 (Atchley, 1958), several evaluations of the deposit have been conducted. An initial exploration program included test pits, auger drilling and power drilling with adapted lightweight equipment on a 100 m grid (Gómez et al., 1979); drilling was carried out to maximum depths of 26 meters (Mejía and Durango, 1982). After determining preliminary reserve estimates, closely spaced drilling was conducted between 1971 and 1977 over a grid pattern in which horizontal distances between drill holes range from 25 to 50 meters; 146 meter depths were reached in some drill holes. Samples were taken continuously at 2 m intervals in both exploration programs.

There are no detailed published studies on the geology at Cerro Matoso. Webber (1972) refers to the Cerro Matoso deposit as a good example of a complete nickel laterite profile, describes in a generalized way the different units comprising the profile, and provides some preliminary information on their chemical characteristics. Gómez et al. (1979) present a very brief review of geological features at the Cerro Matoso deposit but their work deals

mainly with the metallurgical process used in ore dressing.
A generalized geological and chemical description of the
various units comprising the laterite profile is presented
by Mejía and Durango (1982). The Cerro Matoso nickel
laterite deposit is mentioned by McFarlane (1983; 1984) as
an example of a nickel-silicate type ore and by Golightly
(1981) who refers to it as a nickel laterite profile which
probably has an intermediate nontronite zone.

REGIONAL GEOLOGY

Structural elements

The NE part of Colombia (Figure 3), where the Cerro
Matoso nickel deposit is located, is characterized by two
main tectonic elements: a) The San Jorge Basin to the
east, which is a stable platform underlain by continental
crust, and b) The Sinú-San Jacinto terrane to the west,
which is an unstable geosyncline underlain by oceanic crust
(Duque-Caro, 1979) and comprised of two structural elements,
the Sinú Belt and the San Jacinto Belt. The boundary
between the San Jorge Basin and the Sinú-San Jacinto
terrane is marked by the Romeral lineament (Dueñas and
Duque-Caro, 1981).

The San Jorge basement is made up of granitic, quartz
dioritic, and metamorphic rocks (Dueñas and Duque-Caro,
1981) forming a pre-Late Cretaceous rock association similar
to that of the Central Cordillera (Irving, 1975; Case et
al., 1984). The sedimentary sequence is comprised of
Early Oligocene-Early Miocene sandstones with interbedded
coal beds which are overlain by Miocene shales, Pliocene
sandstones, Pleistocene shales and conglomeratic sandstones
and Recent gravels and sands (Dueñas and Duque-Caro, 1981).
The basin is characterized by absence of ultramafic rocks
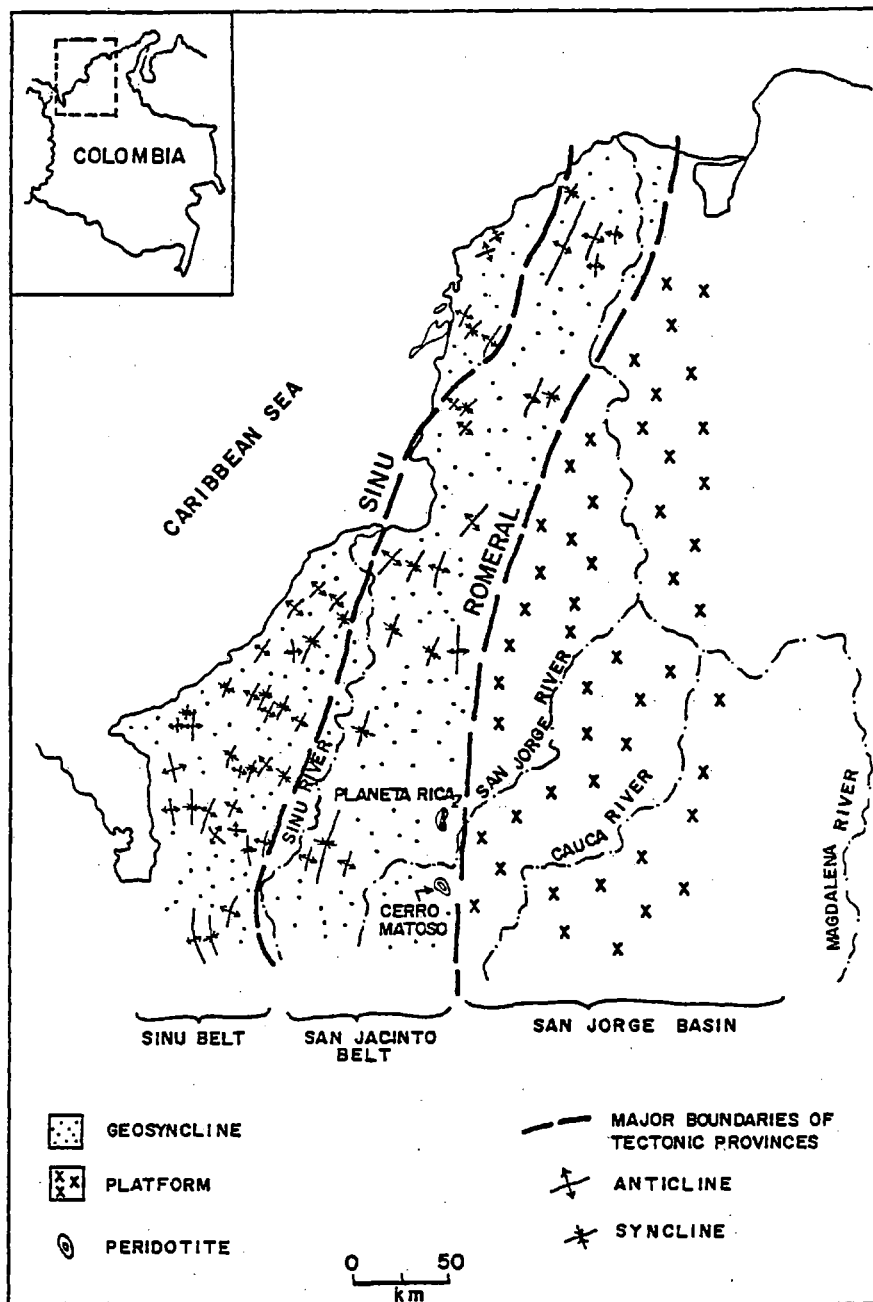
Figure 3. Main regional structural and geo-
tectonic elements of Northwestern
Colombia. Also shown are locations
of the Cerro Matoso and Planeta
Rica peridotites. Modified after
Duque-Caro (1979; 1984).

and abyssal Late Cretaceous-Early Tertiary pelagic sediments and turbidites (Duque-Caro, 1973), strongly negative gravity anomalies (Case et al., 1971; Kellogg, 1983), and a relatively unfolded structural style (Duque-Caro, 1979).

The Sinú Belt is located to the west of the Sinú-San Jacinto terrane and is comprised mostly of highly deformed, Oligocene-Early Pliocene pelagites and hemipelagites overlain by turbidites and floored by oceanic crust (Duque-Caro, 1984). Narrow, steep and elongated anticlinal structures separated by broad synclines characterize this belt and are roughly parallel to the western margin of the belt (Duque-Caro, 1979). The Sinú structural lineament separates the Sinú Belt from the San Jacinto Belt to the east.

The San Jacinto Deformed Belt is comprised of deep marine pelagites and turbidites, shallower marine hemi-pelagites and clastic terrigenous sediments overlain by continental fluvial and lacustrine sediments (Duque-Caro et al., 1983), and floored by oceanic crust (Duque-Caro, 1973; Case et al., 1971, 1984). The oldest sedimentary rocks are Campanian-Maestrichtian cherts and siltstones (Dueñas and Duque-Caro, 1981) that locally overlie peridotite (Duque-Caro et al., 1983) and contain interbedded basaltic flows. The entire sedimentary sequence is described briefly in Table 1. The San Jacinto Belt is characterized by narrow, tight, and elongated anticlinal structures separated by broad gentle synclines (Duque-Caro, 1984) (Figure 3). The

Table 1.   Stratigraphic units near Cerro Matoso.   Modified after Dueñas and Duque-Caro (1981).

Age		Maximum Regional Thickness (m.)	Nomenclature	Character
Holocene			ALLUVIUM	Quartzose sand and gravel with minor clay
Pleistocene		>2,000	SINCELEJO FORMATION	Upper part - yellow, slightly consolidated sandstone with interbedded conglomerate. Middle part - yellow, medium-to coarse-grained, slightly consolidated, partly conglomeratic, cross-stratified sandstone. Lower part - clayey sequence: light-gray shale (locally calcareous) and minor sandstone.
Pliocene		1,000	CERRITO FORMATION	Interbedded yellowish- brown sandstone and claystone; locally, thin arenaceous limestone at base.
Miocene	L M E	400	PORQUERO FORMATION	Variegated, gray, brownish and yellow calcareous shale with some calcareous concretions, locally gypsiferous; changes laterally to sandy facies.
Oligocene	L M E	>2,500	CIENAGA DE ORO FORMATION	Reddish-brown ferruginous sandstone, gray sandy and calcareous shale, black carbonaceous shale; coal beds near top and at base. Local reefal limestone at base.
Eocene	M E	4,000	UPPER SAN CAYETANO FORMATION	Dark-yellow, soft, micaceous graywacke with sporadic calcareous material, and blueish-gray shale; local detrital serpentine. Locally, facies changes laterally to conglomeratic sandstone and conglomerate.
Paleo-cene	L			
Cretaceous Late		700	LOWER SAN CAYETANO FORMATION	Cream coloured, commonly oxidized siltstone at top; changes gradually downwards to black chert with calcite veinlets. Local interbedded diabase and basalt flows, thin sandstone at base
			PERIDOTITE	Peridotitic bodies locally associated with serpentinite and gabbro. Peridotite: mainly harzburgite with minor dunite.

anticlinal structures commonly are truncated by thrust faults along strike (Dueñas and Duque-Caro, 1981). Folds and faults trend north-northeast (Case et al., 1984) and parallel the margin of the unfolded platform to the east (Duque-Caro, 1979). The San Jacinto Belt extends northward to the Caribbean coast of Colombia and three discrete structural units may be recognized (Duque-Caro, 1979): The San Jerónimo, San Jacinto, and Luruaco anticlinoria (Figure 4). The San Jerónimo anticlinorium is the southernmost unit and ultramafic bodies, such as Cerro Matoso and Planeta Rica Peridotites (Figure 3), heve been emplaced near its eastern margin along the Dolores Shear Zone which includes the Romeral Fault.

The Dolores Shear Zone is a major tectonic feature that extends from Guayaquil, Ecuador to Barranquilla, Colombia (Duque-Caro et al., 1983) (Figure 5) and separates oceanic crust on the west from continental crust on the east (Case et al., 1971; 1984). It has been interpreted as the expression of an ancient trench (Duque-Caro, 1979; MacDonald, 1980). Throughout its extent, it includes a mega-melange of ultramafic rocks, ophiolitic fragments, local blueschists, blocks of continental crust, and Mesozoic pelagic and flyschoid strata (Case et al., 1984).

One of the faults within the Dolores Shear Zone, the Romeral Fault, is interpreted by Barrero et al. (1969) as dipping eastward and extending from southern Colombia northward to the Montelíbano area (Figure 5), a distance of
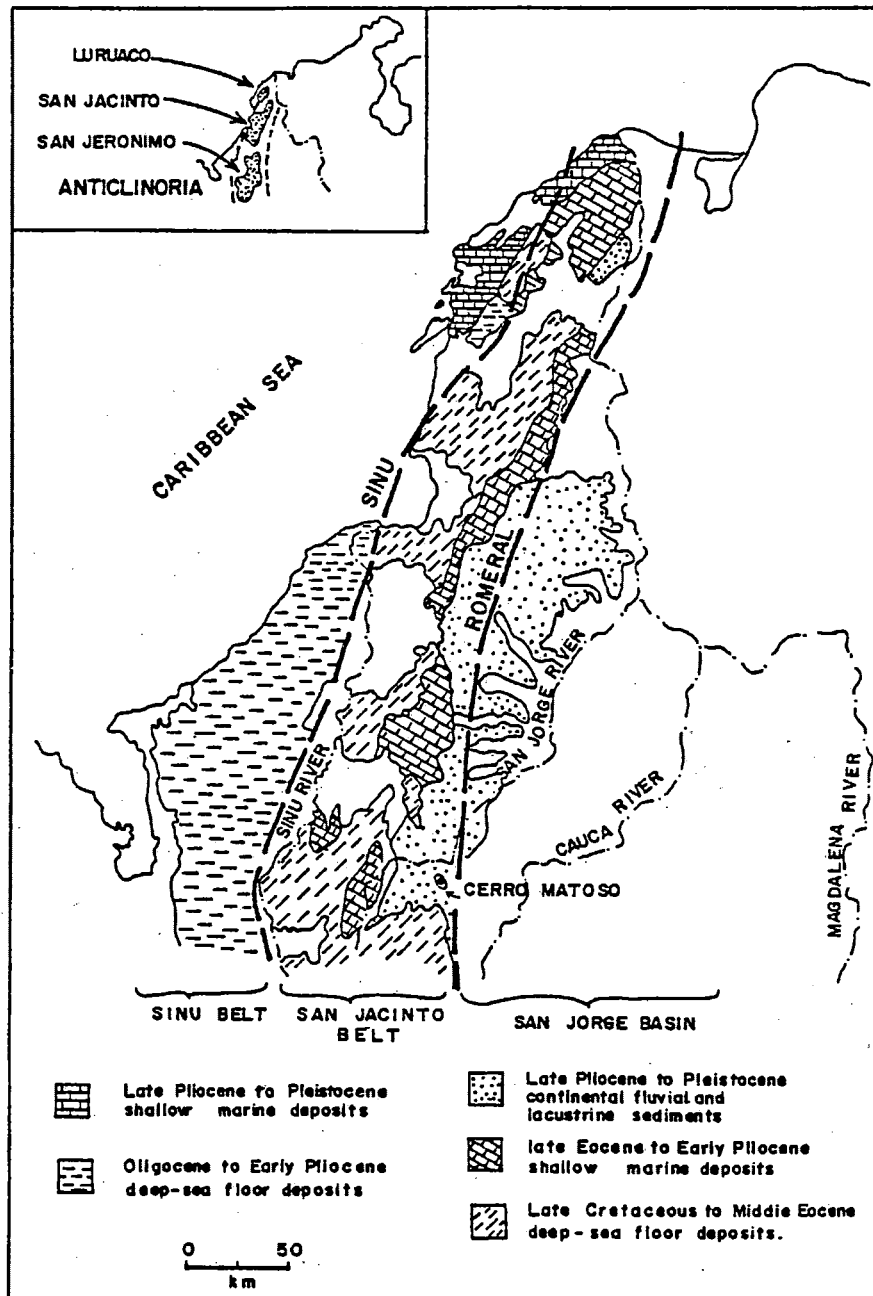
Figure 4. Main regional sedimentary sequence along the San Jacinto and Sinú Belts. Also shown is location of the Cerro Matoso peridotite. Modified after Duque-Caro (1973; 1984).

Figure 5.   Generalized tectonic map of Colombia
            showing major faults, structural
            lineaments, paleosutures, and rift
            margins. Note the Dolores Shear
            zone (36) which extends from Guayaquil,
            Ecuador to Barranquilla, Colombia and
            includes the Río Cauca (25) and Romeral
            (13) fault systems. Arrow points to
            approximate location of the Cerro Matoso
            peridotite. Modified after Ingeominas
            (1983) and James (1985).

Explanation:

1-Colombia lineament
2-Ruma fault
3-Cosinas fault
4-Oca fault
5-Sevilla lineament
6-Cesar lineament
7-Cerrejón fault
8-Cuiza-Tigre fault
9-Arena Blanca fault
10-Santa Marta fault
11-Sinú lineament
12-Montelíbano fault
13-Romeral fault system
14-Murrucucu fault
15-Espíritu Santo fault
16-Ituango fault
17-Santa Rita fault
18-Otú fault

19-Bucaramanga fault
20-San Blas fault
21-Atrato fault system
22-Dabeiba fault
23-Garrapatas fault
24-Dagua fault
25-Río Cauca fault system
26-R.Magdalena fault system
27-Río Sausa fault system
28-Borde Llanero lineament
29-Guaicarama fault
30-Caruru fault
31-Mantecal fault zone
32-Caguán rift
33-Apoporis rift
34-La Trampa lineament
35-La Trampa rift
36-Dolores-Romeral
   Shear Zone
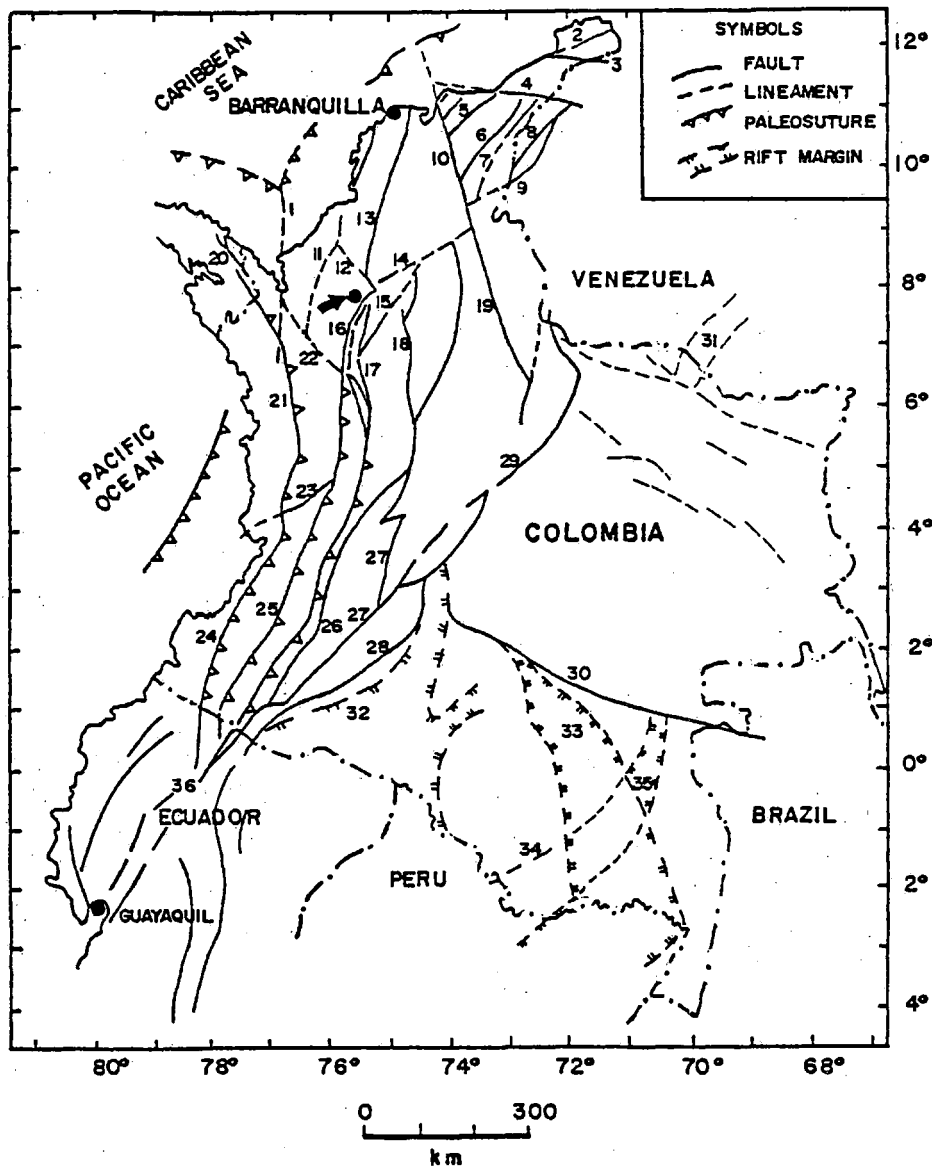
at least 800 kilometers. This fault apparently extends 140 km farther to the north, where it is covered by Late Tertiary-Quaternary sediments of the San Jorge Basin (Feininger, 1970; Duque-Caro, 1979). In the Montelíbano study area, the Romeral Fault zone marks the eastern boundary of the San Jerónimo anticlinorium (Duque-Caro, 1979) and changes from a general northerly trend to a northeasterly trend (Irving, 1975) (Figure 5).

Geologic evolution

The northwestern part of Colombia in the region of the Cerro Matoso nickel deposit has undergone a complex sedimentary and tectonic evolution from Late Cretaceous to Holocene time. A brief description of this evolution is presented with particular emphasis on the San Jerónimo anticlinorium where the Cerro Matoso paridotite occurs.

Late Cretaceous: During Late Cretaceous time, an emerged or positive platform to the east of the study area, in the Central Cordillera region, was subjected to erosion (Case et al., 1971; Dueñas and Duque-Caro, 1981) (Figures 1 and 3). To the west, deep eugeosynclinal type (Bueno, 1970) marine sedimentation of predominantly siliceous material produced the cherts of the Lower San Cayetano Formation (Dueñas and Duque-Caro, 1981). In the San Jerónimo anticlinorium area, tha basal turbidite sequence contains interbedded basaltic flows (Duque-Caro, 1984) that typify Cretaceous volcanism recognized in many other areas of

western Colombia (Malfait and Dinkelman, 1972; Irving, 1975; Duncan and Hargraves, 1984; Mattson, 1984).

Paleocene-Middle Eocene: The Romeral trench along the western margin of the platform was deepened and turbidite deposition continued through the end of the Middle Eocene, giving rise to the Upper San Cayetano Formation (Duque-Caro, 1984). During Paleocene-Middle Eocene time, the Pre-Andean orogeny (van der Hammen, 1958) occurred, apparently in response to the interaction between the Caribbean and the South American plates. Resulting stresses were mainly compressional resulting in uplift of the Central Cordillera (Malfait and Dinkelman, 1972), ultrabasic magmatism and emplacement of some ophiolite complexes (Malfait and Dinkelman, 1972; Dueñas and Duque-Caro, 1981), tight folding, abundant faulting (Mattson, 1984), and diapirism (Duque-Caro, 1984). The San Jerónimo anticlinorium as well as the San Jorge Basin were initiated at this time. The end of the Middle Eocene time is marked by an unconformity (Duque-Caro, 1984; Mattson, 1984).

Middle Eocene-Late Eocene: Additional emplacement of ophiolite complexes, strong folding of sedimentary units and intense shearing and fracturing of peridotitic bodies as a result of intensified lateral compressional stresses (Dueñas and Duque-Caro, 1981) occurred in the San Jacinto Belt area during Middle and Late Eocene time. Because of significant uplift, peridotite was brought to the surface during the late phases of the Pre-Andean orogeny. According to

Duque-Caro (1973), this orogeny was much stronger than the
subsequent Oligocene-Miocene and Late Miocene-Pliocene
diastrophic and orogenic movements and, locally, the sea
floor was uplifted from depths of at least 5,000 m to 600 m
and less. A trench, the Sinú trench, formed to the west of
the San Jacinto Belt area and separated the western flank
of this belt from the abyssal plain (Duque-Caro, 1979)
(Figure 3). From this time on, the San Jacinto Belt consti-
tuted the western limit to the San Jorge Basin (Dueñas and
Duque-Caro, 1981).

Late Eocene-Oligocene: The Pre-Andean orogeny ended
with a period of relative quiescence (Bueno, 1970) and
erosion (Mattson, 1984). The peridotitic bodies, outcrop-
ping since Middle to Late Eocene, were subjected to intense
weathering processes and provided iron-enriched solutions to
nearby shallow marine sites where deposition of the basal
part of the Ciénaga de Oro Formation was initiated during
the Early Oligocene (Duque-Caro, 1979; Dueñas and Duque-
Caro, 1981). In the vicinity of the Cerro Matoso area, a
swampy to deltaic environment apparently prevailed and
clastic sediments with interbedded coals were deposited.

Late Oligocene-Miocene: Towards the end of Oligocene
time, the Oligocene-Miocene diastrophism (Duque-Caro, 1973)
or Proto-Andean orogenic phase (van der Hammen, 1958;
Irving, 1975) was initiated. Tectonic activity apparently
was particularly strong during Early Miocene time (Malfait
and Dinkelman, 1972; Shagam, 1975). The San Jorge Basin

underwent moderate submergence (Duque-Caro, 1973), especially along the Romeral zone (Duque-Caro, 1979), whereas the San Jerónimo anticlinorium and its associated peridotites were subjected to additional moderate uplift. The Ciénaga de Oro Formation was overlain by sediments of the Early Miocene-Middle Miocene Porquero Formation, which also were deposited in a shallow marine environment (Dueñas and Duque-Caro, 1981).

Late Miocene-Pliocene: During Late Miocene, the Andean orogeny was responsible for tectonic activity throughout the San Jorge Basin (Malfait and Dinkelman, 1972; Duque-Caro, 1973). Compression and uplift (Irving, 1975) led to the development of new fault systems through differential vertical movements which also affected the peridotitic bodies. A change towards terrestrial depositional conditions is reflected in the fluvial and lacustrine deposits of the Late Miocene-Pliocene Cerrito Formation (Dueñas and Duque-Caro, 1981), which is separated from the underlying sediments of the Porquero Formation by a gentle angular unconformity (Duque-Caro, 1984).

Pliocene-Pleistocene: The Andean orogeny continued through the Pliocene into Pleistocene time with lateral compression reaching another diastrophic peak. Transcurrent faulting occurred (Duque-Caro, 1979) as well as uplift of the San Jacinto Belt. Intense deformation and uplift also occurred in the Sinú Belt. Large quantities of detrital material were transported and extensive continental

deposition (Irving, 1975) produced the lacustrine and deltaic units of the Sincelejo Formation (Duque-Caro, 1984), which unconformably overlies the Cerrito Formation (Dueñas and Duque-Caro, 1981). The San Jerónimo anticlinorium and associated peridotitic bodies close to the Romeral lineament were uplifted and faulted during a Pleistocene tectonic event (Duque-Caro, 1984).

Late Pleistocene-Holocene: Relative stability prevailed throughout Late Pleistocene and Holocene time (Dueñas and Duque-Caro, 1981), although active erosion continued (Irving, 1975) resulting in deposition of fluvial and deltaic sediments in the San Jorge Basin (Duque-Caro, 1979). Minor local tectonic and climatic oscillations during this time interval (Dueñas and Duque-Caro, 1981) also influenced the present topographic expression of the San Jerónimo anticlinorium. According to Page (1983), Quaternary faults, which generally reflect reactivation of older fault zones, have a tectonic sense different from the earlier displacements, and are common in northwestern Colombia.

GEOLOGY OF THE CERRO MATOSO AREA

Stratigraphic units

The Cerro Matoso study area is situated near the southeastern end of the NNE trending San Jerónimo anticlinorium (Figure 4) where an oval-shaped peridotite body is partially overlain by Tertiary sediments of the Ciénaga de Oro Formation and Holocene alluvial sediments (Plate 1). The NNW trending peridotite body is more resistant than the surrounding sediments and is expressed as a topographic high, Cerro Matoso hill, which has about 200 m of relief.

The Cerro Matoso peridotite body is predominantly harzburgite with minor small lenses of dunite, and is in general only slightly serpentinized. Intense serpentinization is primarily confined to areas of faulting and brecciation particularly along the western and eastern boundaries of the body. The overlying sediments of the Early Oligocene-Early Miocene Ciénaga de Oro Formation (Dueñas and Duque-Caro, 1981) include reddish- to yellowish-brown sandstones with interbedded carbonaceous shales, coal beds, and gray sandy shales in the vicinity of the peridotite body. The sandstones are fine grained to conglomeratic and their colour has been attributed to the

ferruginous character of the clastic components (Duque-Caro, 1973).

Evaluation of chemical analysis of samples from drill holes and examination of outcrops show that lateritization and erosion of the peridotite body were active before and during deposition of the Ciénaga de Oro Formation. Drill holes collared outside the outcropping peridotite penetrate the sediments to depths of as much as 44 m (Figure 6) and show a moderately developed nickel laterite profile in the peridotite which is overlain by sandstones and coal beds (cfr. DDH 2224NE, line 1200 NW). Chemical analyses of sandstones of the Ciénaga de Oro Formation overlying the peridotite body and surrounding the Cerro Matoso hill indicate the presence of nickel and iron values of as much as 1400 ppm and 9%, respectively. High nickel and iron values also are present in the carbonaceous shales, and even in the coal beds (cfr. line 1200 NW, DDH's 2221NE, 2224NE, 2247NE, 2250NE, 2270NE, 2273NE, Appendix 1, and Figure 6). Relatively hardened fragments of iron-rich material occur in gravelly sandstones in upper stratigraphic levels within the Ciénaga de Oro Formation (Figure 6). Iron content of these fragments averages 20% and is similar to that observed locally in the nearby Cerro Matoso hill deposit, particularly at high topographic positions.

Unconsolidated Holocene sediments ranging from silts to gravels with minor clay component are alluvial products
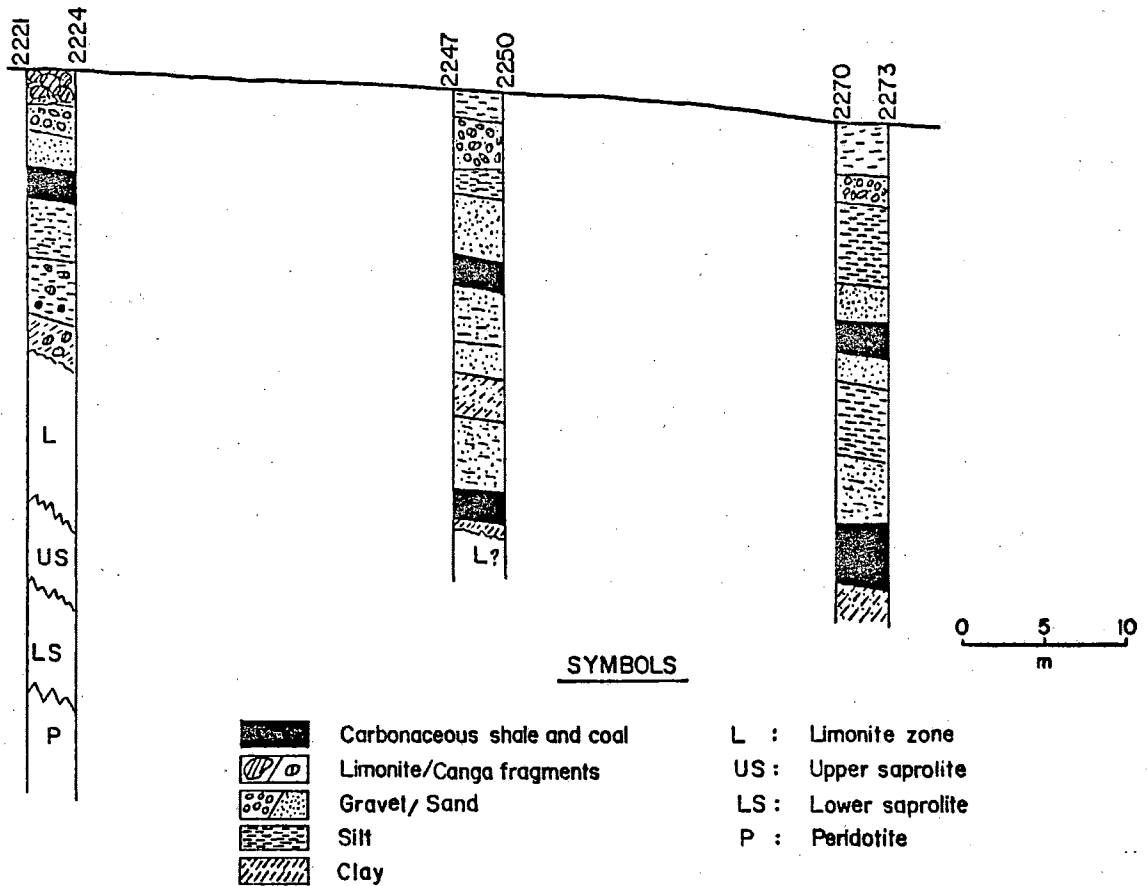
Figure 6. Vertical cross section to the end of Line 1200 NW (Plates 2 and 3) showing relationships between sediments of the Ciénaga de Oro Formation and the Cerro Matoso peridotite.

of the Uré river to the west of the Cerro Matoso peri-
dotite. The Uré river has a meandering character that
is easily recognized on aerial photographs, and successive
changes in its course have resulted in the formation of a
series of terraces up to 5 m in height. These terraces
usually are characterized by gravelly components in the
lower regions whereas fine-grained components dominate near
the top. The gravels consist mainly of rounded quartz
clasts with a sandy matrix but subangular fragments of
hard, iron-rich material also are present locally. Chemical
analysis of some of these fragments shows iron and nickel
contents of as much as 48% and 1%, respectively, thus
suggesting their derivation from the adjacent weathered
peridotite during a period of active erosion.

Structural geology

Two fault systems and abundant joints constitute the
general structural pattern at Cerro Matoso. The first
fault system has a northeast trend and is apparent from
aerial photographs as well as direct ground observation.
Two major NNE trending photogeologic lineaments bordering
the peridotite body along its western and eastern boundaries
apparently are expression of fault breccias and sheared
rock zones described by Mejía and Durango (1982) and
observed in this study. Apparently associated high angle
normal faults with strikes ranging from $N10^{o}E$ to $N57^{o}E$
and dips between 65° and 70° eastward are exposed in benches

at Cerro Matoso. This fault system parallels the trend of the Romeral fault in the Montelíbano area (Barrero et al., 1969) and may be a product of compressional stresses generated during the Pre-Andean orogeny.

The second fault system consists of very high angle normal faults with strikes that range from N30°W to N55°W and with dips greater than 78° to the northeast. Some of these faults appear to extend in to the Ciénaga de Oro Formation, as indicated by photogeologic-topographic lineaments and low escarpments in the sedimentary units northwest and southeast of the peridotite body. This regional NW trending fault system was recognized by Dueñas and Duque-Caro (1981) near Planeta Rica and may be a product of compressional stresses generated during the Andean orogeny (Irving, 1975).

Two general sets of joints observed at Cerro Matoso strike N65-70°W and N70-72°E and dip 30-35°NE and 60-65°NW respectively. They are more clearly identified at the lower levels of the laterite profile, particularly where the rock is only slightly to moderately weathered. Most of these fractures have garnierite accumulation along them, either as thin coatings or as complete fracture fillings.

THE LATERITE PROFILE

The laterite profile at Cerro Matoso consists of five units that can be differentiated on the basis of physical appearance, texture and chemical and mineralogical composition. Terms designating each unit are mainly those used at the mine and are compared in Table 2 with terms established for similar deposits elsewhere. Transitions between units are vertical, lateral and oblique. Consequently, thicknesses of the units are fairly variable. Furthermore, the profile has been truncated locally by erosion.

Peridotite bedrock

Fresh, unweathered peridotite outcrops are scarce in the area. The least altered samples were obtained from a quarry located approximately at the coordinates 2175 NW - 1050 NE (Plate 2) and from drill holes.

Macroscopically, the peridotite is a dark-green to blackish-green, predominantly medium-grained (1 - 5 mm crystals), equigranular rock. Orthopyroxene is easily identified by its larger grain size than the surrounding olivine and its bronze-like color on weathered surfaces.

Table 2. Comparison of nomenclature for silicate-type nickeliferous laterite deposits.

Local terms				General terms	
Cerro Matoso (1)	New Caledonia (2)	Greenvale, Soroako (3,4)	Nickel Mountain (5)	(6)	(7)
Canga	Cuirasse ferrugineuse	Pisolite horizon	----------	Canga	Ferricrete
------------	Terres rouges	----------	----------	----------	------------
Limonite	Saprolite	Limonite	Red soil	Ferralite	In situ limonite
Upper Saprolite	----------------	----------	----------	Saprolite	Intermediate zone
Lower Saprolite	Saprolite	Saprolite	Saprolite	Saprolitic peridotite	------------
Peridotite	Peridotite	Peridotite	Peridotite	Peridotite	Bedrock

(1) This study   (2) Trescases, 1975; Lelong et al., 1976   (3) Burger, 1979
(4) Golightly, 1979b   (5) Durst, 1976   (6) Webber, 1972
(7) Golightly, 1981

Olivine occurs as subhedral crystals that range in color from dark to light green.

Textures ranging from subhedral to anhedral granular (Figure 7) and weakly poikilitic (Figure 8) are evident in thin section. Where the peridotite is slightly to moderately serpentinized, it exhibits a mesh-texture with serpentine veinlets enclosing olivine and orthopyroxene (Figure 9). Average modal composition is 83% olivine, 9% orthopyroxene, and 7% serpentine after olivine, which corresponds to harzburgite (Streckeisen, 1976). Chromite and magnetite are present as accessory minerals. Olivine occurs mostly as equigranular subhedral crystals; it is colorless and exhibits irregular serpentine-bearing fractures. Orthopyroxene occurs as colorless to light brownish-green subhedral crystals that are slightly larger than olivine crystals. Both olivine and orthopyroxene may exhibit undulatory extinction (Figures 10 and 11) and deformation of some orthopyroxene crystal expressed by weak bending of cleavage planes (Figure 12). These features have been interpreted as products of compressional stresses superimposed on these minerals, probably during later tectonic events (MacKenzie et al., 1982). Chromite is present as disseminated subhedral to euhedral crystals, and secondary magnetite occurs as segregations along serpentinized fractures in olivine (Figure 13).

Highly serpentinized zones in the peridotite are characterized by blackish-green, commonly slickensided,

Figure 7. Photomicrograph of Cerro Matoso peridotite
showing subhedral to anhedral granular
texture. Crossed nicols.
Olivine - blue
Serpentine veinlets - black and yellow

Figure 8. Photomicrograph of Cerro Matoso peridotite
showing orthopyroxene (brown)
poikilitically enclosing rounded olivine
crystals. Crossed nicols.
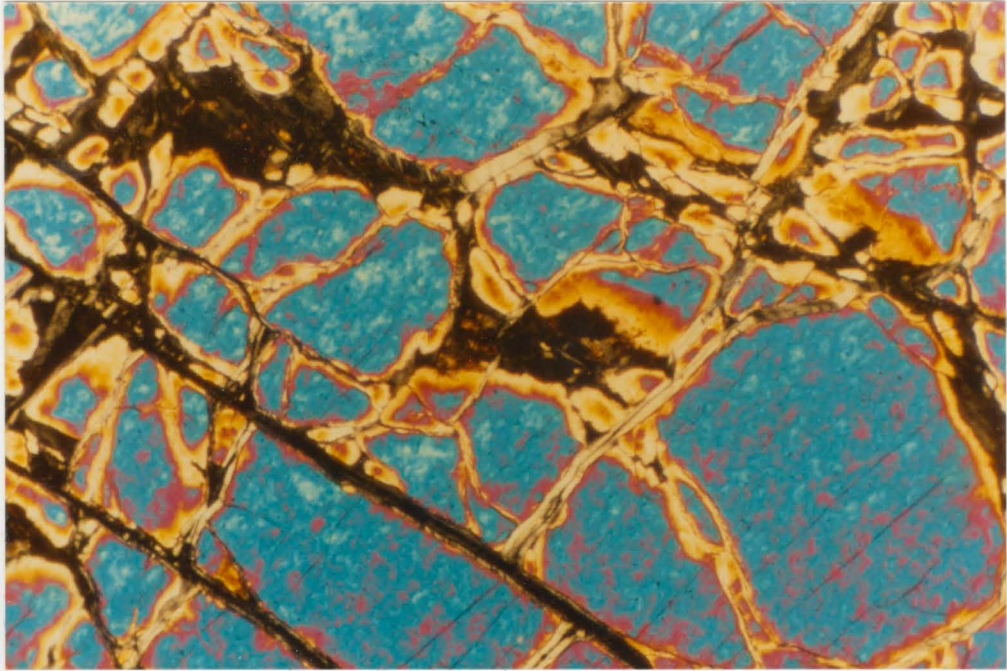
0.2 mm
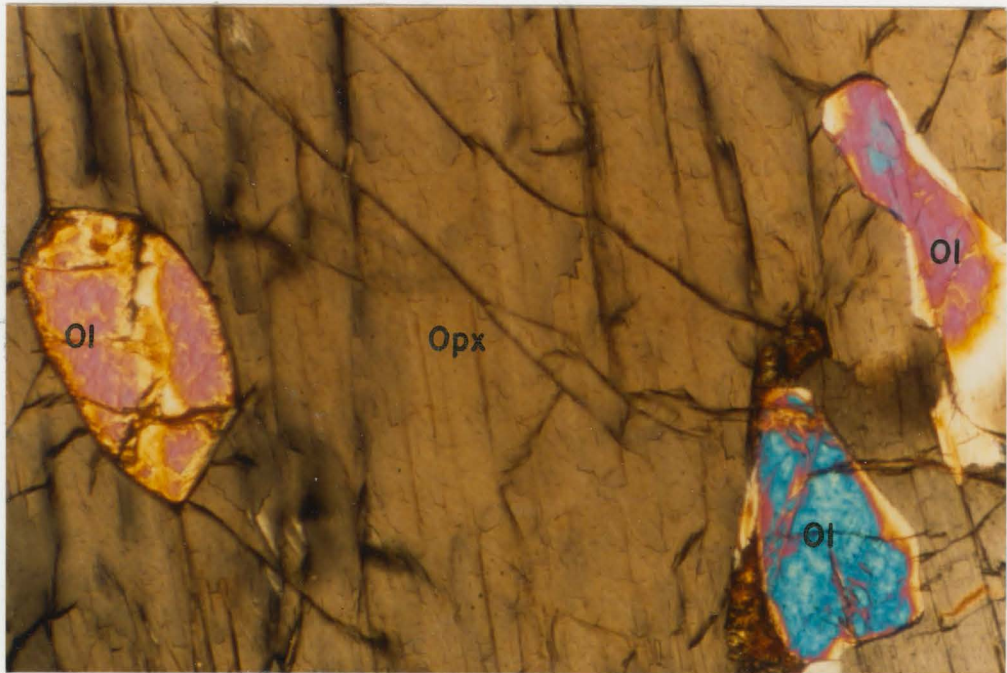
0.2 mm

Figure 9.   Photomicrograph of locally serpentinized
            Cerro Matoso peridotite showing mesh-
            texture with serpentine veinlets enclosing
            olivine.   Crossed nicols.

Figure 10. Photomicrograph of Cerro Matoso
            peridotite showing undulatory extinction
            in olivine (left). Crossed nicols.
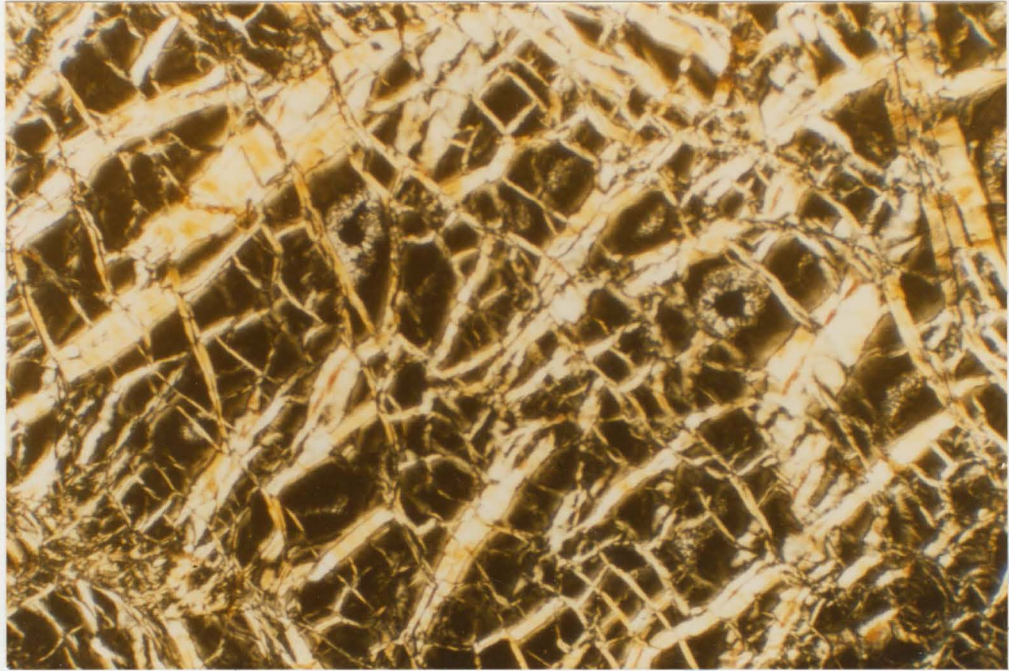
0.5 mm
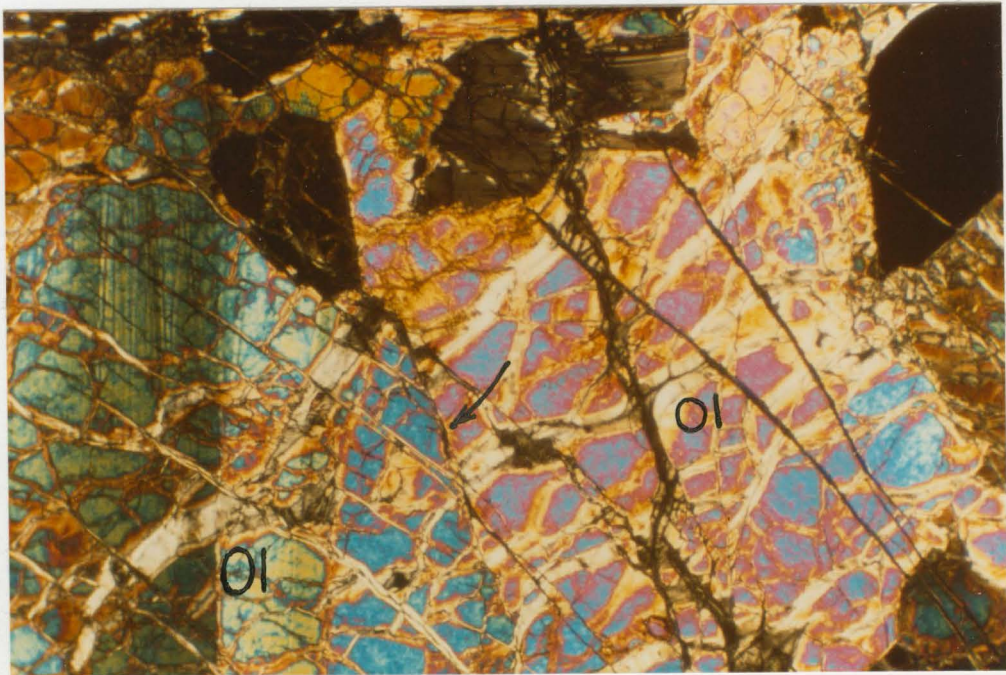
0.5 mm

Figure 11. Photomicrograph of Cerro Matoso
            peridotite showing undulatory extinction
            in orthopyroxene. Crossed nicols.
            Orthopyroxene - opx
            Olivine - Ol

Figure 12. Photomicrograph of Cerro Matoso
            peridotite showing bending of cleavage
            traces in orthopyroxene. Crossed nicols.
            Orthopyroxene - opx
            Olivine - Ol
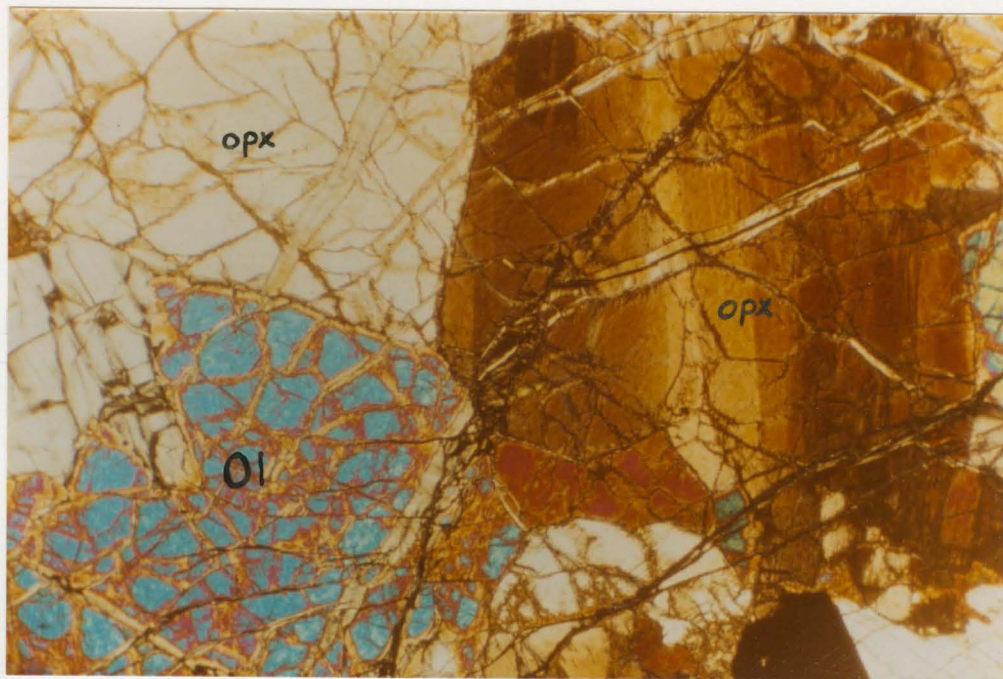
0.5 mm
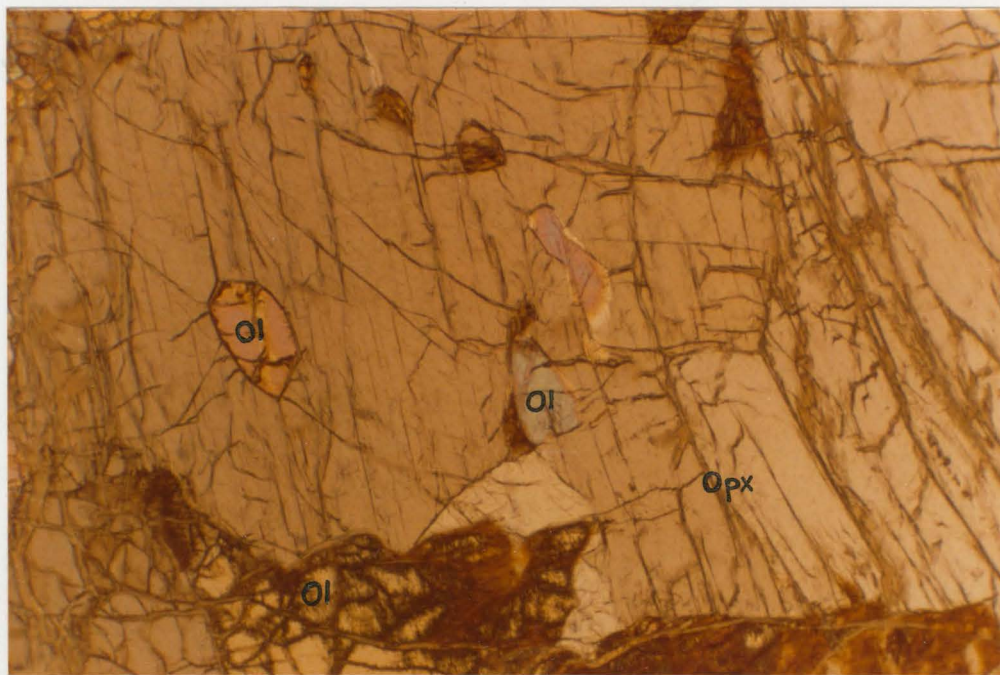
0.5 mm

Figure 13. Photomicrograph of Cerro Matoso
peridotite showing secondary magnetite
(black) as segregations along serpen-
tinized fractures in olivine. Plain
polarized light.

Figure 14. Greenish-black serpentinized peridotite
crisscrossed by white to light-gray
magnesite veinlets. Hammer is 30 cm long.
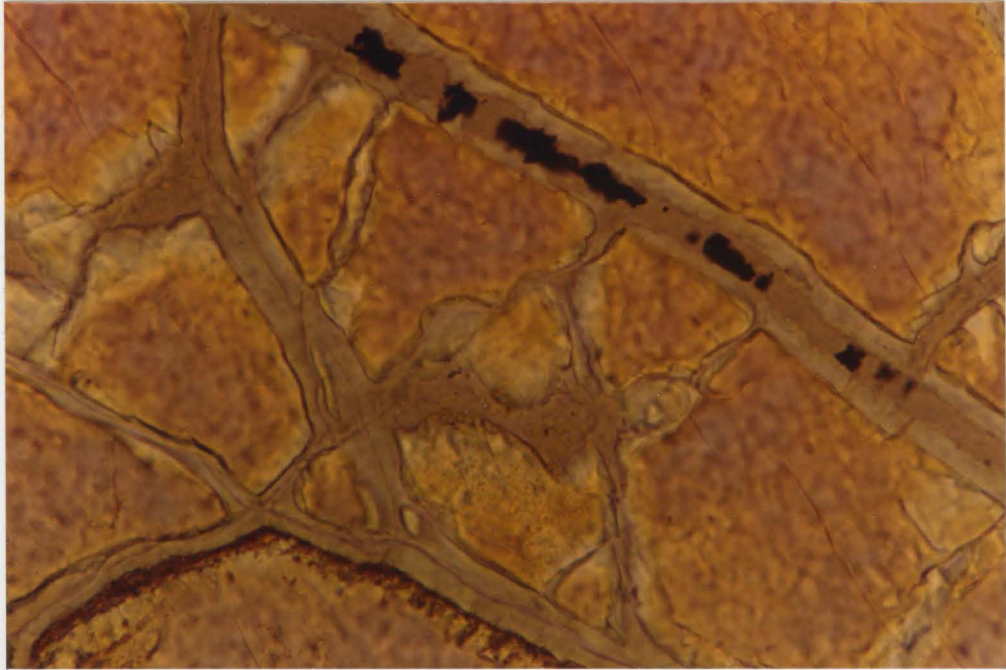
0.05 mm

serpentinite which locally is crisscrossed by numerous magnesite veinlets (Figure 14) that range from 0.2 to 5 cm wide. Serpentinization is preferentially associated with shear zones and has been most effective in the eastern and southeastern parts of the deposit which are proximal to the Romeral fault zone. Similar relationships have been observed by Dueñas and Duque-Caro (1981) in the Planeta Rica peridotite near Cerro Matoso.

Black lenticular bodies present in the peridotite have been described by Mejía and Durango (1982) as probably dunitic in composition. No fresh outcrops of this material were observed, but where weathering is minimal no appreciable amount of pyroxene is evident. These bodies typically are fractured, fractures being filled with goethite and platy chalcedonic silica (Figure 15). Weathered dunite lenses are relatively enriched in nickel (e.g., sample 71, Table 3).

Chemical compositions of selected harzburgite samples from drill holes and outcrops are shown in Table 4 and the general variation intervals are summarized in Table 5. Nickel values are below 0.36% which agrees well with published values for peridotites (Fisher et al., 1969, Table 1; Carmichael et al., 1974, Table 12-4). Values for the other elements are also within the general compositional range for peridotites, except possibly for loss on ignition totals. High L.O.I. values apparently are due to local serpentine present in some samples. The general peridotite (harzburgite) composition given in Table 5 is used as the

Figure 15. Fractured greenish-black dunite.
Fractures are filled with goethite and
platy chalcedonic silica. Hammer is
30 cm long.

Figure 16. Joints in Lower Saprolite zone. Note
light-green garnierite crusts on joint
planes. The bench is 7 m in height.

Table 3. Chemical composition (Wt%), characteristics and
location of representative samples from the
various units of the laterite profile outcropping
along benches. Analytical method: XRF; Analyst:
R. Bustamante; Fe expressed as total iron.

Sample	Ni	Co	Fe	MgO	SiO_2	Al_2O_3	Cr_2O_3	Mn
9	.17	.008	31.6	.1	5.3	14.17	1.12	.18
11	1.05	.067	59.3	2.2	7.4	8.32	3.44	.57
17	.42	.050	44.7	.6	8.1	10.84	2.83	.21
54	.72	.056	55.2	.3	9.3	6.13	3.95	.88
57	1.24	.112	57.5	1.7	11.2	5.16	3.28	1.26
75	.35	.044	38.3	.6	8.2	13.29	4.04	.27
76	1.01	.125	43.8	1.1	17.4	7.68	2.78	1.83
77	.73	.187	37.2	1.8	14.9	6.09	2.97	2.14
88	.43	.020	31.1	.5	9.4	20.31	1.87	.33
90	.97	.120	58.4	.3	8.8	5.73	1.16	.67
91	.54	.013	48.5	.2	10.3	19.82	1.55	.27
92	1.19	.047	44.9	.2	11.6	8.58	4.21	.14
95	.57	.084	41.3	.7	7.3	10.32	3.41	1.01
100	.73	.060	51.0	1.5	6.8	7.71	2.27	1.41
101	.36	.009	44.3	1.2	8.5	9.17	3.96	.87
102	.48	.094	39.4	2.2	12.1	8.45	3.77	.76
7	1.22	.148	28.2	2.6	20.4	5.33	2.19	1.17
8	1.45	.202	33.8	1.9	28.5	3.65	1.43	.67
10	1.04	.187	38.6	1.3	23.1	5.14	2.03	2.77
55	1.10	.288	39.1	.9	31.2	3.72	1.25	4.31
70	.87	.143	28.4	2.9	36.2	2.91	1.35	1.73
97	.96	.221	29.8	1.8	35.1	3.14	1.21	2.96
99	.64	.301	28.7	2.1	12.4	5.12	1.87	4.52
161	1.02	.138	24.3	1.8	29.5	3.27	1.18	2.45
162	.88	.203	31.3	1.3	28.6	1.86	1.44	2.93
163	1.43	.268	35.7	1.2	24.9	1.67	1.75	2.18
164	1.27	.189	33.3	1.6	27.5	1.79	.99	1.14
173	.86	.121	31.2	3.3	34.2	1.14	.87	1.45
174	.57	.302	41.3	.6	30.1	1.26	2.13	3.44
12	4.43	.008	15.2	20.1	38.2	1.13	.74	.25
71	2.02	.082	14.1	27.9	43.2	.87	1.73	.53
84	3.12	.109	16.8	18.2	41.4	2.08	1.01	.57
110	.41	.086	19.5	29.2	33.5	1.87	.45	.27
122	.28	.121	18.4	33.1	31.6	1.03	.66	.21
123	.19	.104	14.3	36.2	24.8	.88	.74	.33
133	1.97	.034	10.2	17.9	46.2	.58	.45	.57
136	2.13	.087	13.1	11.5	53.2	1.35	.61	.71
144	4.45	.034	16.5	13.9	57.2	1.44	.78	.65

Table 3 (Cont.)

147	3.88	.045	19.4	16.4	49.9	1.81	.75	.48
148	5.87	.024	17.8	20.1	43.2	2.12	.89	.54
153	3.57	.065	12.7	24.3	47.1	1.03	.60	.21
168	6.08	.054	10.2	22.4	45.1	1.81	.67	.32
175	3.84	.036	14.3	19.3	48.5	2.55	.78	.56
185	1.57	.025	16.4	17.3	53.1	1.98	.99	.44
37	1.77	.013	11.2	29.8	40.1	1.09	.47	.23
44	2.94	.019	13.3	26.8	43.2	1.42	.87	.08
73	.42	.015	7.6	28.3	45.2	1.25	.53	.10
87	.93	.021	8.2	29.6	44.2	1.10	.66	.11
106	.36	.012	6.3	35.8	42.1	.80	.49	.09
127	.45	.031	7.4	29.3	43.8	.88	.62	.09
128	.88	.025	10.1	30.4	39.6	1.07	.80	.08
129	1.02	.028	9.1	28.8	45.1	.97	.74	.07
131	1.56	.030	12.8	27.6	41.1	1.17	.65	.10
134	.76	.031	13.2	26.9	43.6	1.08	.77	.09
139	1.79	.015	8.7	29.8	39.5	1.21	.84	.12
152	.37	.016	6.8	31.2	41.2	1.10	.57	.06

Characteristics and location

9 Slightly to moderately indurated, Red-Brown Canga; sample from the uppermost level. Bench 210SW

11 Hard Black Canga; laminated texture. Bench 175W

17 Moderately indurated, yellowish-brown to reddish-brown canga; sample from middle level of the Red-Brown Canga. Bench 179N

54 Strongly indurated, reddish-brown canga; middle to lower part of the Red-Brown Canga. Bench 203E

57 Moderately indurated Red-Brown Canga; transition zone from Red-Brown Canga to Black Canga. Bench 182SW

75 Moderately to slightly indurated, reddish-brown to yellowish-brown canga; uppermost part of the Red-Brown Canga. Bench 189N

76 Strongly indurated, brown to reddish-brown canga; middle part of the Red-Brown Canga. Bench 196NE

77 Moderately indurated, Red-Brown Canga; transition zone to Limonite zone. Bench 196NE

88 Moderately indurated, yellowish-red to reddish-brown canga; uppermost part of the Red-Brown Canga. Bench 217E

90 Hard and laminated Black Canga. Bench 182SW

91 Moderately indurated, reddish-brown to yellowish-red canga with segregations of fine-grained quartz as thin silica plates; lower part of the Red-Brown Canga. Bench 217N

Table 3 (Cont.)

92 Strongly indurated, reddish-brown canga; middle part of the Red-Brown Canga. Bench 189NE

95 Strongly indurated, dark brown canga; middle part of the Red-Brown Canga. Bench 196N

100 Moderately indurated, reddish-brown canga; middle part of the Red-Brown Canga; local black Mn oxide coatings on goethite aggregates. Bench 217NE

101 Strongly indurated, brownish-red canga; middle part of the Red-Brown Canga. Bench 217NE

102 Moderately indurated, brownish-red canga; middle part of the Red-Brown Canga. Bench 217NE

7 Moderately soft, yellowish-red Limonite; sample from a 'tongue' of Limonite extending into the Lower Saprolite zone. Bench 161NE

8 Soft, red to yellowish-red Limonite; sample from a 'tongue' of Limonite extending into the Upper Saprolite zone. Bench 175E

10 Soft to moderately hard, light-red to yellowish-red, laminated Limonite. Bench 182NE

55 Moderately hard, yellowish-red Limonite; local Mn oxide stringers. Bench 175NE

70 Moderately hard to soft, reddish-yellow Limonite; transition zone to Upper Saprolite. Bench 182E

97 Moderately hard, massive red Limonite. Bench 189SW

99 Soft, reddish-yellow Limonite; abundant pockets and stringers of Mn oxides. Bench 175N

161 Moderately hard, red to yellowish-red Limonite; some stringers of Mn oxides. Bench 175W

162 Moderately hard, red Limonite; some stringers of Mn oxides. Bench 175W

163 Moderately hard to soft, reddish-yellow Limonite. Bench 175W

164 Soft, yellowish-brown Limonite; some stringers of Mn oxides. Bench 175W

173 Moderately hard, yellowish-brown Limonite; sample from a 'tongue' of Limonite extending into Upper Saprolite. Bench 168S

174 Hard, yellowish-brown to dark brown Limonite; sample from a zone where cavernous structure dominates. Bench 182SW

12 Soft, greenish-brown saprolite; Upper Saprolite zone. Bench 175NW

71 Soft, dark brown to black, weathered dunite (?) lens; Upper Saprolite zone. Bench 175E

84 Soft, greenish-brown saprolite; Upper Saprolite zone. Bench 175NE

Table 3 (Cont.)

110 Soft, green saprolite; thin magnesite veinlets.
Bench 182SW
122 Soft to moderately hard, brownish-green saprolite;
thin magnesite veinlets. Bench 203SW
123 Moderately hard, green saprolite; thin magnesite
veinlets. Bench 210SW
133 Soft, brownish-green saprolite; Upper Saprolite
zone. Bench 175NE
136 Soft, green to greenish-brown saprolite; Upper
Saprolite zone. Bench 175N
144 Soft, brown saprolite; Upper Saprolite zone.
Bench 182NW
147 Soft to moderately hard, greenish-brown saprolite;
Upper Saprolite zone. Bench 168NE
148 Soft, brown saprolite; thin green garnierite veinlets;
Upper Saprolite zone. Bench 168NE
153 Soft, greenish-brown saprolite; Upper Saprolite
zone. Bench 189E
168 Soft, brownish-green saprolite; abundant thin green
garnierite veinlets; Upper Saprolite zone. Bench 182N
175 Soft, green saprolite; Upper Saprolite zone.
Bench 182NE
185 Soft, brown saprolite; Upper Saprolite zone.
Bench 196SW

37 Moderately hard to soft, greenish-brown saprolite;
transition zone from Upper to Lower Saprolite zone.
Bench 175NE
44 Moderately hard, brownish-green saprolite; thick and
widely spaced green garnierite veinlets; Lower
Saprolite zone. Bench 175N
73 Moderately hard, dark green saprolite; lower part
of the Lower Saprolite zone. Bench 168NE
87 Moderately hard, greenish-brown saprolite; Lower
Saprolite zone. Bench 175SW
106 Moderately hard to hard, greenish-brown saprolite;
lower part of the Lower Saprolite zone. Bench 168NW
127 Moderately hard, brown saprolite; lower part of the
Lower Saprolite zone. Bench 182SW
128 Moderately hard, greenish-brown saprolite; Lower
Saprolite zone. Bench 182SW
129 Moderately hard, dark brown saprolite; Lower Saprolite
zone. Bench 182SW
131 Hard, green saprolite; Lower Saprolite zone. Bench 168N
134 Hard, brown saprolite; Lower Saprolite zone. Bench 168N
139 Moderately hard, dark green saprolite; Lower Saprolite
zone. Bench 168NE
152 Moderately hard to hard, dark brown saprolite; lower
part of the Lower Saprolite zone. Bench 175SW

Table 4. Chemical analysis (Wt%) of harzburgite samples. Analytical method: XRF; Analyst: R. Bustamante; Fe expressed as total iron.

Sample	Coordinates	Depth (m)	Ni	Co	Fe	MgO	SiO_2	Al_2O_3	Cr_2O_3	Mn	LOI
72-100	2000 NW 1378 NE	21	.30	.010	6.2	35.7	42.9	.71	nd	nd	10.6
72-3628	2000 NW 1574 NE	49	.36	.015	6.1	33.8	43.4	1.24	.51	nd	8.4
73-3769	2000 NW 1657 NE	37	.30	.013	6.2	37.0	40.8	1.22	.41	nd	10.3
40-7161	1200 NW 1128 NE	25	.25	.009	5.7	32.1	41.9	1.26	nd	nd	10.0
40-7126	1300 NW 800 NE	29	.31	.012	6.6	35.1	42.7	1.22	nd	nd	4.8
43-A	2100 NW 1000 NE	0	.34	.020	6.1	40.6	42.2	.47	.29	.09	4.2
106-A	1800 NW	0	.32	.013	5.8	38.2	40.5	.80	.28	.06	4.3

Table 5. Generalized variation intervals in chemical composition for characteristic components (Wt%) in the Cerro Matoso laterite profile. Established from chemical data corresponding to drill hole and outcrop samples (Appendix 1, Table 3).

	Canga	Limonite	Upper Saprolite	Lower Saprolite	Harzburgite
Ni	< 1.1	< 1.5	$1.5 - 5.0$	$.36 - 3.0$	$< .36$
Co	$< .100$	$< .300$	$.010 - .200$	$< .030$	$< .020$
Fe*	> 44	$20 - 45$	$14 - 20$	$6.6 - 14$	$5.7 - 6.6$
MgO	< 1	< 2	$8 - 25$	$25 - 30$	$30 - 40$
SiO_2	< 10	$10 - 38$	> 45	$38 - 45$	$40 - 45$
Al_2O_3	$6-20$	$3 - 10$	$1.2 - 3.0$	$.8 - 1.5$	< 1.3
Cr_2O_3	$2-4$	$1.2 - 2.5$	$.6 - 1.5$	$.5 - .8$	$< .5$
Mn	$.2-1$	$.8 - 4.5$	$< .7$	$< .1$	$< .1$
LOI	$6-10$	$8 - 12$	< 12	< 11	< 10

* Fe expressed as total iron and mostly Fe^{2+} for harzburgite

bulk chemical starting point in evaluating chemical trends associated with weathering processes that were responsible for the development of the laterite profile.

Saprolite

Saprolite is a zone of relatively intensely decomposed peridotite in which most of the structural features of the original peridotite are preserved. Typical colors range from green through greenish-brown to reddish- and yellowish-brown to brown. Two saprolite zones, Lower and Upper, may be identified based upon relative hardness, degree of preservation of original structures, and composition.

The Lower Saprolite zone is characterized by relatively fresh-looking rock in which joints and faults are readily discernible (Figures 16 and 17). Blocky and moderately hard, this zone reflects a low degree of weathering of the peridotite and is equivalent to 'saprolitic peridotite' of Webber (1972). Chemical compositions of samples from drill holes and outcrops (Tables 3 and 5) indicate that magnesium is slightly leached from this zone as compared to the original peridotite whereas iron is relatively enriched and silica remains essentially unchanged. The significant enrichment of nickel is related primarily to the introduction of nickel-bearing silicates along fractures and to a lesser extent with partial block saprolitization.

The Upper Saprolite zone corresponds to intensely weathered peridotite in which original rock structures are

Figure 17. Fault preserved in Lower Saprolite zone.
Greenish-brown brecciated zone above
geologist is enriched in nickel. Note
reddish-brown 'tongue' of Limonite
(center of photograph). Geologist is
1.7 m in height.

Figure 18. Light-brown and greenish brown saprolites.
Light-brown saprolite is located
preferentially along fractures and grades
to greenish-brown saprolite away from
fractures. Book is 16 cm long.

still preserved but much less so than in the Lower Saprolite zone. The rock of the Upper Saprolite level lacks the blocky appearance of Lower Saprolite and is soft enough to be cut by a knife blade. Gómez et al. (1979) differentiated two varieties of soft saprolite, green and brown; green saprolite has a higher ferrous iron and lower ferric iron content than brown saprolite (Mejía and Durango, 1982). Bench examinations conducted in this study established that green and brown saprolites reflect variable structural control on oxidizing solutions. Brown saprolite occurs preferentially along fractures and grades to green saprolite away from fractures (Figure 18). With progressive alteration, only small local patches of green saprolite engulfed by brown saprolite are observed (Figure 19). It is apparent that these two saprolites do not correspond to different levels of the profile in a vertical sense but rather are the products of differential weathering processes controlled mainly by structures. That solutions advance from fractures inward toward the cores of individual blocks also is indicated by the presence of spheroidal blocks cored by less weathered peridotite surrounded by saprolitized shells (Figure 20).

The chemical composition of the Upper Saprolite reflects a more evolved degree of alteration as compared to the Lower Saprolite (Tables 3 and 5). Nickel enrichment is very strong in this zone and it is the most important site for silicate-type nickel ore reserves. Average nickel content

Figure 19. Light-brown saprolite engulfing greenish-
           brown saprolite indicating progressive
           alteration. Some small patches of
           greenish-brown saprolite are completely
           surrounded by light-brown saprolite.
           Hammer is 30 cm long.

Figure 20. Spheroidal weathering in Upper Saprolite
           zone. Brown nuclei of slightly weathered
           peridotite (top center) are surrounded by
           saprolitic shells or rims. Knife is 8 cm
           long.

is approximately 3.0% Ni, but grades of as much as 8% have been observed locally. Iron content increases and magnesium content decreases compared to the Lower Saprolite zone.

Several types of silicification products are present at Cerro Matoso, especially in the Upper Saprolite zone. Irregular to lenticular, porous silica accumulations consisting of very fine-grained quartz are abundant at intermediate levels of the Upper Saprolite (Figure 21). Veinlets of fine-grained quartz are present at lower levels of the Upper Saprolite (Figure 22). Silica boxworks in which chalcedonic silica plates are arranged in a honeycomb-like texture occur principally in zones of abundant fractures at upper levels of the Lower Saprolite but also are locally present at lower levels of the Upper Saprolite (Figure 23). Zones of massive silicification consisting of nearly horizontal fine-grained quartz accumulations having varying thickness, occur principally in the Upper Saprolite (Figure 24) and are locally disrupted by normal faults (Figure 25).

Limonite zone

This zone consists of slightly indurated, brown to reddish-brown to yellowish-brown iron-rich material (Figure 26) in which no preservation of the original parent rock structures is evident. Iron is principally in goethite, but moderate amounts of maghemite also were observed by Webber (1972, Figure 6). This corresponds to a more

Figure 21.   Light-brown to gray, porous silica
             accumulations consisting of very fine-
             grained quartz in Upper Saprolite zone.
             Note the lenticular shape.   Hammer is
             30 cm long.

Figure 22.   Light-gray to brown, fine-grained quartz
             veinlet in Upper Saprolite zone.   Knife
             is 15 cm in total length.

Figure 23. Silica boxwork in Upper Saprolite zone.
Grayish-white to cream, chalcedonic
silica plates are arranged in a honeycomb-
like texture and enclose light-brown
saprolite material. Hammer is 30 cm
long.

Figure 24. Massive silicification in Upper Saprolite
zone. The nearly horizontal, grayish-
brown, silica 'layer' above the hard hat
consists of fine-grained quartz and is
about 15 cm thick. Hard hat is 25 cm
long.

Figure 25.   Grayish-yellow to light-brown massive
             silica zone in Upper Saprolite disrupted
             by normal fault.   Also shown light-brown
             to cream, fine-grained quartz veinlets
             (bottom right).   Hammer is 30 cm long.

Figure 26.   Outcrop of reddish-brown Limonite zone.
             Geologist is 1.7 m in height.

advanced degree of alteration than is reflected by the Upper Saprolite zone.

Only local variations in the physical appearance of the Limonite zone have been observed. In some places the zone consists of a homogeneous, relatively indurated, massive, fine-grained and fractured goethite-rich material in which the fractures are filled with hematite (Figure 27). These fracture fillings apparently were deposited from iron-bearing solutions derived from upper parts of the profile. Dissolution in the Limonite zone has produced cavernous structures (Figure 28) lined with botryoidal aggregates of limonitic material, principally goethite, hematite, and amorphous iron compounds (Figure 29). Dissolution also may have favoured slump and/or creep processes that may have been responsible for the development of local laminations in this zone (Figure 30).

The contact of the Limonite zone with the underlying saprolite is usually irregular to tongue-shaped (Figure 31), and locally limonitic 'tongues' may extend as far as the Lower Saprolite zone (Figure 17). In the latter case, a fault generally serves as a lateral or oblique permeability conduit that promotes the advance of the Limonite zone. Tectonic activity that occurred after the formation of the Limonite zone is reflected by joints (Figure 32), faults (Figure 33), and arcuated structures (Figure 34).

Some features related to the chemical composition (Tables 3 and 5) of the Limonite zone deserve attention.

Figure 27.   Massive fine-grained Limonite zone
             showing abundant fractures filled with
             hematite.   Book is 16 cm long.

Figure 28.   Cavernous structures (left center) in the
             Limonite zone.   Fault contact between
             brownish Limonite zone and yellowish
             Upper Saprolite zone is present toward
             the right part of the photograph.   Book is
             16 cm long.

Figure 29. Botryoidal aggregates of limonitic
material consisting principally of
goethite and hematite from cavities
in the Limonite zone. Scale in cm.

Figure 30. Goethite- and maghemite-rich laminae
in Limonite zone. Hammer is 30 cm long.

Figure 31. Tongues of reddish-brown Limonite zone
            extending into underlying light
            yellowish-brown Upper Saprolite zone.
            Note black manganese oxide stringers
            in Limonite zone. Book is 16 cm long.

Figure 32. Prominent joints in Limonite zone.
            Book is 16 cm long.

Figure 33. Layered Limonite zone (right) in fault
contact with Upper Saprolite zone (left).
Hammer at contact is 30 cm long.

Figure 34. Arcuated structures in Limonite zone.
Hard hat is 25 cm long.

Drill hole samples from the Limonite zone (Appendix 1) exhibit MgO contents that generally are less than 1.0%, and samples taken from outcrops in which either iron hydroxides or manganese oxides are abundant (e.g. samples 55 and 99, Table 3) also show very low MgO contents. This indicates an almost complete absence of magnesium hydrous-silicates and suggests that nickel values, usually on the order of 1.0%, may be associated with iron hydroxides and/or manganese oxides. Manganese tends to accumulate preferentially toward the lower part of the Limonite zone as stringers and pockets of manganese oxide associated with moderate amounts of silica (Figure 35). Silica content usually ranges between 10 and 25%, eventually reaching values of as much as 38%, and increases downward in the Limonite zone. Evidence of massive silicification is reflected locally by elongated and lenticular bodies of fine-grained quartz (Figure 36) that range to 2 m in length and 0.3 m in thickness. Platy and very fine-grained quartz accumulations associated with concretionary ferruginous material also are common (Figure 37).

Canga

The uppermost unit in the laterite profile at Cerro Matoso is referred to as Canga. It is dominantly red-brown, moderately indurated to hard, highly enriched in iron, and shows no preservation of original parent rock structures. Iron minerals are goethite and maghemite.

Two general varieties of canga are recognized: Red-brown Canga and Black Canga. The Red-brown Canga is by far

Figure 35.   Pockets and stringers of black manganese
              oxide in Limonite zone.   Hammer is 30 cm
              long.

Figure 36.   Gray to light-gray, massive silica lenses
              consisting of fine-grained quartz (middle
              to upper part of the photograph) in the
              Limonite zone.   Blackish stains are
              manganese oxide films.   Hammer is 30 cm
              long.
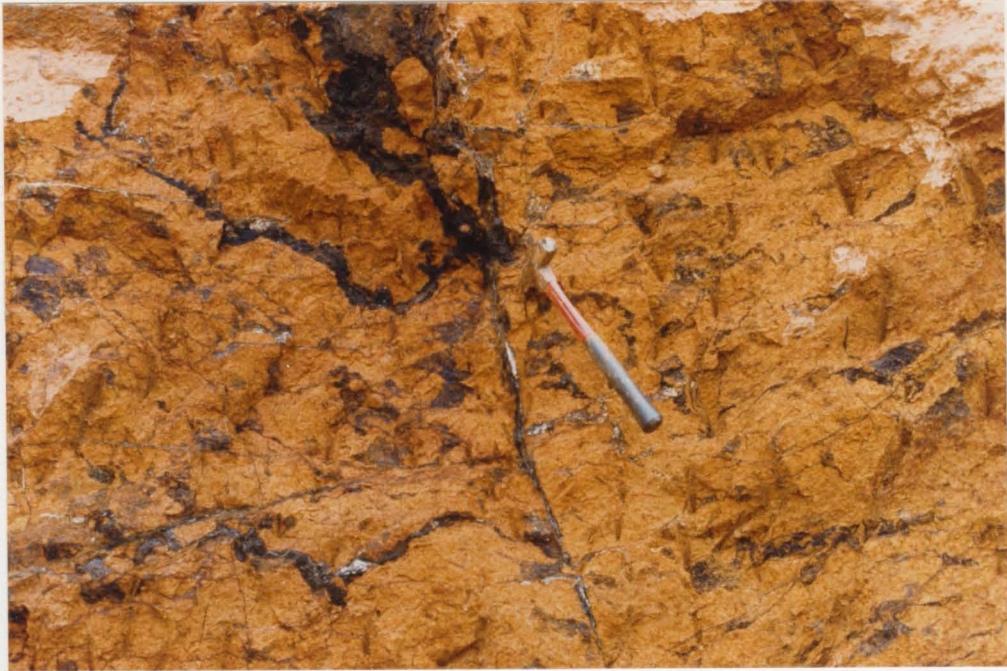
Figure 37. Grayish-white, platy silica accumulation
consisting of very fine-grained quartz
associated with concretionary ferruginous
material in Limonite zone. Knife is
8 cm long.

Figure 38. Red-brown Canga showing concretionary
structure. Hard hat is 25 cm long.

the most abundant variety; it exhibits a concretionary structure (Figure 38) but also may be dense and moderately fine-grained. It occurs over a wide area, particularly in the northeastern part of the deposit (Plate 2) where, due to its toughness, it has largely protected the underlying materials from erosion. The presence of Red-brown Canga generally correlates with highest nickel grades observed in associated saprolite.

Black Canga occurs as local elongated accumulations which may grade laterally either into Red-brown Canga or Limonite zone material (Figure 39). It is greenish-black to black-brown and exhibits a laminated texture that apparently formed by slumping processes associated with dissolution of goethite (Figure 40). Fine-grained quartz occurs as segregations in the Black Canga in the form of thin plates which parallel the lamination direction (Figure 41) and locally as lenticular massive accumulations and stringers (Figure 42).

Chemical analyses of Canga zone samples (Tables 3 and 5) show several significant differences relative to other units in the profile. Cobalt and manganese contents are greater than in the peridotite parent rock but lower than in the underlying Limonite zone. Chromium values in Canga are the highest observed in the laterite profile and probably reflect the relative resistance of chromite to weathering. The highest iron values observed in the profile also are found in the Canga zone, and contents over 44% total Fe are common. Nickel values generally are low, usually ranging

Figure 39. Elongated body of Black Canga grading
           laterally and downwards into Limonite
           zone.   Book is 16 cm long.

Figure 40. Laminated texture in Black Canga.
           Hammer is 30 cm long.

Figure 41.   Cream to white, fine-grained quartz
             plates paralleling the lamination
             direction in Black Canga.   Hammer is
             30 cm long.

Figure 42.   Black Canga showing lenticular massive
             silica accumulations (cream colour, center
             of photograph) and stringers (bottom
             left).   Both silica occurrences involve
             fine-grained quartz.   Hard hat is 25 cm
             long.

from 0.4 to 0.9%. In Black Canga, nickel appears to be in a relatively mobile form, probably loosely bounded on iron hydroxides. In dry days following a rainy period, greenish-white efflorescences of hydrated nickel compounds (Mejía and Durango, 1982) form on Black Canga outcrops (Figure 43). Individual separates of the material comprising these efflorescences show nickel values of as much as 14% (Mejía and Durango, 1982). Alumina content may be as high as 20%. Gibbsite was not detected during the mineralogical analyses, but Al probably occurs associated with Fe as Al-goethite as observed experimentally by Lewis and Schwertmann (1979).

Figure 43.   Greenish-white nickeliferous
             efflorescences on Black Canga outcrops.
             Book is 16 cm long.

Figure 44.   Soft saprolite mottled by green
             garnierite; Upper Saprolite zone.
             Scale in cm.
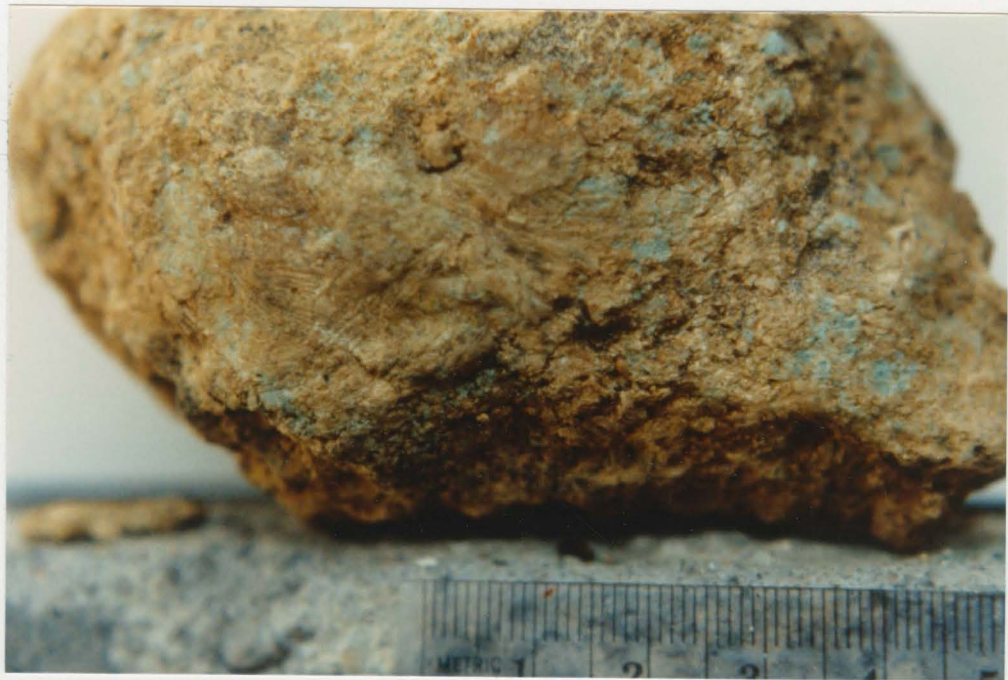
ORE TYPES AND DISTRIBUTION

Ore grade nickeliferous laterite at Cerro Matoso has been defined as material having a nickel content in excess of 1.5% (Gómez et al., 1979). Utilizing this cutoff grade, analytical results from outcrop and drill hole samples (Table 3 and Appendix 1) indicate that ore at Cerro Matoso is contained principally in the Upper Saprolite zone with lesser amounts in the Lower Saprolite zone. Several types of ore grade materials occur in both saprolite zones and ore types described herein are named on the basis of their geological occurrence. Table 6 shows chemical compositions of the various ore types.

Massive ore

This type of ore occurs primarily in the Upper Saprolite zone, and represents a direct weathering product of peridotite. It constitutes the principal ore of the deposit. Nickel content in saprolite is quite variable, for example, saprolite developed on highly serpentinized peridotite has a very low nickel content, usually less than 1.0%. Magnesite has been observed only in saprolite derived from highly serpentinized peridotite. Where there is no magnesite and the saprolite zone exhibits an advanced degree of

Table 6. Chemical compositions (in Wt%), characteristics,
and location of different ore types. Analytical
method: XRF; Analyst: R. Bustamante;
Fe expressed as total iron.

	Sample	Ni	Co	Fe	MgO	SiO_2	Al_2O_3	Cr_2O_3	Mn
Massive ore	35	3.57	.02	7.9	32.2	40.4	.52	.56	.13
	51	3.65	.04	12.1	24.1	43.4	.91	.92	.24
	81	2.49	.02	9.6	21.6	45.9	1.69	.70	.12
	86	.36	.01	7.2	29.5	46.1	1.49	.43	.05
	36	2.03	.03	14.4	15.2	50.3	1.53	1.21	.03
Fracture fillings	34V	23.36	.02	2.6	8.8	39.7	.12	.03	.72
	34N	19.47	.04	1.7	9.5	40.2	.17	.01	1.17
	39	15.23	.02	1.9	10.4	39.8	.14	.02	.55
	114	4.72	.23	.9	10.7	48.4	.08	.02	10.26
	96	2.82	.10	8.9	19.6	41.6	5.74	.35	.29
	98	30.12	.12	4.4	9.2	33.6	3.98	.06	.20
	48	7.40	.01	2.0	23.2	53.0	.45	.13	.04
	66	10.75	.01	.6	19.6	50.3	.29	.04	.11
	32	13.27	.01	1.8	9.4	52.3	.20	.02	.08
	25	22.14	.08	.7	11.3	47.7	.25	.03	.33
	52	18.31	.02	.6	8.9	57.2	.13	.01	.85

Ore type, characteristics, and sample location

35 Massive ore; moderately to slightly weathered peri-
dotite; Upper Saprolite, near its base. Bench 175SW

51 Massive ore; completely weathered core of a soft
joint controlled 'parallelepiped' block; located in
the middle of the Upper Saprolite. Bench 189W

81 Massive ore; completely weathered peridotite; upper
part of the Upper Saprolite. Bench 203N

86 Massive ore; completely weathered peridotite; from
zone where intensely serpentinized peridotite is
associated with abundant magnesite boxworks;
location within the laterite profile is equivalent
to that of sample 81. Bench 210SW

36 Massive ore; completely weathered peridotite; upper-
most part of the Upper Saprolite, near overlying
Limonite zone. Bench 196NE

34V Green garnierite-rich fracture fillings; Lower
Saprolite. Bench 175SW

34N Mn oxide-bearing green garnierite-rich fracture
fillings; Upper Saprolite. Bench 196SW

39 Pale green garnierite-rich fracture fillings; Lower
Saprolite. Bench 182N

114 Mn-oxide-rich fracture fillings; Upper Saprolite.
Bench 189W

Table 6 (Cont.)

96   Chloritic material along shear zones; Lower
      Saprolite.   Bench 175NE
98   Chloritic material-rich fracture fillings; Upper
      Saprolite.   Bench 189NE
48   Soft, white sepiolitic material fracture fillings;
      Upper Saprolite.   Bench 189W
66   Soft, spongy, light-green to white sepiolitic
      material fracture fillings; Upper Saprolite.
      Bench 196SW
32   Green garnierite coating joints; Lower Saprolite.
      Bench 175SW
25   Green garnierite veinlets; Upper Saprolite.
      Bench 196N
52   Cavity fillings of green garnierite in botryoidal
      aggregates; Lower Saprolite.   Bench 175SW

development, it is difficult to differentiate between saprolite derived from highly serpentinized versus only slightly serpentinized peridotite.

After a material has been identified as saprolite, a chemical analysis for nickel generally is necessary to determine if it constitutes massive ore, although an analysis might not be needed if the saprolite is mottled with abundant garnierite (Figure 44). Garnierite as used here is a general field term for a fine-grained material containing hydrous nickel-magnesium silicates and does not connote a specific mineralogical composition unless specifically indicated as such. Garnierite generally is pale green but ranges from dark green to greenish white. It may be soft or moderately hard and ranges from massive to botryoidal in form.

Fracture fillings

Ore grade fracture fillings in both Upper and Lower Saprolite zones may be distinguished based upon colour variations, hardness, habit of the nickel-bearing minerals, mineralogical association, particular textures and site of occurrence.

Major fractures, usually fault related, commonly are filled with garnieritic material. In the Lower Saprolite zone, a soft (hardness 2-2.5), fine-grained, pale- to dark-green garnierite commonly is associated with minor serpentine in fracture fillings (Figure 45). Towards the base of the

Figure 45. Fractures filled with garnierite and
            serpentine; Lower Saprolite zone.
            Hammer is 30 cm long.

Figure 46. Light-green garnierite veinlets near the
            base of the Upper Saprolite zone. Knife
            is 8 cm long.
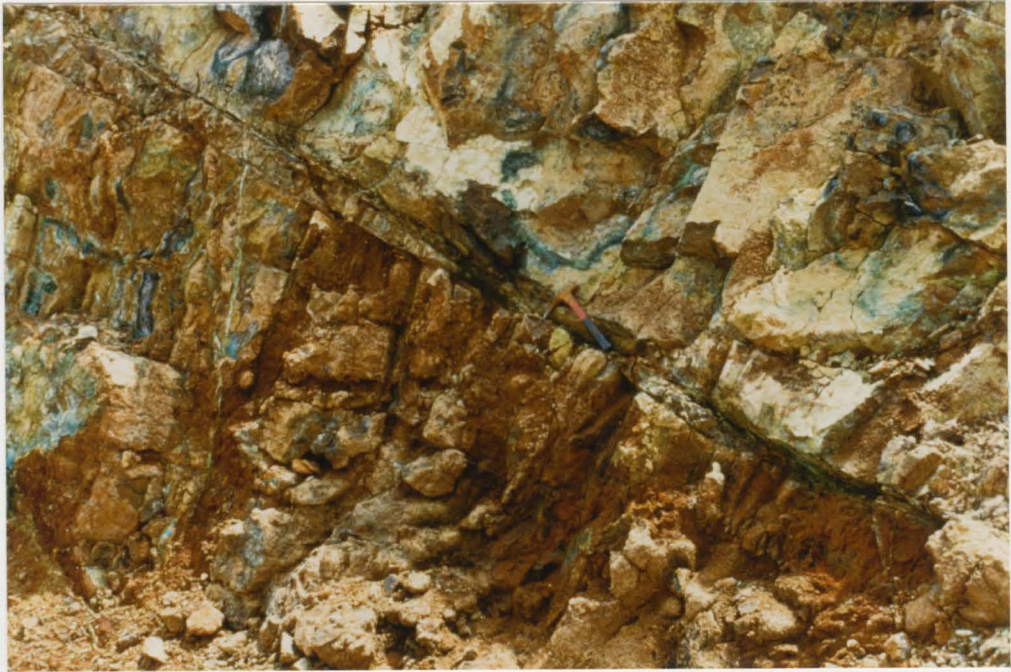
Upper Saprolite zone, veins consist predominantly of massive, fine-grained, light-green garnierite (Figure 46); however, a bright green chloritic phase locally constitutes the dominant nickel-bearing mineral (Figure 47). Green to whitish-green garnierite veins may be stained with black manganese oxides, particularly in the Upper Saprolite zone. Manganese oxides may dominate in some veins to the point that garnierite is not readily identified in outcrop (Figure 48). At intermediate depths in the Upper Saprolite zone, fractures also may be filled with soft, spongy, light greenish-white ore grade material composed primarily of sepiolite (Figures 49, 50 and 51).

Coatings or thin crusts as much as 5 mm thick of relatively hard (hardness about 3.5), fine-grained, greenish garnierite are relatively abundant in the Lower Saprolite. Roughly parallel fractures in the Upper Saprolite are completely filled with soft, fine-grained, greenish garnierite (Figure 52). Spheroidally weathered areas are characterized by joint controlled rims of saprolitic material mottled with green garnierite (Figures 53 and 54).

Some fractures have variable amounts of open space and can be subdivided into two types: a) those containing breccia-like bodies in which fragments of saprolite ranging from millimeters to centimeters in size are cemented by garnierite and chalcedonic silica and generally reflect more than one stage of garnierite-silica deposition, garnierite being deposited after silica (Figures 55 and 56),

Figure 47.   Green, nickel-bearing chlorite filling
             fractures near the base of the Upper
             Saprolite zone.   Hard hat is 25 cm long.

Figure 48.   Black manganese oxide with subordinate
             green garnierite; Upper Saprolite zone.
             Knife is 8 cm long.
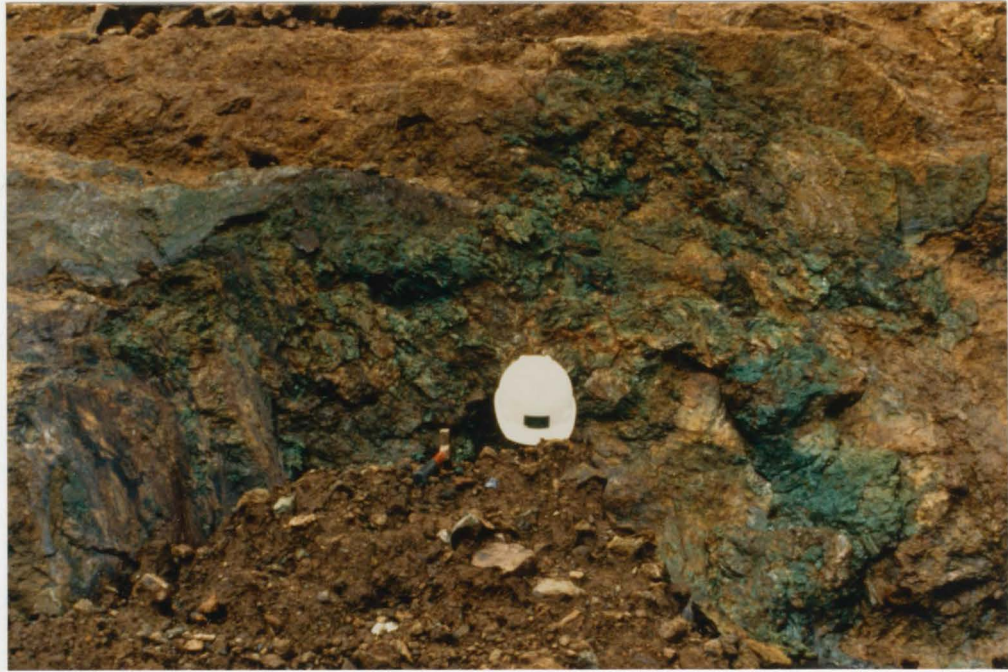
Figure 49. Light-green to greenish-white, spongy
nickel-bearing sepiolite filling
fractures; Upper Saprolite. Knife is
8 cm long.

Figure 50. Light-green to white, nickel-bearing
sepiolite filling cracks; Upper
Saprolite. Hammer is 30 cm long.

Figure 51. Greenish-white to light-gray nickel-
bearing sepiolite with dessication
cracks developed after exposure to
air.   Scale in cm.

Figure 52. Light-green garnierite veinlet cutting
soft light-brown saprolite; Upper
Saprolite.   Coin is about 2.3 cm in
diameter.

Figure 53.   Rims of yellowish-brown saprolitic
             material surrounding spheroidal blocks
             of slightly weathered peridotite; Upper
             Saprolite.   Hammer is 30 cm long.

Figure 54.   Close-up of central vein area in Figure
             53.   Rims mottled by light-green
             garnierite indicated by knife.   Knife is
             8 cm long.

Figure 55. Breccia ore showing multiple stages of
            garnierite (green) and chalcedonic silica
            (grayish-white) engulfing brownish
            fragments of weathered peridotite.
            Scale in cm.

Figure 56. Breccia ore with green to dark-green
            garnierite and light-gray to white
            chalcedonic silica cement surrounding
            dark-brown to greenish-brown saprolite
            fragments. Garnierite deposited after
            silica. Scale in cm.
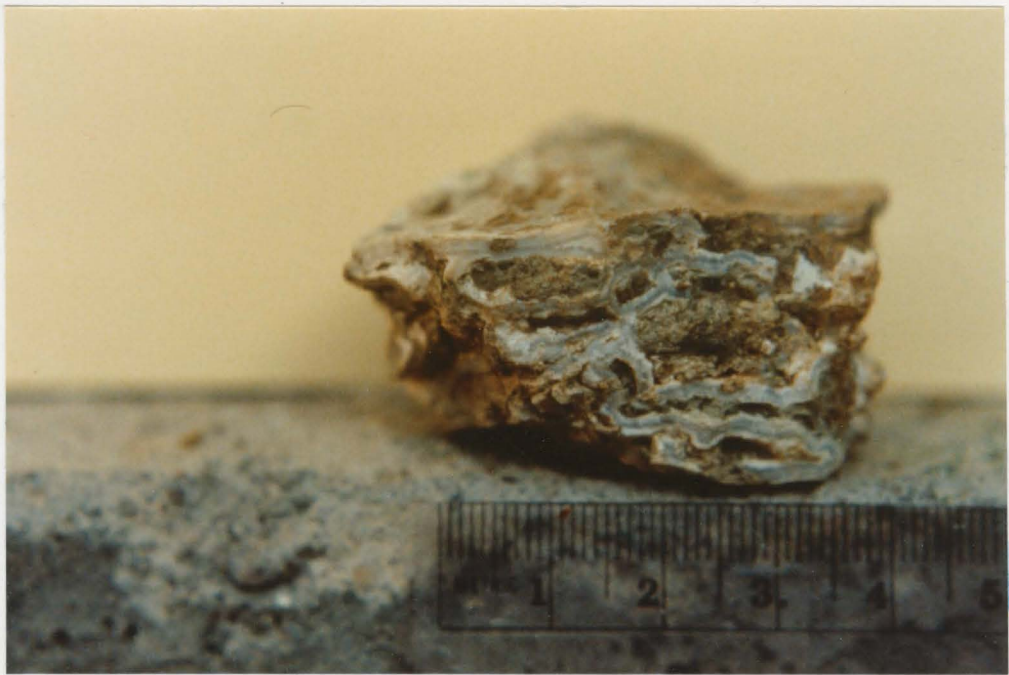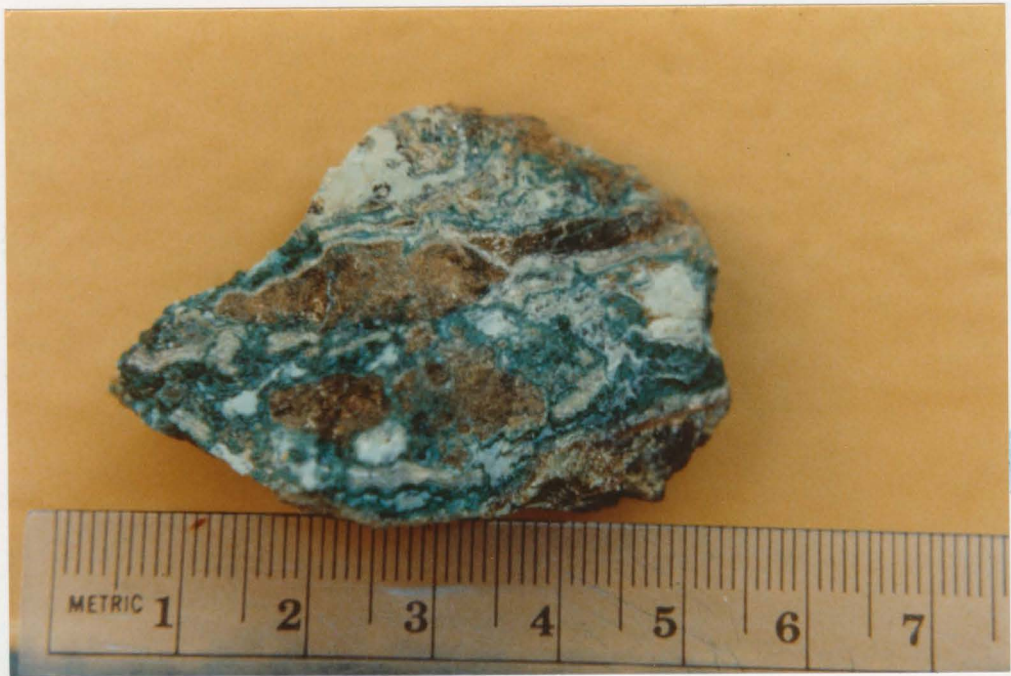
b) botryoidal garnierite aggregates commonly developed
over chalcedonic silica or chalcedonic silica + manganese
oxides (Figure 57).

Figure 57. Botryoidal garnierite encrustations in
            open fractures. Light-green botryoidal
            garnierite aggregates deposited over
            whitish to cream chalcedonic silica and
            black manganese oxides. Scale in cm.
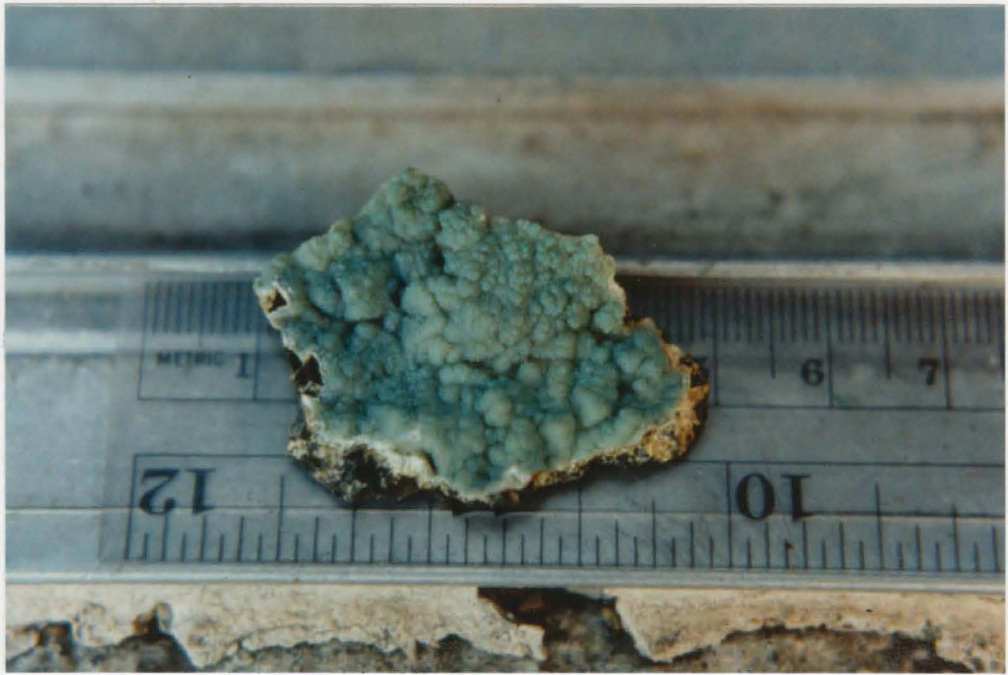
NICKEL ORE MINERALOGY

General Statement

The Cerro Matoso nickeliferous laterite has been referred to as silicate-type ore (Gómez et al., 1979; Golightly, 1981; McFarlane, 1983; McFarlane, 1984) but no studies have been conducted on the mineralogical composition of the Ni-bearing compounds occurring in the various zones throughout the deposit profile.

Silicate-type nickel laterite ore minerals comprise a suite of hydrous nickel-silicate phases ranging from serpentine- to smectite-group minerals which can be identified, in many cases, on the basis of their X-ray diffraction characteristics. The most abundant hydrous nickel-bearing silicate minerals appear to be the non-swelling 7Å and 10Å layered types that generally occur as intimate mixtures in which one or the other type may dominate. These mixtures are mostly fine-grained, usually display a low degree of crystallinity, and commonly are referred to as garnierites. The term garnierite implies a nickel content in contrast to deweylites which also are poorly crystallized fine-grained mixtures of 7Å and 10Å type layered structures but in which nickel is not an essential constituent. Hydrous nickel-bearing silicates

other than 7Å and 10Å layered types have been identified locally.

7Å and 10Å type structures:

Garnierites from Nickel Mountain, Oregon, studied by Pecora et al. (1949), revealed the presence of mixtures of two or more hydrous silicates as their components rather than a single mineral species. In a later study of this locality, Hotz (1964) identified garnierites as mixtures of serpentine and 10Å layered material. One of his samples was referred to as having a poorly ordered serpentine pattern; however, the resolution of the diffraction peaks for poorly crystalline, mostly fine-grained, garnierite is in many cases so low that the other components also present may not be clearly identified (Brindley and Pham Thi Hang, 1973).

Brindley and Pham Thi Hang (1973) examined forty garnierite separates from various localities and concluded that garnierites have components with basal spacings near 7.2-7.3Å and 10Å. They emphasize the resemblance of the 7Å-type component to the serpentine group minerals chrysotile and lizardite, and of the 10Å-type component to a talc-like mineral with a high degree of layer stacking disorder (Brindley and Pham Thi Hang, 1973). Chrysotile and lizardite are the more commonly reported members of the serpentine group present in garnierites but Trescases (1975), in an extensive study of the New Caledonia nickeliferous deposits, indicates that garnierites are talc-like minerals having

varying amounts of antigorite. Montoya and Baur (1963) have identified a nickel-bearing antigorite in lateritic ore from Humboldt County, California.

Brindley and Maksimovic (1974) and Brindley (1978) re-evaluated the multiple names in the literature for definite 7Å and 10Å type nickel-bearing minerals, and their conclusions are presented in Table 7. Table 8 shows the generalized mineral composition for hydrous nickel-bearing silicates described in Table 7. A nickel analog of clinochrysotile, pecoraite, was described by Faust et al. (1969), and a nickel analog of lizardite, nepouite, may be considered as the nickeliferous end members of the chrysotile-pecoraite and lizardite-nepouite series, respectively (Brindley and Maksimovic, 1974; Brindley and Wan, 1975; Bailey, 1980). Brindleyite is the Ni analog of berthierine (Brindley, 1978).

In re-evaluating the names for 10Å type minerals, Brindley and Maksimovic (1974) suggest the use of two series based upon the basal spacing position in X-ray diffraction patterns. Willemseite, a nickel-rich mineral with well-defined talc structure (i.e. basal spacing around 9.36Å), described by de Waal (1970b), may be considered as the nickeliferous end member of a series having talc as the magnesian end member. With respect to Ni-Mg minerals with a disordered talc-like structure (i.e. basal spacing around 10Å), the suggestion of keeping them in the kerolite-pimelite series appears to be reasonable. Maksimovic (1966) found beta-kerolite and pimelite from Goles Mountain,

Table 7. Hydrous nickel-bearing silicates (modified after Brindley and
          Maksimovic, 1974, and Brindley, 1978).

7Å-type minerals	References
Antigorite	Montoya and Baur, 1963; Trescases, 1975.
Chrysotile-Pecoraite series	Montoya and Baur, 1963; Faust et al., 1969; Brindley and Maksimovic, 1974.
Lizardite-Nepouite series	Brindley and Wan, 1975.
Berthierine-Brindleyite	Brindley, 1978.

10Å-type minerals	
Talc-Willemseite series	De Waal, 1970b; Brindley and Maksimovic, 1974.
Kerolite-Pimelite series	Maksimovic, 1966; Brindley et al., 1979; Wiewiora et al., 1982.

12Å-type minerals	
Sepiolite-Falcondoite series	Hotz, 1964; Brindley, 1978.

14Å-type minerals	
Chlorite Ia	Montoya and Baur, 1963; Zeissink, 1969; Brindley and de Souza Santos, 1975.
Clinochlore-Nimite series	De Waal, 1970a; Brindley and Maksimovic, 1974; Bailey, 1980.
Vermiculite	Felicissimo, 1965 (in Brindley and de Souza Santos, 1975).
Fe^{3+}-Montmorillonite	Zeissink, 1969; Brindley and de Souza Santos, 1975.

Table 8. General formulae for hydrous nickel-bearing silicates.

7Å-type minerals

    Antigorite: $Mg_3Si_2O_5(OH)_4$

    Chrysotile-Pecoraite series: $(Mg,Ni)_3Si_2O_5(OH)_4$

    Lizardite-Nepouite series: $(Mg,Ni)_3Si_2O_5(OH)_4$

    Berthierine-Brindleyite series: $[(Fe^{2+},Ni)_{2.25}Al_{.75}](Si_{1.25}Al_{.75})O_5(OH)_4$

10Å-type minerals

    Talc-Willemseite series: $(Mg,Ni)_3Si_4O_{10}(OH)_2$

    Kerolite-Pimelite series: $(Mg,Ni)_{3.04}(Al,Fe)_{.01}(Si_{3.93}Al_{.02}Fe_{.02})O_{10}(OH)_2 \cdot .89H_2O$

12Å-type minerals

    Sepiolite-Falcondoite series: $Si_{12}(Mg,Ni)_9O_{30}(OH)_6(OH_2)_4\ 6H_2O$

14Å-type minerals

    Clinochlore-Nimite series: $[(Mg,Fe,Ni)_6(SiAl)_8O_{20}(OH)_4](Mg,Al,Ni)_6(OH)_{12}$

    Ni-Vermiculite: $(Mg,Fe,Ni)_6(Si_{8-x}Al_x)O_{20}(OH)_4(Mg,Ca,Ni)_x \cdot yH_2O$

    Ni-Smectite: $(Fe^{3+},Ni)_4(Si_{7.34}Al_{.66})(Ca,Ni)_{.66}O_{20}(OH)_4$

Modified after: Bailey, 1980; Brindley, 1978; Brindley and Maksimovic, 1974; Brindley and Wan, 1975; Faust et al.,1969; Grim, 1968; Montoya and Baur, 1963; Wiewiora et al., 1982; Zeissink, 1969.

Yugoslavia to be 10Å, mostly non-swelling, hydrous layered minerals forming a series of solid solutions with beta-kerolite as the magnesian and pimelite as the nickeliferous end members. In another study of kerolites from Goles Mountain and other localities, Brindley et al. (1977) emphasize the chemical and structural similarity to talc but note that secondary differences arise from extreme layer-stacking disorder. Additional work by Brindley et al. (1979) defines kerolite-pimelite as a series of hydrous magnesium-nickel silicates with talc-like structure and composition but with additional water and with a highly disordered and non-swelling stacking of layers. Using this revised classification, Wiewiora et al. (1982) include nickel-bearing talc-like minerals from Szklary, Poland in the kerolite-pimelite series.

As for divisions between end members within the above three series, Brindley and Maksimovic (1974) suggest a ratio of Ni/(Ni+Mg) such as twenty percent, taking into account the common relatively small proportion of Ni as compared to Mg in naturally occurring Ni-Mg hydrous silicate minerals.

Other 7Å and 10Å type mixtures:

Other mixtures of talc-like and serpentine-like compo-nents have been described as deweylites. Speakman and Majumdar (1971, p. 225) found deweylites to be mixtures of poorly crystallized talc and serpentine wherein "nickel is not an essential constituent, but it greatly assists the

development of the talc-like and serpentine-like phases from the intermediate material ". From their description, it would appear that at least some garnierites could be referred to as Ni-bearing deweylites (Speakman and Majumdar, 1971). The character of deweylite, with or without nickel in its composition, as an intimate mixture of a hydrous highly dis-ordered form of talc and a poorly crystalline hydrous serpen-tine mineral resembling a disordered chrysotile, is furtherly pointed out by Bish and Brindley (1978) who also suggest that this name be retained as a field term for mixtures of poorly crystalline hydrous magnesium silicates of variable compo-sition and mineralogy.

Sepiolite:

A nickel-bearing sepiolite from Nickel Mountain, Oregon has been described by Hotz (1964). This sepiolite displayed the typical basal spacing near 12Å, an intermediate degree of crystallinity, and a Ni content of 1.46%. The possibility of having Ni-bearing sepiolite as a relatively common mineral in weathered ultramafic rocks is also indicated by Brindley and Maksimovic (1974).

Vermiculite and smectite:

Ni-bearing vermiculite has been reported from Jacupiranga, Brazil (Felicissimo, 1965, in Brindley and de Souza Santos, 1975). Brindley and de Souza Santos (1975) report Ni-bearing ferric iron montmorillonites from

Nickelandia, Brazil, and differentiate them from nontronites
in that the layer charge for Nickelandia minerals originates
largely in the octahedral sheet.

Ni-bearing compounds at Cerro Matoso

7Å-15Å garnierites:

This garnierite group includes those Ni-bearing com-
pounds characterized by the presence of 7Å and 15Å basal
reflections in their X-ray diffraction patterns. They occur
as a massive product of weathering processes and comprise
the previously defined massive ore which is found principal-
ly in the Upper Saprolite zone and to a lesser extent in the
Lower Saprolite zone.

Several samples of massive ore (numbers 35, 51, 81, 86,
36) were selected for discussion purposes. These samples
represent different depth locations within the nickeliferous
Upper Saprolite level. Variations in mineralogical composi-
tion and relative abundance of Ni-bearing compounds are thus
correlated with degree of weathering in the saprolite zones.
Samples are ordered, according to increasing weathering from
No.35 (slightly to moderately weathered peridotite) to No.36
(completely weathered peridotite). Chemical compositions
and locations of these samples are presented in Table 6.

X-ray diffraction data: X-ray diffraction patterns of
massive ore samples listed in Table 6 are shown in Figure 58.
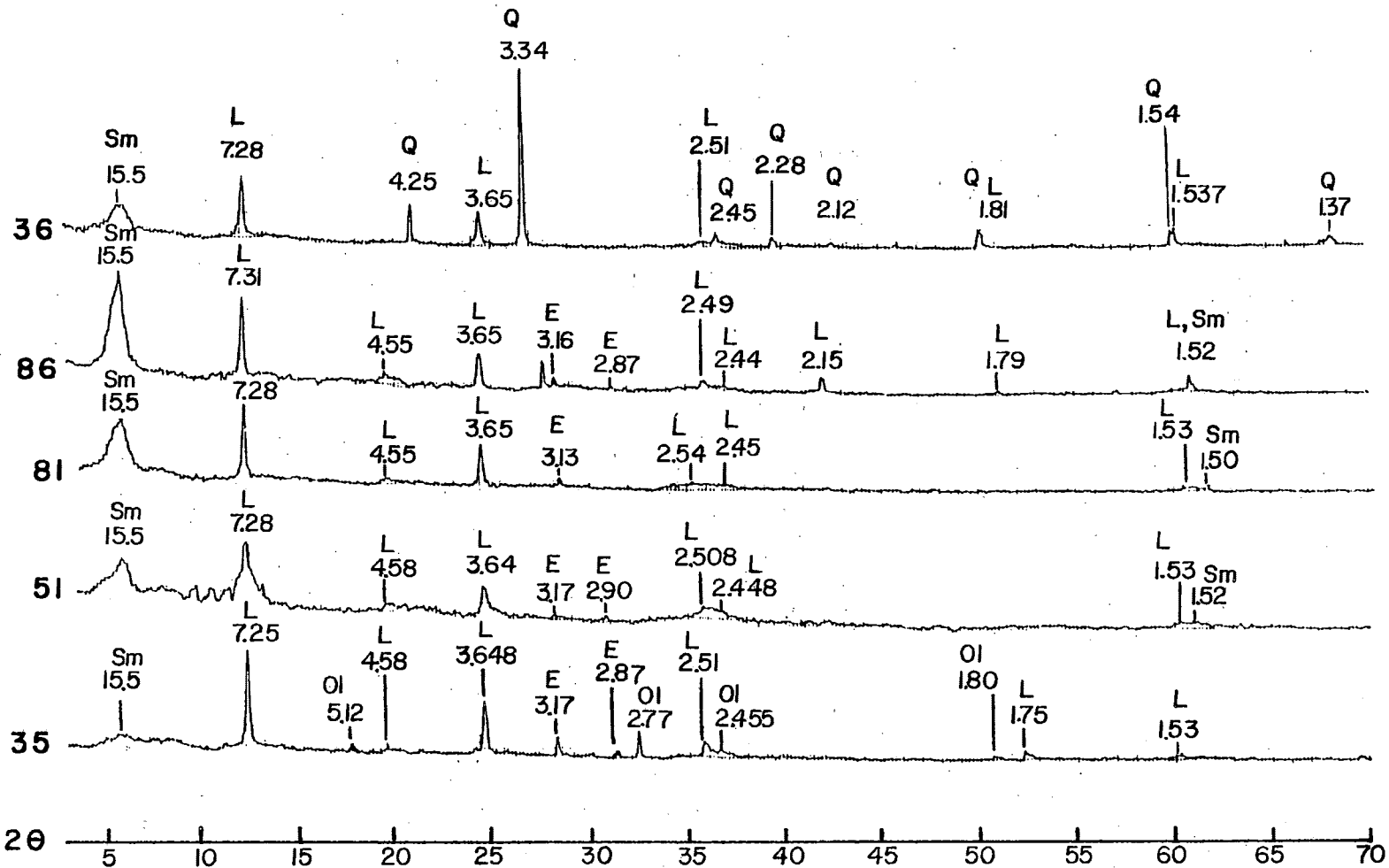
Figure 58. X-ray diffraction patterns for 7Å-15Å garnierites in Upper Saprolite zone. Sm: Smectite L: Lizardite Ol: Olivine E: Enstatite Q: Quartz

The samples are ordered according to their relative positions within the Upper Saprolite zone from bottom (sample 35) to top (sample 36).

7Å and 15Å type components characterize these samples. Ethylene-glycol treatment expands the lattice displacing the 15.5Å reflection to 17.3Å, which indicates the presence of smectite component. Intensity of the smectite reflection ranges from slight in samples towards the base of the Upper Saprolite zone, through moderately strong in middle zone samples, to moderately slight in those towards the top. 7Å reflections are recognizable in all samples. Table 9 presents the main reflections, ordered according to decreasing relative intensities, for the 7Å component as well as examples for lizardites and nepouite from the literature. When comparing the main reflections that have relative intensities over 20% for the 7Å component in massive ore samples with those corresponding to the reference minerals lizardite and nepouite, a striking resemblance is present between the 7Å component in massive ore and lizardite. When considering relative intensities over 30% as suggested by Berry (1974), the similarity is even greater. These observations indicate that a lizardite-type component has been preserved for the most part through the Upper Saprolite zone.

When compared to each other, individual sample diffraction patterns have striking differences that relate to relative intensity of weathering (Figure 58). In weakly altered samples (sample 35), lizardite is prominent,

Table 9. Comparison of X-ray diffraction peaks for serpentine component in samples from the Upper Saprolite zone (Table 6) with reference lizardites.

No. 36	7.28^*_{100}	3.65_{54}	1.82_{25}	1.537_{22}	2.51_{10}	4.55_4
No. 86	7.31_{100}	3.65_{45}	1.523_{19}	4.55_{13}	2.49_8	1.79_3
No. 81	7.28_{100}	3.65_{57}	2.49_{10}	4.55_8	1.53_6	
No. 51	7.28_{100}	3.64_{50}	2.508_{22}	4.58_{13}	1.53_{12}	
No. 35	7.25_{100}	3.648_{55}	2.51_{16}	4.58_5	1.53_4	
(1)	7.30_{100}	3.65_{90}	2.493_{50}	1.53_{35}	4.55_{30}	
(2)	7.28_{100}	3.63_{43}	2.475_{40B}	1.527_{23}	4.57_{20}	
(3)	7.40_{vs}	2.505_{vs}	4.60_s	3.67_s	1.538_s	1.799_m
(4)	7.25_{100}	3.65_{60}	2.499_{35}	1.536_{20}	4.55_{15}	

(1) Nickel-bearing lizardite, Valojoro, Madagascar (Brindley and Wan, 1975)
(2) Nepouite, Ba, Yugoslavia (Maksimovic, 1973)
(3) Lizardite, Kennack Cove, Cornwall, England (Rucklidge and Zussman, 1965)
(4) Nickel-bearing lizardite, New Caledonia (Montoya and Baur, 1963)

* d_I : d(obs., Å) $\quad$ I (relative intensity)

B: band $\quad$ vs: very strong $\quad$ s: strong $\quad$ m: moderate

114

smectite component is minor, and small amounts of olivine and enstatite are still identifiable. With increasing alteration (sample 51), smectite is more abundant and it and lizardite are the principal phases. Barely recognizable traces of enstatite may also occur, particularly towards the core of individual blocks. In the upper part of the Upper Saprolite zone, smectite and lizardite are the only components identifiable in X-ray diffraction patterns (sample 81). The uppermost part of the Upper Saprolite zone (sample 36) is characterized by diffraction patterns that indicate a decrease in smectite associated with the appearance of quartz; lizardite remains prominent.

Differential Thermal Analysis: DTA curves for samples from the Upper Saprolite zone (Figure 59) reflect the same mineralogical variations determined by X-ray diffraction analysis. The first endothermic peak, around $100^{\circ}C$, corresponds to loss of hydration of interlayer water in smectite component, and is more pronounced for those samples in which the 15.5Å reflection is better developed (Figure 58). A second small endothermic peak at around $270^{\circ}C$ may correspond to dehydroxylation of cryptocrystalline nickel hydroxide which has also been observed by Trescases (1975) as a minor component in garnierites. The third endothermic peak, at $595\text{-}615^{\circ}C$ is attributed to dehydroxylation of serpentine component present in garnierite materials (Brindley and Pham Thi Hang, 1973; Wiewiora et al., 1982;
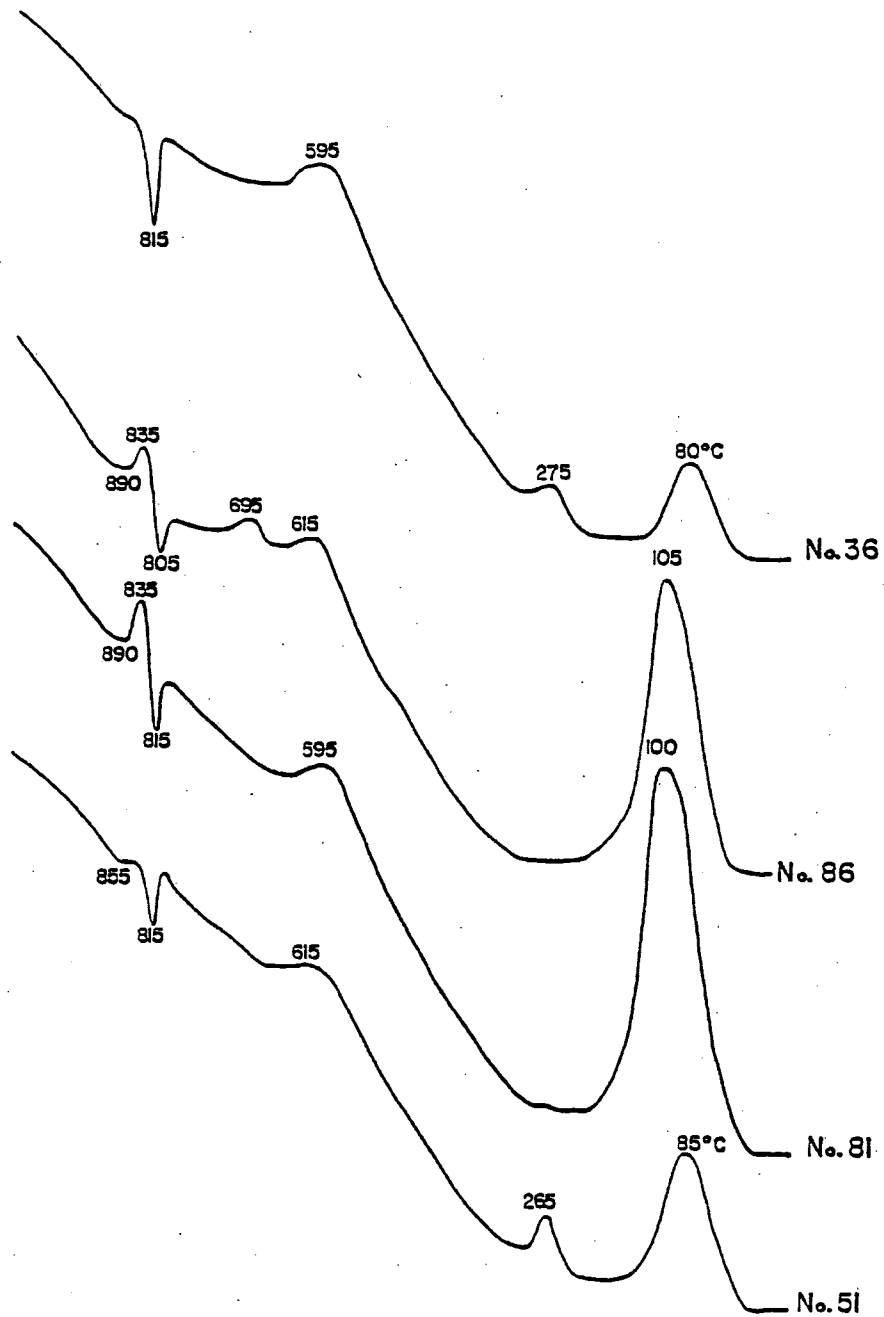
Figure 59. DTA curves for massive ore samples from
the Upper Saprolite zone.

Gerard and Herbillon, 1983), a component that is common throughout the Upper Saprolite zone. A fourth endothermic peak, observed only in sample 86 at about $700^{\circ}C$ (possibly masked in other samples), may reflect lizardite (Faust and Fahey, 1962, Fig. 36). The exothermic peak at $815^{\circ}C$ represents formation of a new mineral phase from lizardite component (Faust and Fahey, 1962), which in low NiO systems is primarily olivine with minor enstatite (Pham Thi Hang and Brindley, 1973). A fifth endothermic peak at around $835^{\circ}C$, followed by an exothermic peak at $855-890^{\circ}C$, correspond to the final dehydroxylation and reconstitution into new phases, respectively, of the smectite component (Sudo and Hayashi, 1959; Takeshi, 1978).

Chemical data: Chemical analyses of the selected samples of the Upper Saprolite zone listed in Table 6 reflect a major variation in the nickel enrichment environment. Changes in parent-rock material characteristics appear to control to a certain extent nickel distribution. Samples 81 and 86 are from equivalent locations within the weathering profile and correspond to completely weathered peridotite. However, there is a basic difference in their occurrence: sample 86 represents weathered peridotite from the strongly serpentinized part of the deposit, whereas sample 81 represents moderately to slightly serpentinized peridotite. Although samples 86 and 81 are mineralogically similar (Figure 58), nickel content in sample 86 (Table 6) is very

different to that in sample 81 and is close to the average nickel content in the peridotite country rock. Nickel content in sample 81 corresponds to ore grade. This difference may be due to the relative degree of serpentinization of the parent ultramafic rock. Strongly serpentinized parent rock may be less permeable than little or moderately serpentinized peridotite (McFarlane, 1983) and, under similar weathering conditions, the latter is more favourable to nickel laterite development (Lelong et al., 1976).

Summary: X-ray diffraction data, DTA, and chemical analyses indicate that the bulk of the ore at Cerro Matoso is principally made up of a mixture of lizardite and smectite components, which is referred to as $7\text{\AA}$–$15\text{\AA}$ garnierite. General similarity in qualitative mineralogical composition between high- and low-Ni samples from the Upper Saprolite zone necessitate that chemical analysis be conducted in order to verify the presence of Ni-rich intervals. Furthermore, it appears that strongly serpentinized zones are not favourable enrichment sites for Ni-rich laterite deposits.

$10\text{\AA}$ garnierites:

This group of Ni-bearing minerals include those specimens in which diffraction patterns showed a dominant diffraction peak centered at about 10.0–$10.3\text{\AA}$. All of the Cerro Matoso samples analyzed in this study show minor

amounts of serpentine group minerals and/or quartz as con-
taminants. This type of ore corresponds to pale- to dark-
green, fine-grained, soft to moderately hard (hardness:
2.0-3.5), massive garnierite which occurs principally as
fracture fillings and to a lesser extent as cavity fillings,
both in the Lower and Upper Saprolite zones. Samples 34V,
34N, and 39 were selected to illustrate the general charac-
teristics of the $10\overset{\circ}{A}$ garnierites. Their locations and
chemical compositions are presented in Table 6.

X-ray diffraction data: Figure 60 shows diffraction
patterns for samples 34V, 34N, and 39 grouped according to
decreasing dominance of the $10\overset{\circ}{A}$ type component. Kerolite-
like material dominates the patterns. The broad [001]
diffraction peak at about $10\overset{\circ}{A}$, as well as the other main
peaks at around 1.52, 2.56, 4.53, 3.21, and $1.32\overset{\circ}{A}$
(decreasing order of relative intensity), agree well with
reference patterns for kerolite (Maksimovic, 1966, Fig. 3;
Brindley et al., 1977, Fig. 1; Brindley et al., 1979, Table
1; Cole and Shaw, 1983, Table 1) and for $10\overset{\circ}{A}$-type garnier-
ites (Brindley and Pham Thi Hang, 1973, Fig. 2). Association
of kerolite with minor amounts of serpentine group component
is not uncommon (Maksimovic, 1966; Brindley et al., 1977;
Wiewiora et al., 1982), and 7.25 and $3.63\overset{\circ}{A}$ peaks (Figure 60)
reflect the presence of serpentine component.

Table 10 compares the observed intensities in sample 34V
to those in a nickeliferous beta-kerolite from Goles
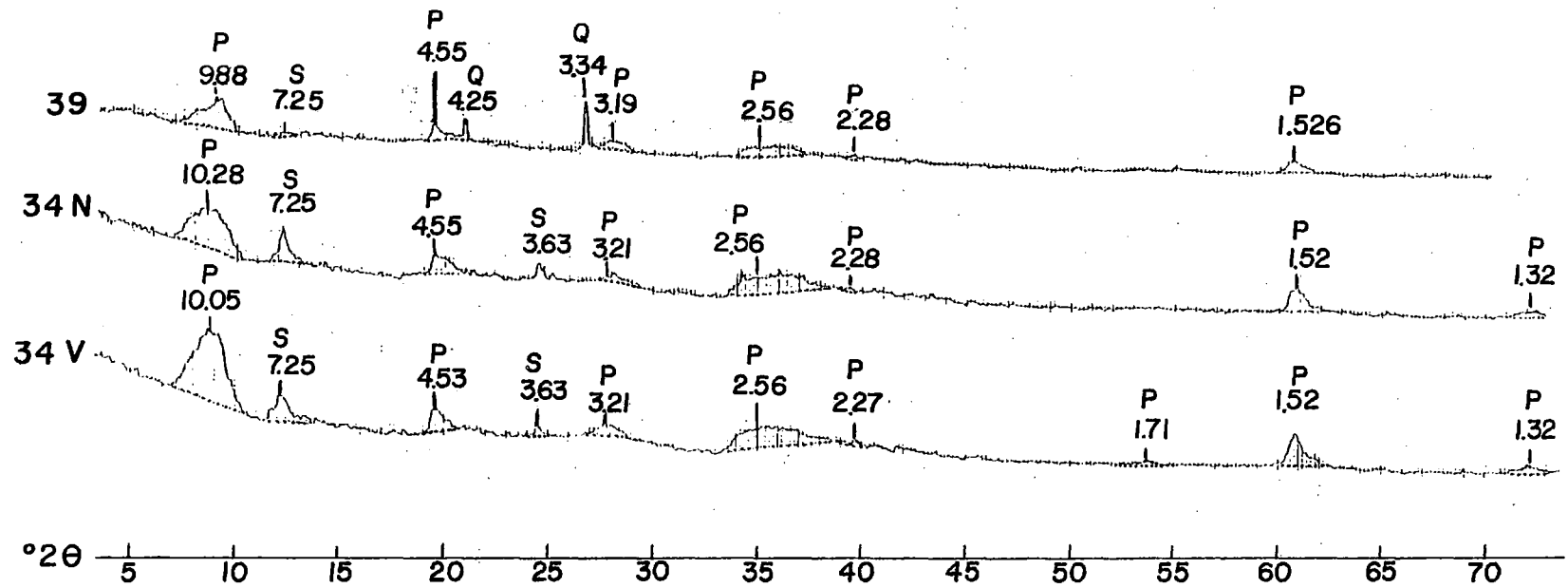
Figure 60. X-ray diffraction patterns for 10Å garnierites.
P: Pimelite   S: Serpentine   Q: Quartz

120

Table 10. X-ray diffraction data and chemical characteristics for sample 34V and a reference nickeliferous beta-kerolite.

34V		B			34V	B
d_{obs}(Å)	I_{obs}	d_{obs}(Å)	I_{obs}			
10.05	100	10.26	100	SiO_2	39.7	48.65
7.25	*	7.35	*	Al_2O_3	0.12	0.26
4.53	38	4.60	60	Fe_2O_3	3.72	0.10
3.63	*	3.66	*	NiO	29.73	17.12
3.21	25	3.25	50	MgO	8.8	18.43
2.56	42	2.57	60	CaO	0.09	0.44
2.27	8	2.29	5	Cr_2O_3	0.03	----
1.71	6	1.737	30	MnO	0.93	----
1.52	56	1.530	90	CoO	0.03	----
1.31	12	1.321	30	H_2O^-	7.74	6.49
				H_2O^+	9.27	8.41
					100.16	99.90

* serpentine component
Sample B: light-green, nickeliferous beta-kerolite, Goles Mountain, Yugoslavia (Maksimovic, 1966, Table I)
No. 34V : Analytical method: XRF; Analyst: R. Bustamante (Cerro Matoso S.A.)

Mountain, Yugoslavia (Maksimovic, 1966, sample B). Although the absolute values do not coincide, the order of decreasing intensity does, as well as the position of the peaks (10.05, 1.52, 2.56, 4.53, 3.21, 1.32, 1.71, 2.27Å). Therefore, based on X-ray diffraction data, this 10Å-type material may be referenced as kerolite.

Differential Thermal Analysis: DTA curves for samples 34V and 39 (Figure 61) show endothermic peaks at about $100^{\circ}C$ and $850^{\circ}C$. A very weak, hardly recognizable, broad endothermic peak at approximately $590^{\circ}C$ is attributed to minor serpentine-type component. The general behaviour exhibited by both samples is similar to that of pimelites from Goles Mountain, Yugoslavia (Maksimovic, 1966, Fig. 1) and Szklary, Poland (Wiewiora et al., 1982, Fig. 10). According to Brindley et al. (1977), adsorbed molecular water and surface hydroxyls (held at surface imperfection sites) are lost up to about $650^{\circ}C$; above $800^{\circ}C$, structure hydroxyls are completely lost and crystalline reorganization to an enstatite product takes place (Brindley et al., 1979).

Chemical data: Chemical composition of sample 34V compares with that of nickeliferous beta-kerolite from Goles Mountain (Table 10), although the Cerro Matoso sample is more enriched in nickel and has lower silica content. Additional nickel may be present in garnierites as cryptocrystalline nickel hydroxide (Trescases, 1975) and, if this
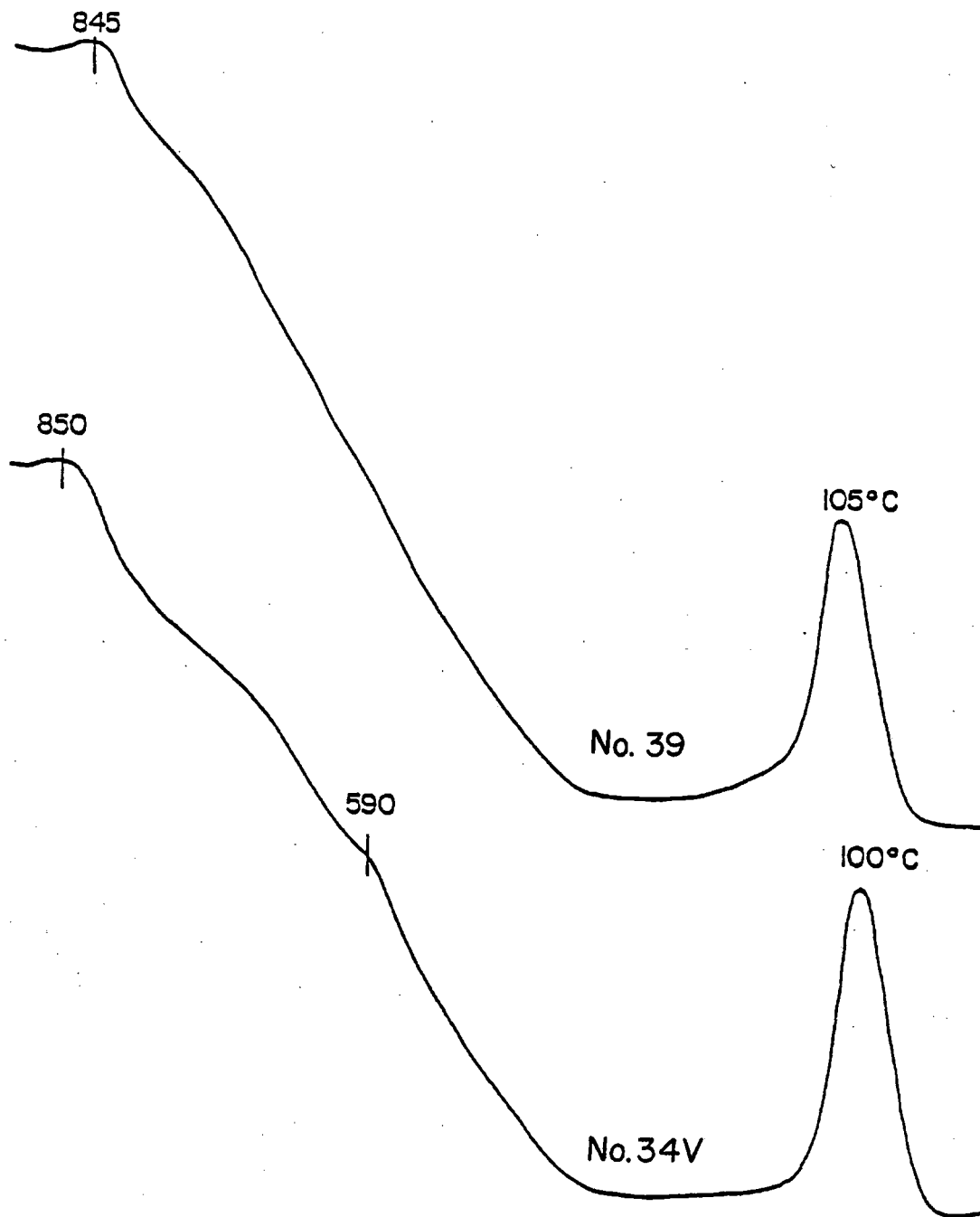
Figure 61. DTA curves for 10Å garnierites.

is the case for sample 34V, it would partly explain the difference in silica content with the beta-kerolite from Goles Mountain. Nickeliferous beta-kerolite is included in the kerolite-pimelite series by Maksimovic (1966). Brindley and Maksimovic (1974) suggest a division within this series at a Ni/(Ni+Mg) atomic ratio such as 20 to 25%. Sample 34V has a Ni/(Ni+Mg) ratio of about 65% which indicates pimelite. However, the Nomenclature Committee of AIPEA (International Association for the Study of Clays) still recommends the usage of pimelite as Ni-analogue of kerolite when Ni is greater than Mg content. For sample 34V, Ni=1.82Mg which further supports the designation of the 10Å component in the Cerro Matoso ore minerals as pimelite.

Ni-rich sepiolite:

Nickel-rich sepiolite at Cerro Matoso occurs in three separate modes: 1) Soft (hardness less than 2.5), fine-grained, greenish-gray sepiolite in fault breccia zones; elongated accumulations as much as 30 cm thick and 2 m long follow fault plane surfaces between fault breccia and peridotite country rock (e.g. sample 48); 2) Very soft, somewhat greasy, brownish-white, fine-grained sepiolite occurring in veins (1-2 cm thick) in the Upper Saprolite zone within moderately to strongly weathered peridotite in which original texture is destroyed (e.g. sample 80); 3) Soft, spongy, low density, light green-white, very fine-grained sepiolite crack fillings (5-7 cm wide) occurring

near the base of the Upper Saprolite zone in moderately weathered peridotite (e.g. sample 66).

X-ray diffraction data: Figure 62 shows diffraction patterns for selected samples corresponding to the three types of Ni-rich sepiolite occurrences. The main reflection at about 12.28$\overset{o}{A}$ is attributed to sepiolite, and is best developed in samples from fault breccia zones (sample 48). Sepiolite from veins in the Upper Saprolite zone (sample 80) also contains quartz as a minor component (weak reflection at 3.34$\overset{o}{A}$). Minor amounts of other components present in sepiolite from crack fillings in the Upper Saprolite zone (sample 66) probably are smectite, talc, and serpentine admixtures represented by weak reflections at about 15.5, 10.0, and 7.2$\overset{o}{A}$, respectively.

The main reflections for the best Cerro Matoso sepiolite sample (No. 48), are shown in Table 11 along with data for sepiolite from Oregon, Utah and Asia. Reflections for sample 48 conform with a pattern for sepiolite with a moderate degree of crystallinity. Sepiolites commonly are poorly crystalline in character (Brindley, 1959).

Differential Thermal Analysis: Differential thermal analysis may be particularly useful in the identification of sepiolites (Caillere, 1951). DTA curves (Figure 63) for samples 66 (poorly crystalline) and 48 (moderately crys-talline) exhibit peaks similar to those of sepiolites
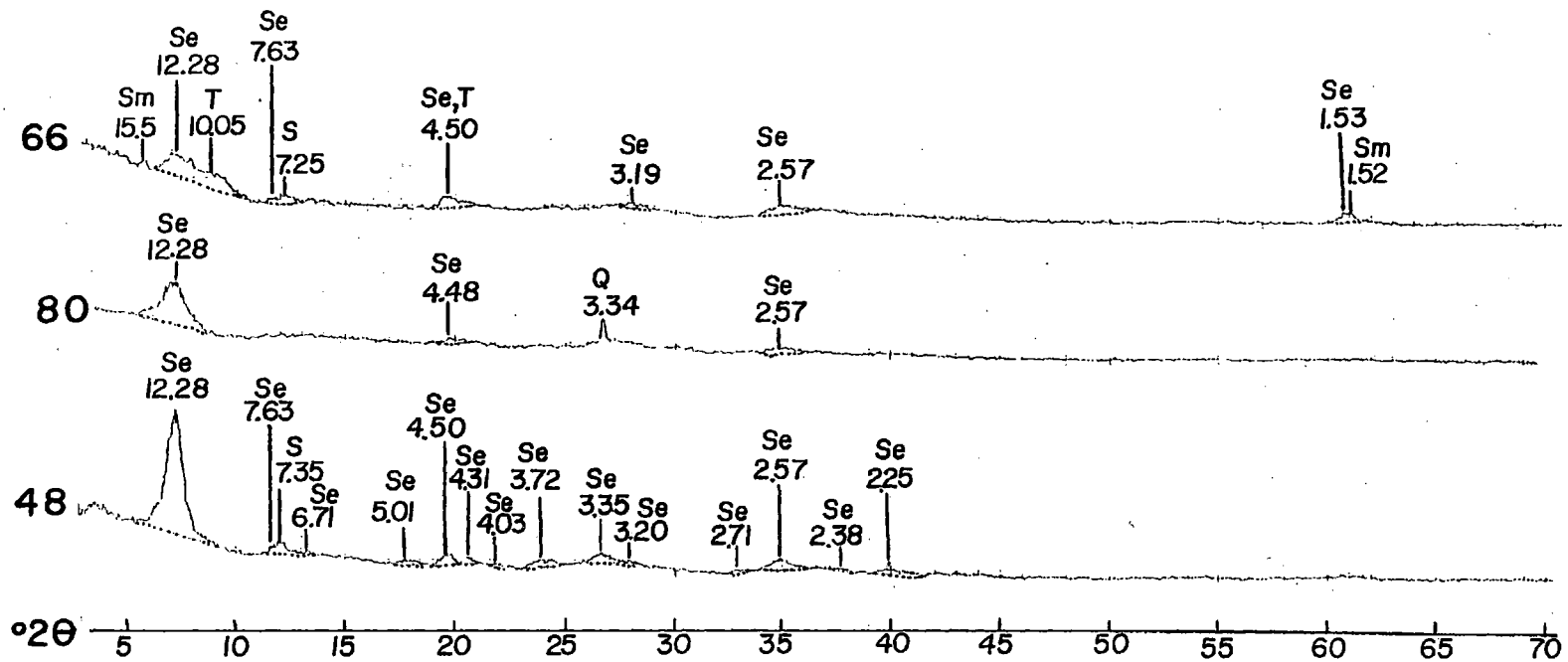
Figure 62. X-ray diffraction patterns for nickel-bearing sepiolites.
Se: Sepiolite S: Serpentine Sm: Smectite T: Talc-like Q: Quartz

126

Table 11.   X-ray diffraction data for sepiolites.

Sample No.48		(1)		(2)		(3)	
d_{obs}(Å)	I_{obs}	d_{obs}(Å)	I_{obs}	d_{obs}(Å)	I_{obs}	d_{obs}(Å)	I_{obs}
12.18	100	12.30	60	12.05	100	12.30	vs
7.63	5	7.6	5			7.58	m
7.38	*			7.47	10		
6.71	5			6.73	5	6.61	w
5.01	3	4.9	6B	5.01	7	5.04	w
4.50	10	4.5 ⎤		4.498	25	4.53	m
		⎟ 20nR					
4.31	8	4.3 ⎦		4.306	40	4.26	m
4.03	3			4.022	7		
3.72	7	3.746	20B	3.753	30	3.74	m
				3.533	12		
		3.49	5				
3.35	12	3.34 ⎤		3.366	30	3.35	m
3.20	4	⎟ 20B,nR		3.196	35		
		2.98 ⎦		2.932	4		
				2.771	4		
		2.67 ⎤		2.691	20		
		⎟		2.617	30		
		⎟ 40B,nR					
2.57	13	⎟		2.56	55	2.58	m
		2.49 ⎦		2.479	5	2.46	m
		2.43 ⎤		2.449	25	2.44	m
		⎟ 10nR		2.406	15		
		2.36 ⎦					
2.25	5	2.24	20B	2.263	30	2.28	m
				2.206	3		
				2.125	7	2.13	wB
		2.08	6B	2.069	20	2.06	w
				2.033	4	2.03	w

(1) Sepiolite from Eski Chehir, Asia Minor (Brindley, 1959)
(2) Sepiolite from Little Cottonwood, Utah (Brindley, 1959)
(3) Fibrous sepiolite, Nickel Mountain, Oregon (Hotz, 1964)
 *   serpentine admixture   ]: Band
vs: very strong m: medium w: weak
 B: broad   nR: not resolved
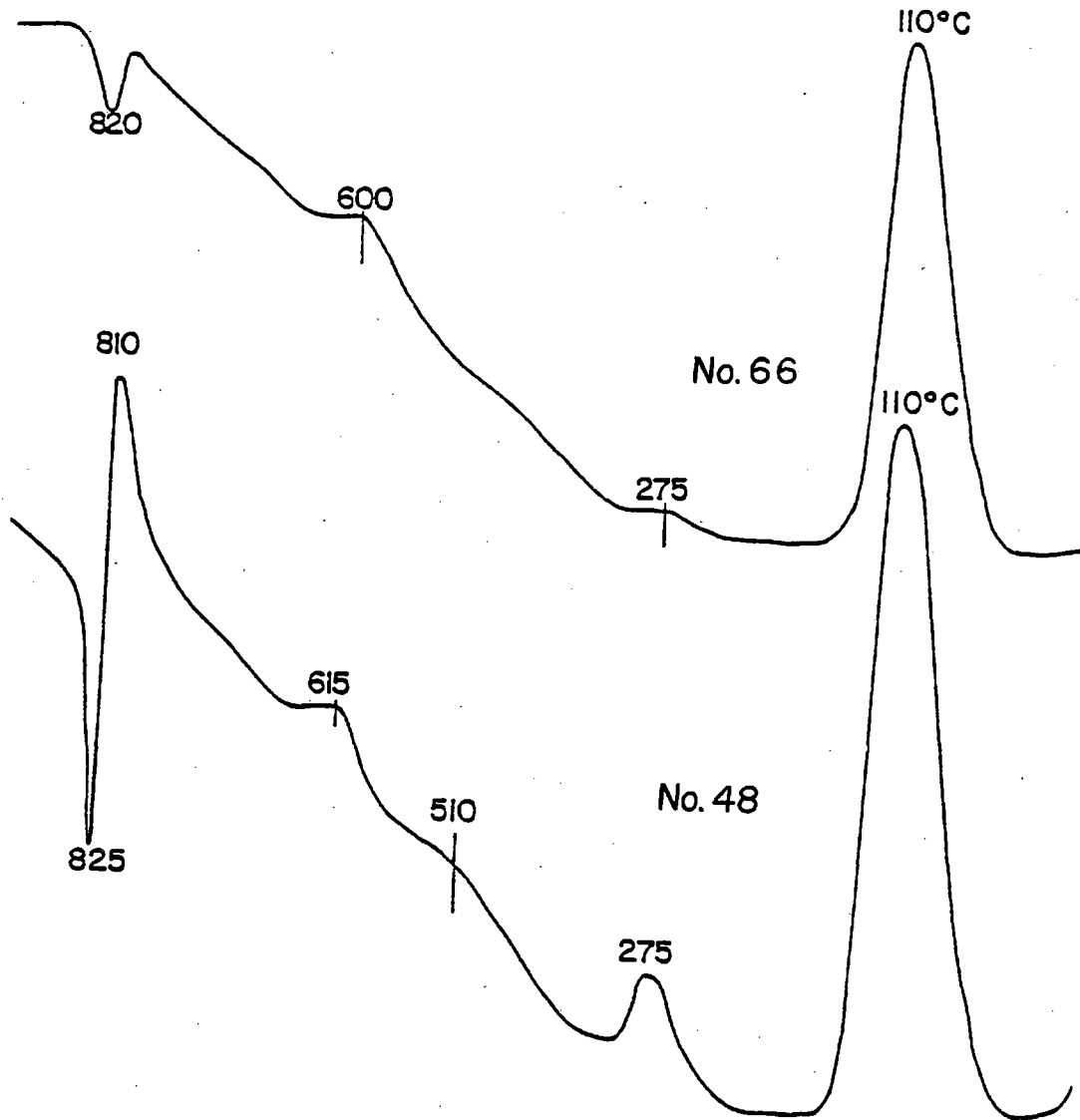
Figure 63. DTA curves for nickel-bearing sepiolites.

described in the literature (Grim, 1968, Fig. 9.13; Papke, 1972, Fig. 4; Rautureau and Caillere, 1974, Fig. 2; Kuhnel et al., 1978, Table 8).

Utilizing electron microscope diffraction and infrared studies, Rautureau and Mifsud (1977) define water losses in sepiolite, losses which also are reflected in DTA peaks. Zeolitic water (water present in the structural channels) is lost up to about $200^{\circ}C$ and corresponds with the first endothermic peak in DTA curves. Loss of crystallization water (surface-adsorbed water) occurs in two distinct stages at about $300^{\circ}C$ and $500^{\circ}C$, and is represented by the well-resolved endothermic peak at $275^{\circ}C$ and the weak, broad, endothermic peak at $510^{\circ}C$. From $510^{\circ}C$ to $810^{\circ}C$, dehydroxylation takes place, particularly at about $615^{\circ}C$. Dehydroxylation culminates sharply at around $825^{\circ}C$, corresponding to crystalline reorganization to form enstatite.

Chemical data: Table 6 indicates that both moderately and poorly crystalline sepiolites from Cerro Matoso have relatively high nickel content. A molecular ratio value for SiO_2/MgO may be used to confirm sepiolite, particularly for the relatively pure sample 48. Sepiolites are characterized by a SiO_2/MgO of 1.21-1.80, with a mean ratio of 1.50 (Caillere, 1951). If magnesium has not been replaced by nickel in the sepiolite structure, the ratio SiO_2/MgO for sample 48 is 1.53. If nickel is substituting for magnesium, a molecular ratio $SiO_2/(MgO+NiO)$ of 1.26 is obtained.

Both values fall within Caillere's suggested interval for sepiolites.

Ni-bearing chlorites:

Admixtures dominated by chlorite occur along shear zones and towards the base of the Upper Saprolite zone in two distinct modes: 1) Bright green, flaky aggregates of chloritic material, with individual flakes as much as 7 mm in longest dimension; local lens-shaped pockets as much as 20 cm wide and 1-2 m long. The highest nickel enrichment for chlorite was observed in such a pocket (sample 98); 2) Light-green to light-gray, somewhat greasy, massive schistose chlorite (sample 96) with lower nickel content than that in the flaky aggregates.

X-ray diffraction data: X-ray diffraction patterns for the two types of nickel-bearing chlorites (samples 98 and 96, Figure 64) indicate a chlorite-type component as an abundant phase. An ethylene-glycol test did not show lattice expansion thus verifying chlorite-type component. Minor amounts of serpentine are intermixed with flaky chlorite (sample 98), whereas massive schistose chlorite (sample 96) has minor talc admixture.

Table 12 compares X-ray diffraction data for samples 98 and 96 and the original nimite described from Barberton, South Africa (de Waal, 1970a). Similarity is apparent for both the position of the first basal reflections and their
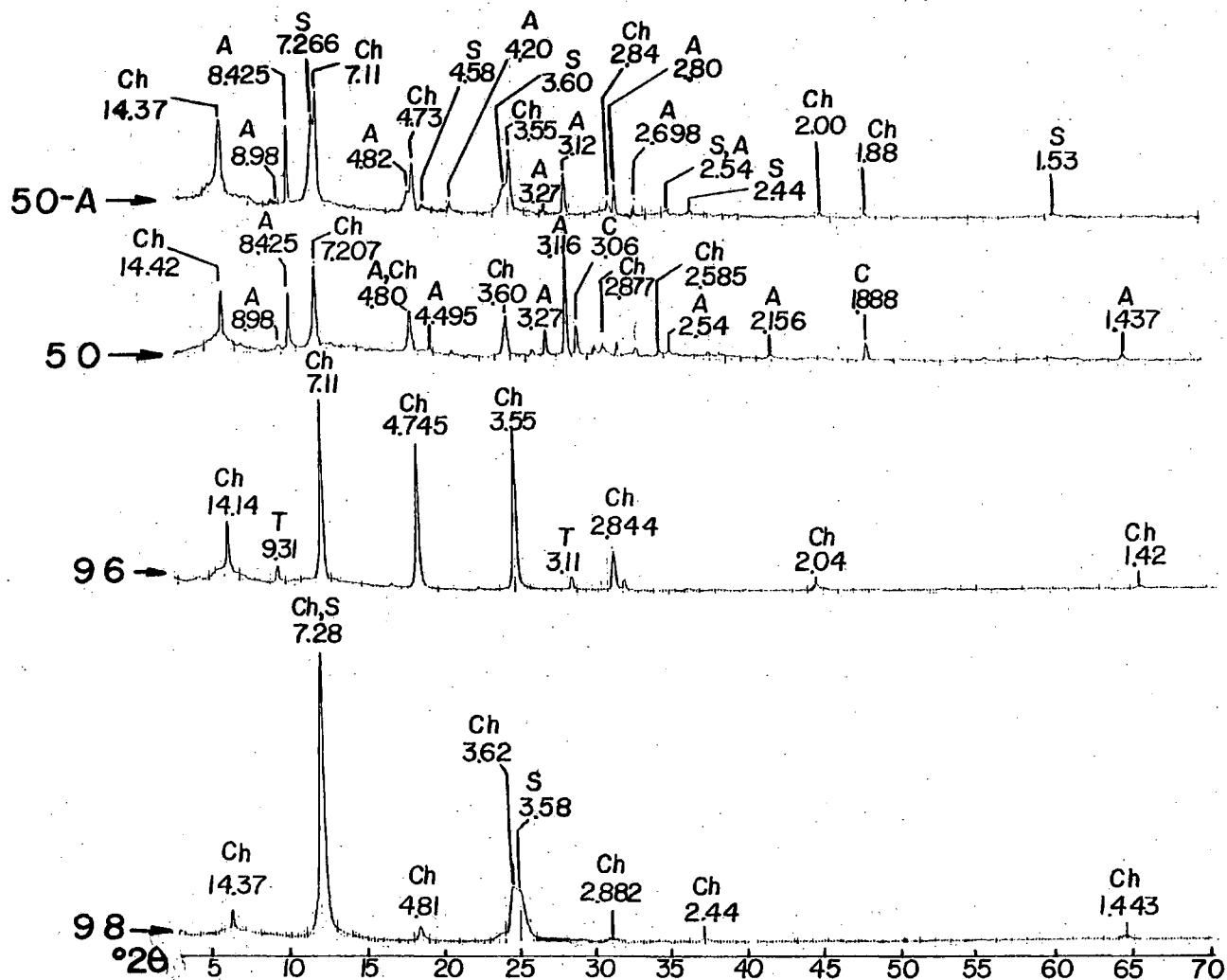
Figure 64. X-ray diffraction patterns for nickel-bearing chlorites.
Ch: Chlorite   S: Serpentine   T: Talc   A: Amphibole   C: Calcite

Table 12. X-ray diffraction data for nickel-rich chlorites.

Sample No.96		Sample No.98		Nimite[1]	
d_{obs} (Å)	I_{obs}	d_{obs} (Å)	I_{obs}	d_{obs} (Å)	I_{obs}
14.14	30	14.37	8	14.2	25
9.31	**				
7.11	100	7.28	100	7.10	100
4.745	80	4.81	5	4.74	16
				4.60	1
3.55	90	3.62	20	3.55	45
		3.58	*		
3.11	**				
2.844	20	2.882	1B	2.841	7
				2.644	1
				2.582	3
				2.540	2
2.48	**				
		2.44	1B	2.438	2
				2.379	2
				2.258	2
				2.062	<1
				2.028	1
				2.003	3
				1.8827	1
				1.8253	<1
				1.6620	1
				1.5661	2
				1.5349	2
				1.5012	1
		1.443	1B	1.4188	1B
				1.4101	1B
				1.3948	1
				1.3190	1B
				1.3001	<1
				1.2901	1
				1.2179	1B
				1.1821	1B

(1) De Waal (1970a)
* minor serpentine admixture   ** minor talc admixture

relative decreasing intensity. The abrupt change in relative intensity between the 7.28Å and the other peaks for sample 98 as compared to nimite, may have to do with the presence of minor amount of serpentine-type component in sample 98 which may be reinforcing the intensity at 7.28Å. A clearly visible peak at 3.58Å that may be attributed to serpentine component supports the above observation.

Although in the same sequential order, the first basal reflections for sample 98 appear somewhat displaced towards lower 2θ angle values. This displacement may reflect a certain degree of structural degradation. A degraded chlorite structure has losened layers and produces an X-ray diffraction pattern with a limited number of peaks (Lucas, 1962). Only four peaks are distinctly resolved on the sample 98 pattern and a slightly less compact stacking of the unit structure may be reflected in displacement of the spacings towards higher values.

The effective Ni^{2+} ionic radius also appear to be significant in this structural transformation. Six-fold coordinated Ni^{2+} and Mg^{2+} have effective ionic radii of 0.700 and 0.720Å respectively (Shannon and Prewitt, 1969), which gives a net difference of 0.02Å which is close to the value 0.03Å obtained from the values 0.77 and 0.80Å proposed by Whittaker and Muntus (1970). Based upon experimental work on silicates, White et al. (1971) observed contraction of the structure in pyroxenes when large amounts of Ni^{2+} substituted for Mg^{2+}. Chemical composition of sample 98

(Table 6) suggests the possibility of a high degree of
nickel substituting for magnesium in the chlorite structure.
If this substitution brought about structural contraction of
the chlorite, it could at least partly attenuate the other-
wise contrary effect, that is, structural expansion due to
degradation. Therefore, the net effect could have been a
slight structural expansion reflected in the displacement of
the first basal spacings towards higher values.

Differential Thermal Analysis: Differential thermal
analysis of sample 98 strongly indicates the presence of
chlorite. The ethylene-glycol test ruled out the presence
of smectite, but the X-ray diffraction peak at 14.37Å may
be attributed either to chlorite- or vermiculite-type
component. Four endothermic peaks and one exothermic peak
characterize the DTA curve (Figure 65), and are classified
according to their relative intensities as strong (610°C),
moderate to weak (90°C), and weak (690, 820, 870°C).

Some characteristics may differentiate vermiculites
from chlorites in DTA curves (Walker, 1951, Fig. VII, 2, A;
Grim, 1953, Fig. 75, D, E). Molecular water is present in
the interlayer space of vermiculites as "unbound" or free
water and also as magnesium-bound water molecules. Ver-
miculites show a strongly intense endothermic reaction at
about 153°C, manifested in many cases as a doublet, which
corresponds to the release not only of all "unbound" water
but also of part of the magnesium-bound water that is
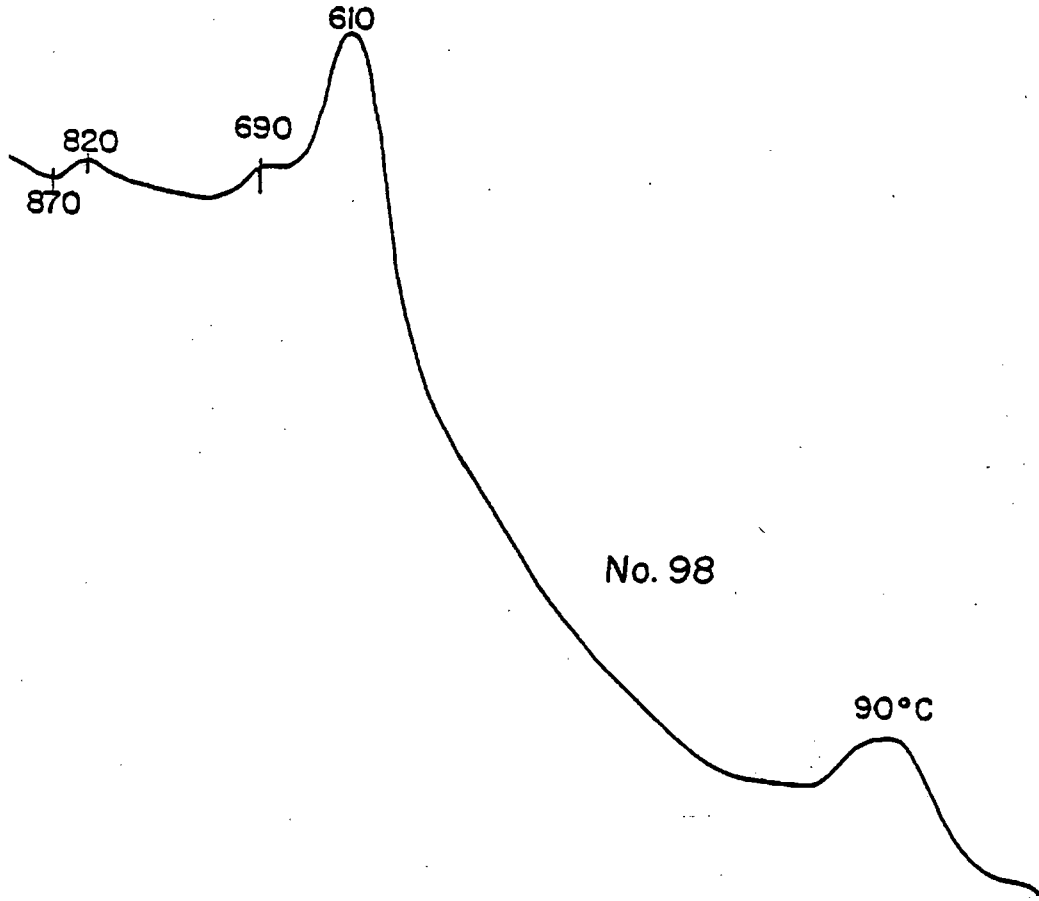
Figure 65. DTA curve for nickel-bearing chlorite.

present in the interlayer space (Walker, 1951). The endo-thermic reaction at 272^OC represents the release of the remaining magnesium-bound water from the interlayer space. At about 850^OC the hydroxyl groups are removed (endothermic reaction) and recrystallization to enstatite (exothermic reaction) takes place at about 882^OC.

It is apparent that the thermal behaviour of sample 98 does not correspond to that of vermiculite, particularly through the temperature interval 25 to 800^OC. Below 500^OC, neither the first strong doublet nor the endothermic reaction peak at about 272^OC are present; only a single, moderate to low intensity, endothermic peak occurs at about 100^OC. From 500 to 800^OC, the strong endothermic peak at 610^OC, and the weak endothermic peak at 690^OC are not characteristic of vermiculite thermal decomposition.

The thermal curve for sample 98 (Figure 65) shows a dominant chlorite component which apparently is associated with minor amounts of serpentine-type component. Thermal curves for chlorites may exhibit a weak endothermic reaction around 100^OC caused by expulsion of small amounts of inter-layer water, and all chlorites show a strong endothermic reaction around 600^OC followed, in most, by a less intense endothermic reaction at about 800^OC and an exothermic reaction around 850^OC (Walker, 1951; Grim, 1953). Hydroxyl water is driven off in two stages corresponding to the endo-thermic peaks around 600^OC and 800^OC (Brindley and Ali, 1950; Grim, 1953; Lucas, 1962), and an olivine- and/or spinel-type

structure is formed after the exothermic reaction around 850°C is completed. This overall thermal behaviour for chlorites has been confirmed by X-ray diffraction work (Brindley and Chang, 1974). A serpentine-type component probably is responsible for the weak to very weak endothermic reaction at 690°C, and may contribute at least in part to the first endothermic reaction at around 100°C (Faust and Fahey, 1962).

A thermal study of penninite-clinochlore-sheridanite by Brindley and Ali (1950) differentiates the chlorites in this series according to the temperature of disappearance of chlorite structure and the temperature at which olivine is first clearly visible in X-ray diffractograms (or films). Comparison of data presented in Table 13 (see also Lucas, 1962, p. 147) with the thermal behaviour of sample 98 (Figure 65) suggests that this sample has a clinochlore structure.

Chemical data: Chemical analyses for samples 96 and 98 shown in Table 6 indicate ore grade for these two chlorites, that is Ni content greater than 1.5%. Both chlorites have a trioctahedral character reflected by the relatively high (Ni+Mg) content as compared to Al. The AIPEA Nomenclature Committee recommends that trioctahedral chlorites be named according to the dominant divalent octahedral cation present, for example clinochlore for Mg-dominant and nimite for Ni-dominant (Bailey, 1980). Dominance of Mg over Ni for the chlorite component in sample 96 (MgO=19.60% vs. NiO=2.8%,

Table 13. Comparison of thermal changes in chlorites in the Penninite-Clinochlore-Sheridanite series (after Brindley and Ali, 1950).

	Penninite	Clinochlore	Sheridanite
Range of temperature in which modified chlorite structure occurs	600–700°C	600–760°C	600–800°C
Temperature of disappearance of chlorite structure when powdered minerals are heated	760°C	800°C	850–900°C
Temperature at which olivine is first clearly visible in diffractograms or X-ray films	800°C	850°C	950°C

Table 6) indicates that this component is a clinochlore-type material. The chlorite component in sample 98 is Ni-dominant (NiO=32.7% vs MgO=9.20%, Table 6) thus should be called nimite.

Other Ni-bearing chloritic mixtures:

Nickel-bearing mixtures of chlorite with associated serpentine and amphibole-type minerals occur along shear zones in slightly weathered peridotite. Light-green to grayish-green, moderately hard (hardness: 3-3.5) material that fractures into splinters characterizes this occurrence.

X-ray diffraction data: Varying proportions of chlorite, serpentine, amphibole-type component and minor calcite, were observed in X-ray diffraction patterns of selected samples (50 and 50-A, Figure 64). X-ray reflections for chlorite indicate the presence of thuringite-type component. The main reflections of the chlorite component in samples 50 and 50-A are compared in Table 14 with those of a reference thuringite from Transvaal, South Africa (Berry, 1974, File 7-78). The position of the characteristic reflections and the relative intensities of the Cerro Matoso samples closely resemble those for the reference thuringite, indicating a similarity in the chlorites.

The presence of a thuringite-type structure may be useful to genetic interpretations. Brown and Bailey (1962) determined the polytype of the Transvaal reference

Table 14. Comparison of X-ray diffraction characteristics for chlorite and serpentine-type components in samples 50 and 50-A, and selected reference minerals; listed according to decreasing intensities.

	Characteristic reflections					
Chlorite:						
(1)	7.07^*_{100}	14.1_{90}	3.54_{60}	4.726_{30}	2.845_{30}	
Sample 50	7.207_{100}	14.42_{67}	3.60_{48}	4.80_{35}	2.877_{10}	
Sample 50-A	7.11_{100}	14.37_{65}	3.55_{55}	4.73_{43}	2.84_{7}	
Serpentine:						
(2)	7.30_{100}	3.65_{90}	2.493_{50}	1.53_{35}	4.55_{30}	2.442_{15}
Sample 50-A	7.266_{100}	3.60_{31}	2.54_{5}	1.53_{4}	4.58_{4}	2.44_{4}

$*$ d_I, with $d = d_{obs}$ (Å) and $I = I_{obs}$

(1) Thuringite, IIb polytype, Limpopo, Transvaal, South Africa (Brown and Bailey, 1962; Berry, 1974, File 7-78)

(2) Ni-bearing lizardite, Valojoro, Madagascar (Brindley and Wan, 1975)

thuringite as IIb, which corresponds to a stacking polytype based on a monoclinic cell (Hayes, 1970). The IIb chlorite polytype has been observed in igneous and metamorphic rocks (Brown and Bailey, 1962), and also can form authigenically at temperatures approaching those of low-grade metamorphism (Hayes, 1970). Thus, if the chlorite in samples 50 and 50-A is IIb polytype as suggested by the close resemblance with the Transvaal reference thuringite, it could not have been formed by weathering processes. Occurrence of these thuringitic samples along shear zones in peridotite, and their association with serpentine and amphibole-type material, suggests the possibility of metamorphic origin for their chlorite component.

Serpentine reflections from sample 50-A along with those for a Ni-bearing lizardite from Valojoro, Madagascar, studied by Brindley and Wan (1975) are shown in Table 14. The similarity of the serpentine component in sample 50-A to the reference Ni-bearing lizardite is apparent.

Two high intensity peaks, namely 3.116$\overset{\circ}{A}$ and 8.425$\overset{\circ}{A}$ reflections in samples 50 and 50-A appear to reflect clinoamphibole. Table 15 presents the four strongest reflections and the largest spacing in the diffraction pattern for several clinoamphiboles described in the literature (Berry, 1974, Files 13-437, 19-1061, 20-481, 20-656, 23-665) and the suspected clinoamphibole. The unknown in sample 50-A approaches the X-ray diffraction behaviour of either magnesio-riebeckite or tremolite,

Table 15. Comparison of X-ray diffraction characteristics for clinoamphibole-type component in samples 50 and 50-A, and selected standard minerals.

	Strongest reflections				Largest spacing
Hornblende (1)	8.40^{*}_{100}	3.10_{70}	3.26_{20}	2.697_{20}	8.96_{6}
Richterite (2)	3.15_{100}	3.28_{50}	8.48_{45}	4.80_{14}	9.01_{6}
Riebeckite (3)	8.40_{100}	3.12_{55}	2.726_{40}	2.801_{18}	9.02_{4}
Magnesio-riebeckite (4)	8.45_{100}	3.12_{90}	2.89_{60}	3.27_{30}	9.03_{8}
Tremolite (5)	8.38_{100}	3.12_{100}	2.705_{90}	3.27_{75}	8.98_{16}
Sample No. 50	3.116_{100}	8.425_{53}	4.80_{40}	3.27_{25}	8.98_{8}
Sample No. 50-A	8.425_{100}	3.12_{55}	2.80_{32}	4.82_{28}	8.98_{4}

* d_I , with $d=d_{obs}$ (Å) and $I=I_{obs}$

(1) Sample from Naustdal, Norway (Berry, 1974, File 20-481)
(2) Synthetic form, 75% Richterite, 25% Tremolite (Berry, 1974, File 23-665)
(3) Sample from Doubrutscha, Rumania (Berry, 1974, File 19-1061)
(4) Sample from Ambatofinandrahana, Torendrika, Madagascar (Berry, 1974 File 20-656)
(5) Sample from St. Gotthard, Switzerland (Berry, 1974, File 13-437)

whereas richterite is suggested for sample 50. Deviations from close similarity between unknown samples and reference materials may in part be related to the preparation procedure for analyses of standard materials which are either mineral separates or individually synthesized compounds. Samples 50 and 50-A appear to be composed of mixed components.

Additional reflections in the X-ray diffraction pattern of Figure 64 indicate that minor calcite is present in sample 50. Reflections at $3.05\overset{\circ}{A}$ and $1.88\overset{\circ}{A}$ agree well with those in the pattern for a synthetic standard reference calcite (Berry, 1974, File 5-586).

Chemical data: Chemical data for samples 50 and 50-A along with generalized structural formulas for mineral species identified by X-ray diffraction are presented in Table 16. Calcium and sodium contents are possibly related to the presence of clinoamphibole (probably calcian richterite) and calcite in sample 50, and to the presence of clinoamphibole (probably magnesio-riebeckite) in sample 50-A. Chlorite, clinoamphibole and serpentine may explain magnesium content in both samples.

Contrasting nickel contents between the two samples may in large part be due to the serpentine component present in sample 50-A. It is apparent that samples 50 and 50-A are enriched in nickel; Ni=0.72% in sample 50 and 1.73% in sample 50-A. Both samples have similar types of silicates (chlorite and clinoamphibole) in their mineralogical

Table 16. Chemical data for shear zone samples 50 and 50-A, and generalized structural formulae, from the literature, for mineral species suggested as principal components in both samples.
Analytical method: XRF; Analyst: R. Bustamante.

	No.50	No.50-A
SiO_2	43.1	43.2
Al_2O_3	8.65	10.05
Fe_2O_3	5.25	6.19
Cr_2O_3	0.32	0.16
NiO	0.92	2.20
MgO	27.20	25.70
MnO	0.06	0.09
CaO	5.09	5.16
Na_2O	2.17	0.84
CoO	0.01	0.03
LOI	7.39[1]	6.46
	100.16	100.08

[1] some CO_2 may be present

Generalized structural formulae
for selected standard minerals:

Calcian Richterite (Berry, 1974, File 23-665):
   $Na_{.75}(Ca_{1.25}Na_{.75})Mg_5Si_8O_{22}(OH)_2$
Magnesioriebeckite (Berry, 1974, File 20-656):
   $(Na,Ca)_2(Mg,Fe^{2+},Fe^{3+})_5Si_8O_{22}(OH)_2$
Thuringite (Berry, 1974, File 7-78):
   $(Mg_{2.8}Fe^{2+}_{.7}Fe^{3+}_{1.4}Al_{1.2})(Si_{2.5}Al_{1.5})O_{10}(OH)_8$
Ni-bearing lizardite (Brindley and Wan, 1975):
   $(Mg_{2.87}Fe^{3+}_{.03}Al_{.02}Ni_{.05})Si_2O_5(OH)_4$
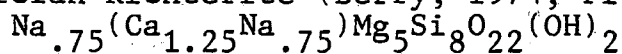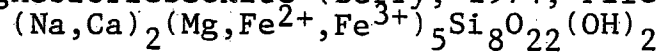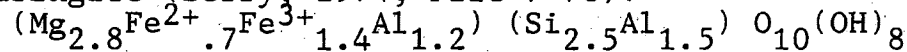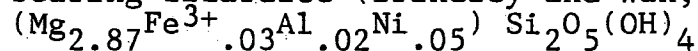
composition except that sample 50-A has additional serpentine component. Serpentines commonly are enriched in nickel derived from the parent olivines and, if this is the case for sample 50-A, it would partly explain the difference in nickel content with sample 50.

GENERAL CHEMISTRY OF THE LATERITE PROFILE

The section 1200 NW, between the coordinates 1572NE and 1707NE (Plate 2) was chosen as representative of the general vertical distribution of Ni, Co, Fe, MgO, SiO_2, Al_2O_3, Cr_2O_3, and Mn in the laterite profile at Cerro Matoso. The laterite at this zone displays near maximum vertical extent (depth to peridotite bedrock is 136 m), and all units recognized in the profile are present (Plate 3).

Figure 66 shows the generalized vertical distribution of chemical components of interest and represents average chemical compositions of equivalent samples from drill holes 1572NE, 1590NE, 1660NE, and 1707NE (line 1200 NW). Because not all components were determined for some samples in original chemical analyses of drill hole samples (Appendix 1), these samples were re-analyzed to provide information about Co, SiO_2, Al_2O_3, Cr_2O_3, and Mn distribution through the entire profile. Analytical results used in the following discussion are shown in Table 17.

Nickel

Nickel is concentrated primarily in the Upper Saprolite zone (generally greater than 3.0%) with lesser concentration in the Lower Saprolite zone (mostly 1.0-3.0%), Limonite
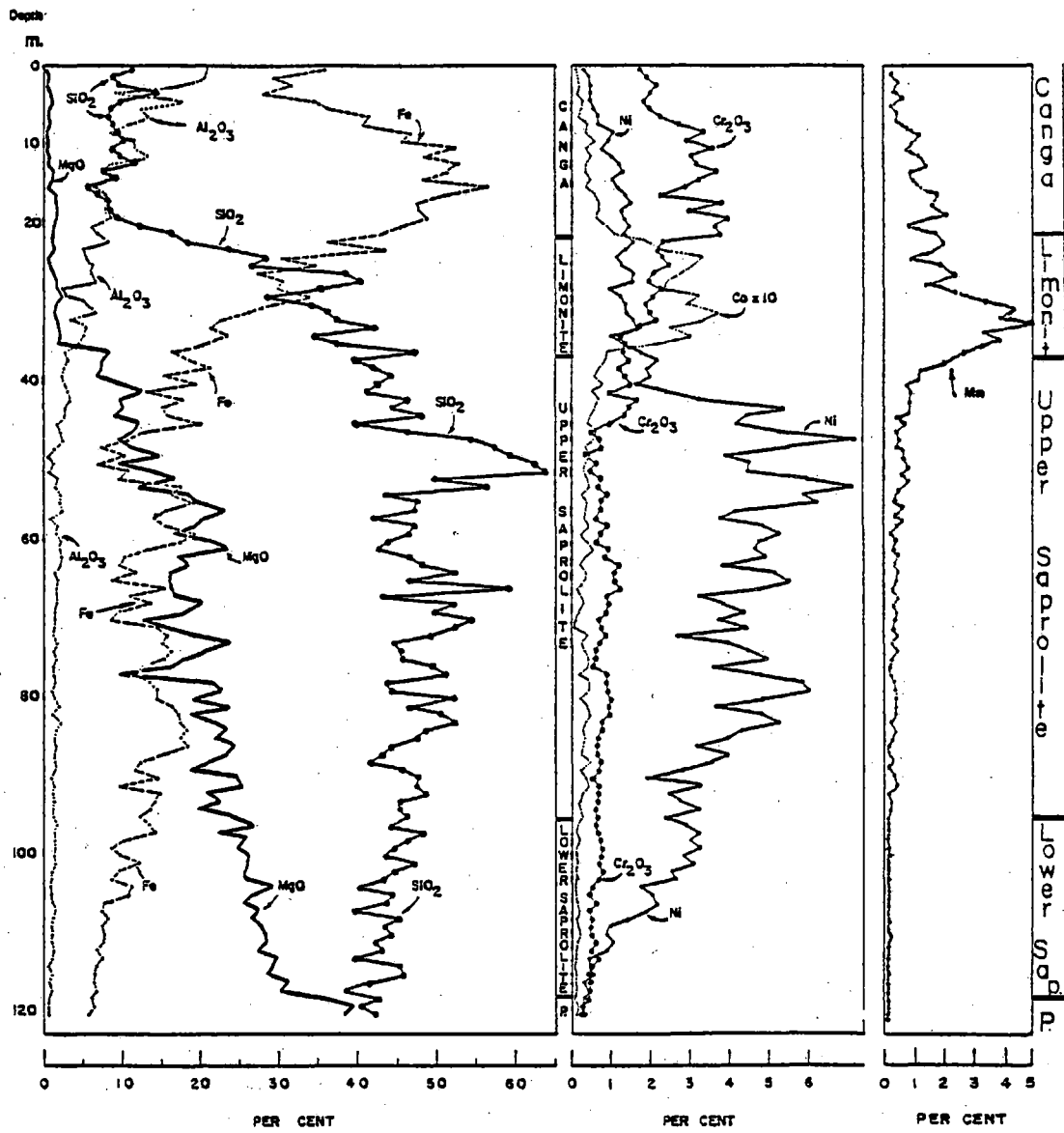
Figure 66. Generalized vertical distribution of selected
            components in the laterite profile.

Table 17.   Chemical composition (Wt%) of a generalized
            laterite profile derived from drill hole samples
            corresponding to the Line 1200 NW   (DDH's
            1572NE, 1590NE, 1660NE, and 1707NE).
            Analytical method: XRF; Analyst: R. Bustamante;
            Fe expressed as total iron.

Depth (m)	Unit	Ni	Co	Fe	MgO	SiO_2	Al_2O_3	Cr_2O_3	Mn
1	C	.26	.011	35.9	.2	11.1	20.84	1.72	.20
2	C	.40	.017	29.3	.7	8.7	20.65	1.87	.31
3	C	.44	.020	31.7	.6	9.5	17.06	2.15	.27
4	C	.46	.019	28.0	.8	14.5	9.04	1.95	.59
5	C	.45	.031	34.5	1.2	9.7	17.48	1.80	.17
6	C	.56	.028	36.4	.8	8.6	12.46	1.97	.42
7	C	.62	.020	41.5	.7	8.4	13.12	2.24	.40
8	C	.68	.041	40.9	.9	8.7	10.68	2.70	.72
9	C	1.02	.036	46.8	.6	9.3	8.60	3.35	1.24
10	C	.91	.057	47.9	.5	10.2	11.36	2.87	.85
11	C	.75	.039	52.3	.6	8.9	11.77	3.55	.67
12	C	1.03	.047	48.6	.9	9.7	13.22	3.03	1.17
13	C	1.19	.038	52.7	.8	11.8	8.83	3.16	1.25
14	C	1.27	.034	51.2	1.2	7.5	7.70	3.65	.88
15	C	1.05	.047	48.4	1.1	9.3	8.47	3.22	.97
16	C	1.17	.036	56.3	.7	5.6	6.29	2.87	1.17
17	C	1.37	.060	51.0	1.5	6.9	7.74	2.25	1.71
18	C	1.48	.067	47.6	1.6	8.1	8.13	3.81	1.55
19	C	1.26	.064	47.7	1.7	8.3	8.88	2.95	2.17
20	C	1.37	.062	48.7	1.7	9.3	8.51	3.95	.88
21	C	1.45	.087	45.4	1.4	12.3	6.14	3.63	1.68
22	C	1.36	.110	43.0	1.2	16.2	6.97	3.75	1.92
23	L	1.55	.192	36.4	1.1	18.4	8.04	2.31	1.41
24	L	1.35	.240	43.2	1.6	23.7	5.15	2.22	.87
25	L	1.17	.330	30.3	.8	28.7	5.65	2.32	1.85
26	L	1.28	.310	34.7	.9	26.6	6.13	2.48	2.39
27	L	1.59	.275	27.5	1.3	38.6	6.08	2.14	1.35
28	L	1.54	.219	30.5	1.7	40.5	6.78	1.98	2.44
29	L	.98	.215	30.0	1.9	35.5	2.62	2.27	3.41
30	L	1.23	.320	33.9	2.2	28.3	3.41	2.05	4.32
31	L	1.37	.287	29.2	1.6	34.1	5.78	1.87	3.83
32	L	1.40	.368	26.1	1.5	36.2	6.64	1.95	4.98
33	L	1.57	.325	22.6	1.8	37.4	3.52	2.17	3.44
34	L	1.66	.253	21.4	2.0	42.2	5.42	1.63	3.88
35	L	1.01	.304	23.2	2.1	34.4	5.06	1.21	2.60
36	L	1.36	.207	20.1	1.9	37.2	4.62	1.36	1.73
37	US	1.75	.093	16.5	8.5	47.4	2.93	1.35	1.09
38	US	2.15	.085	18.7	7.7	39.7	3.11	1.48	1.05
39	US	1.87	.067	20.1	7.4	42.0	2.77	1.21	.87

Table 17 (Cont.)

40	US	1.98	.059	21.2	6.8	44.3	2.51	1.37	.92
41	US	1.65	.078	15.5	9.5	42.7	2.87	1.52	.81
42	US	2.41	.054	19.4	12.4	41.2	3.15	.99	.77
43	US	3.25	.067	13.2	9.7	46.5	3.24	1.65	.43
44	US	5.37	.061	17.7	10.1	44.5	2.99	1.43	.62
45	US	4.43	.049	15.3	8.9	48.2	2.85	1.37	.44
46	US	4.19	.042	15.7	12.2	39.8	1.77	.95	.47
47	US	5.28	.062	20.0	11.5	46.2	2.13	.57	.45
48	US	7.16	.058	13.1	9.8	54.2	2.61	.70	.64
49	US	5.48	.037	10.9	10.8	57.5	1.47	.75	.67
50	US	3.89	.046	7.5	14.9	59.1	.58	.44	.71
51	US	4.50	.039	10.2	9.4	62.6	1.35	.61	.57
52	US	4.44	.034	7.0	13.8	63.9	.78	.45	.65
53	US	6.02	.042	10.8	16.7	49.9	1.81	.75	.48
54	US	7.11	.046	9.9	12.1	56.6	1.67	.67	.32
55	US	5.87	.027	17.5	18.1	43.5	2.25	.89	.54
56	US	6.21	.041	16.6	19.7	47.4	2.17	.74	.43
57	US	4.15	.038	19.2	23.1	47.1	2.55	.78	.54
58	US	3.79	.035	15.8	20.4	42.0	.99	.61	.42
59	US	4.85	.037	14.3	19.3	47.1	1.77	.91	.22
60	US	5.25	.044	15.5	16.7	46.6	1.68	.77	.44
61	US	4.77	.024	19.2	21.4	43.9	2.22	.62	.37
62	US	4.65	.044	17.4	23.5	42.7	2.10	.92	.47
63	US	4.87	.057	13.4	17.1	46.6	2.37	.84	.39
64	US	3.85	.038	10.1	18.3	48.2	2.20	1.21	.40
65	US	5.15	.022	9.8	16.2	52.3	1.50	1.14	.38
66	US	5.49	.039	11.7	16.1	46.3	1.74	1.13	.41
67	US	4.77	.035	8.9	16.2	59.1	1.68	1.25	.46
68	US	3.25	.019	15.2	16.5	43.0	1.67	.87	.38
69	US	3.86	.024	11.3	20.1	52.2	1.73	.92	.41
70	US	4.37	.034	13.4	17.8	49.7	1.46	.84	.39
71	US	3.75	.020	9.9	12.7	54.5	1.49	.67	.37
72	US	4.41	.013	8.7	15.4	52.1	1.35	.77	.44
73	US	2.70	.009	14.4	18.7	49.1	1.36	.85	.27
74	US	3.89	.040	15.8	23.7	44.8	1.80	.67	.35
75	US	4.44	.025	15.4	20.1	45.3	1.32	.60	.28
76	US	4.87	.033	16.2	18.0	45.6	1.77	.61	.27
77	US	3.59	.045	15.4	16.1	49.4	1.34	.55	.33
78	US	4.79	.041	12.8	9.7	51.2	1.51	.87	.42
79	US	5.85	.022	11.9	21.0	43.9	1.61	.84	.44
80	US	6.00	.047	14.3	22.6	44.2	1.10	.88	.47
81	US	4.86	.043	14.7	19.0	52.2	1.53	1.02	.44
82	US	3.70	.025	16.5	23.7	46.4	2.05	.90	.43
83	US	4.79	.041	17.2	18.9	50.8	1.26	.95	.29
84	US	5.23	.048	17.4	21.8	52.5	2.33	.75	.40
85	US	4.34	.039	18.2	23.4	48.4	1.66	.77	.25
86	US	3.90	.032	17.6	21.9	47.8	1.44	.67	.17
87	US	3.21	.038	18.5	24.3	44.3	1.84	.65	.18
88	US	3.87	.033	15.4	23.6	43.2	1.42	.63	.23

Table 17 (Cont.)

89	US	3.57	.027	12.4	20.9	41.8	1.60	.72	.15
90	US	2.85	.051	11.8	18.7	45.6	1.62	.69	.31
91	US	1.90	.025	14.3	24.8	47.7	1.05	.53	.47
92	US	3.25	.039	9.8	25.3	47.8	1.27	.72	.12
93	US	2.47	.044	14.8	20.8	48.9	1.18	.67	.21
94	US	2.75	.032	14.1	22.3	45.4	1.35	.66	.17
95	US	3.21	.024	13.8	19.7	45.3	1.20	.60	.14
96	US	2.37	.026	12.5	24.0	46.2	1.37	.63	.12
97	LS	2.91	.019	13.5	26.8	44.2	1.72	.60	.13
98	LS	3.23	.015	14.1	22.3	48.3	1.43	.65	.09
99	LS	3.02	.021	10.2	25.7	46.3	1.54	.74	.12
100	LS	3.25	.016	8.7	24.8	44.8	1.56	.91	.14
101	LS	2.87	.017	9.9	26.2	43.4	1.42	.87	.11
102	LS	3.13	.018	12.1	26.1	47.4	1.65	.67	.11
103	LS	2.57	.015	9.8	25.9	44.9	1.25	.80	.08
104	LS	2.65	.016	8.9	25.7	43.4	1.17	.72	.10
105	LS	1.77	.011	11.2	29.2	40.1	1.03	.55	.09
106	LS	2.13	.013	10.9	26.7	44.7	1.10	.47	.08
107	LS	2.19	.015	7.8	25.4	43.9	1.33	.61	.09
108	LS	1.87	.021	7.7	27.3	39.5	1.35	.48	.12
109	LS	1.45	.016	8.1	26.5	45.3	1.28	.53	.08
110	LS	.98	.020	7.6	27.4	43.6	1.06	.50	.13
111	LS	.91	.023	7.7	28.2	44.2	1.20	.56	.12
112	LS	1.07	.018	7.7	28.4	42.2	1.10	.61	.14
113	LS	.93	.015	6.9	27.5	43.1	1.38	.51	.07
114	LS	.45	.015	7.4	29.8	39.8	1.15	.67	.08
115	LS	.51	.010	6.8	29.2	45.6	.87	.53	.11
116	LS	.57	.016	6.6	28.7	45.8	1.23	.48	.08
117	LS	.36	.012	6.5	31.2	41.4	.95	.51	.06
118	LS	.42	.016	6.6	30.4	38.5	1.03	.53	.10
119	P	.36	.011	6.3	36.2	42.9	.71	.49	.06
120	P	.32	.020	6.4	39.6	40.5	.80	.28	.09
121	P	.34	.015	5.8	38.3	42.2	.79	.29	.08

C: Canga   L: Limonite zone   US: Upper Saprolite zone
LS: Lower Saprolite zone   P: Peridotite bedrock

zone (1.0-1.5%) and Canga (0.5-1.5%). The highest nickel values correlate with high SiO_2. This nickel distribution is characteristic of silicate-type lateritic nickel ores (Dissanayake, 1982).

Nickel apparently is associated with iron hydroxides and manganese oxides in the Canga and Limonite zones. Part of the nickel released during weathering of peridotite becomes incorporated in goethite where it is present either as adsorbed ions on grains or substituted in lattice sites (Trescases, 1975; Kuhnel et al., 1978; Schellmann, 1978; Maynard, 1983). In addition, stringers and pockets of Mn oxides occurring from the middle to the lower part of the Limonite zone contain nickel values of as much as 1.8% (Table 3). Such an association also has been observed in profiles at other nickel laterite deposits (Golightly, 1979a; 1981).

Nickel abundance in the saprolite zone is probably chiefly the result of supergene enrichment processes. Nickel is relatively mobile under oxidizing acidic conditions, but mobility decreases substantially in alkaline conditions (Levinson, 1980). As weathering proceeds and bases are leached from the upper part of the profile, the environment there becomes relatively less alkaline, pH decreases (Trescases, 1975), and nickel mobilization is progressively favoured. When downward percolating solutions reach a horizon where more abundant magnesia and silica are available and alkalinity is increased, nickel becomes relatively

immobilized and is redeposited in the hydrous silicates that form in the saprolite zone. Ni particularly substitutes for Mg in the octahedral layer of smectites where it becomes strongly stabilized as demonstrated experimentally by Decarreau (1981). As the weathering front moves progressively downward, and the process of nickel mobilization from upper levels of the profile and deposition at lower levels is successively repeated, the net result is a cumulative buildup of the nickel content in the saprolite zone (McFarlane, 1983). Part of the nickel in the saprolite zone occurs as garnierite accumulations filling fractures and cavities. These accumulations contribute to the general trend shown in Figure 66.

Cobalt

Cobalt is accumulated primarily in the Limonite zone, above the zone of greatest nickel enrichment, where it is preferentially associated with Mn oxides and to a lesser extent with goethite (cfr. samples 99 and 55, Table 3). Although both Co and Ni are relatively mobile in the weathering environment (Levinson, 1980), observed distribution (Figure 66) indicates that Co precipitates more readily than Ni. The accumulation mechanism appears to be similar to that of Ni, that is dissolution in the uppermost part of the profile and deposition downwards (McFarlane, 1976). The presence of Mn oxides in the Limonite zone apparently favours Co deposition, thus impeding its migration to deeper levels

in the profile. The association of Co with Mn oxides is related to the high capacity of these oxides for the adsorption of transition group metals (Maynard, 1983), and is common in Ni laterite profiles (Zeissink, 1969; Zeissink, 1971; Kuhnel et al., 1978; Golightly, 1979a; Golightly, 1981).

Co is slightly enriched in the Canga zone, particularly towards the base of this zone where goethite and maghemite are abundant. Co adsorption on grains or substitution in lattices of goethite and maghemite may explain this Co relative accumulation (Kuhnel et al., 1978). Although less so than in the Canga zone, Co is slightly enriched in the saprolite zone, particularly towards the top where it seems to be associated with smectite. Enrichment of as much as 6 times the value in the peridotite parent rock has been observed. Experimental work by Tiller and Hodgson (1962) on adsorption of Co by layer silicates shows that the amount of Co adsorbed by smectites may be relatively significant and that as pH increases up to values of about 7.5, the amount is greater than at lower pH's.

Iron

Iron is concentrated in the Canga and Limonite zones. The highest iron contents occur at middle and lower levels of the Canga zone. Variation in iron content appears to be related to both residual enrichment and partial remobilization of iron. Oxidizing and slightly acidic conditions, with Eh's generally over 0.3 volts and pH's around 5.0, are

usually present at the Limonite and Canga zone levels (Trescases, 1975; McFarlane, 1976). Under these conditions, soluble Fe^{2+} is converted to Fe^{3+} (Pickering, 1962; Levinson, 1980) and iron readily precipitates as goethite (Krauskopf, 1979; Schwertmann and Murad, 1983). Intense leaching of more mobile constituents such as magnesia and silica results in a relative residual concentration of iron.

In addition, supergene enrichment by iron remobilization from the uppermost part of the laterite profile may occur over short distances. Locally, pH may reach values as low as 3.0 or less, particularly at the top of the Canga zone (McFarlane, 1976). This decrease in pH may be accomplished by introduction of carbon dioxide from the atmosphere and of organic acids derived from decaying organic matter into the weathering solutions (Krauskopf, 1979). Under these strongly acidic conditions, ferric iron from goethite may be reduced to ferrous iron and downward remobilization of solubilized iron may occur (McFarlane, 1976; Krauskopf, 1979). However, downward remobilization of iron is limited to a few meters (Dorr, 1964) and changes to slightly less acidic conditions induce iron reprecipitation; iron is thus re-accumulated toward the middle and lower parts of the Canga zone.

Magnesia

Strong depletion of magnesia from the uppermost part of the Upper Saprolite zone upwards to the top of the profile is

in accordance with the mobility characteristics of this component. In the weathering environment, magnesium is highly mobile under acid, neutral, and alkaline conditions (Levinson, 1980), especially in the range of pH 4 to 9 (Lelong et al., 1976). Leaching of Mg is particularly pronounced in the Limonite and Canga zones where it has been almost completely removed.

In the saprolite zone, comparison between the general decreasing trends of magnesia and silica seems to indicate that magnesia is leached more rapidly than silica. This difference in leaching rates between magnesia and silica in laterite profiles developed on peridotite has been observed at other peridotite localities (Zeissink, 1969; Trescases, 1975; Lelong et al., 1976).

Silica

Silica is relatively depleted in the upper part of the laterite profile. This general distribution pattern of sharply decreasing silica from the Limonite zone upwards has been observed in other silicate-type nickel laterites (Trescases, 1975; Golightly, 1979b; Burger, 1979). Silica released during weathering of silicates may be partly removed from the weathering environment (Trescases, 1975), particularly when the solutions have pH's in the range of 3 to 5 (Maynard, 1983) and leaching conditions are favourable. Leaching of silica is promoted during rainy seasons when water is available (Trescases, 1975), and also if the rock

is fractured and permeable enough to provide channelways to the solutions. Some of the silica apparently migrates downwards and deposits along fractures as chalcedony associated with garnierite.

Alumina

In general, alumina exhibits concentration at the Canga and Limonite levels (Figure 66), probably because of its relative insolubility in weathering environments (Keller, 1964; Levinson, 1980; Maynard, 1983). Relatively high alumina values in the uppermost part of the laterite profile may be explained by a residual enrichment through removal of other constituents such as magnesia and silica and incorporation into goethite structures (Zeissink, 1969; Lewis and Schwertmann, 1979; Golightly, 1981). Additionally, aluminium released by weathering of primary silicates also probably is incorporated in smectite structures, particularly towards the uppermost part of the saprolite (Zeissink, 1969).

Chromium

Chromium is residually concentrated upwards in the profile and is preferentially enriched in the Canga zone, except at its top. This general compositional trend probably relates to the resistance of chromite to weathering (McFarlane, 1976) and, as a result, chromium content through the laterite profile commonly is used as an index for

assessing the relative concentration or leaching of other elements (Zeissink, 1969).

Although chromite in general is a fairly resistant mineral, it may be partially dissolved, particularly at the top of the Canga zone where pH may be as low as 3.0 or less (Schellmann, 1978; McFarlane, 1983; Maynard, 1983). A slight decrease in Cr_2O_3 content towards the uppermost part of the Canga zone seems to reflect the very limited mobilization of chromium in the Cerro Matoso laterite profile.

Manganese

The general distribution of manganese indicates preferential accumulation in the Limonite zone and, to a lesser extent, in the Canga zone. The highest accumulation of manganese is slightly below that of iron in the laterite profile, which may be explained on the basis of differences in precipitation conditions between iron and manganese in the weathering environment. Oxidizing conditions, with Eh's above 0.3 volts, are commonly observed in the Limonite and Canga zones (McFarlane, 1976). In this oxidizing environment, both iron and manganese may precipitate as iron hydroxide and manganese oxide, respectively. In the laterite profile, pH increases from values around 5.0 or less in the Canga zone downwards to 8.5-9.0 and slightly greater values in the Lower Saprolite zone (Trescases, 1969; 1975). According to Krauskopf (1979), with slow increase

in pH, iron compounds reach the limit of solubility before manganese compounds and can precipitate while manganese is left in solution. Manganese probably is mobilized as Mn^{2+} (Ahmad and Morris, 1978) through short distances in the Canga and Limonite zones and readily converted to Mn^{4+} (López-Eyzaguirre and Bisque, 1975) at pH's above around 6.0 (Trescases, 1975), and it is precipitated as manganese oxide in the upper part of the laterite profile in stringers, pockets, and coatings on goethite concretions.

ZONAL DISTRIBUTION OF SELECTED CHEMICAL COMPONENTS

In order to evaluate the lateral and vertical distribution of selected elements in the laterite profile at Cerro Matoso, longitudinal vertical profiles showing zones defined by contours of equal concentration for a given component were constructed for the lines 500 NW, 1200 NW, 1300 NW, and 2000 NW. These lines represent the southeastern, central and northwestern parts of the deposit (Plate 2), and they cut across the general SE–NW trend of the peridotite body and the main faults (Figures 67, 68, 69, and 70).

Chemical data utilized for the construction of the profiles appear in Appendix 1 and are from samples recovered at 2 m depth intervals from the original drill holes. The following profiles were constructed: Line 500 NW – Ni, Fe, MgO; Line 1200 NW – Ni, Co, Fe, MgO, SiO_2, Al_2O_3; Line 1300 NW – Ni, Co, Fe, MgO, SiO_2, Al_2O_3; Line 2000 NW – Ni, Fe, MgO, SiO_2. The vertical scale in these profiles was exaggerated by 5 with respect to the horizontal scale in order to accentuate local characteristics in the element distribution.

Nickel

The nickel profiles (Figures 71, 72, 73, and 74) exhibit several features that reflect the behaviour of
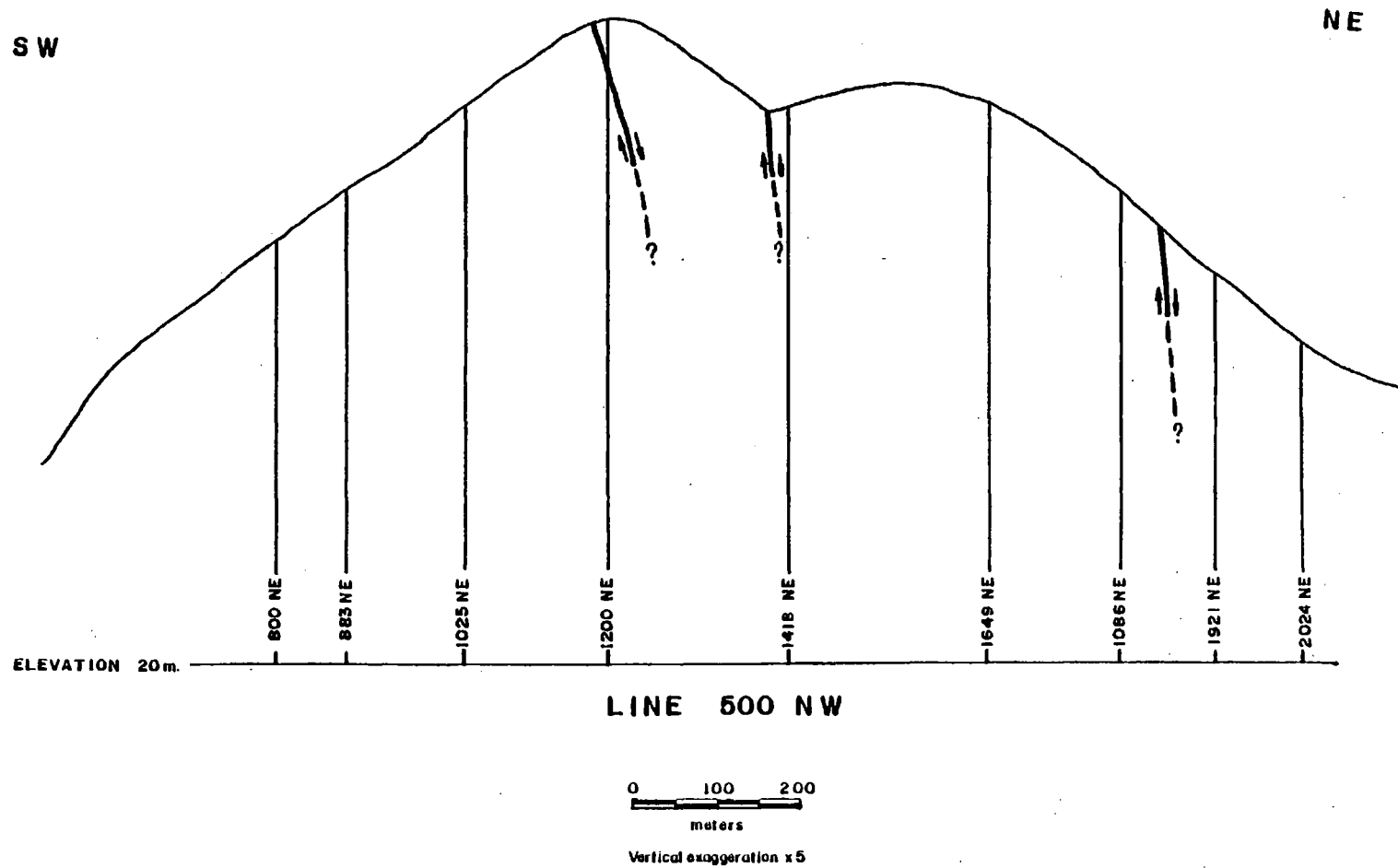
Figure 67. Line 500 NW, Longitudinal vertical profile showing drill hole distribution and location of faults.
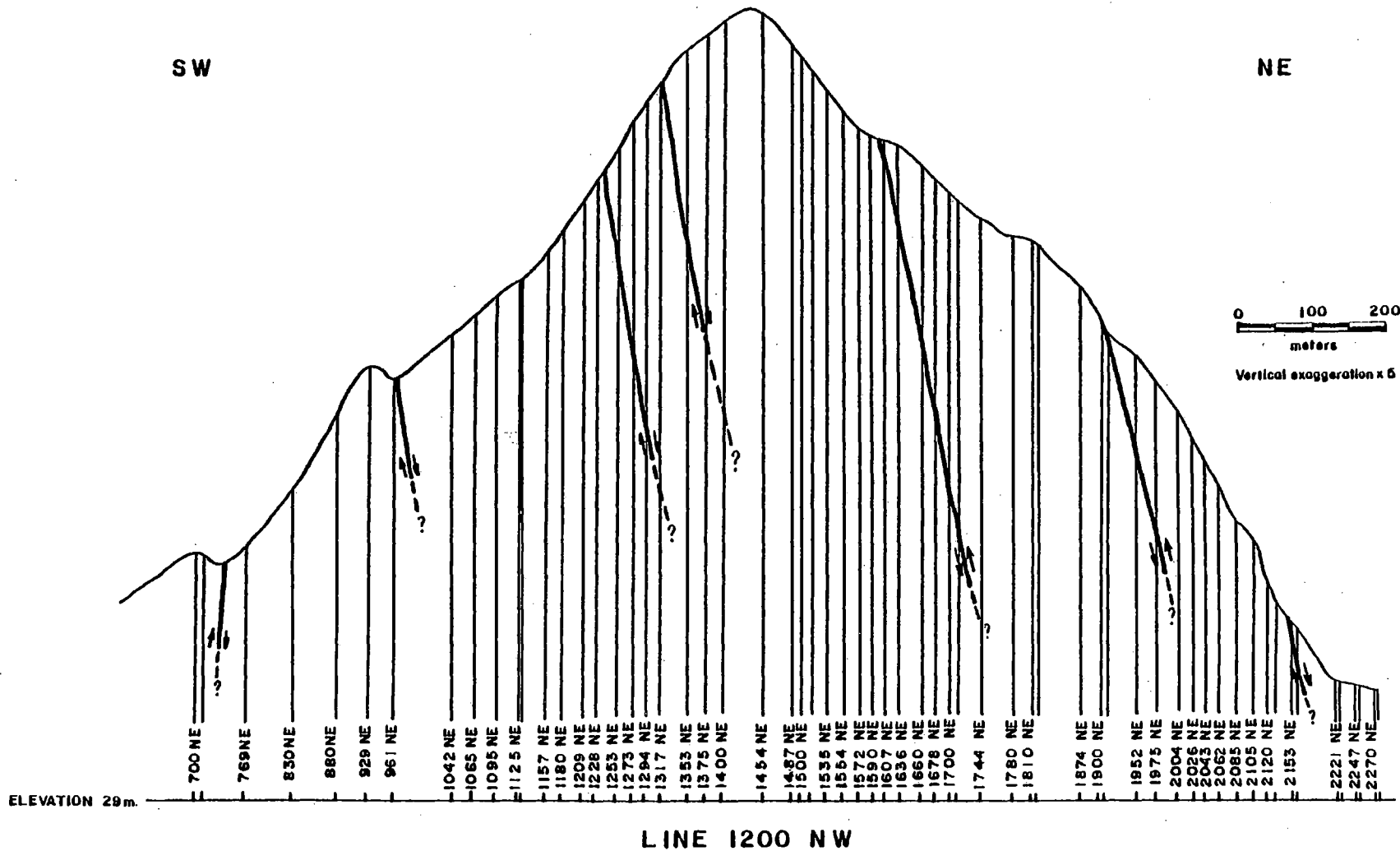
Figure 68. Line 1200 NW, Longitudinal vertical profile showing drill hole distribution and location of faults.

161
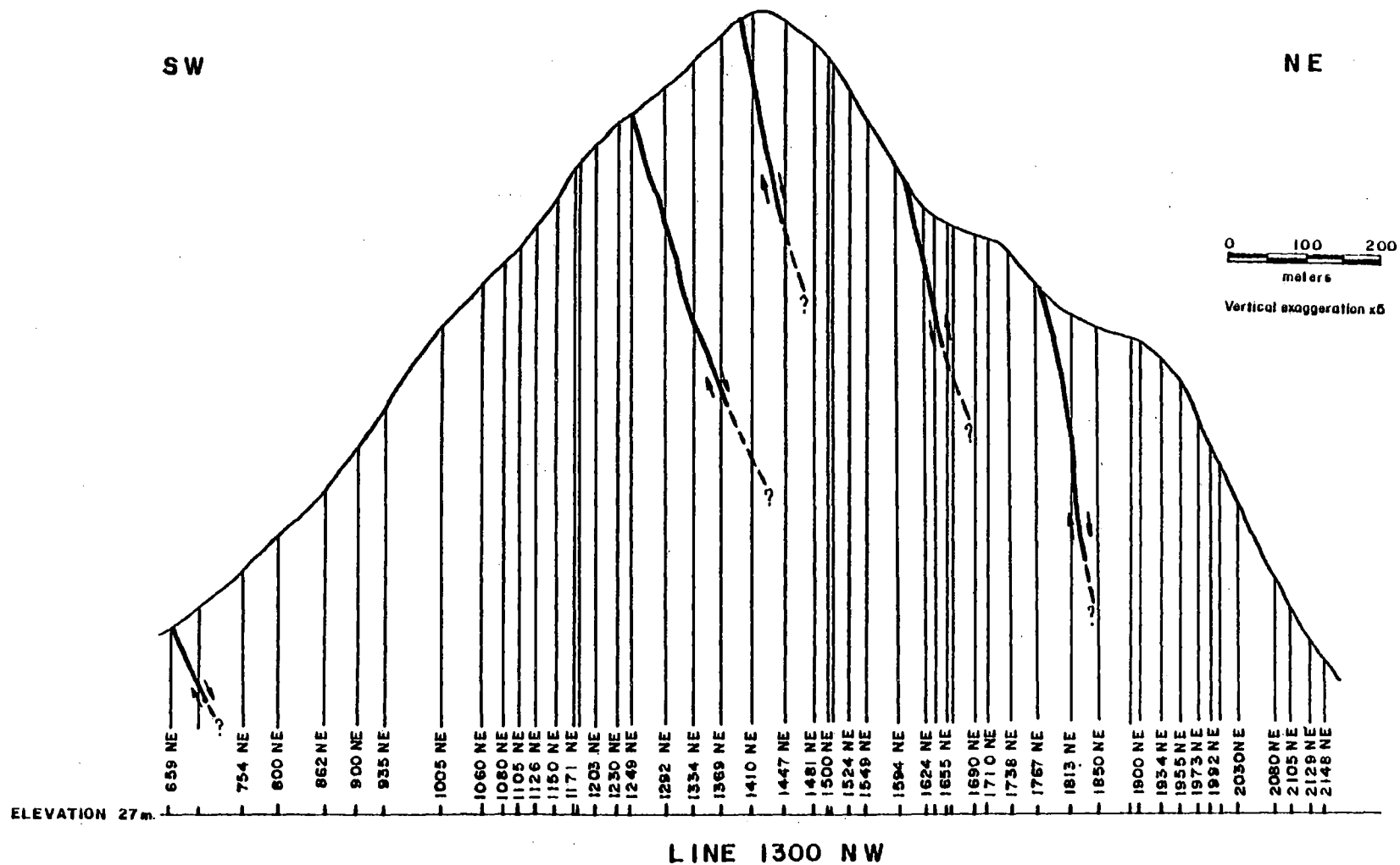
Figure 69. Line 1300 NW, Longitudinal vertical profile showing drill hole
distribution and location of faults.

SW

NE

ELEVATION 0m.
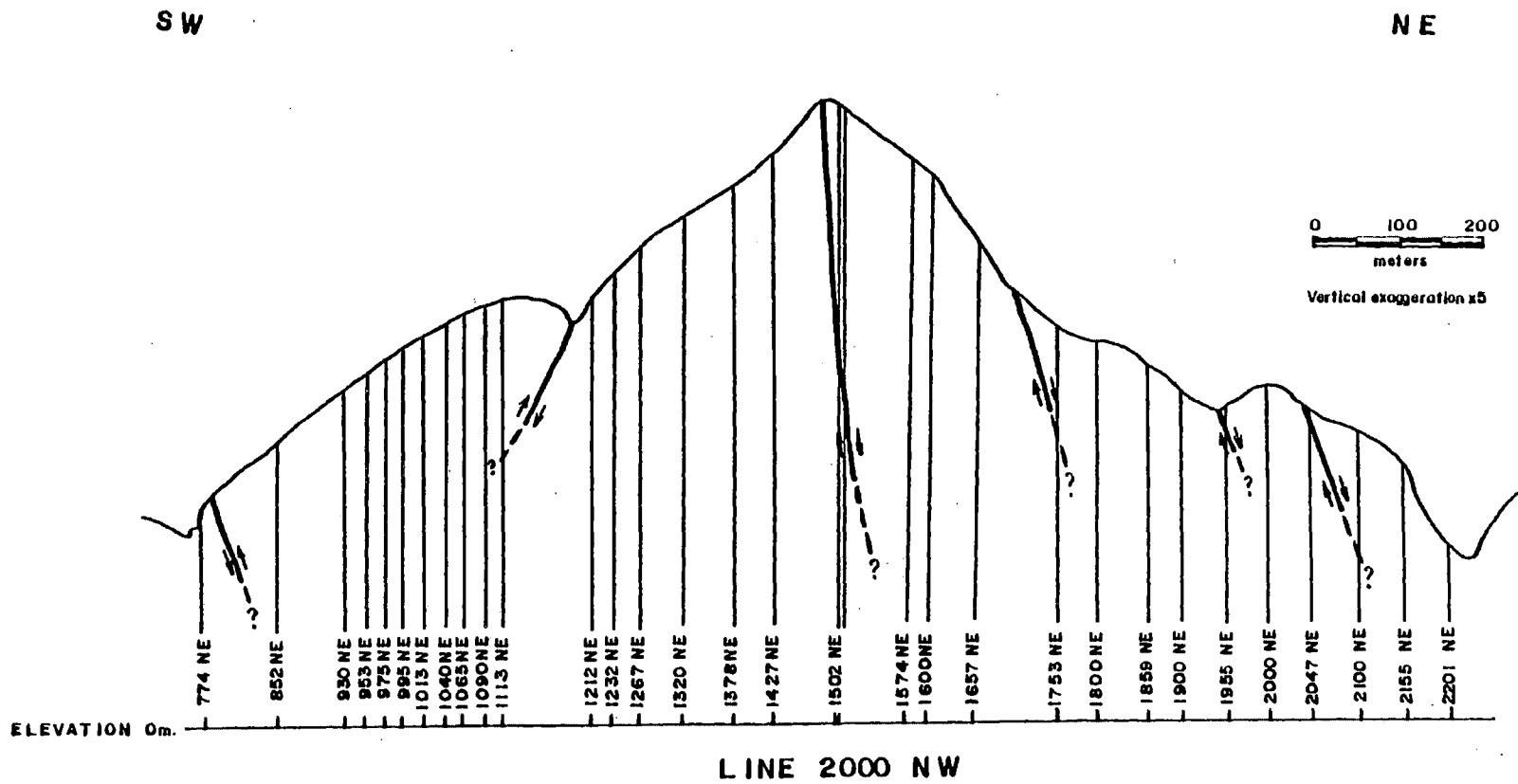
LINE 2000 NW

Figure 70. Line 2000 NW, Longitudinal vertical profile showing drill hole distribution and location of faults.

163
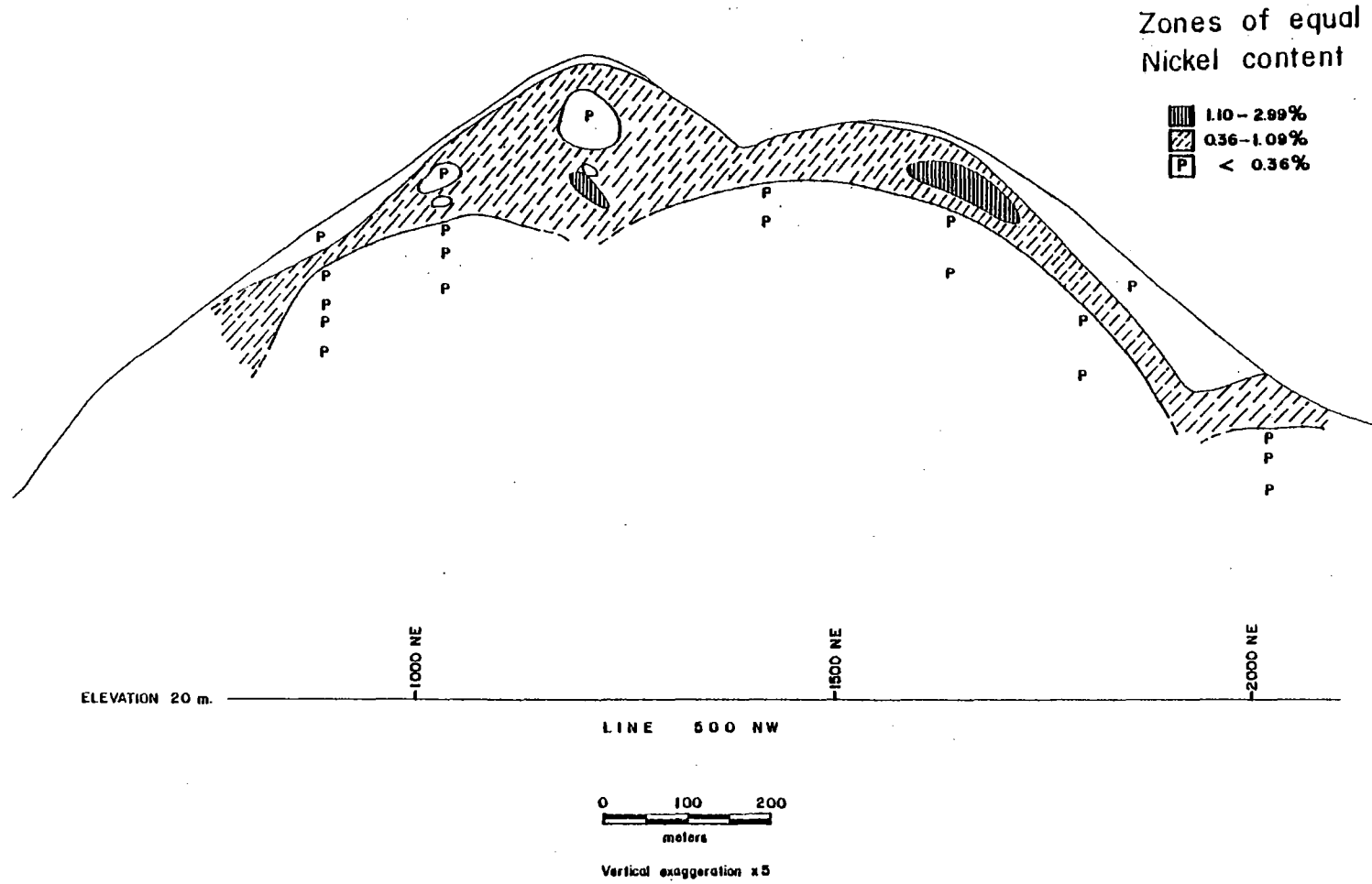
Figure 71. Line 500 NW, Longitudinal vertical profile showing zones of equal nickel concentration.
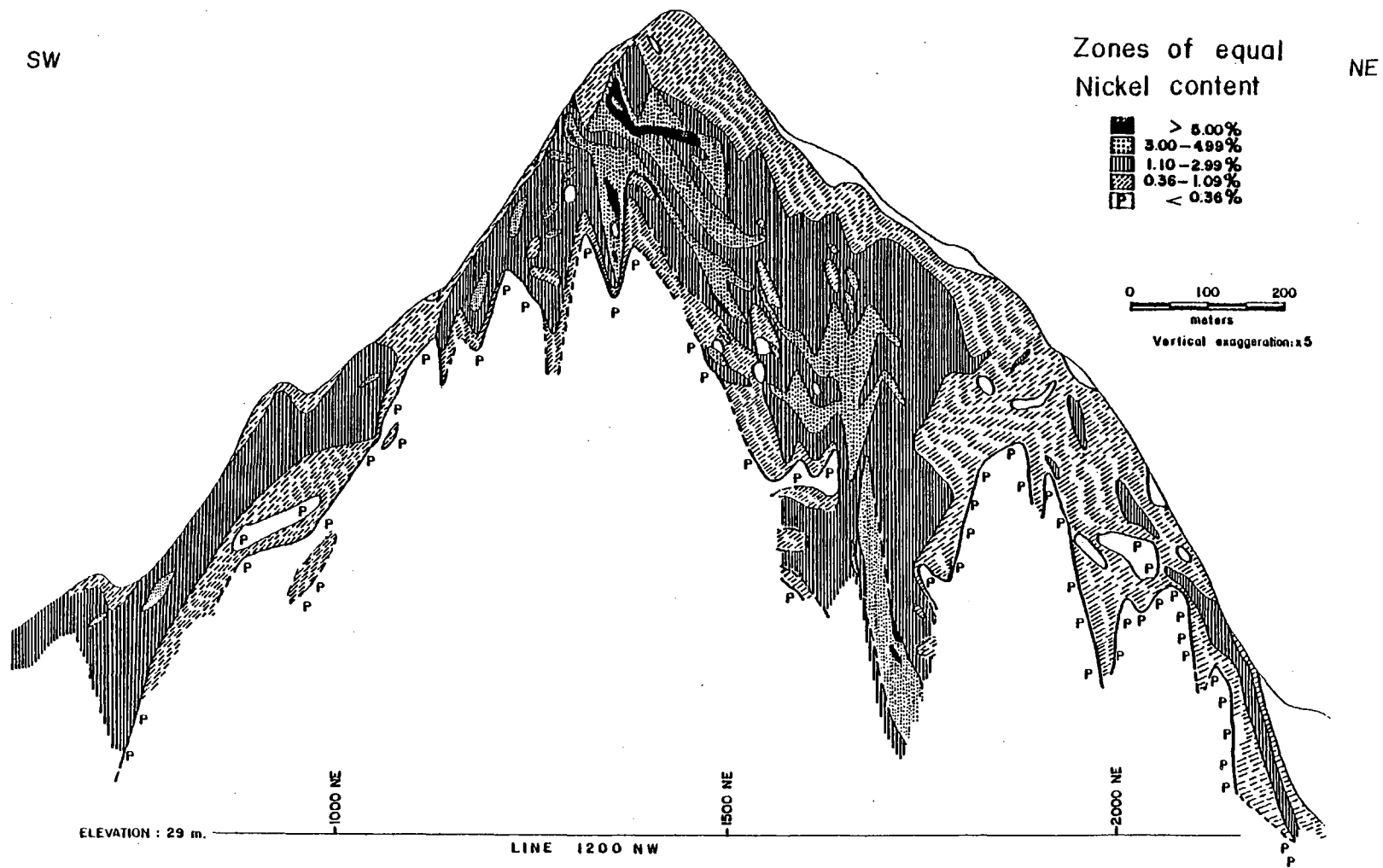
Figure 72.   Line 1200 NW, Longitudinal vertical profile showing zones
of equal nickel concentration.

SW   NE

Zones of equal
Nickel content

> 5.00%
3.00 – 4.99%
1.10 – 2.99%
0.36 – 1.09%
P   < 0.36%

0   100   200

meters
Vertical exaggeration: x5

ELEVATION 27 m.
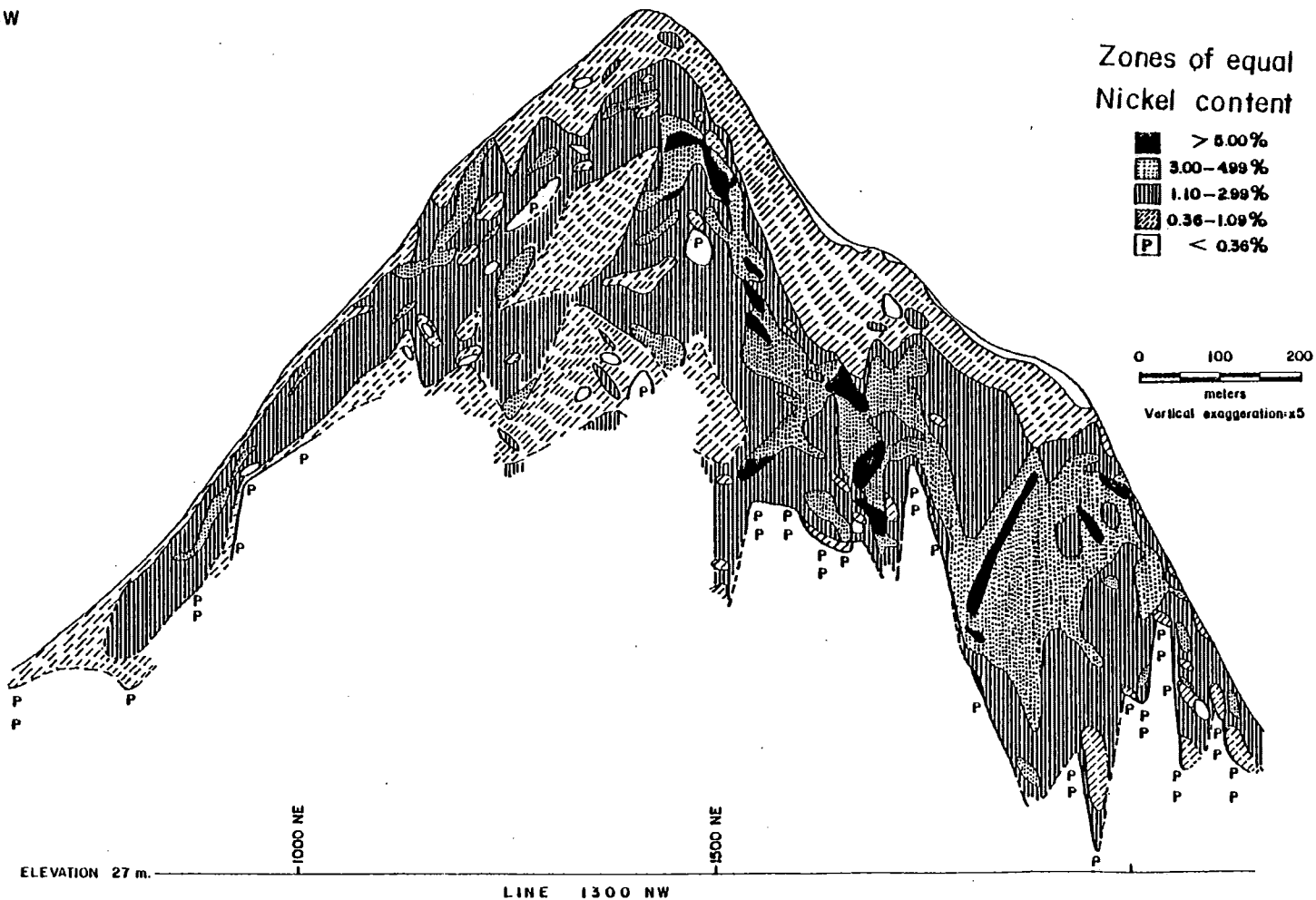
LINE 1300 NW

Figure 73.   Line 1300 NW, Longitudinal vertical profile showing zones of equal nickel concentration.

SW   NE

Zones of equal Nickel content

- 3.00–4.99%
- 1.10–2.99%
- 0.36–1.09%
- P   < 0.36%

ELEVATION 0 m

1000 NE

1500 NE

2000 NE

LINE 2000 NW

0   100   200

meters

Vertical exaggeration x 5
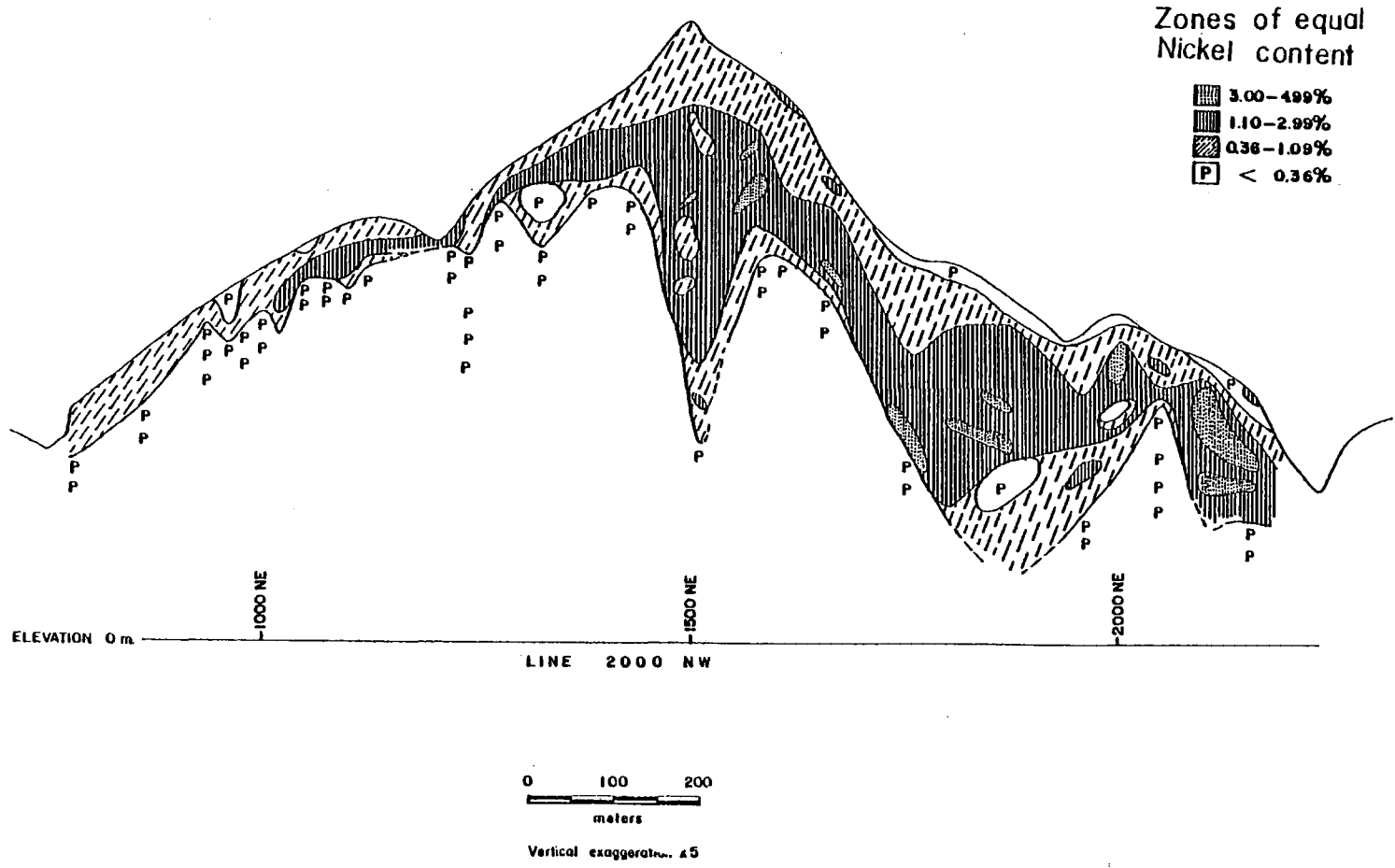
Figure 74.   Line 2000 NW, Longitudinal vertical profile showing zones of equal nickel concentration.

nickel in the weathering environment as well as differences in the degree of lateritization of the peridotite body. Weathering did not proceed uniformly throughout the entire rock mass. Depth to peridotite bedrock shows marked variations both along a single profile and between profiles. Zones having nickel concentrations of less than 0.36% (i.e. the reference content in the original peridotite) occur locally at intermediate levels in the profiles. These zones are surrounded by higher grade materials and correspond to isolated nuclei of relatively fresh to slightly weathered peridotite within Ni-rich saprolite as previously described.

The general shape of the zones defined by contours of equal concentration for nickel, particularly those corresponding to high Ni grades, seems to indicate local structural control. Narrow, elongated, steeply dipping zones showing sharp lateral transitions from high to low Ni values may be discerned in the profiles (cfr. at the approximate coordinates 1200NW-1275NE, 1200NW-1700NE, 1300NW-1250NE, 1300NW-1710NE, 2000NW-1500NE). In general, these narrow zones correspond with faults and major joint sets observed along the benches.

The best developed ore occurs towards the northeastern part of the peridotite body, particularly along the profiles 1200 NW and 1300 NW. This distribution may be explained by uplift of the southwestern portion of the hill along a NW trending fault that post-dated the main lateritization event. Erosion that was preferentially active on

the uplifted block may have resulted in only slight weathering of peridotite at that site, and a less evolved laterite profile developed thereafter.

Except for those zones where structural control apparently led to the development of elongated and vertical high grade ore masses, Ni accumulation appears to have proceeded in a somewhat regular fashion related to supergene enrichment. Very low Ni values characterize the top of the laterite profile whereas the highest values occur at intermediate depths in the Upper Saprolite zone.

Comparison between the southeastern, northwestern, and central areas of the peridotite body indicates a significant difference in the degree of nickel enrichment which is apparently related to variations in the relative degree of serpentinization of the parent peridotite. Strongly serpentinized peridotite occurs to the southeast of the Cerro Matoso hill, near the Romeral fault zone. This area is represented by the profile 500 NW (Figure 71) which is characterized by a thin laterite profile and low nickel values. Moderately to slightly serpentinized peridotite occurs to the northwest of the Cerro Matoso hill (profile 2000 NW, Figure 74). A thicker laterite profile and greater nickel enrichment are apparent along the profile 2000 NW as compared to the profile 500 NW. The central parts of the Cerro Matoso hill are characterized by slightly serpentinized peridotite and represented by the profiles 1200 NW and 1300 NW. These two profiles (Figures 72 and 73)

exhibit the thickest laterite profile development and the greatest nickel enrichment.

Cobalt

The profiles of equal concentration for Co (Figures 75 and 76) also emphasize variations in the weathering profile. Similar to nickel distribution, cobalt profiles indicate that the northeastern part of the peridotite body is relatively more evolved with respect to laterite profile development than is the southwestern part of the body.

Cobalt values from samples collected at the uppermost part of the profile are lower than those obtained in samples from underlying zones and appear to indicate relative leaching and downwards mobilization of Co. The highest concentration zones (i.e. >0.10% Co) are approximately coincident with the Limonite zone. Comparison between the highest concentration zones for Co and those for Ni (Figures 72 and 73) shows that Co accumulates preferentially at a level slightly above that of maximum Ni enrichment.

The shape of the zones of equal concentration for cobalt seems to be structurally controlled locally. Some V-shaped accumulations at intermediate levels in the profile (e.g. the 0.10% zone) may reflect such control.

Iron

Iron distribution profiles (Figures 77, 78, 79 and 80) express the relative immobility of this element in the
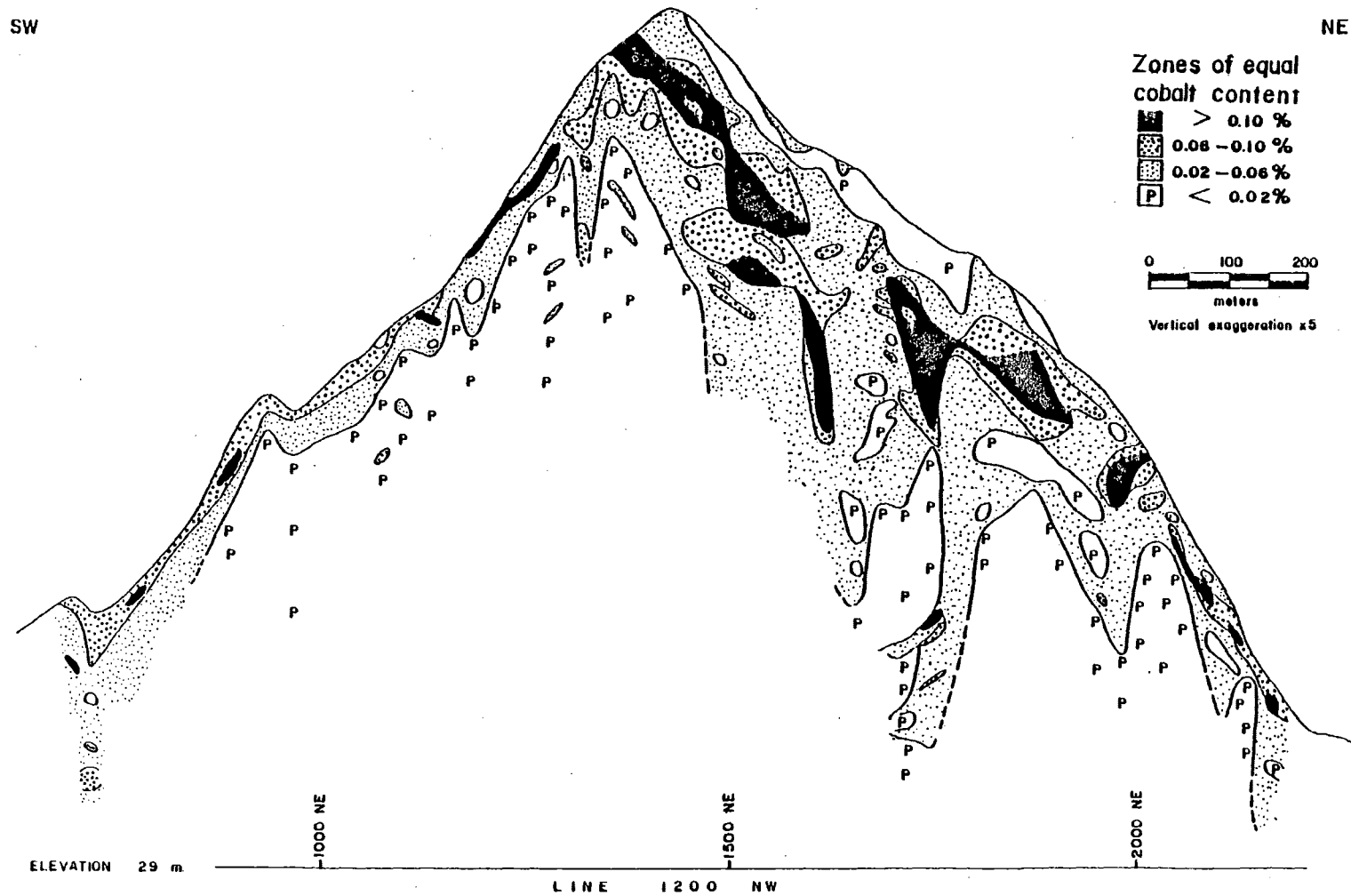
Figure 75. Line 1200 NW, Longitudinal vertical profile showing zones of equal cobalt concentration.
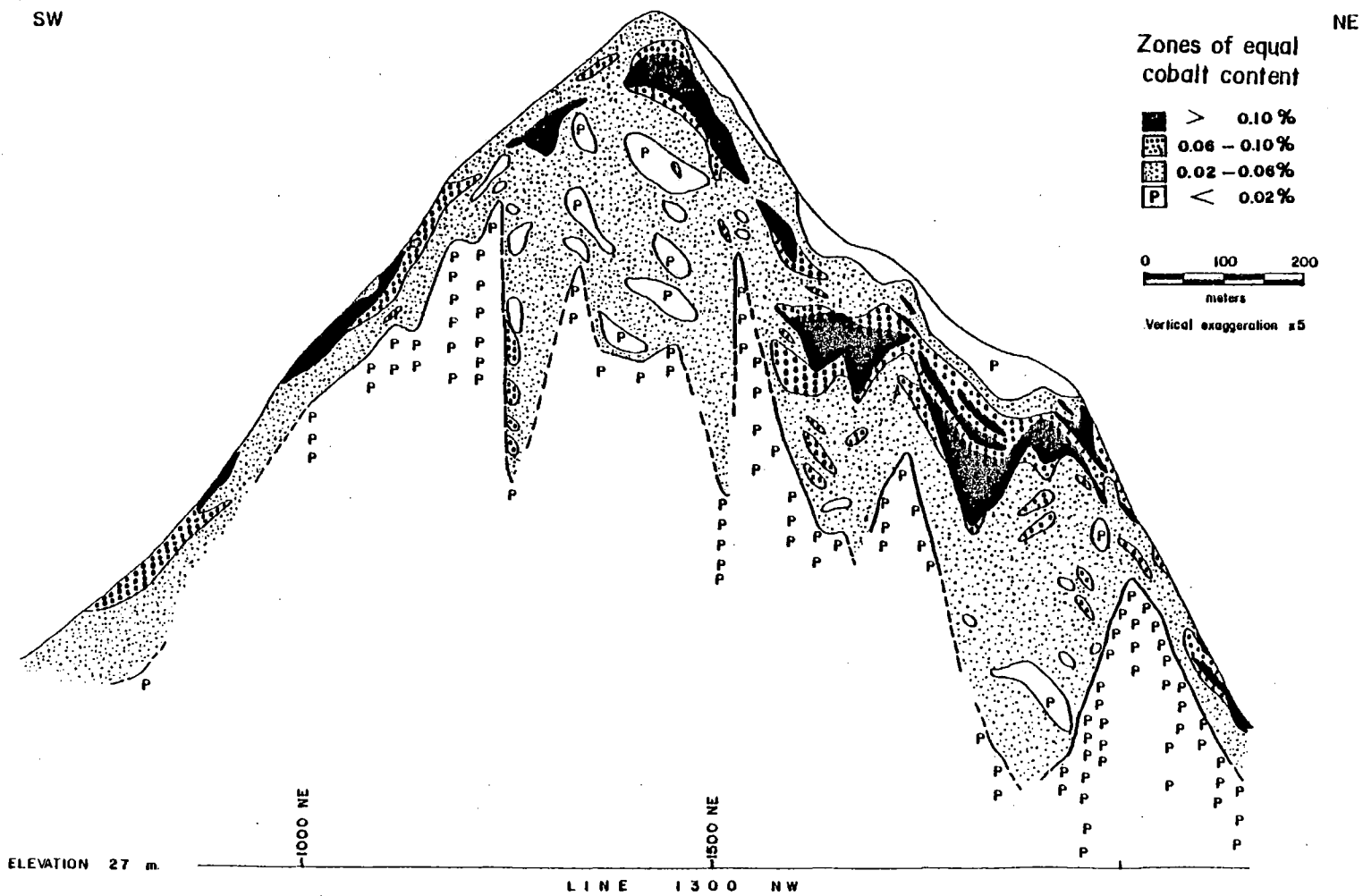
Figure 76. Line 1300 NW, Longitudinal vertical profile showing zones of
equal cobalt concentration.
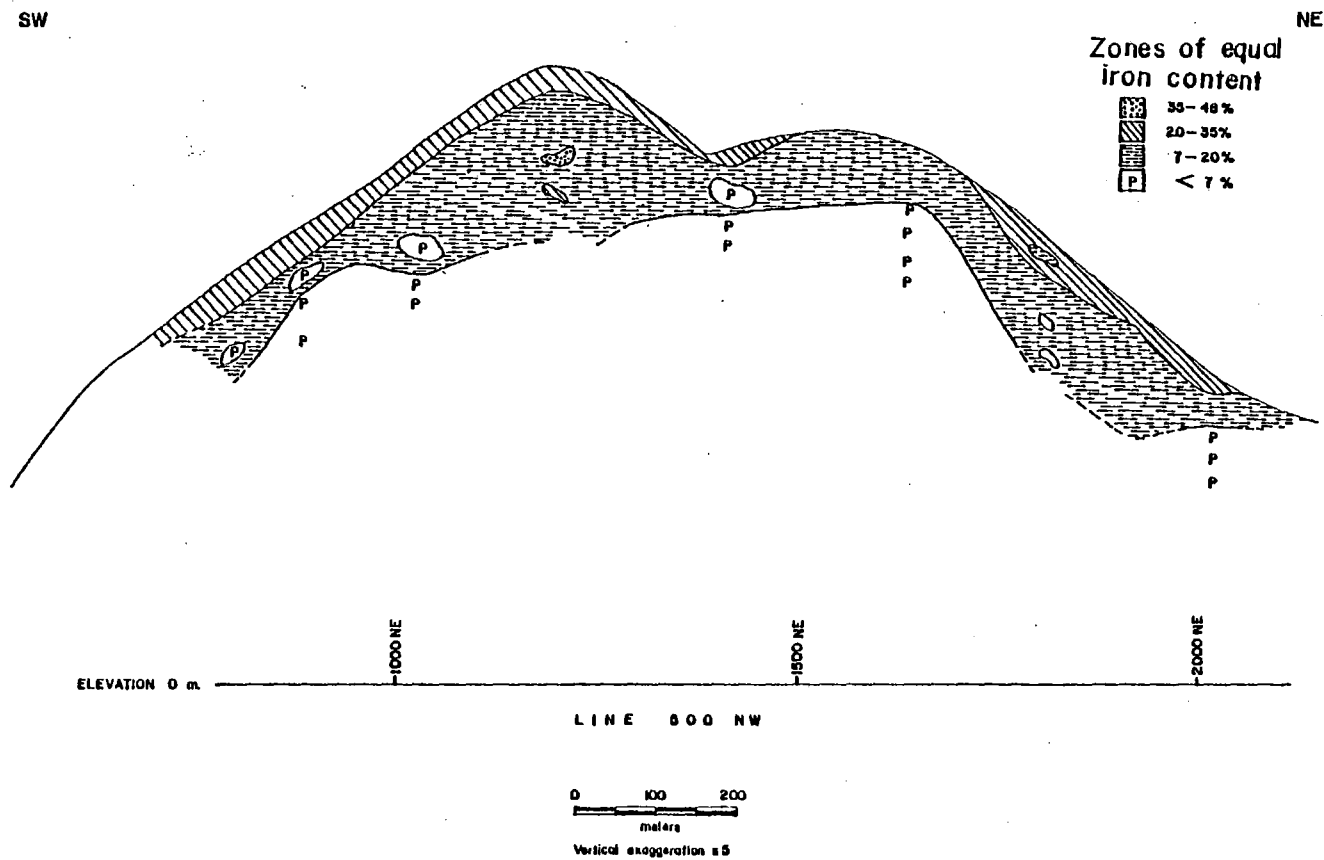
Figure 77.   Line 500 NW, Longitudinal vertical profile showing zones
of equal iron concentration.

SW NE

Zones of equal
Iron content

> 40%
35 — 48%
20 — 35%
7 — 20%
P < 7%

0   100   200
meters

Vertical exaggeration x 5

ELEVATION 29 m

LINE 1200 NW

1000 NE   1500 NE   2000 NE

174
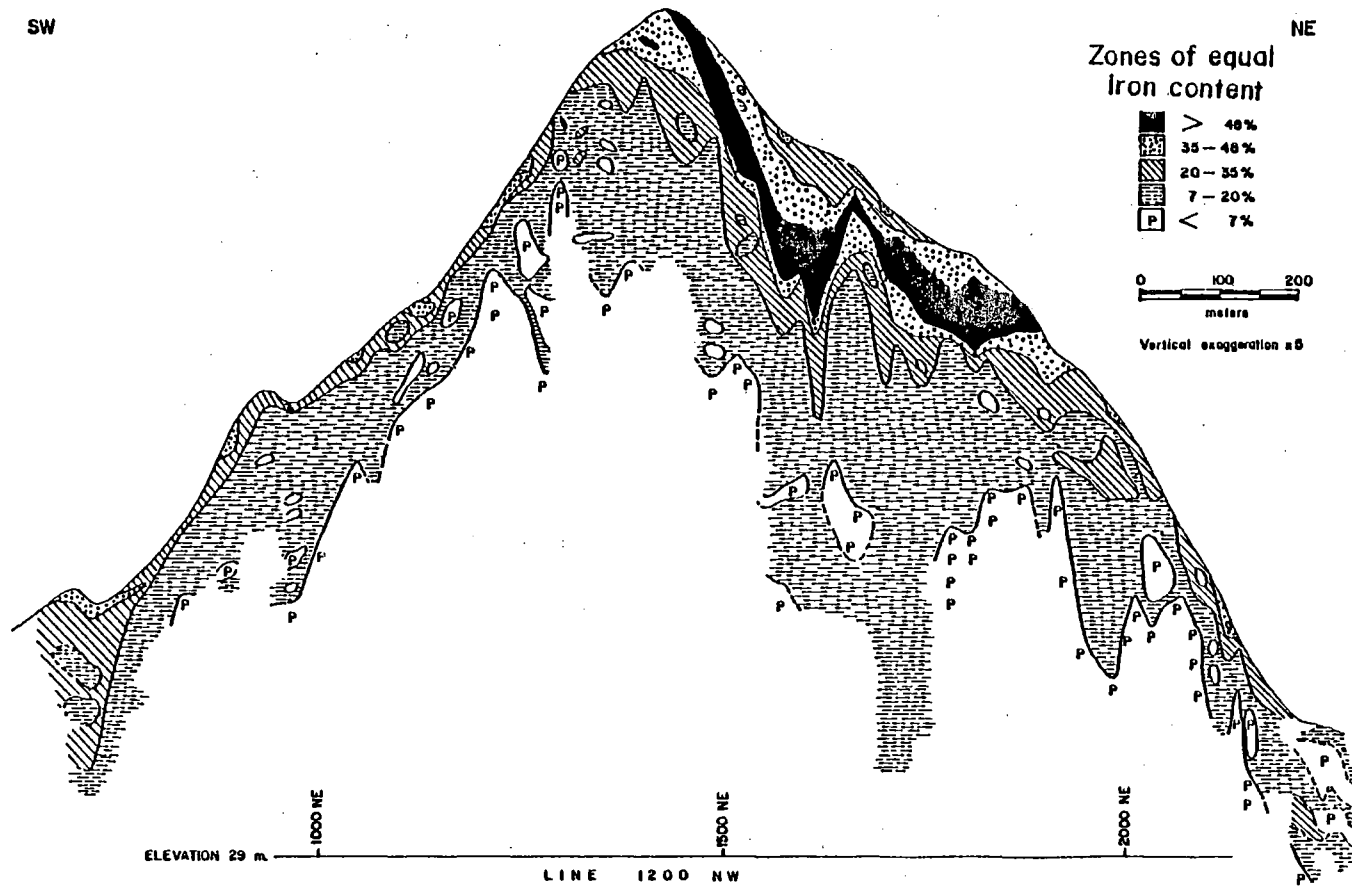
Figure 78.   Line 1200 NW, Longitudinal vertical profile showing zones
of equal iron concentration.
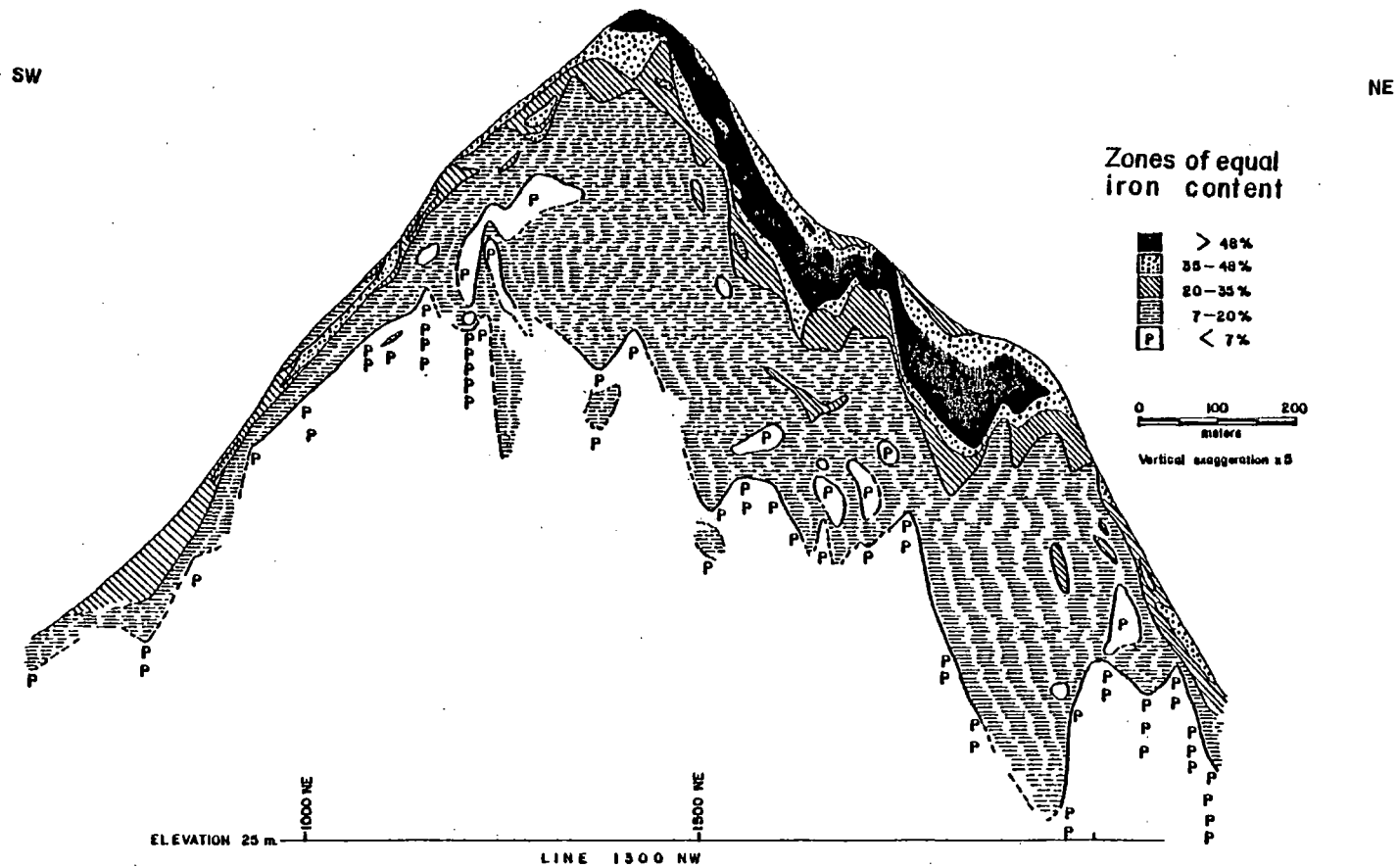
Figure 79.   Line 1300 NW, Longitudinal vertical profile showing
zones of equal iron concentration.
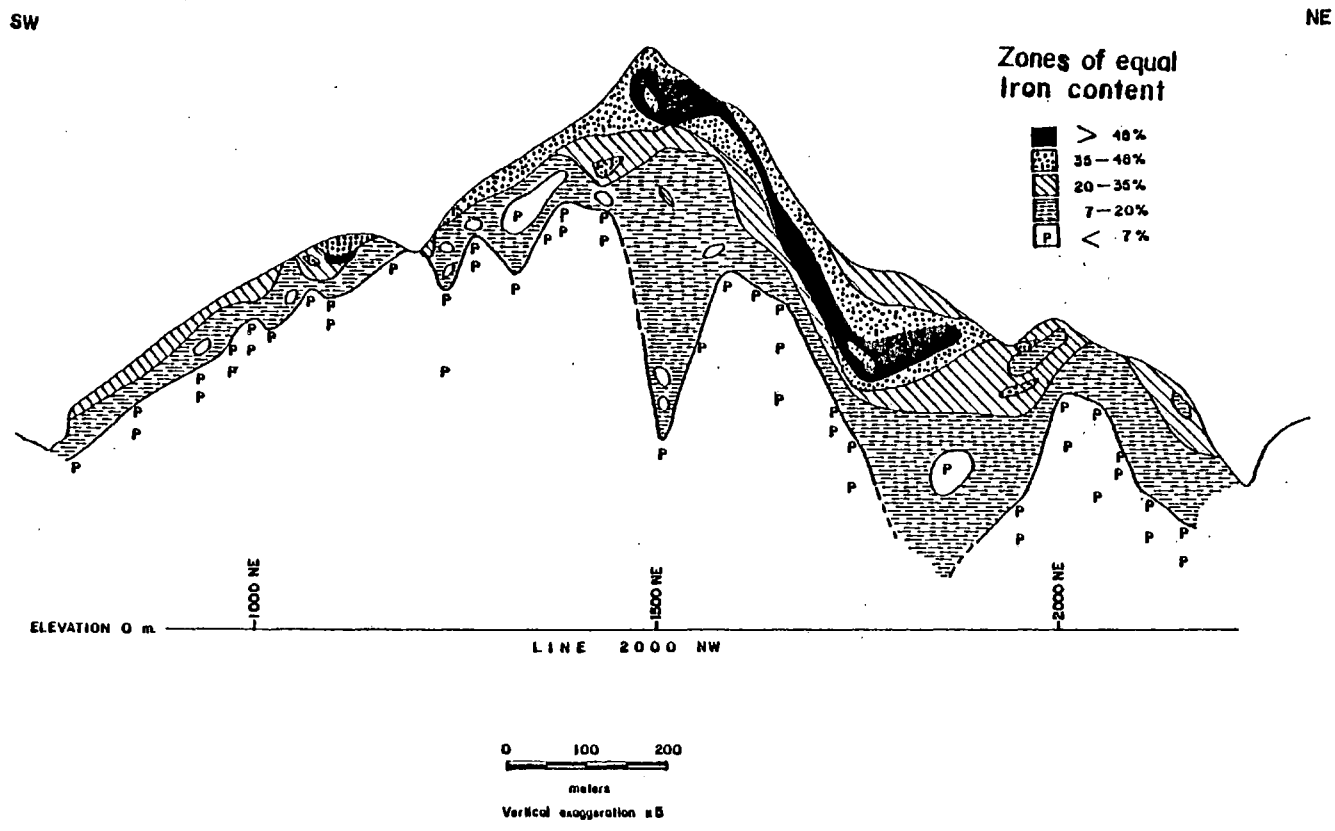
Figure 80.   Line 2000 NW, Longitudinal vertical profile showing
             zones of equal iron concentration.

weathering environment. Iron accumulates preferentially at upper levels in the profile, and zones of highest Fe concentration (i.e. >48% Fe) are approximately coincident with the position of the Canga. These zones occur in the NE part of the deposit and overlie the thickest saprolite sections. The presence of lower value Fe zones overlying those of highest Fe concentration in the Canga level indicate Fe solution at the top of the profile and redeposition at the Canga level.

The distribution of equal concentration zones for Fe also reflect variations in the degree of evolution of the laterite profile across the peridotite body. The NE part of the hill (Figures 78, 79 and 80) shows intense lateritization. All equal concentration intervals are well developed and extend to relatively great depths as compared to the SW part of the hill. To the southeast (profile 500 NW, Figure 77), a low degree of laterite profile evolution is apparent. There is no Canga, and saprolitic material is poorly developed.

Differential weathering conditions are reflected by Fe in the distribution profiles. Some zones or nuclei having low Fe content (i.e. <7% Fe) occur within equal concentration zones that have higher Fe values. These zones represent remnants of relatively unweathered to slightly weathered peridotite within saprolite material.

Magnesium

The highly mobile nature of magnesium is characterized by equal concentration profiles for MgO (Figures 81, 82, 83
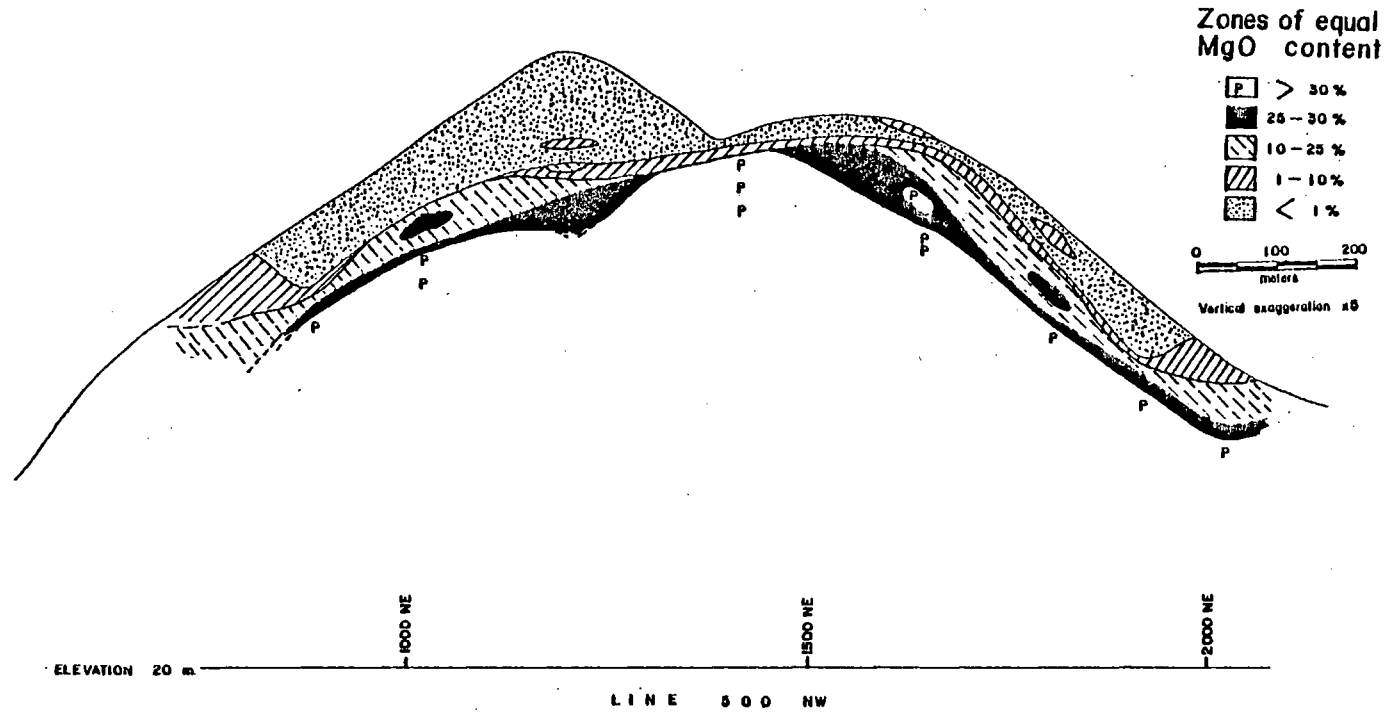
Figure 81. Line 500 NW, Longitudinal vertical profile showing zones
of equal MgO concentration.
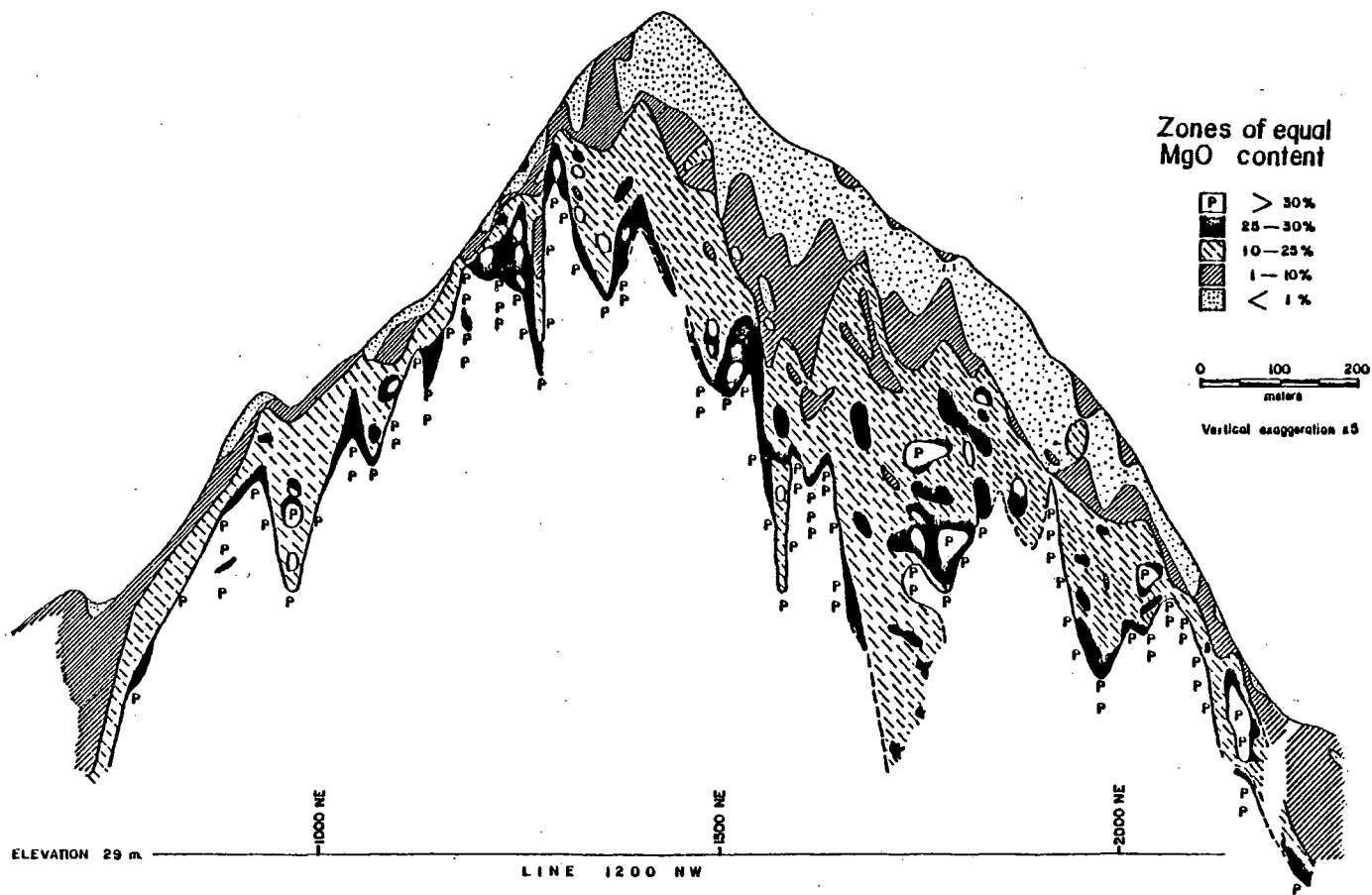
Figure 82. Line 1200 NW, Longitudinal vertical profile showing zones of equal MgO concentration.
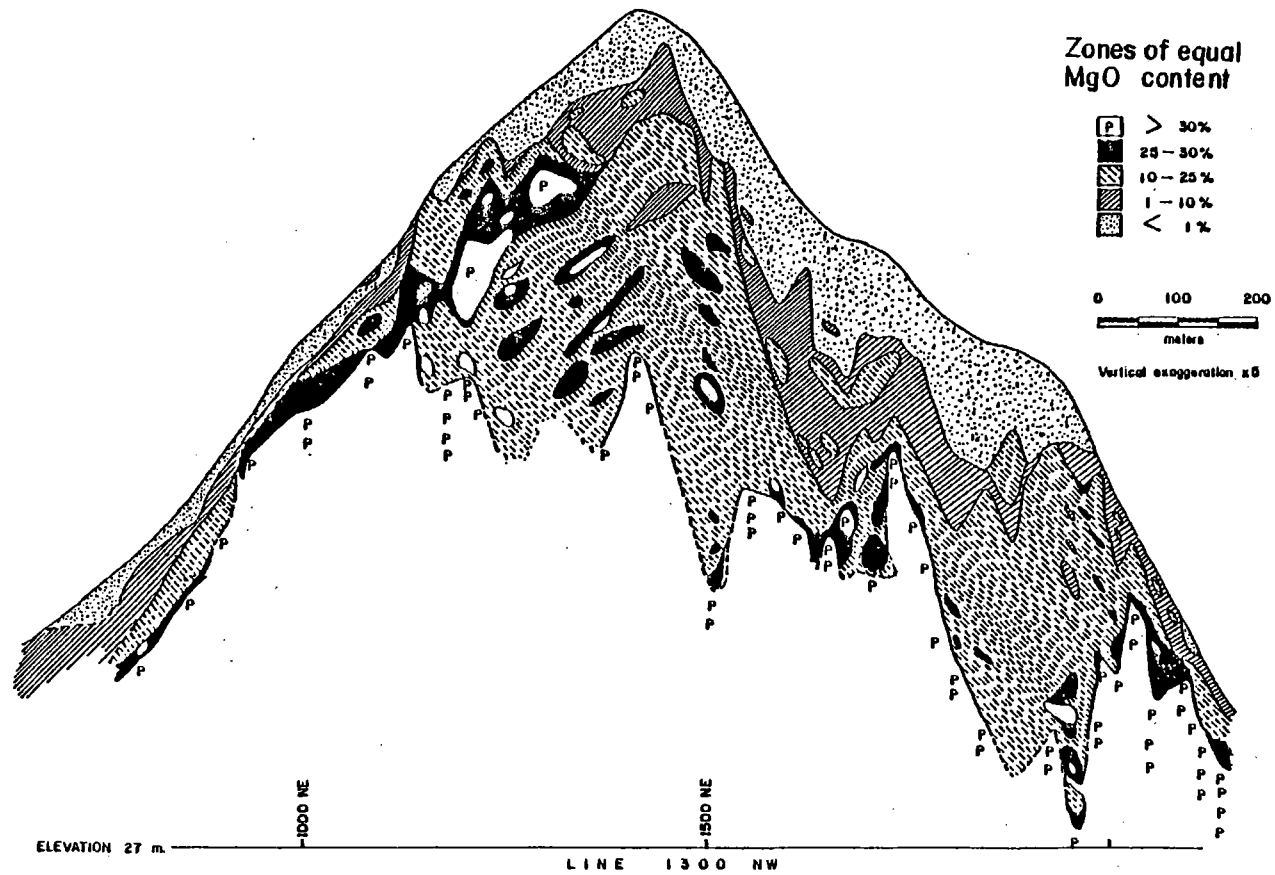
Figure 83. Line 1300 NW, Longitudinal vertical profile showing zones of equal MgO concentration.
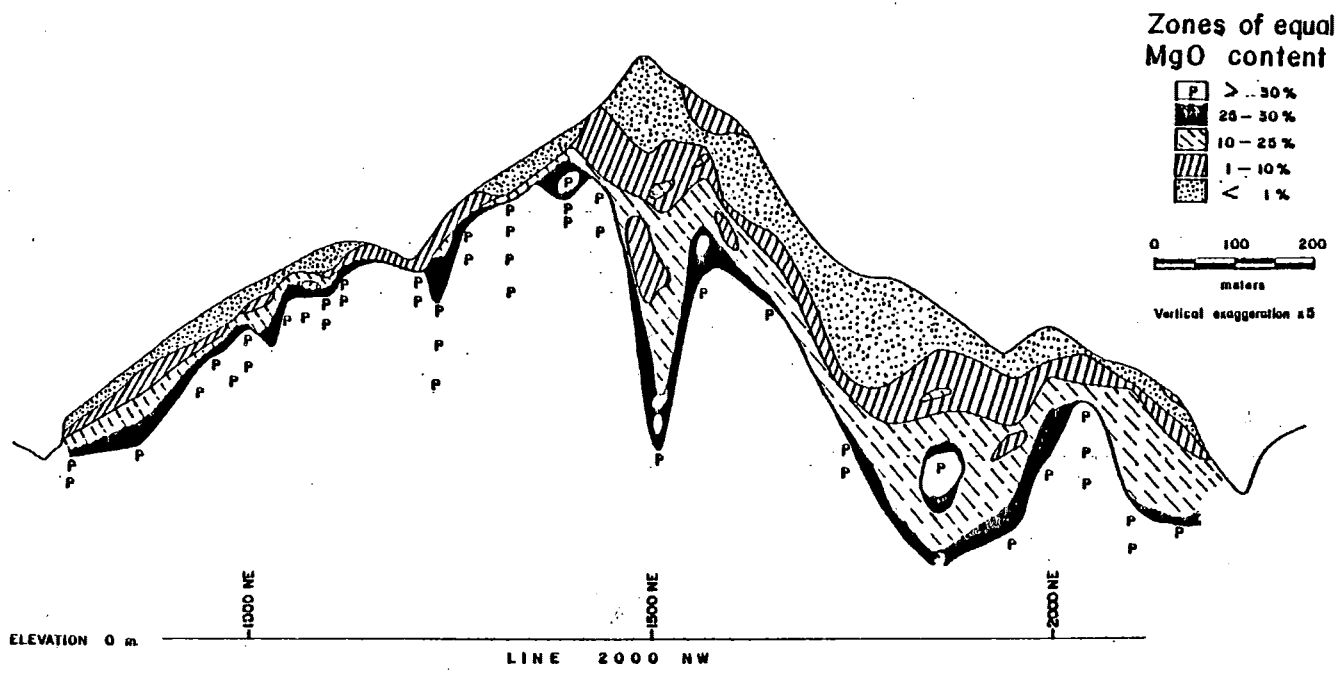
Figure 84.   Line 2000 NW, Longitudinal vertical profile showing
zones of equal MgO concentration.

and 84) which clearly reflect the weathering process at Cerro Matoso. Weathering intensity relates directly to degree of magnesium leaching which is greater on the NE part of the peridotite body. Depth to bedrock is highly variable and magnesium is preferentially leached from upper levels in the profile.

Locally narrow and elongated shapes of equal concentration zones apparently indicate structural control on magnesium leaching. Very low MgO values ($<$1.0%) at intermediate to deep levels also may be the result of deep migration of leaching waters along structures. Where major joint sets are present, weathering proceeds from the outer surface of individual blocks progressively inwards to the cores. Zones of high MgO values ($>$30%) surrounded by lower MgO zones at intermediate to deep levels appear to indicate the presence of relatively fresh to slightly weathered peridotite nuclei within saprolite material. Some of these nuclei attain diameters of 8 m. Even in the most intensely leached zones where MgO is less than 1.0% there are still remnants of relatively less weathered peridotite nuclei with MgO contents of as much as 10%.

Silica

Equal concentration profiles for silica (Figures 85, 86 and 87) show that the highest values (i.e. $>$ 55% SiO_2) occur preferentially at intermediate depths. This corresponds to the Upper Saprolite level where the shapes of
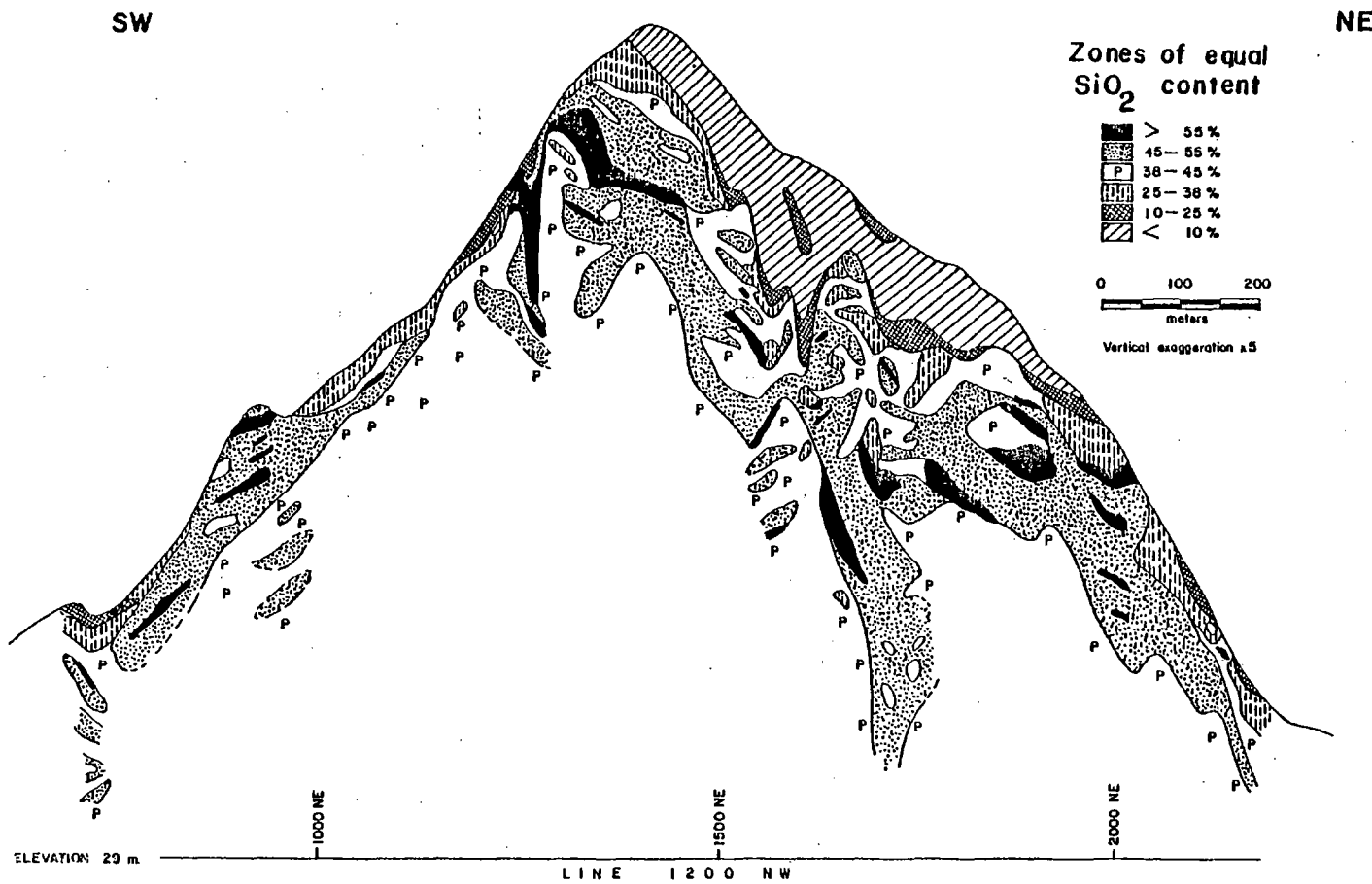
Figure 85. Line 1200 NW, Longitudinal vertical profile showing zones
of equal SiO_2 concentration.
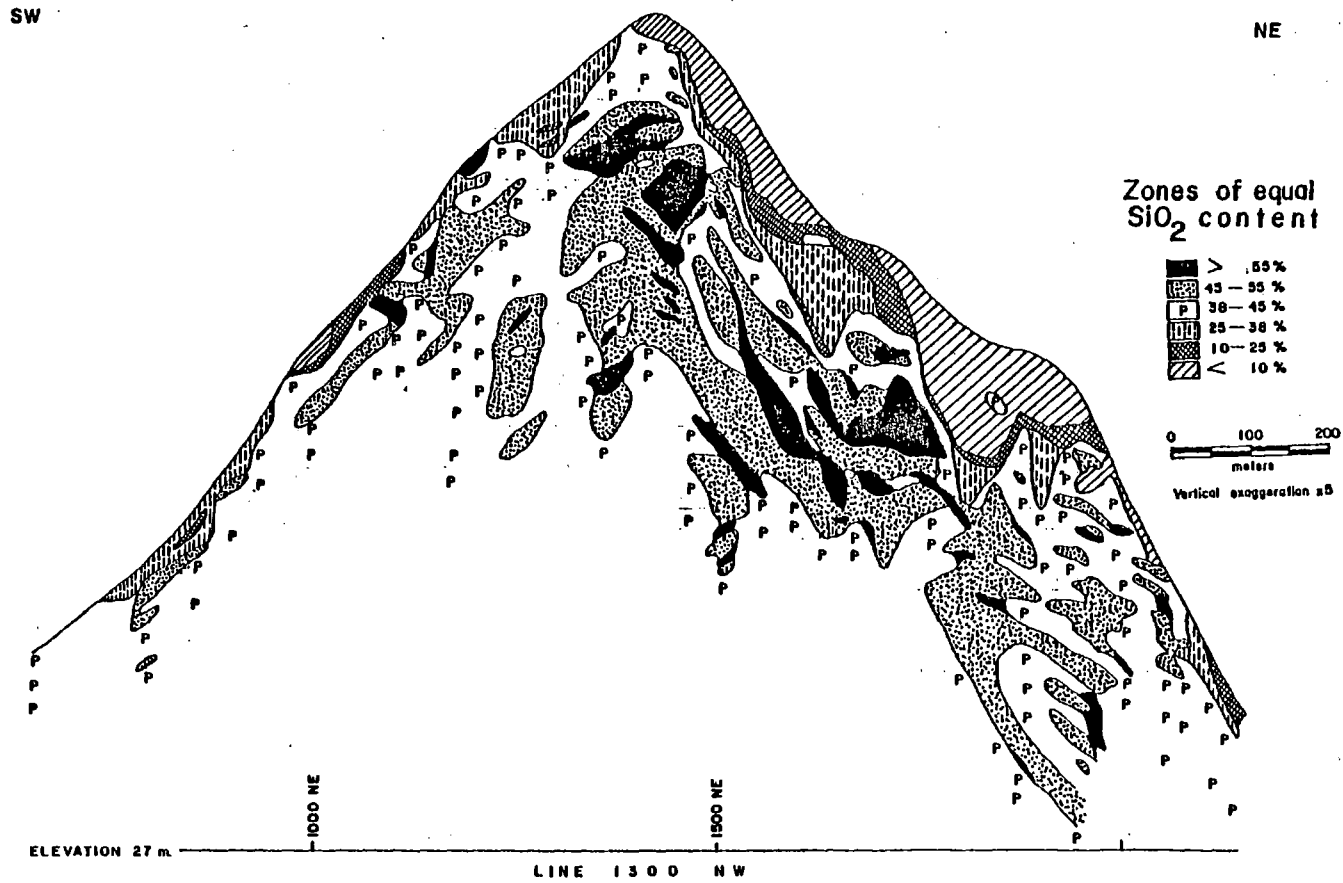
Figure 86.   Line 1300 NW, Longitudinal vertical profile showing zones of equal SiO_2 concentration.
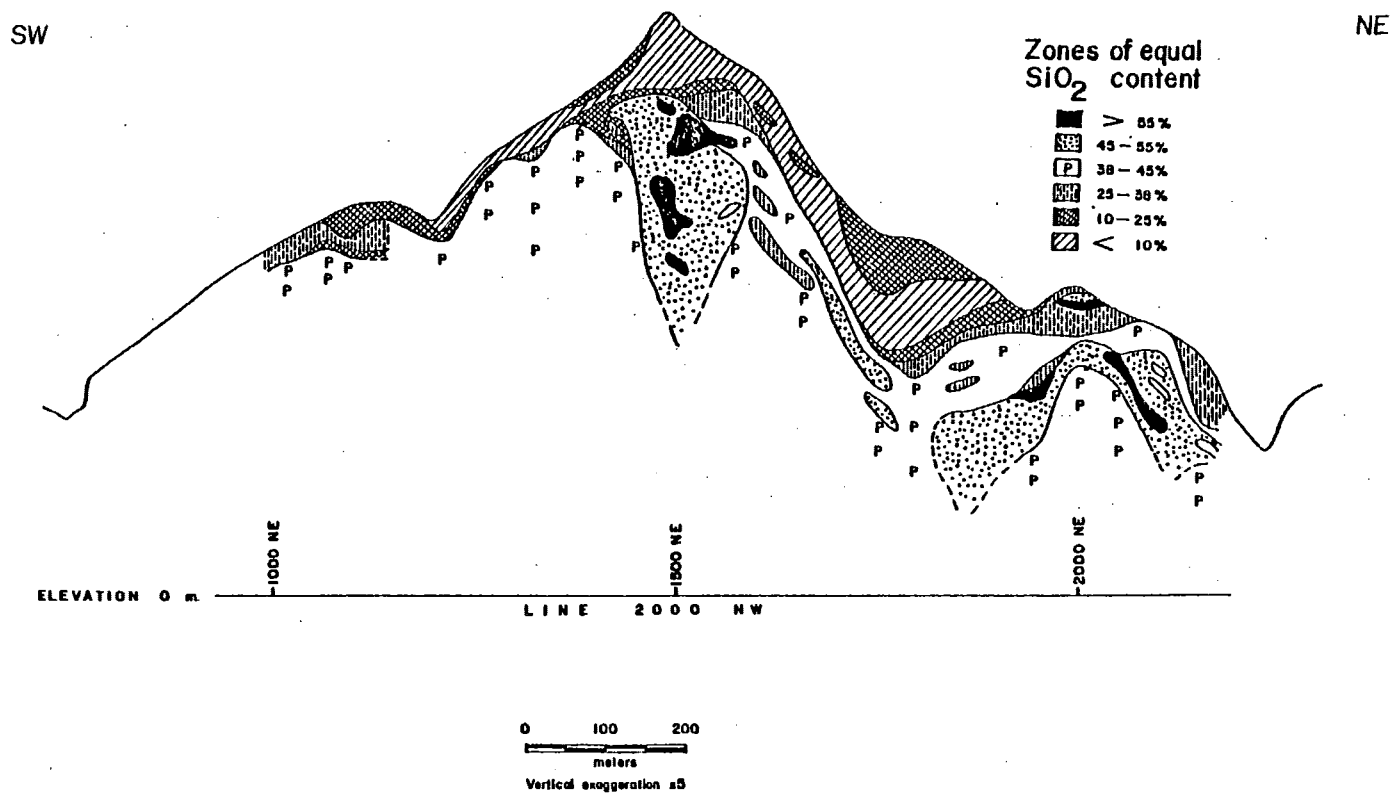
Figure 87.   Line 2000 NW, Longitudinal vertical profile showing
             zones of equal SiO_2 concentration.

these high silica value zones are roughly tabular or lensoid (e.g. profile 1300 NW, Figure 86). In general, high silica values correlate with high nickel contents (Figures 72, 73 and 74). This is reflected by the abundance of silicates, particularly smectite and serpentine, constituting the massive ore at Cerro Matoso.

Some local alignment of silica equal concentration zones corresponds approximately to fault zones and joints. Boxwork-type silica accumulations are represented on the silica profiles by roughly elongated, vertical zones where silica content exceeds 55%.

Locally, high silica values are associated with relatively high iron values (Figures 78 and 85) in material that crops out at the surface (e.g. at the coordinates 1200NW-920NE) in the form of small mounds.

Alumina

Alumina distribution profiles (Figures 88 and 89) confirm the relatively immobile character of aluminium under weathering conditions at Cerro Matoso. The highest Al_2O_3 concentrations ($>$ 10%) occur at and near surface, particularly over the NE part of the hill where a prominent progression from high alumina downwards to low alumina may be observed. These trends indicate the residual nature of the Al_2O_3 enrichment.

Isolated blocks or nuclei of relatively unweathered peridotite at intermediate levels within the laterite

SW ... NE

Zones of equal
Al_2O_3 content

■ > 10.0%
▦ 5.0–10.0%
▨ 2.5–5.0%
▧ 0.8–2.5%
P < 0.8%

0   100   200
meters

Vertical exaggeration x5

ELEVATION 29 m

1000 NE   1500 NE   2000 NE
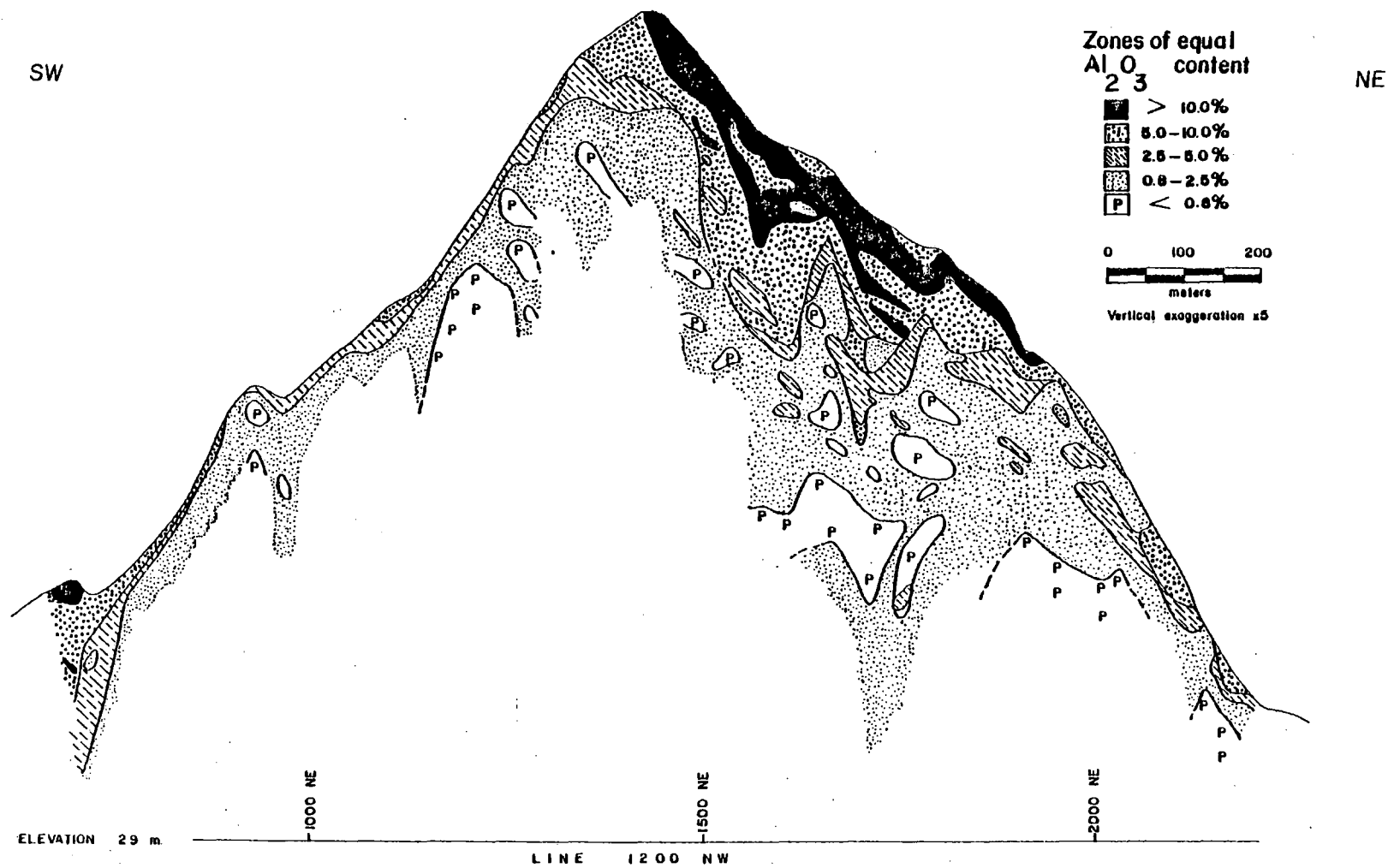
LINE   1200 NW

Figure 88.   Line 1200 NW, Longitudinal vertical profile showing zones of equal Al_2O_3 concentration.
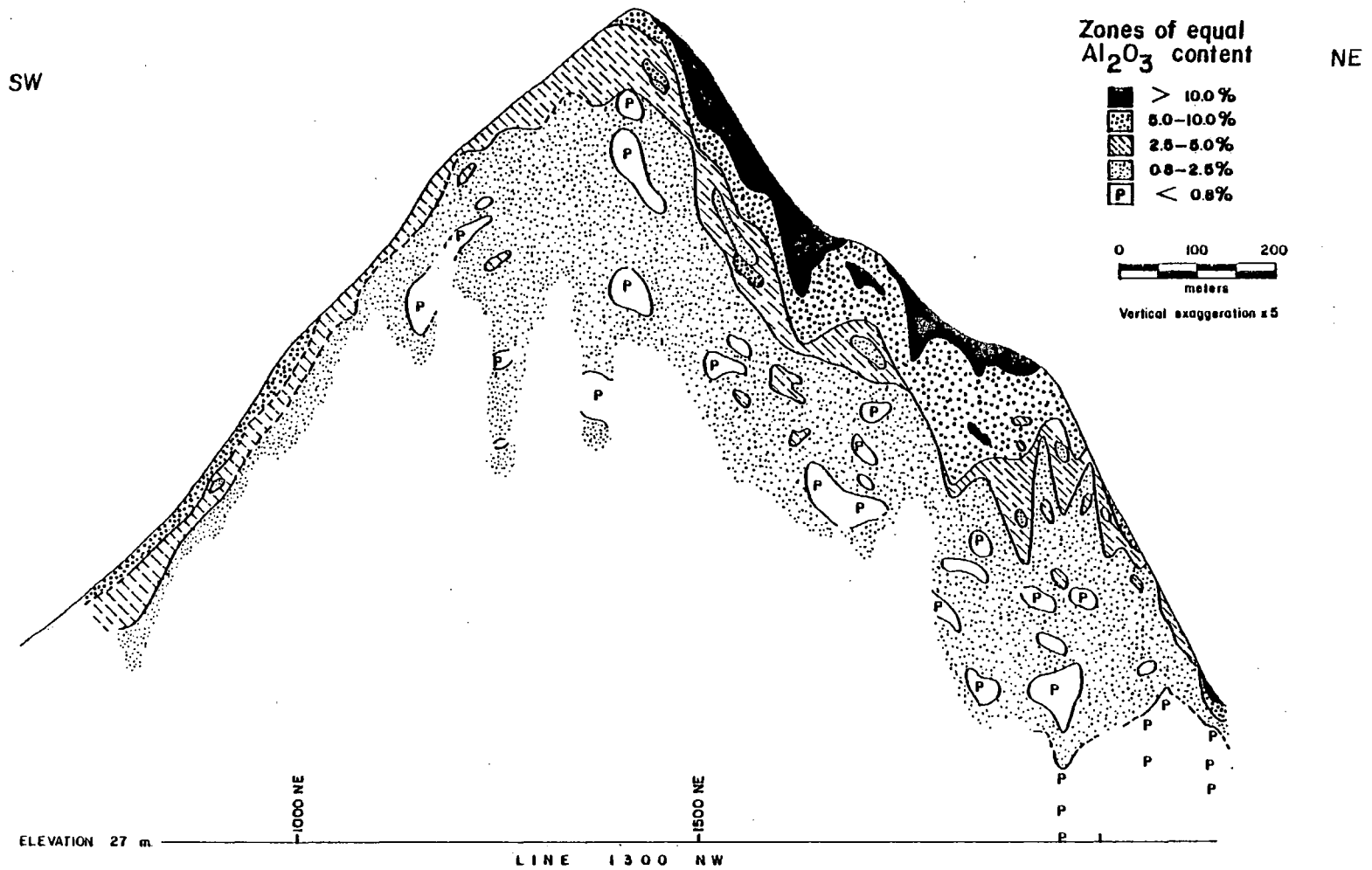
Figure 89. Line 1300 NW, Longitudinal vertical profile showing zones of equal Al_2O_3 concentration.

profile have low to very low Al_2O_3 contents. Local elongated, vertical zones of equal concentration for alumina (e.g. 0.8 – 2.5% Al_2O_3 equal concentration zone, profile 1200 NW, Figure 88) indicate the relative intensity of weathering along structures.

CORRELATION BETWEEN SELECTED CHEMICAL COMPONENTS

Statistical treatment of chemical data for drill hole samples along the profiles 500NW, 1200NW, 1300NW, and 2000NW (Appendix 1) allows generalizations to be made regarding relationships between individual components. Two features of the Minitab computer program were utilized in treating the Cerro Matoso data: X-Y graphs for pairs of elements, and first order linear regressions based upon least squares fit. The graphic approach permits visualization of general trends of point distribution, that is, whether there is a localized concentration of points, a general tendency or a random distribution in the position of the (x,y) pairs. Linear regression between elements, and particularly the determination of R-squared (coefficient of determination, or the square of the correlation coefficient), helps to establish the relative degree of correlation present between the two variables X and Y. Table 18 shows the tested regression pairs, regression equations, number of samples utilized, and resulting R-squared values.

Nickel

Relationships between Ni and Co, Fe, MgO, SiO_2, Al_2O_3, Cr_2O_3, and SiO_2+MgO were established. In all cases no

Table 18. Correlations between components, Regression equations and R-squared values.

Regression Y vs X	Regression equation Y = a + bX	Number of samples	R-squared R^2(%)
Ni,Co	Ni = 2.09 − 1.36Co	2325	0.4
Ni,Fe	Ni = 1.93 − 0.0161Fe	3618	2.8
Ni,MgO	Ni = 1.62 + 0.0017MgO	3618	0.0
Ni,MgO *	Ni = 2.87 + 0.0043MgO	1517	0.1
Ni,SiO$_2$	Ni = 1.45 + 0.0198SiO$_2$	2189	4.3
Ni,(SiO$_2$+MgO)	Ni = 1.62 + 0.0118(SiO$_2$+MgO)	2189	3.0
Ni,Al$_2$O$_3$	Ni = 2.56 − 0.107Al$_2$O$_3$	1612	7.1
Ni,Cr$_2$O$_3$	Ni = 2.66 − 0.224Cr$_2$O$_3$	1289	1.4
$\dfrac{Al_2O_3}{SiO_2}, \dfrac{Cr_2O_3}{SiO_2}$	$\dfrac{Al_2O_3}{SiO_2} = 0.0235 + 3.14\dfrac{Cr_2O_3}{SiO_2}$	1289	79.7
SiO$_2$,MgO	SiO$_2$ = 36.7 + 0.432MgO	2189	9.5
MgO,Fe	MgO = 26.3 + 0.636Fe	3618	55.0
(SiO$_2$+MgO),Fe	(SiO$_2$+MgO) = 85.4 − 1.65Fe	2189	95.7
Cr$_2$O$_3$,Fe	Cr$_2$O$_3$ = 0.168 + 0.061Fe	1289	83.3

* For Ni greater than 1.5%

correlation or very low correlation was found, which also is indicated by R-squared values that range from 0.0 (Ni versus MgO) to 7.1 (Ni versus Al_2O_3).

No correlation exists between Ni and Co, as shown by an R-squared value of 0.4 and the point distribution for (Co,Ni) pairs (Figure 90). Both elements occur in low concentrations in the original peridotite. They have a tendency to accumulate mostly by supergene enrichment, but their relative mobility appears to be different. Lack of linear correlation probably relates to differences in mobility which, in turn, accounts for the difference in their zones of maximum enrichment.

There is no simple correlation between Ni and Fe. A similar result was obtained by Trescases (1975) in his study of New Caledonia Ni laterites. General areas of (Fe,Ni) pairs concentration may be differentiated on Figure 91. For Fe values over about 30%, there is a tendency for low Ni (between 0.30-1.75%, i.e. the approximate distribution in the Limonite and Canga zones). For low Fe values under about 20%, there are two general trends: towards high Ni values (between about 1.75% to 5.0%, which corresponds to Upper Saprolite) and towards low Ni values (less than about 1.75%, corresponding to Lower Saprolite and, to a certain extent, peridotite). For Fe values between about 20% and 30%, low and high Ni values (majority at about 0.8%) correspond to the transition from Upper Saprolite zone to Limonite zone. This complexity in the Ni-Fe relationship
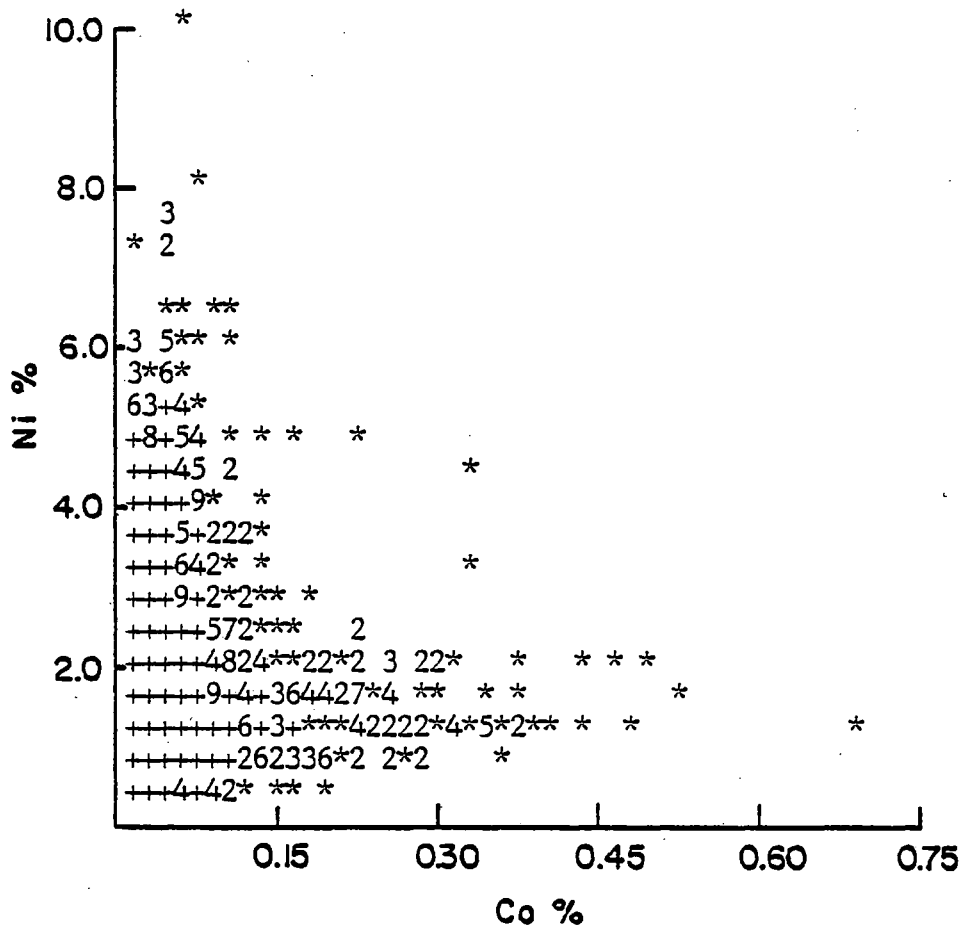
Figure 90. Point distribution for (Co,Ni) pairs.
Symbols:

+   greater than ten samples have
        this (x,y) value
*   one sample with this (x,y) value
3   all others as indicated by value
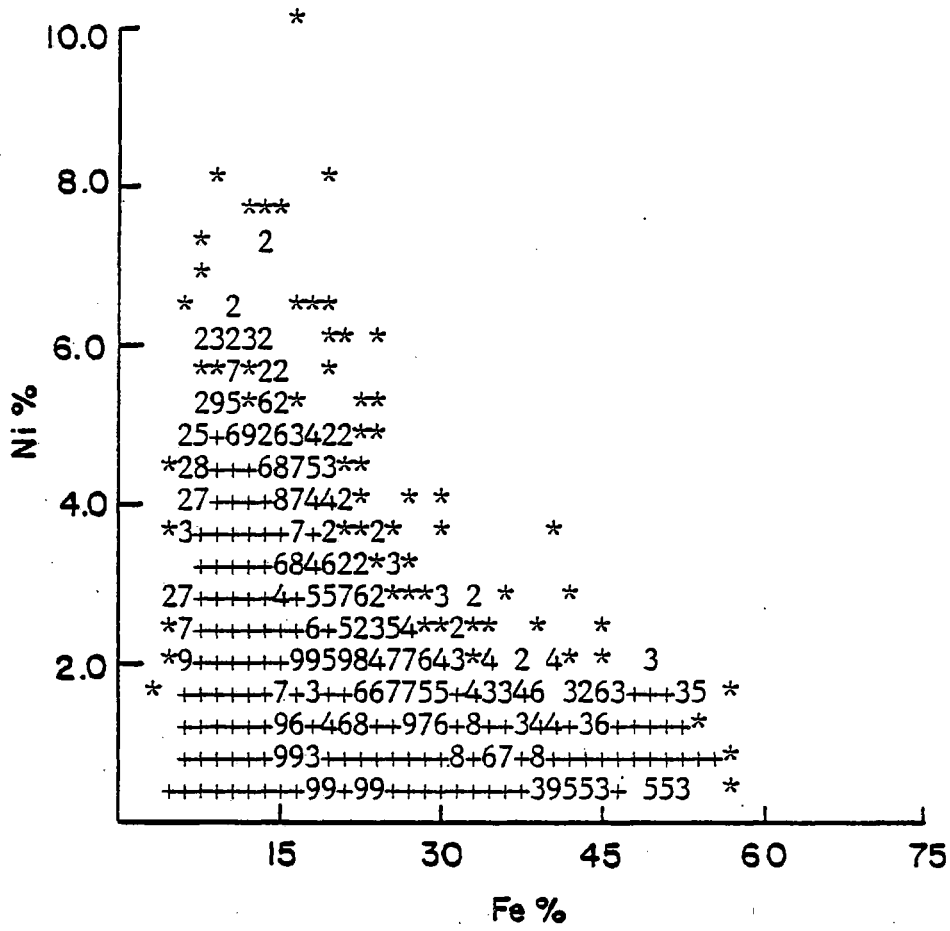
Figure 91. Point distribution for (Fe,Ni) pairs. Symbols as in Figure 90.

most likely is a function of differences in basic behaviour
of these elements: iron concentration is mostly residual in
character (Golightly, 1981) whereas Ni may be accumulated
by supergene as well as residual processes.

Ni and MgO show no correlation whether all MgO-Ni pairs
are considered (Figure 92) or if the regression is
restricted to Ni values over 1.5% cutoff grade (Figure 93).
This lack of correlation probably relates to differences
in the mobility of these components through the laterite
profile. Magnesium is a highly mobile element and MgO
content tends to progressively decrease from peridotite
bedrock upwards to Canga. Ni is less mobile than Mg and
accumulates both by supergene and residual processes. As a
result, Ni distribution does not correlate with that of MgO
but fluctuates from low (in Peridotite and Lower Saprolite)
through high (at the base and middle levels in Upper
Saprolite), to moderate (upper part of the Upper Saprolite)
and back to low (Limonite and Canga zones) contents.

Lack of correlation between Ni and SiO_2 is shown in the
graphical representation of the (SiO_2,Ni) pairs distribution
(Figure 94) and by a very low R-squared (4.3%) from the re-
gression analysis. However, Ni enrichment clearly relates
to intermediate SiO_2 concentrations of 38-60% which corre-
sponds to the Upper and Lower Saprolite zones.

Observations for Ni versus MgO+SiO_2 distribution are
similar to those found for Ni versus MgO and Ni versus SiO_2.
Although there is no linear correlation between Ni and

```
10.0 ┌        *

 8.0 ├    *       *
            **  *
        *       **
                    *
 6.0 ├  *   **  *   **
     ***  * * 2 * *22*    *
          *3 ** 3*4*
     2* **2*** *22 2232 4
     **  **432276443*56*2 *
     2* *2242634887755658234    *
 4.0 ├*22333525263+83636944332*
     *2* *54347548+5+88+7+6872224   *
     25 **34323263573986++8888 322 *
     23772524534345657+++++++++745252 2
     *885532462559975++++79+++7++6 2*
 2.0 ├+7++5437575+63449+96+6+98+734532** *
     +++7+87443*26659459++++9+837776423
     +++6242245328444746378699+++7957732*
     +++3872*8*255369677++++9+8++8+++7+44*
     +997***** **2 *28++8++++++++++++++++8*
     └─────┬────┬────┬────┬────┬
          10    20   30   40   50
```

Ni %

MgO %
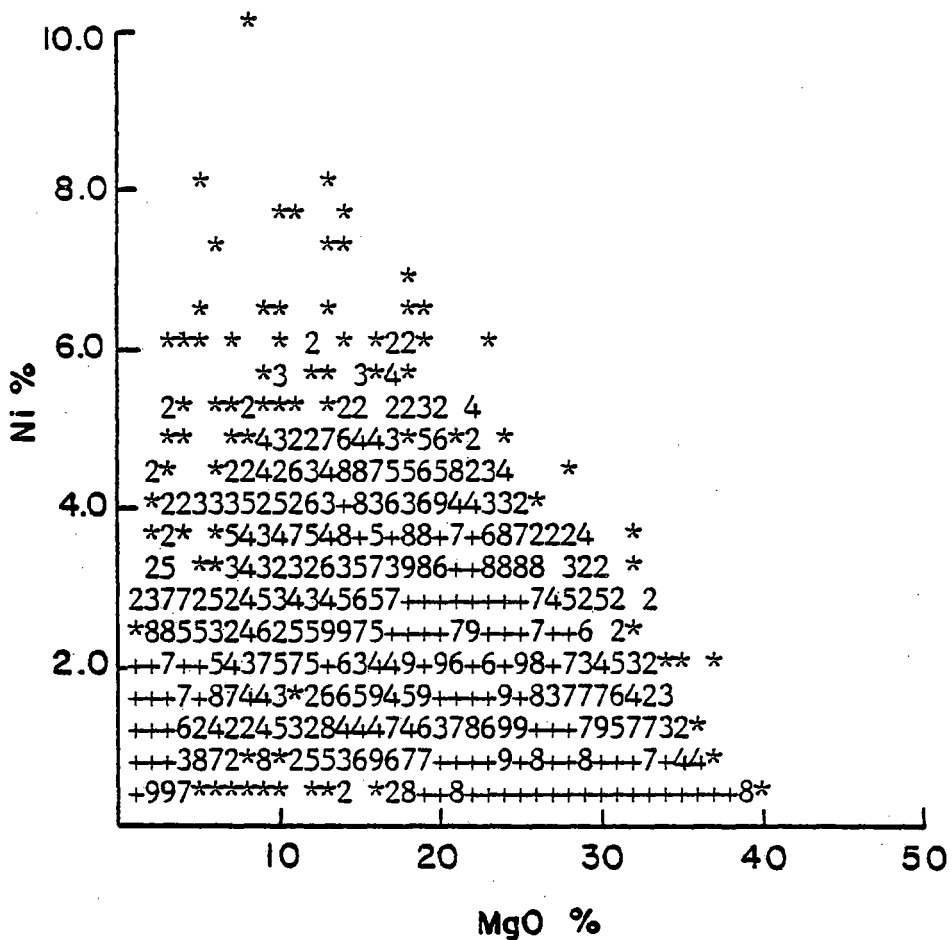
Figure 92. Point distribution for (MgO,Ni) pairs. Symbols as in Figure 90.
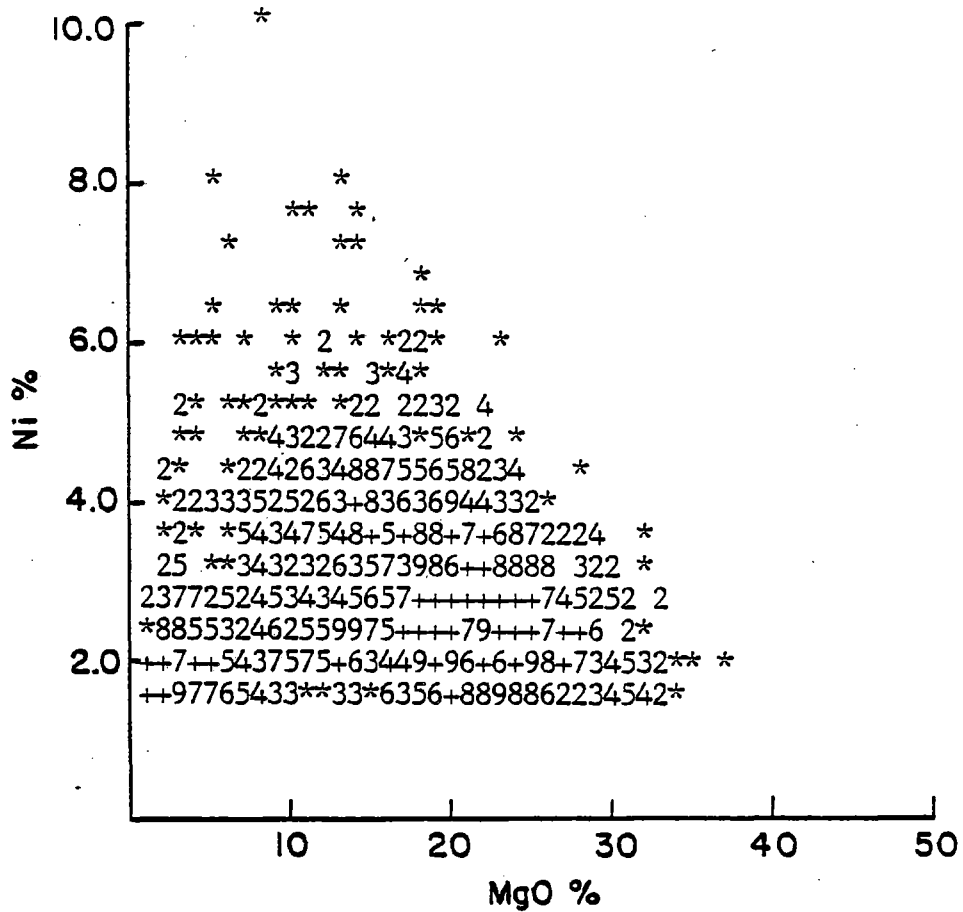
Figure 93. Point distribution for (MgO,Ni) pairs, and
Ni greater than 1.5%. Symbols as in Figure 90.
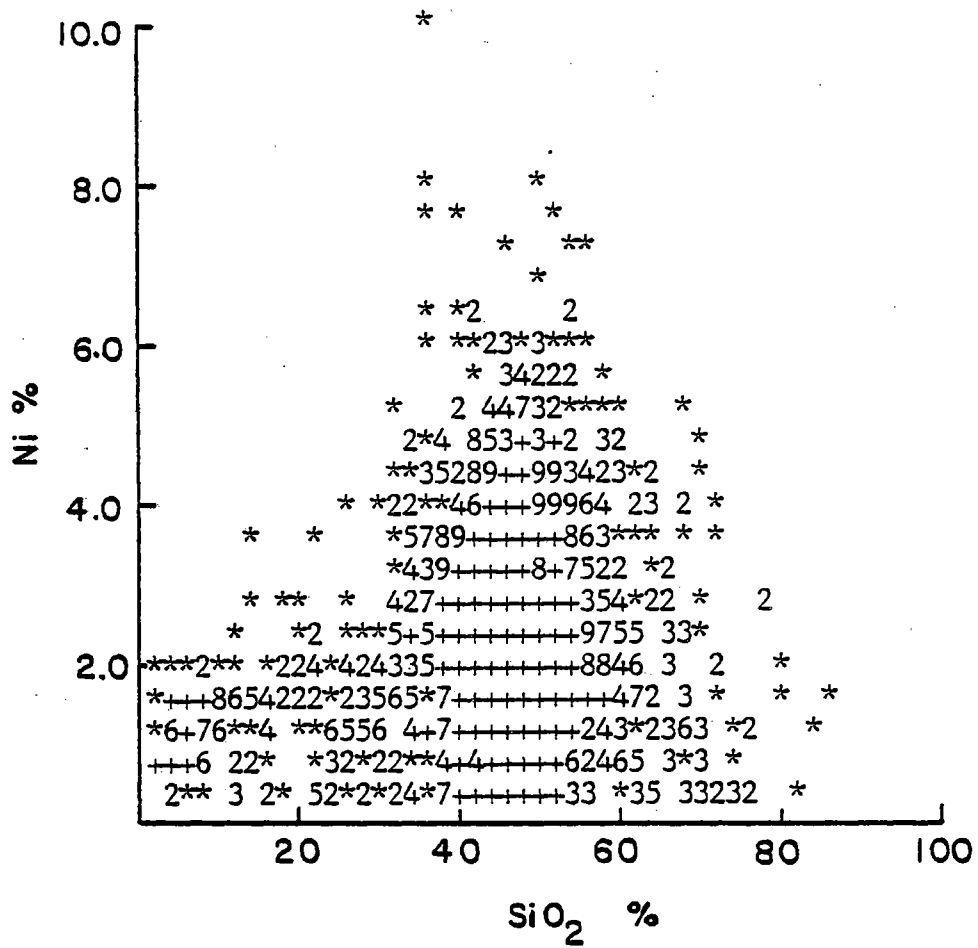
Figure 94. Point distribution for (SiO₂,Ni) pairs. Symbols as in Figure 90.

$MgO+SiO_2$, the highest Ni values correspond to high $MgO+SiO_2$ values (Figure 95). This relates to the presence of Ni-bearing silicates found at the saprolite level in which smectite- and serpentine-type minerals are the most abundant mineral components.

Plots of Ni versus Al_2O_3 (Figure 96) and Ni versus Cr_2O_3 (Figure 97) show a general tendency for Al_2O_3 and Cr_2O_3 to behave similarly with respect to Ni. No correlation was found in either case, although the saprolite zone, which is characterized by Ni enrichment (values ranging from 0.8 to 5.0%), typically contains relatively low Al_2O_3 and Cr_2O_3. This seems to suggest that the high variability in the point distribution diagram is mostly influenced by the variable behaviour of nickel.

Al_2O_3 and Cr_2O_3 behaviour can be best tested by ratioing both components with respect to a leached component such as SiO_2. (x,y) pairs distribution and regression analysis for Al_2O_3/SiO_2 versus Cr_2O_3/SiO_2 (Figure 98, Table 18) give a relatively good positive correlation with an R-squared value of 79.9%. Al_2O_3 and Cr_2O_3 appear to behave in a similar manner, both being residually enriched in the laterite profile (Golightly, 1981).

SiO_2, MgO, Fe, Cr_2O_3

The general distribution observed in Figure 99 for (MgO,SiO_2) pairs and an R-squared value of 9.5% indicate no simple linear relationship between these components. From
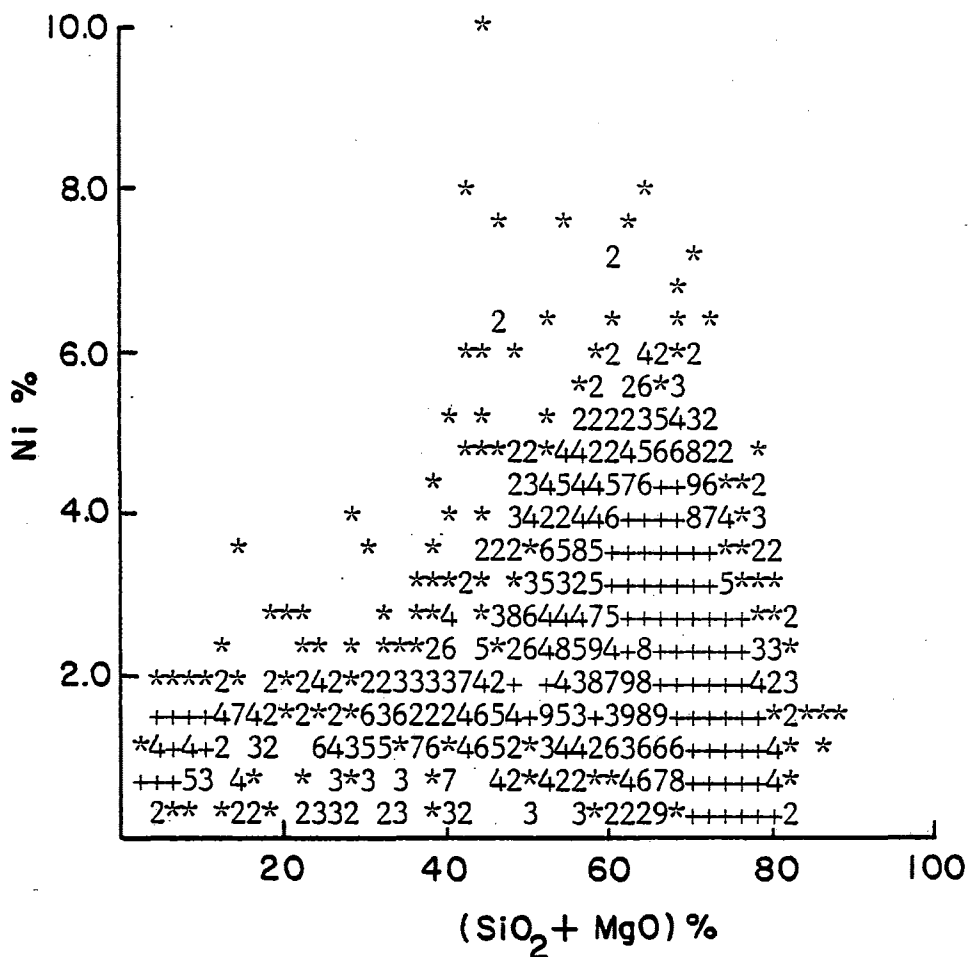
Figure 95. Point distribution for $[(SiO_2+MgO),Ni]$ pairs. Symbols as in Figure 90.
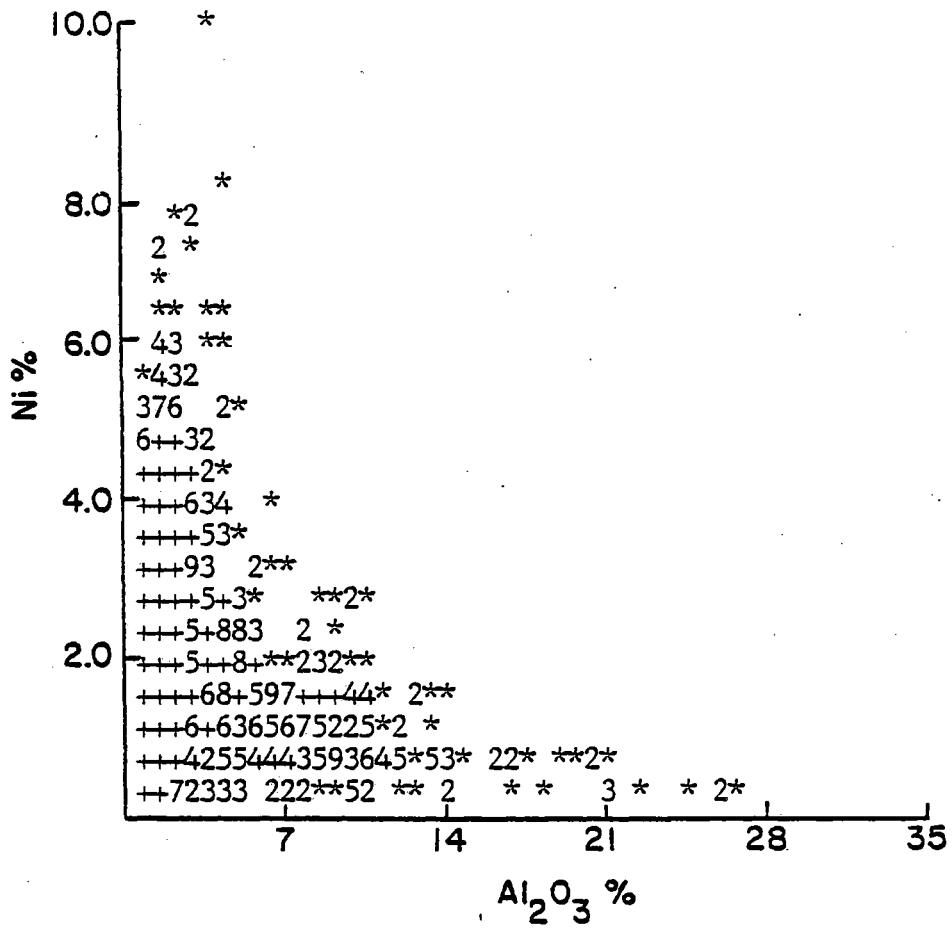
Figure 96. Point distribution for (Al_2O_3, Ni) pairs.
Symbols as in Figure 90.
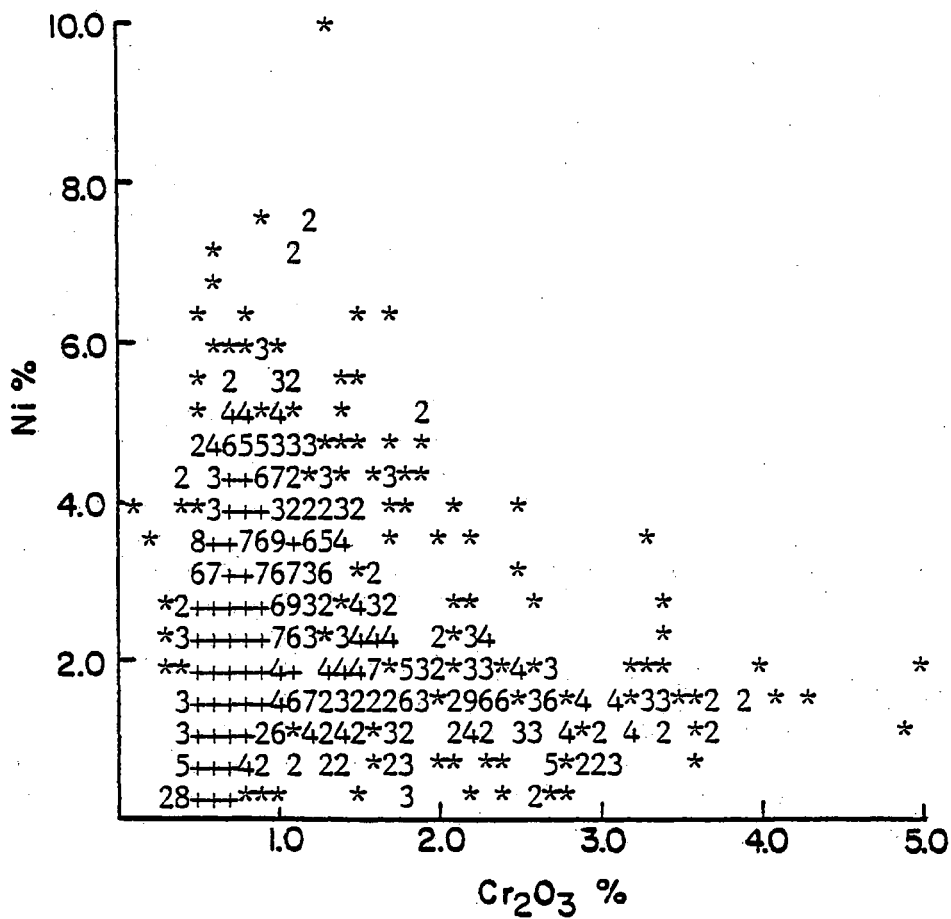
Figure 97. Point distribution for (Cr_2O_3, Ni) pairs. Symbols as in Figure 90.
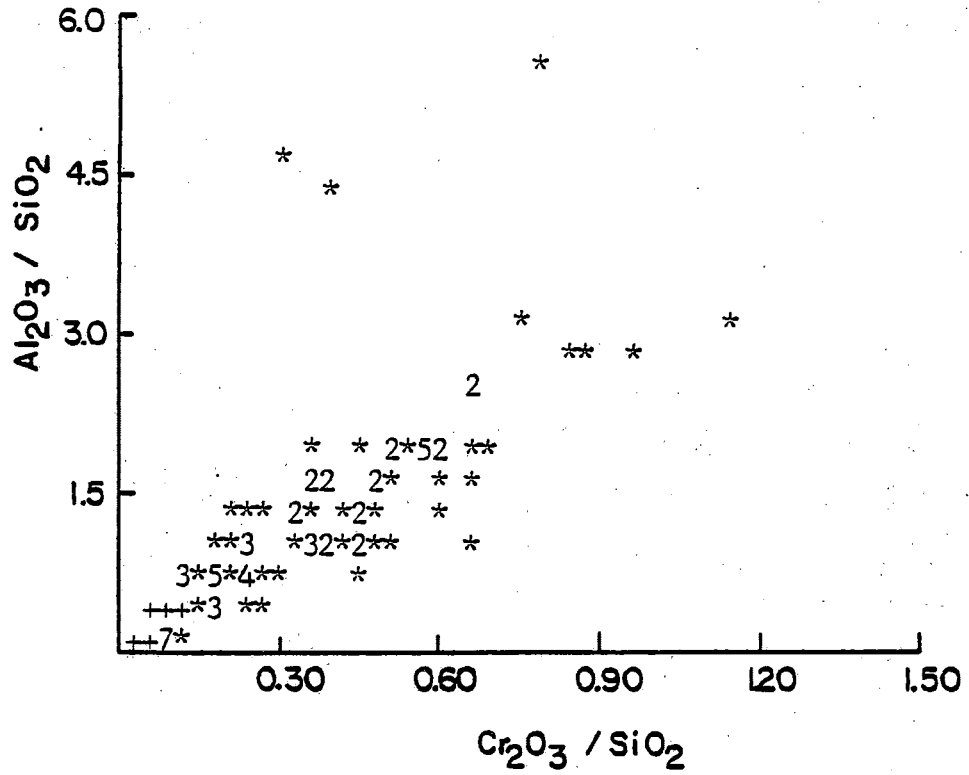
Figure 98. Point distribution for $(Cr_2O_3/SiO_2, Al_2O_3/SiO_2)$ pairs. Symbols as in Figure 90.
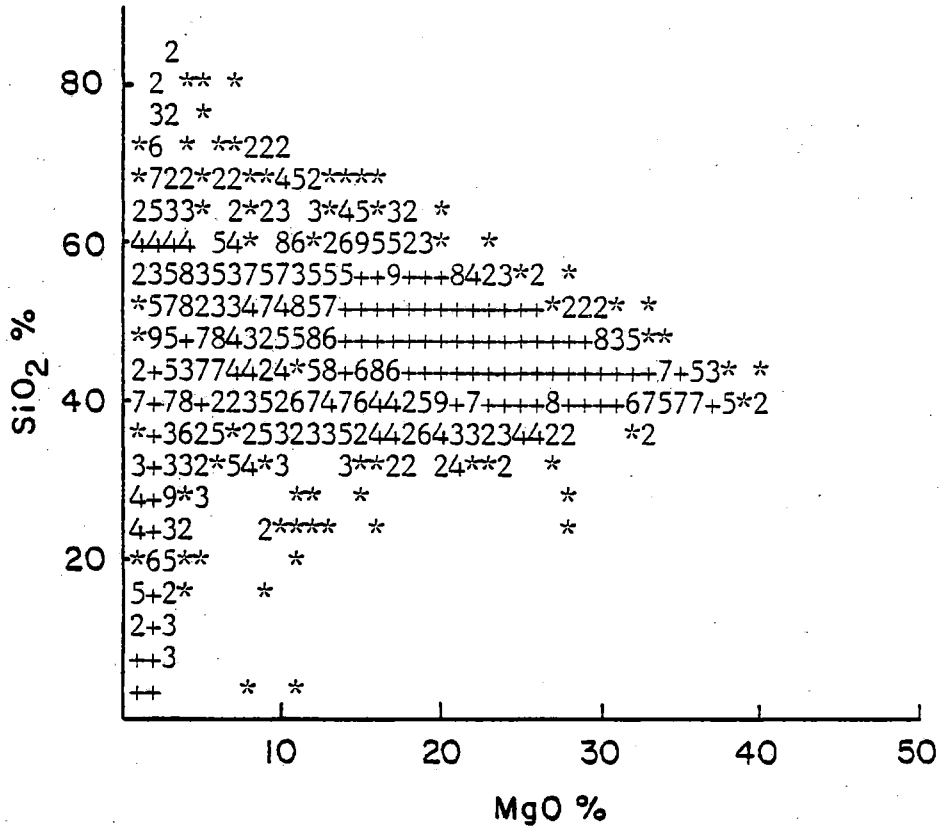
Figure 99. Point distribution for (MgO,SiO$_2$) pairs. Symbols as in Figure 90.

high to moderate MgO values (i.e. from about 40 to 12% MgO), silica values remain relatively high; silica decreases in zones where MgO values are low to very low. One possible explanation for this behaviour may be the greater mobility of MgO over SiO_2; MgO apparently is removed more rapidly from the profile than SiO_2 (Zeissink, 1969; Trescases, 1975). Another possible explanation may be related to sampling density through the different units of the laterite profile: most samples are from slightly to moderately weathered horizons (Lower to Upper Saprolite zones), and the general distribution for (MgO, SiO_2) pairs also may be reflecting magmatic trends.

In the case of MgO and Fe, a low to moderate correlation is indicated by an R-squared value of 55.0%. The general trend of the point distribution (Figure 100) appears to be somewhat hyperbolic. Fe values under about 20% are approximately related to higher MgO values (majority between about 10% and 40%, which corresponds to Upper and Lower Saprolite zones). For Fe values over about 30%, there is a tendency for low MgO (less than about 4%, which corresponds to the Limonite and Canga zones). The 'inflection' zone in this general trend is between about 20 and 30% Fe which probably reflects the transition from the Upper Saprolite to the Limonite zone. Differences in mobility between iron and magnesium, and the character of iron concentration may explain the Fe-MgO relationship: Mg is a highly mobile element, whereas Fe has a significantly lesser
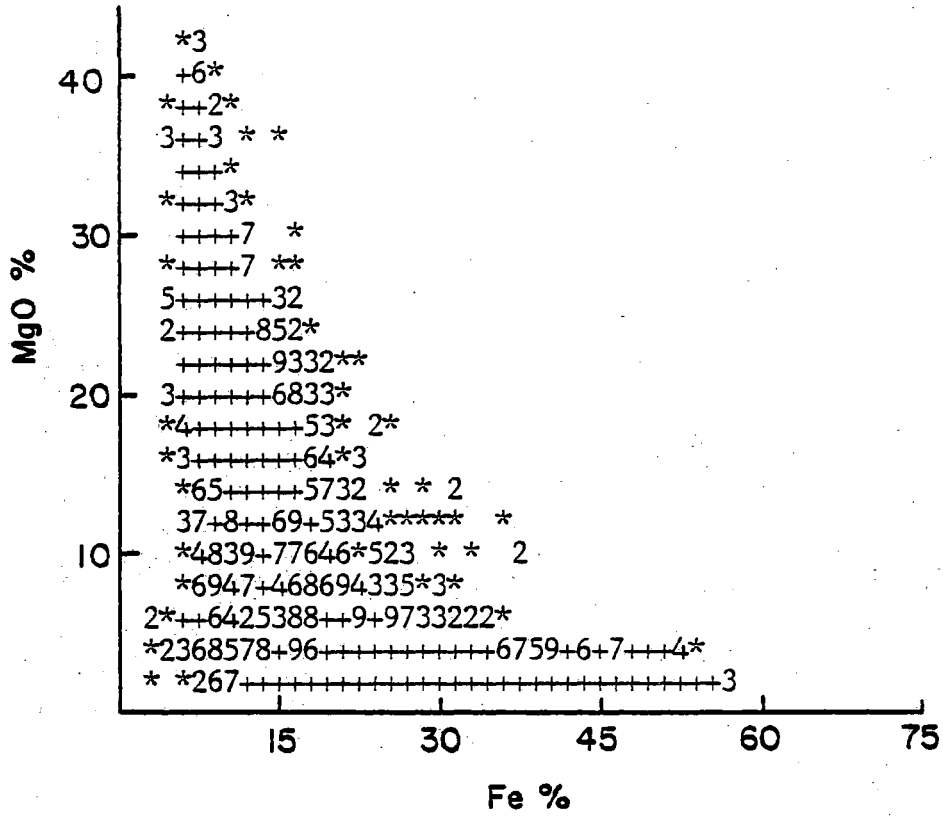
Figure 100. Point distribution for (Fe,MgO) pairs.
Symbols as in Figure 90.

mobility than Mg and tends to accumulate mostly by residual processes.

If Fe is plotted against (SiO_2+MgO) (Figure 101) and a regression is determined, the R-squared value increases dramatically to 95.7% and a very good negative linear relationship is apparent. Low Fe values correspond to high (SiO_2+MgO) values and vice versa. This suggests that MgO and SiO_2 are leached out at about the same time that Fe is being accumulated. Furthermore, it also reflects the decreasing proportion of silicates and increasing proportion of goethite upwards in the profile (Golightly, 1979a).

The relatively residual character of Fe may be tested if its distribution is compared with other resistant components. When Fe is plotted with the highly immobile component Cr_2O_3 (McFarlane, 1976), a general linear trend is observed (Figure 102). The linear regression of the (Fe, Cr_2O_3) pair gives an R-squared value of 83.3% and indicates a relatively good positive correlation between both components, i.e. Fe content tends to increase upwards in the profile with increase in Cr_2O_3, which indicates the residual nature of both components.
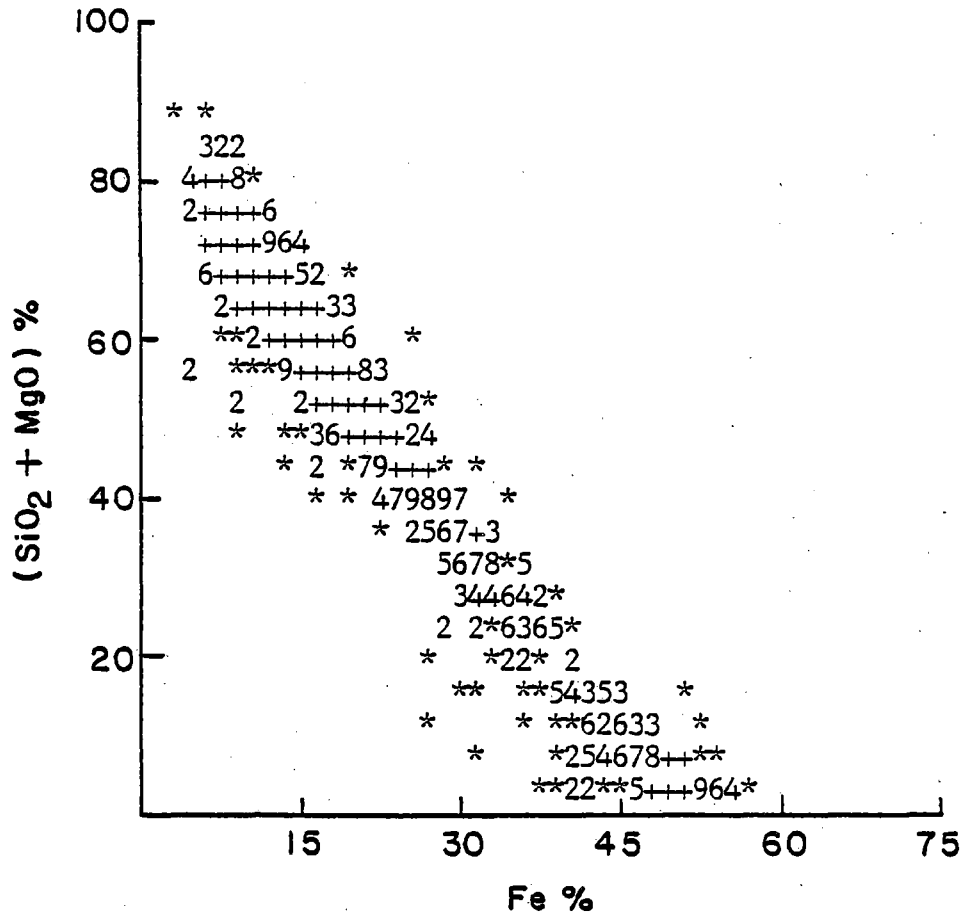
Figure 101. Point distribution for $[Fe, (SiO_2+MgO)]$ pairs. Symbols as in Figure 90.
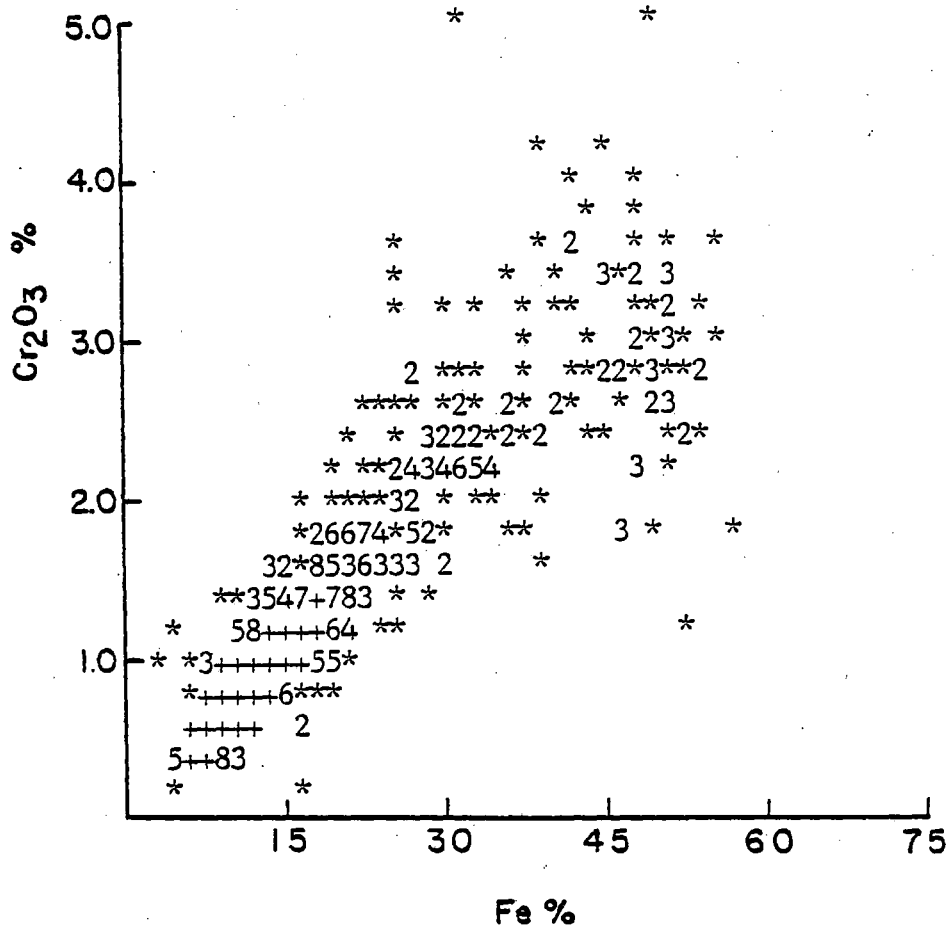
Figure 102.   Point distribution for (Fe, Cr_2O_3) pairs.
Symbols as in Figure 90.

FACTORS IN DEPOSIT GENESIS

The conjunction of several factors led to the development of the Cerro Matoso nickeliferous laterite deposit. Although each factor is described separately, it must be kept in mind that the efficiency of nickel enrichment by the lateritization process does not depend exclusively upon one factor but is the result of the combined influence of all relevant factors.

Parent material

The peridotite body at Cerro Matoso is composed almost exclusively of harzburgite in which olivine dominates (83%) and orthopyroxene and secondary serpentine occur as subordinate components (9% and 7%, respectively). Nickel content in this parent rock ranges from 0.28 to 0.36%.

It has been recognized by many workers that lateritic weathering of peridotite has a good probability of generating sufficiently high nickel values to be of economic interest. The most favourable peridotites are harzburgite and dunite (de Vletter, 1978; McFarlane, 1983) but, due to the relatively high mobility of nickel, original contents of this element in the parent rock must be relatively high for economic nickeliferous laterite deposits to form

(McFarlane, 1983). In this context, there is considerable disagreement between authors regarding the minimum nickel content required in the original peridotite. Minimum contents of 0.2%, 0.3% or even 0.4%Ni have been established as a compositional requisite for parent peridotite by various workers (e.g. Golightly, 1979a; Golightly, 1981; McFarlane, 1983).

The degree of serpentinization of the peridotite appears to be very important in the development of silicate-type nickeliferous laterites as serpentines may have an important effect on the physico-chemical response of peridotite to weathering. There is no apparent loss or enrichment of nickel during the serpentinization of olivine (Faust and Fahey, 1962; Perruchot, 1971), thus the nickel distribution in the original peridotite seems to be retained regardless of the degree of serpentinization (Avias, 1978). However, serpentinization products do influence the relative response of peridotite to weathering. Troly et al. (1979) observed that olivine in New Caledonia peridotites is broken down more easily than serpentine and alteration of weakly serpentinized peridotite was stronger than in highly serpentinized peridotite. Development of the laterite profile was greater in weakly serpentinized peridotite both in vertical extent and in the degree of enrichment of nickel-rich secondary products. This behaviour probably also is influenced by relative differences in permeability as intense serpentinization appears to create a relatively impermeable rock

mass (Maynard, 1983; McFarlane, 1983). Water circulation would be inhibited in the serpentinized rock in such a way that even though general conditions may be favourable to Ni enrichment, the development of economic nickel accumulations appears to be restricted principally to near surface units such as Limonite and Canga (Lelong et al., 1976).

The Cerro Matoso peridotite appears suitable as parent material for Ni laterite development from the stand point of original nickel content, harzburgite composition, and low degree of serpentinization for most of the rock mass. Localized areas of intense serpentinization, particularly along shear zones in the southeast part of the body, exhibit saprolite with nickel concentrations that are considerably lower than values in saprolite over only slightly serpentinized harzburgite. Nickel values in saprolite developed from intensely serpentinized harzburgite commonly are similar to those in unweathered harzburgite (0.36%), although locally values may reach 1.0%Ni.

Climate

Although there is no direct evidence for the climatic conditions that prevailed at the time of the Cerro Matoso laterite formation, relationships between the peridotite body and adjacent sediments of the Ciénaga de Oro Formation provide climatic inferences. Partially lateritized peridotite (i.e. Ni laterite profile without a great vertical extent) is overlain locally by sediments of the early

Oligocene-early Miocene Ciénaga de Oro Formation along the northeastern boundary of the Cerro Matoso hill (Plate 3, Figure 6). Chemical weathering must have been active slightly before and during the earlier stages of deposition of the sedimentary sequence, and nickel and iron were leached from the peridotite body and incorporated within the sediments, not only in the siltstones and sandstones but also in the interbedded carbonaceous shales and coals. Clearly, water was available for the transport of elements from the peridotite into the adjacent sedimentary basin.

The presence of interbedded coals in the Ciénaga de Oro Formation suggests a warm humid climate (Blatt, 1982) with moderate to heavy rainfall (Jensen and Bateman, 1981). Palynological studies of coals from different beds within the Ciénaga de Oro Formation (Dueñas, 1980) show that they formed for the most part from a mangrove type vegetation similar to that currently growing in other places in Colombia. These sites correspond to swampy areas and are characterized by temperatures in excess of $26^{\circ}C$, average annual rainfall greater than 3,500 mm and relative humidity on the order of 80% (Espinal, 1977).

It appears, therefore, that at least during part of the time in which the Cerro Matoso Ni laterite was forming, there was a tropical humid and rainy climate with probable alternating wet-relatively dry seasons. It has been recognized that in the lateritization process dissolution and leaching of metals take place during rainy seasons

(de Vletter, 1978) and formation of some secondary compo-
nents in the laterite profile may occur during relatively
dry seasons (Golightly, 1979a). Alternating conditions
have been suggested as necessary for sesquioxide precipita-
tion (McFarlane, 1976) as well as for smectite formation
(Harder, 1977; Golightly, 1981) and silica deposition
(Golightly, 1979a). The above conditions probably prevailed
during at least part if not all of the development of the
Canga, Limonite and Saprolite zones, and silica boxworks at
Cerro Matoso.

Tectonics

Tectonic activity has played an important role in the
evolution of the laterite profile at Cerro Matoso, either
through generation of structures such as faults and joints
or providing favourable conditions for successive rejuve-
nation of the profile which resulted in greater nickel
enrichment.

Initial structural preparation of the Cerro Matoso
peridotite body probably was related to the Pre-Andean
orogeny. The Pre-Andean orogeny (van der Hammen, 1958)
occurred during Paleocene-Middle Eocene time, apparently
in response to the interaction between the Caribbean and
the South American plates (Mattson, 1984). Resulting
stresses were mainly compressional and particularly intense
during the late phases of this orogeny (Malfait and
Dinkelman, 1972; Irving, 1975). According to Dueñas and

Duque-Caro (1981), regional NNE trending faults formed in northwestern Colombia as a result of these intense lateral compressional stresses. The Cerro Matoso peridotite body, which has been exposed at least in part since Middle Eocene time (Duque-Caro, 1979; Dueñas and Duque-Caro, 1981), exhibits a NNE trending fault system which apparently resulted from tectonic activity related to the Pre-Andean orogeny.

Fracturing of the parent peridotite has influenced the development of the laterite profile and the nickel mineralization at Cerro Matoso. Fractures are important in that they permit ready access to meteoric solutions for leaching of soluble components and formation of secondary products. In the saprolite zone, isolated blocks in which the inner part is less weathered and has lower nickel content than the outer part indicate that weathering has proceeded preferentially from joints and fractures inwards to the core of the blocks leading to the development of massive ore. Locally, tongues of intensely weathered material occur in the Lower Saprolite zone and are fault-limited, indicating that faults may serve as conduits for weathering to proceed to relatively great depths. This effect was observed along benches and is readily inferred from geochemical profiles of element distribution. Part of the ore occurs along zones of intense fracturing, either as fracture fillings, colloform deposits in cavities along fractures, or crusts coating joints and fractures. Although this ore type is not the most important part of the deposit

volumetrically, locally it may attain grades up to 30% Ni thus emphasizing the importance of fractures as effective channelways for migration of nickel-rich solutions.

Additional nickel enrichment and thickening of the massive ore at Cerro Matoso appear to have occurred as the result of renewed episodes of laterite development. Tectonic effects such as uplift and block faulting involving a lateritized terrain may result in rejuvenation of the weathering process. As the groundwater table is lowered and new faults, fractures, and/or joints are formed or old structures are reactivated, fluid circulation increases (de Vletter, 1978), differential leaching is activated by the return to vadose conditions in the upper part of the profile (McFarlane, 1983), and the process of nickel enrichment is enhanced. Faulting of massive silica accumulations and of garnieritic fracture fillings indicates that tectonic reactivation with resulting slight to moderate uplift has occurred at Cerro Matoso.

In order for additional vertical development of the laterite profile and enhancement of nickel contents in the saprolite zone to occur, a balance between uplift and erosion must have existed (McFarlane, 1983). If uplift had been intense, the laterite profile probably would have undergone strong dissection and original units would have been rapidly eroded (Lelong et al., 1976). A NW trending fault system developed at Cerro Matoso during the late Miocene-Pliocene Andean orogeny and the southwestern part

of the weathered peridotite was uplifted relative to the
northeastern part. This uplift apparently was sufficient
for intense erosion to remove most of the laterite profile
from the uplifted block while the northeastern block was
being only slightly modified. In the northeastern block,
minor uplift apparently occurred such that erosion was not
so intense as in the southwestern block; the groundwater
table was lowered and an increase in the vertical extent
of the laterite profile as well as local nickel redistri-
bution probably were favoured (McFarlane, 1983).

Role of pH-Eh

Variations in pH, and to a lesser extent in Eh, of the
weathering solutions have resulted in selective differential
element accumulation and mineral formation throughout the
laterite profile. In particular, nickel was enriched at
intermediate depths where nickel-bearing silicates devel-
oped in the saprolite zone.

The distribution of nickel and iron in the laterite
profile may be evaluated in terms of a pH-Eh diagram
(Figure 103). It may be inferred from the diagram that
slight shifts in the pH or Eh of the weathering solutions
may drastically alter the relative chemical mobility of
iron and lead to changes in its oxidation state (Krauskopf,
1967; Norton, 1973). At the uppermost part of the profile
where slightly acidic and relatively oxygenated solutions,
with Eh's generally over 0.3 volts and pH's around 5.0,
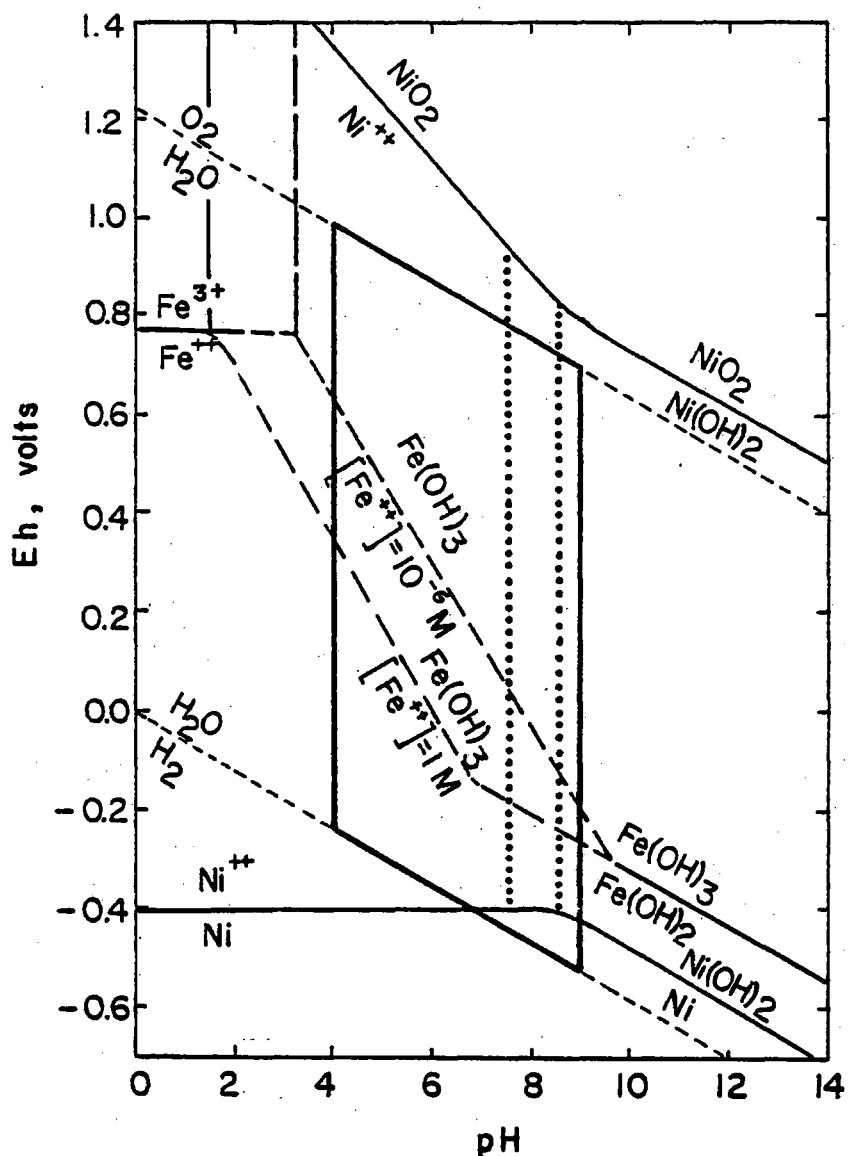
Figure 103. pH-Eh diagram for iron and nickel at 25°C. Parallelogram in center indicates approximate pH-Eh conditions found in weathering environment. pH value for the boundary between Fe^{3+} and $Fe(OH)_3$ is near 3 (long dashed lines), the exact value being a function of the total iron concentration. Boundary between Ni^{2+} and $Ni(OH)_2$ may range from 7.5-8.5 pH values (dotted lines) and depends on total nickel concentration. Modified after Krauskopf (1967), Trescases (1975) and Levinson (1980).

commonly dominate (Trescases, 1975; McFarlane, 1976), iron is oxidized from the ferrous to ferric state, and precipitates as goethite, $Fe(OH)_3$. On the other hand, if pH decreases (e.g. to about 3.5), Fe^{3+} may be reduced to the soluble Fe^{2+} state and be remobilized (Schorin, 1981). Locally, decrease in pH to values as low as 3.0 or less have been observed at the top of the Canga zone (McFarlane, 1976) and may be accomplished by introduction of atmospheric CO_2 in rainfall and of organic acids derived from decaying organic matter (Keller, 1968; Krauskopf, 1979). Soluble iron may be either leached out of the system or migrate downwards through relatively short distances in the profile. Downward iron remobilization is limited to a few meters in the Canga zone (Dorr, 1964), and pH rapidly changes from about 3.0 at the top of the Canga zone to slightly over 5.0 at middle and lower levels of the Canga zone (Trescases, 1975; Golightly, 1981). Under these conditions (pH above 5.0 and Eh near or greater than 0.3 volts), Fe^{2+} is readily oxidized to Fe^{3+} and goethite precipitates (Krauskopf, 1979; Levinson, 1980). This probably explains the dramatic increase in iron accumulation observed at middle and lower levels of the Canga zone.

The high mobility of nickel is readily inferred from Figure 103. In the laterite profile, Eh may range from as high as 0.7 down to about 0.1 volts (Levinson, 1980) whereas pH may range from around 3.5 to 9.0 and slightly greater (Krauskopf, 1967; Trescases, 1969; Trescases, 1975). Under

these Eh and pH conditions, Eh variations do not appear to affect nickel solubility, whereas pH shifts towards alkaline conditions promote nickel precipitation. As iron precipitates at the pH conditions found at the upper part of the laterite profile, the more soluble nickel may be either partially incorporated into the goethite structure (Sahoo et al., 1981), leached out of the system, or migrate downwards to deeper levels. pH increases with depth (Golightly, 1981) and when alkaline conditions are reached, nickel solubility decreases drastically and nickel supergene enrichment occurs. Alkaline conditions are attained at the saprolite level where secondary nickel silicates are formed.

Silica behaviour in the weathering profile also is important in laterite nickel systems in that the principal Ni ore is composed of silicate minerals. Silica solubility increases sharply at pH's above 9, but in the pH range 4 to 9 it appears to be modest and essentially independent of pH (Krauskopf, 1959). However, experimental work by Marshall (1980a; 1980b) and Marshall and Warakomski (1980) has shown that, for solutions in the pH range 5 to 7.5, silica solubility may decrease significantly in the presence of dissolved cations, particularly Mg^{2+} (Figure 104). This decrease is essentially dependent on the nature of the cation, and high hydration number cations such as Mg^{2+} appear to have the greatest influence in decreasing silica solubility.

These observations may be useful in the interpretation of chemical reactions that occur during development of the
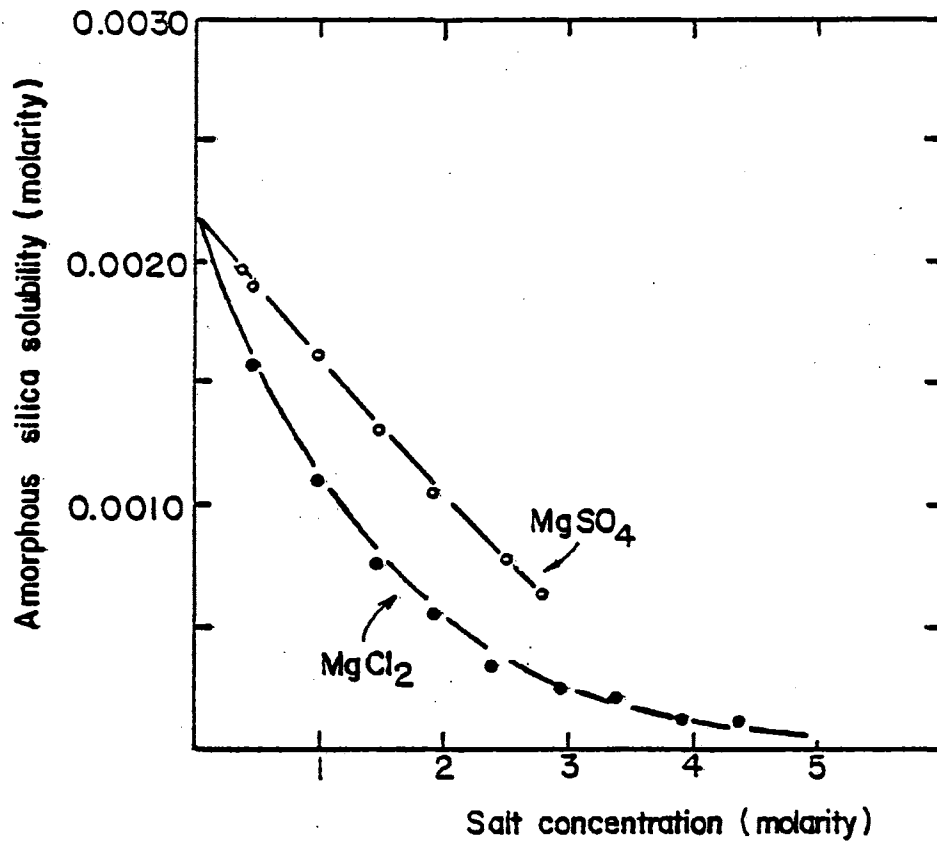
Figure 104. Solubility of amorphous silica in aqueous salt solutions at 25°C (after Marshall and Warakomski, 1980).

laterite profile. Silica and magnesia constitute as much as 80% of the original peridotite composition. During weathering, both components are released from the parent rock (Golightly, 1981), magnesium being more mobile than silica (Trescases, 1975). At the upper parts of the profile, magnesium is readily leached out of the system. At intermediate levels dissolved magnesium content may build up relatively rapidly (Golightly, 1979) and be accompanied by increase in the pH of the solution. Trescases (1975) reports pH values of about 7.5 in groundwater samples from weathered peridotites in New Caledonia. Increase in dissolved magnesium is associated with decrease in silica solubility at a depth (Upper Saprolite zone) where nickel also is relatively immobile. These conditions are favourable for the precipitation of nickel silicates (i.e. the massive ore minerals). The combined behaviour of nickel, magnesium, and silica in the laterite weathering environment also explains the formation of pimelite associated with chalcedony as fracture fillings associated with massive ore in the Upper Saprolite zone.

CONCLUSIONS

Geological and geochemical aspects and history
of the Cerro Matoso nickeliferous laterite

The Cerro Matoso harzburgite is situated along the
Romeral fault zone and was brought to the surface during the
late phases of the Pre-Andean orogeny in middle Eocene-late
Eocene time (Dueñas and Duque-Caro, 1981). The Pre-Andean
orogeny apparently occurred in response to the interaction
between the Caribbean and the South American plates (Burke
et al., 1984; Mattson, 1984). Resulting stresses were main-
ly compressional and particularly intense during the late
phases of this orogeny (Malfait and Dinkelman, 1972; Irving,
1975). Compressional stresses gave rise to faults in the
peridotite body that roughly parallel the NNE trend of the
Romeral paleo-trench. Serpentinization occurred locally
during the Pre-Andean orogeny, particularly along fault
zones towards the eastern and western margins of the perido-
tite body. Serpentinization was accompanied locally by the
development of silica-magnesite veinlets along fractures.
Peridotite chemistry coupled with structural preparation fa-
voured subsequent intense lateritization and supergene
nickel ore development.

Lateritization of the harzburgite probably began in
late Eocene-early Oligocene time and chemical weathering

and erosion continued throughout the Oligocene period. The development of a thick laterite profile (as much as 140 m) was made possible by a climate in which high rainfall, relative humidity and temperatures, resulted in intense chemical weathering of the peridotite. The process apparently was polycyclic as evidenced by the presence of limited displacement vertical faults that cut previously formed Saprolite and Limonite zones.

A thick, well developed laterite profile was formed in the Cerro Matoso peridotite body. The laterite profile consists from top to bottom of Canga, Limonite, Upper Saprolite, and Lower Saprolite zones overlying peridotite. Original rock structures are absent in the Canga and Limonite zones but are preserved in saprolite, particularly in the Lower Saprolite level. Canga exhibits a concretionary texture formed by successive accretion of goethite aggregates which is particularly well developed towards the lower part of the zone. The Limonite zone consists of material that is softer and less iron-rich than the overlying Canga. It has an earthy appearance locally and also contains some concretionary goethite. Material in the Upper Saprolite level is relatively soft, but hardness increases progressively downwards into the Lower Saprolite zone and becomes significantly greater as peridotite bedrock is approached.

The different profile units also show pronounced variations in element distribution. Iron and chromium accumulated preferentially in the Canga level, whereas alumina

is preferentially concentrated in the uppermost part of the Canga. The Limonite zone contains the maximum observed values of cobalt and manganese; iron content is high but not as much so as in Canga. Saprolite exhibits significant enrichment in nickel, grades of as much as 7% Ni having been recognized. Nickel is preferentially concentrated in the Upper Saprolite zone, although the Lower Saprolite zone also may show local nickel enrichment. Magnesium concentration is very low in the Canga and Limonite zones but increases progressively downwards in to the saprolite zones and the underlying peridotite bedrock. Silica concentrations in the Limonite and Canga zones are considerably less than values observed in the saprolite zones.

Element distribution in the weathering profile can be explained in terms of variations in relative mobility of the various elements in this chemical environment. Magnesium is highly mobile in the upper parts of the profile and it tends to be almost entirely leached from the Canga and Limonite zones. Magnesium mobility decreases at intermediate and deeper levels, thus concentrations increase accordingly. Chromium has very low mobility and is concentrated residually. Iron is precipitated under oxidizing and slightly acidic conditions that prevail in the Canga and Limonite zones. Locally, decrease in pH at the top of the Canga zone may result in iron remobilization downwards through a few meters and reprecipitation in the lower part of the Canga zone, thus leading to significant increase

in iron content at this level. Manganese mobility in the
Canga and Limonite zones appears to be somewhat higher than
that of iron and Mn is readily precipitated in the neutral
to slightly alkaline conditions that occur in the lower
part of the Limonite zone. Nickel and cobalt are fairly
mobile elements but the preferential accumulation of cobalt
above the zone of maximum nickel enrichment indicates a rela-
tively higher mobility downwards in the profile for nickel
over cobalt. Alumina is a highly immobile component, and
is concentrated primarily in the near surface portion of the
profile (Canga). Moderate mobility of silica occurs in upper
profile levels but mobility decreases rapidly at intermediate
levels which is due at least in part to the presence of
higher amounts of dissolved magnesium in the weathering
solutions.

Vertical longitudinal profiles for element distribution
reflect the behaviour of each element in the laterite pro-
file. Lateral chemical variations appear to be related to
structural features such as faults and joints which greatly
facilitated solution migration. The vertical longitudinal
profiles of element distribution clearly indicate the
variable thickness of the laterite profile.

Using an ore grade cutoff of 1.5% Ni, it is apparent
that the most intense nickel mineralization is located
principally in the Upper Saprolite zone. Two varieties of
silicate-type nickel ore have been recognized: massive and
fracture fillings. Massive ore occurs as a product of

pervasive weathering of parent peridotite and nickel is concentrated in smectite- and serpentine-type minerals. This ore type constitutes the most important part of the deposit economically and exhibits an average nickel grade that exceeds 3%. Fracture filling ore is comprised of nickel-bearing minerals that completely fill major fractures, coat joint surfaces as thin crusts, or fill cavities as botryoidal aggregates where fractures widen. In this ore, nickel appears to be concentrated primarily in the silicates pimelite, sepiolite, and chlorite. Although volumetrically less important than massive ore, fracture filling ore is important in that nickel may attain concentrations of as much as 30% and thus may contribute considerably to the overall recoverable reserves being developed by open pit mining methods.

Nickel enrichment above the 1.5% cutoff grade is primarily a supergene process and apparently was partially restricted by local characteristics of the parent rock, in particular the degree of serpentinization. The overall process was controlled by nickel dissolution in the more acidic upper part of the laterite profile and downwards migration and accumulation at intermediate levels where alkaline conditions were present and nickel mobility was reduced. This enrichment process was particularly efficient where nickel migration was not restricted by low rock permeability. Nickel distribution profiles indicate preferential nickel enrichment in harzburgite that has

undergone minimum serpentinization; highly serpentinized parent rock exhibits nickel values that are below the 1.5% Ni cutoff grade. Strongly serpentinized parent rock acts as a relative permeability barrier that restricts the nickel enrichment process (Lelong et al., 1976; Maynard, 1983; McFarlane, 1983).

Tectonic effects associated with the Andean orogeny are reflected in the location of the zone of maximum nickel enrichment. A NW trending fault system developed at Cerro Matoso during the late Miocene-Pliocene Andean orogeny and the southwestern part of the weathered peridotite body was uplifted relative to the northeastern part. This uplift apparently was sufficient for intense erosion to remove most of laterite profile from the uplifted block while the northeastern block was only slightly modified. This erosional event is reflected by the presence of abundant ferruginous debris in the post-Pliocene sediments that occur along the southwest flank of the peridotite body. Uplift of the northeastern block appears to have been sufficiently minor that erosion was minimal; the ground-water table was lowered and an increase in the vertical extent of the laterite profile as well as local nickel redistribution probably were favoured.

Suggestions for exploration

Once a deposit has been established as having economic potential, care must be taken in determining drill hole

locations and depths. The wide variations in element distribution at Cerro Matoso, both vertically and laterally, indicate that evaluation based on a widely spaced drill hole grid (e.g. 50 m intervals or greater) may lead to major misinterpretation of the actual profile. A closely spaced drill hole grid (e.g. 25 m intervals or less) is required for accurate interpretation and evaluation of the deposit. Furthermore, longitudinal vertical profiles of equal content for several components constructed for this study reveal the presence of nuclei of less altered peridotite at intermediate levels in the profile that could be misinterpreted as representing the bottom of the laterite profile. It is advisable, therefore, to drill several meters into any less altered peridotite in order to avoid the possibility of terminating a hole in such a nucleus. It is recommended that longitudinal vertical profiles showing element distribution be constructed as drilling operations proceed in order to provide the continuous chemical control that reflects level in the laterite profile and depth to bedrock.

Accurate evaluation of laterite nickel deposits requires proper identification of units present in each drill hole. Common exploration practice is to chemically determine a pre-established set of elements (e.g. Ni, Fe, MgO) in samples taken continuously at 2 m depth intervals, and obtain analyses of additional elements at intercepts that appear to show more economic potential (Appendix 1).

It is suggested that mineralogical studies also be conducted in order to determine if a high nickel intercept corresponds to massive ore (smectite, serpentine) or to a fracture filling type of ore (pimelite, sepiolite, chlorite). Furthermore, better definition of the distribution of the various profile units could be obtained if mineralogical data are available.

Chemical analyses for noble metals should be included in the evaluation of laterite nickel deposits with great vertical extent. Au, Pt, Pd and Ir may become enriched in the Canga and Limonite zones relative to the parent peridotite as shown by Ahmad et al. (1977) and Ahmad and Morris (1978) for some nickel laterite deposits from Lake Izabal (Guatemala), Pamalea (Indonesia) and New Caledonia which have maximum vertical extent of as much as 26 m. The Cerro Matoso nickeliferous laterite deposit has vertical extent of as much as 136 m and appears to be a promisory target for noble metals.

In summary, parameters important to exploration for silicate-type nickel ore comparable to the Cerro Matoso deposit are as follows: a) favourable parent material – ultramafic rocks, fresh to only slightly serpentinized harzburgites particularly promising; b) structural preparation – faults and joints particularly important in pervasive weathering processes; c) polycyclic uplift – minor uplift favourable to rejuvenation of the laterite

profile; d) paleoclimates with alternating high rainfall and relatively dry seasons. Local target exploration procedures should include the following: a) geochemical surveys of surface materials (distribution of chromium, cobalt, manganese, alumina); b) drilling at closely spaced intervals (grid of 25 m or less); c) chemical analyses of material in drill holes at closely spaced (2 m) depth intervals for Ni, Fe, MgO, SiO_2; d) construction of longitudinal vertical profiles showing zones of equal content for components such as Ni, Fe, MgO, SiO_2, Al_2O_3, Co, Mn; e) mineralogical analyses of drill hole material to establish the type of ore corresponding to a high nickel intercept and to better define the distribution of the various profile units; f) drilling of several meters in to less altered peridotite to determine the bottom of the laterite profile.

REFERENCES CITED

Ahmad, I., Ahmad, S., and Morris, D.F.C., 1977,
  Determination of noble metals in geologic materials by
  radiochemical neutron-activation analysis: Analyst,
  v. 102, p. 17-24.

Ahmad, S., and Morris, D.F.C., 1978, Geochemistry of some
  lateritic nickel-ores with particular reference to the
  distribution of noble metals: Mineral. Mag., v. 42,
  p. M4-M8.

Atchley, F.W., 1958, Preliminary exploration of
  nickeliferous laterite deposits, Córdoba, Colombia:
  Unpublished Report for Richmond Oil Company, Cerro
  Matoso S.A. file, 57 p.

Avias, J., 1978, L'evolution des idees et des connaissances
  sur la genese et sur la nature des minerais de nickel, en
  particulier lateritiques, de leur decouverte a nous
  jours: Bull. B.R.G.M., 2nd series, Section II, No. 3,
  p. 165-172.

Bailey, S.W., 1980, Summary of recommendations of AIPEA
  Nomenclature Committee: Clay Minerals, v. 15, p. 85-93.

Barrero, D., Alvarez, J., and Kassem, T., 1969, Actividad
  ígnea y tectónica en la cordillera central: Colombia
  Instituto Nacional de Investigaciones Geológico-Mineras,
  Boletín Geológico, v. 17, No. 1-3, p. 145-173.

Berry, L.G., ed., 1974, Selected Powder Diffraction Data
  for Minerals, Data Book, First edition, Joint Committee
  on Powder Diffraction Standards, Swarthmore,
  Pennsylvania.

Bish, D.L., and Brindley, G.W., 1978, Deweylites, mixtures
  of poorly crystalline hydrous serpentine and talc-like
  minerals: Mineral. Mag., v. 42, p. 75-79.

Blatt, H., 1982, Sedimentary Petrology: W.H. Freeman and
  Co., San Francisco, 564 p.

Brindley, G.W., 1959, X-ray and electron diffraction data
  for sepiolite: Am. Mineral., v. 44, p. 495-500.

Brindley, G.W., 1978, The structure and chemistry of hydrous nickel-containing silicate and aluminate minerals: Bull. B.R.G.M., 2nd series, Section II, No. 3, p. 233-245.

Brindley, G.W., and Ali, S.Z., 1950, X-ray study of thermal transformations in some magnesian chlorite minerals: Acta Cryst., v. 3, p. 25-30.

Brindley, G.W., Bish, D.L., and Wan, H.M., 1977, The nature of kerolite, its relation to talc and stevensite: Mineral. Mag., v. 41, p. 443-452.

Brindley, G.W., Bish, D.L., and Wan, H.M., 1979, Compositions, structures, and properties of nickel-containing minerals in the Kerolite-Pimelite series: Am. Mineral., v. 64, p. 615-625.

Brindley, G.W., and Chang, T.S., 1974, Development of long basal spacings in chlorites by thermal treatment: Am. Mineral., v. 59, p. 152-158.

Brindley, G.W., and Maksimovic, Z., 1974, The nature and nomenclature of hydrous nickel-containing silicates: Clay Minerals, v. 10, p. 271-277.

Brindley, G.W., and Pham Thi Hang, 1973, The nature of garnierites-I: Structures, chemical composition and color characteristics: Clays Clay Minerals, v. 21, p. 27-40.

Brindley, G.W., and de Souza Santos, J.V., 1975, Nickel-containing montmorillonites and chlorites from Brazil, with remarks on Schuchardtite: Mineral. Mag., v. 40, p. 141-152.

Brindley, G.W., and Wan, H.M., 1975, Compositions, structures, and thermal behavior of nickel-containing minerals in the Lizardite-Nepouite series: Am. Mineral., v. 60, p. 863-871.

Brown, B.E., and Bailey, S.W., 1962, Chlorite polytypism: I. Regular and semi-random one-layer structures: Am. Mineral., v. 47, p. 819-850.

Bueno, R., 1970, The geology of the Tubara region, Lower Magdalena Basin: Colombia Society of Petroleum Geologists and Geophysicists, Eleventh Annual Field Conf., February 27-28, 1970, Guidebook, p. 299-324.

Burger, P.A., 1979, The Greenvale nickel laterite orebody: in D.J.I. Evans, R.S. Shoemaker, and H. Veltman, eds., International Laterite Symposium-New Orleans, February 1979, A.I.M.E., New York, p. 24-37.

Burke, K., Cooper, C., Dewey, J.F., Mann, P., and Pindell, J.L., 1984, Caribbean tectonics and relative plate motions: Geol. Soc. Am., Memoir 162, p. 31-63.

Caillere, S., 1951, Sepiolite: in G.W. Brindley, ed., X-ray identification and crystal structures of clay minerals, The Mineralogical Society (Clay Minerals Group), London, p. 224-233.

Carmichael, I.S.E., Turner, F.J., and Verhoogen, J., 1974, Igneous Petrology: McGraw-Hill Book Co., New York, 739 p.

Case, J.E., Durán , L.G., López, A., and Moore, W.R., 1971, Tectonic investigations in western Colombia and eastern Panama: Geol. Soc. Am. Bull., v. 82, p. 2685-2712.

Case, J.E., Holcombe, T.L., and Martin, R.G., 1984, Map of geologic provinces in the Caribbean region: Geol. Soc. Am., Memoir 162, p. 1-30.

Cole, T.G., and Shaw, H.F., 1983, Kerolite associated with Anhydrite in sediments from the Atlantis II Deep, Red Sea: Clay Minerals, v. 18, p. 325-331.

De Vletter, D.R., 1978, Criteria and problems in estimating global lateritic nickel resources: Mathem. Geol., v. 10, p. 533-542.

De Waal, S.A., 1970a, Nickel minerals from Barberton, South Africa: II. Nimite, a nickel-rich chlorite: Am. Mineral., v. 55, p. 18-30.

De Waal, S.A., 1970b, Nickel minerals from Barberton, South Africa: III. Willemseite, a nickel-rich talc: Am. Mineral., v. 55, p. 31-42.

Decarreau, A., 1981, Mesure experimentale des coefficients de partage solide/solution pour les elements de transition A2+ dans les smectites magnesiennes (A = Ni, Co, Zn, Fe, Cu, Mn): C.R. Acad. Sci. Paris, v. 292, series II, p. 459-462.

Dissanayake, C.B., 1982, Recognition of ultramafic rocks and nickeliferous laterites in humid tropical terrains: Some guidelines: in D.J.L. Laming and A.K. Gibbs, eds., Hidden Wealth: Mineral Exploration Techniques in Tropical Forest Areas, A.G.I.D., Report No. 7, New York, p. 51-58.

Dorr, J.V.N. II, 1964, Supergene iron ores of Minas Gerais, Brazil: Econ. Geol., v. 59, p. 1203-1240.

Dueñas, H., 1980, Verruperiporites y syntricolporites nuevos géneros del polen fósil del Terciario del norte de Colombia: Memorias, IV Coloquio sobre Paleobotánica y Palinología, México, D.F., p. 77-85.

Dueñas, H., and Duque-Caro, H., 1981, Geología del cuadrángulo F-8, Planeta Rica: Colombia Instituto Nacional de Investigaciones Geológico-Mineras, Boletín Geológico, v. 24, No. 1, p. 1-35.

Duncan, R.A., and Hargraves, R.B., 1984, Plate tectonic evolution of the Caribbean region in the mantle reference frame: Geol. Soc. Am., Memoir 162, p. 81-93.

Duque-Caro, H., 1973, The geology of the Montería area: Colombia Society of Petroleum Geologists and Geophysicists, Fourteenth Annual Field Conf., October 19-21, 1973, Guidebook, p. 397-431.

Duque-Caro, H., 1979, Major structural elements and evolution of northwestern Colombia: Am. Assoc. Pet. Geol., Memoir 29, p. 329-351.

Duque-Caro, H., 1984, Structural style, diapirism, and accretionary episodes of the Sinu-San Jacinto terrane, southwestern Caribbean borderland: Geol. Soc. Am., Memoir 162, p. 303-316.

Duque-Caro, H., Page, W.D., and Cuellar, J., 1983, General geology, geomorphology and neotectonics of northwestern Colombia (southeastern Caribbean borderland): 10th Caribbean Geol. Conf., Cartagena, Colombia, 1983, Field Trip C, 18 p.

Durst, T.L., 1976, The mineralogical and chemical development of the Nickel Mountain (Oregon) nickel laterite deposit: Unpub. Ph. D. thesis, Case Western Reserve Univ., 261 p.

Espinal, T.S., 1977, Zonas de Vida ó Formaciones Vegetales de Colombia: Colombia Instituto Geográfico Agustín Codazzi, Revista I.G.A.C., v. 13, No. 11, 238 p.

Faust, G.T., and Fahey, J.J., 1962, The serpentine-group minerals: U.S. Geol. Surv., Prof. Paper 384-A, 92 p.

Faust, G.T., Fahey, J.J., Mason, B., and Dwornik, E.J., 1969, Pecoraite, $Ni_6Si_4O_{10}(OH)_8$, the nickel analog of clinochrysotile, formed in the Wolf Creek meteorite: Science, v. 165, p. 59-60.

Feininger, T., 1970, The Palestina fault, Colombia: Geol. Soc. Am. Bull., v. 81, p. 1201-1216.

Fisher, D.E., Joensuu, O., and Bostrom, K., 1969, Elemental abundances in ultramafic rocks and their relation to the upper mantle: Jour. Geophys. Res., v. 74, No. 15, p. 3865-3873.

Gerard, P., and Herbillon, A.J., 1983, Infrared studies of Ni-bearing clay minerals of the kerolite-pimelite series: Clays Clay Minerals, v. 31, p. 143-151.

Golightly, J.P., 1979a, Nickeliferous laterites: A general description: in D.J.I. Evans, R.S. Shoemaker, and H. Veltman, eds., International Laterite Symposium-New Orleans, February 1979, A.I.M.E., New York, p. 24-37.

Golightly, J.P., 1979b, Geology of the Soroako nickeliferous laterite deposits: in D.J.I. Evans, R.S. Shoemaker, and H. Veltman, eds., International Laterite Symposium-New Orleans, February 1979, A.I.M.E., New York, p. 38-56.

Golightly, J.P., 1981, Nickeliferous laterite deposits: Econ Geol., Seventy-Fifth Anniversary Volume, p. 710-735.

Gómez, R., Ogryzlo, C.T., and Dor, A.A., 1979, The Cerro Matoso nickel project: in D.J.I. Evans, R.S. Shoemaker, and H. Veltman, eds., International Laterite Symposium-New Orleans, February 1979, A.I.M.E., New York, p. 412-458.

Grim, R.E., 1953, Clay Mineralogy: McGraw-Hill Book Co., New York, 384 p.

Grim, R.E., 1968, Clay Mineralogy: McGraw-Hill Book Co., New York, 2nd ed., 596 p.

Harder, H., 1977, Clay mineral formation under lateritic weathering conditions: Clay Minerals, v. 12, p. 281-288.

Hayes, J.B., 1970, Polytypism of chlorite in sedimentary rocks: Clays Clay Minerals, v. 18, p. 285-306.

Hotz, P.E., 1964, Nickeliferous laterites in southwestern Oregon and northwestern California: Econ. Geol., v. 59, p. 355-396.

Ingeominas, 1983, Mapa de terrenos geológicos de Colombia: Publicaciones Geológicas Especiales, No. 14, 135 p.

Irving, E.M., 1975, Structural evolution of the northernmost Andes: U.S. Geol. Surv., Prof. Paper 846, 47 p.

James, M.E., 1985, Evidencia de colisión entre la miniplaca Bloque Andino y la placa Norteamericana desde el Mioceno Medio: VI Congreso Latinoamericano de Geología, Bogotá, Octubre 9-12, 1985, Memorias, Tomo I, p. 69-89.

Jensen, M.L., and Bateman, A.M., 1981, Economic Mineral Deposits: John Wiley and Sons, New York, 593 p.

Keller, W.D., 1964, The origin of high-alumina clay minerals - A review: Clays Clay Minerals, 12th Natl. Conf. Proc., p. 129-151.

Keller, W.D., 1968, Principles of Chemical Weathering: Lucas and Brothers Pub. Co., 111 p.

Kellogg, J., 1983, Gravity-tectonic study of the Caribbean-Nazca-South America triple junction or convergent zone: 10th Caribbean Geol. Conf., Cartagena, Colombia, 1983, Abs. of Papers, p. 44.

Kerr, P.F., Kulp, J.L., and Hamilton, P.K., 1949, Differential Thermal Analysis of Reference clay mineral specimens: A.P.I. Project 49, Preliminary Rept. No. 3, Columbia Univ., New York, 48 p.

Krauskopf, K.B., 1959, The geochemistry of silica in sedimentary environments: in H.A. Ireland, ed., Silica in Sediments, Soc. Econ. Paleont. Mineral., Spec. Pub. No. 7, Tulsa, Oklahoma, p. 4-19.

Krauskopf, K.B., 1967, Introduction to Geochemistry: McGraw-Hill Book Co., New York, 721 p.

Krauskopf, K.B., 1979, Introduction to Geochemistry: McGraw-Hill Book Co., 2nd ed.

Kuhnel, R.A., Roorda, H.J., and Steensma, J.J.S., 1978, Distribution and partitioning of elements in nickeliferous laterites: Bull. B.R.G.M., 2nd series, Section II, No. 3, p. 191-206.

Lelong, F., Tardy, Y., Grandin, G., Trescases, J.J., and Boulange, B., 1976, Pedogenesis, chemical weathering and processes of formation of some supergene ore deposits: in K.H. Wolf, ed., Handbook of Strata-bound and Stratiform Ore Deposits, v. 3, Elsevier Sci. Pub. Co., Amsterdam, p. 93-173.

Levinson, A.A., 1980, Introduction to Exploration Geochemistry: Applied Pub. Ltd., Wilmette, Illinois, 2nd ed., 924 p.

Lewis, D.G., and Schwertmann, U., 1979, The influence of Al on iron oxides. Part III. Preparation of Al goethites in M KOH: Clay Minerals, v. 14, p. 115-126.

López-Eyzaguirre, C., and Bisque, R.E., 1975, Study of weathering of basic, intermediate, and acidic rocks under tropical humid conditions: Quart. Colo. Sch. Mines, v. 70, p. 1-59.

Lucas, J., 1962, La transformation des mineraux argileux dans la sedimentation. Etudes sur les argiles du Trias: Mem. Serv. Carte Geol. Als.-Lorr., Rept. No. 23, 187 p.

MacDonald, W.D., 1980, Anomalous paleomagnetic directions in Late Tertiary andesitic intrusions of the Cauca depression, Colombian Andes: Tectonophys., v. 68, p. 339-348.

MacKenzie, W.S., Donaldson, C.H., and Guilford, C., 1982, Atlas of igneous rocks and their textures: John Wiley and Sons, Inc., New York, 148 p.

Maksimovic, Z., 1966, Beta-kerolite - Pimelite series from Goles Mountain, Yugoslavia: Proc. Intern. Clay Conf., Jerusalem, 1966, v. I, p. 97-105.

Maksimovic, Z., 1973, Nickel clay minerals in some laterites, bauxites and oolitic iron ores: 6th Conf. Clay Mineral. and Petrol., Prague, 1973, p. 119-134.

Malfait, B.T., and Dinkelman, M.G., 1972, Circum-Caribbean tectonic and igneous activity and the evolution of the Caribbean plate: Geol. Soc. Am. Bull., v. 83, p. 251-272.

Marshall, W.L., 1980a, Amorphous silica solubilities – I. Behavior in aqueous sodium nitrate solutions; 25-300°C, 0-6 molal: Geochim. Cosmochim. Acta, v. 44, p. 907-913.

Marshall, W.L., 1980b, Amorphous silica solubilities – III. Activity coefficient relations and predictions of solubility behavior in salt solutions, 0-350°C: Geochim. Cosmochim. Acta, v. 44, p. 925-931.

Marshall, W.L., and Warakomski, J.M., 1980, Amorphous silica solubilities – II. Effect of aqueous salt solutions at 25°C: Geochim. Cosmochim. Acta, v. 44, p. 915-924.

Mattson, P.H., 1984, Caribbean structural breaks and plate movements: Geol. Soc. Am., Memoir 162, p. 131-152.

Maynard, J.B., 1983, Geochemistry of Sedimentary Ore Deposits: Springer-Verlag, New York, 305 p.

McFarlane, M.J., 1976, Laterite and Landscape: Academic Press, London, 151 p.

McFarlane, M.J., 1983, Laterites: in M. Woakes and J.S. Carman, eds., A.G.I.D. Guide to Mineral Resources and Development, Report No. 10, A.G.I.D., Bangkok, p. 441-488.

McFarlane, M.J., 1984, International interdisciplinary Laterite Reference Collection: in P.K. Banerji, ed., International Geological Correlation Programme-Project 129, Lateritisation Processes, Newsletter-VI, S.K. Mukerjee, Pub., Hyderabad (India), p. 13-21.

Mejía, V.M., and Durango, J., 1982, Geología de las lateritas niquelíferas de Cerro Matoso: Revista Univ. Industrial de Santander, 1981-1982, Boletín de Geología, v. 15, p. 99-116.

Montoya, J.W., and Baur, G.S., 1963, Nickeliferous serpentines, chlorites, and related minerals found in two lateritic ores: Am. Mineral., v. 48, p. 1227-1238.

Norton, S.A., 1973, Laterite and bauxite formation: Econ. Geol., v. 68, p. 353-361.

Page, W.D., 1983, Quaternary faulting in northwestern Colombia: 10th Caribbean Geol. Conf., Cartagena, Colombia, 1983, Abs. of Papers, p. 56.

Papke, K.G., 1972, A sepiolite-rich playa deposit in southern Nevada: Clays Clay Minerals, v. 20, p. 211-215.

Pecora, W.T., Hobbs, S.W., and Murata, K.J., 1949, Variations in garnierite from the nickel deposit near Riddle, Oregon: Econ. Geol., v. 44, p. 13-23.

Perruchot, A., 1971, Sur le partage du nickel entre serpentine et brucite au cours de la serpentinisation du peridot: C.R. Acad. Sci. Paris, v. 273, Series D, p. 125-127.

Pham Thi Hang, and Brindley, G.W., 1973, The nature of garnierites - III. Thermal transformations: Clays Clay Minerals, v. 21, p. 51-57.

Pickering, R.J., 1962, Some leaching experiments on three quartz-free silicate rocks and their contribution to an understanding of lateritization: Econ. Geol., v. 57, p. 1185-1206.

Rautureau, M., and Caillere, S., 1974, Interpretation des courbes thermiques en fonction des donnees structurales de la sepiolite: C.R. Acad. Sci. Paris, v. 278, Series D, p. 1661-1664.

Rautureau, M., and Mifsud, A., 1977, Etude par microscope electronique des differents etats d'hydration de la sepiolite: Clay Minerals, v. 12, p. 309-318.

Rucklidge, J.C., and Zussman, J., 1965, The crystal structure of the serpentine mineral, lizardite, $Mg_3Si_2O_5(OH)_4$: Acta Cryst., v. 19, p. 381-389.

Sahoo, R.K., Kaaden, G.V.D., and Muller, G., 1981, The mineralogy and geochemistry of nickeliferous laterite of Sukinda, Orissa, India: Proc. Intern. Seminar on Lateritisation Processes, Trivandrum (India), December 11-14, 1979, Oxford and I.B.H. Pub. Co., New Delhi, p. 77-85.

Schellmann, W., 1978, Behaviour of nickel, cobalt and chromium in ferruginous lateritic nickel ores: Bull. B.R.G.M., 2nd series, Section II, No. 3, p. 275-282.

Schorin, H., 1981, Geochemical comparison of two laterite profiles from Serrania de los Guaicas, Venezuela: Proc. Intern. Seminar on Lateritisation Processes, Trivandrum (India), December 11-14, 1979, Oxford and I.B.H. Pub. Co., New Delhi, p. 154-162.

Schwertmann, U., and Murad, E., 1983, Effect of pH on the formation of goethite and hematite from ferrihydrite: Clays Clay Minerals, v. 31, p. 277-284.

Shagam, R., 1975, The northern termination of the Andes: in A.E.M. Nairn and F.G. Stehli, eds., The Ocean Basins and Margins, v. 3, The Gulf of Mexico and the Caribbean, Plenum Press, New York, p. 325-420.

Shannon, R.D., and Prewitt, 1969, Effective ionic radii in oxides and fluorides: Acta Cryst., v. 25, p. 925-946.

Speakman, K., and Majumdar, A.J., 1971, Synthetic "Deweylite": Mineral. Mag., v. 38, p. 225-234.

Streckeisen, A., 1976, To each plutonic rock its proper name: Earth-Science Rev., v. 12, p. 1-33.

Sudo, T., and Hayashi, H., 1959, Mineralogical aspects of montmorillonite from Japan: XX Intern. Geol. Cong., Mexico, Rept. Comité Internacional para el Estudio de las Arcillas, p. 43-52.

Takeshi, H., 1978, Smectites: in T. Sudo and S. Shimoda, eds., Clays and Clay Minerals of Japan, Kodansha Ltd.-Elsevier Sci. Pub. Co., Tokyo-Amsterdam, p. 221-242.

Tiller, K.G., and Hodgson, J.F., 1962, The specific sorption of cobalt and zinc by layer silicates: Clays Clay Minerals, 9th Natl. Conf. Proc., Lafayette (Indiana), 1960, p. 393-403.

Trescases, J.J., 1969, Geochemie des alterations et des eaux de surface dans le massif ultrabasique du sud de la Nouvelle-Caledonie: Bull. Serv. Carte Geol. Als. Lorr., v. 22, No. 4, p. 329-354.

Trescases, J.J., 1975, L'evolution geochimique supergene des roches ultrabasiques en zone tropicale - Formation des gisements nickeliferes de Nouvelle-Caledonie: Memoires O.R.S.T.O.M., No. 78, Paris, 259 p.

Troly, G., Esterle, M., Pelletier, B., and Reibell, W., 1979, Nickel deposits in New Caledonia, some factors influencing their formation: in D.J.I. Evans, R.S. Shoemaker, and H. Veltman, eds., International Laterite Symposium-New Orleans, February 1979, A.I.M.E., New York, p. 85-119.

Van der Hammen, T., 1958, Estratigrafía del Terciario y Maestrichtiano continentales y tectogénesis de los Andes Colombianos: Colombia Servicio Geológico Nacional, Boletín Geológico, v. 6, No. 1-3, p. 67-128.

Walker, G.F., 1951, Vermiculites and some related mixed-layer minerals: in G.W. Brindley, ed., X-ray Identification and Crystal Structures of Clay Minerals, The Mineralogical Society (Clay Minerals Group), London, p. 199-223.

Webber, B.N., 1972, Supergene nickel deposits: A.I.M.E. Trans., v. 252, p. 333-347.

White, W.B., McCarthy, G.J., and Scheetz, B.E., 1971, Optical spectra of chromium, nickel, and cobalt-containing pyroxenes: Am. Mineral., v. 56, p. 72-89.

Whittaker, E.J.W., and Muntus, R., 1970, Ionic radii for use in geochemistry: Geochim. Cosmochim. Acta, v. 34, p. 945-956.

Wiewiora, A., Dubinska, E., and Iwasinska, I., 1982, Mixed-layering in Ni-containing talc-like minerals from Szklary, Lower Silesia, Poland: Proc. VII Intern. Clay Conf., Bologna-Pavia (Italy), September 6-12, 1981, Elsevier Sci. Pub. Co., Amsterdam, p. 111-125.

Zeissink, H.E., 1969, The mineralogy and geochemistry of a nickeliferous laterite profile (Greenvale, Queensland, Australia): Mineralium Deposita, v. 4, p. 132–152.

Zeissink, H.E., 1971, Trace element behaviour in two nickeliferous laterite profiles: Chem. Geol., v. 7, p. 25–36.

APPENDIX 1

CHEMICAL COMPOSITION OF DRILL HOLE SAMPLES

Analytical Method: X-ray fluorescence analysis

Laboratory   :   XRF-laboratory of Cerro Matoso S.A.,
Montelíbano, Colombia

Analysts   :   Rafael Bustamante (Chief)
Luis Paternina
Nydia Rojas
Enrique Jaraba
Juan Londoño
Jorge Rivera

Samples   :   From drill holes along the Lines
500 NW (p. 244-248), 1200 NW (p. 249-
297), 1300 NW (p. 298-340) and 2000 NW
(p. 341-357) (Plate 2)

Explanation   :

DDH   :   Drill Hole, northeast coordinate
ELEV   :   Elevation above sea level for the
top of the drill hole (in meters)
Depth   :   Sampling depth (2 m intervals)
%   :   Weight percent
0.000, 0.00,
0.0   :   Indicate that analysis was not made
LOI   :   Loss On Ignition
Fe   :   Fe expressed as total iron

DDH = 800NE   LINE 500 NW   ELEV = 123 m

Depth (m)	Ni (%)	Co (%)	Fe (%)	MgO (%)	SiO$_2$ (%)	Al$_2$O$_3$ (%)	Cr$_2$O$_3$ (%)	LOI (%)
0-2	.27	0.000	24.50	1.00	40.0	9.98	0.00	0.00
2-4	.32	0.000	24.60	1.14	38.0	10.79	0.00	0.00
4-6	.41	0.000	22.90	1.12	49.4	6.17	0.00	0.00
6-8	.63	.112	20.30	1.46	54.7	4.60	0.00	5.00
8-10	1.14	.093	20.50	2.63	52.0	4.50	0.00	5.61
10-12	.84	.049	16.10	5.92	60.4	2.67	0.00	4.74
12-14	.52	.026	10.90	7.20	70.8	1.61	0.00	3.77
14-16	.70	0.000	0.00	0.00	0.0	0.00	0.00	0.00
16-18	.67	0.000	11.00	11.80	65.1	1.51	0.00	0.00
18-20	.50	0.000	0.00	0.00	0.0	0.00	0.00	0.00
20-22	.35	0.000	7.00	13.10	62.3	1.16	0.00	0.00
22-24	.43	0.000	8.20	14.00	64.9	1.09	0.00	0.00

DDH = 883NE   LINE 500 NW   ELEV = 133 m

Depth (m)	Ni (%)	Co (%)	Fe (%)	MgO (%)	SiO$_2$ (%)	Al$_2$O$_3$ (%)	Cr$_2$O$_3$ (%)	LOI (%)
0-2	.31	0.000	25.11	.58	0.0	0.00	0.00	0.00
2-4	.31	0.000	25.07	.78	0.0	0.00	0.00	0.00
4-6	.30	0.000	22.40	1.00	0.0	0.00	0.00	0.00
6-8	.55	0.000	22.23	.84	0.0	0.00	0.00	0.00
8-10	.52	0.000	18.40	.55	0.0	0.00	0.00	0.00
10-12	.07	0.000	2.83	.34	0.0	0.00	0.00	0.00
12-14	.16	0.000	5.83	.37	0.0	0.00	0.00	0.00
14-16	.27	0.000	8.36	.42	0.0	0.00	0.00	0.00
16-18	.28	0.000	5.65	3.69	0.0	0.00	0.00	0.00
18-20	.19	0.000	4.01	17.09	0.0	0.00	0.00	0.00
20-22	.21	0.000	5.20	26.26	0.0	0.00	0.00	0.00
22-24	.21	0.000	4.94	31.00	0.0	0.00	0.00	0.00
24-26	.24	0.000	6.30	38.29	0.0	0.00	0.00	0.00
26-28	.22	0.000	5.63	38.42	0.0	0.00	0.00	0.00

DDH = 1025NE   LINE 500 NW   ELEV = 154 m

Depth (m)	Ni (%)	Co (%)	Fe (%)	MgO (%)	SiO_2 (%)	Al_2O_3 (%)	Cr_2O_3 (%)	LOI (%)
0-2	.34	0.000	27.45	.76	0.0	0.00	0.00	0.00
2-4	.58	0.000	25.80	.63	0.0	0.00	0.00	0.00
4-6	.66	0.000	29.38	.64	0.0	0.00	0.00	0.00
6-8	.43	0.000	16.36	.51	0.0	0.00	0.00	0.00
8-10	.31	0.000	11.80	.51	0.0	0.00	0.00	0.00
10-12	.32	0.000	12.35	.49	0.0	0.00	0.00	0.00
12-14	.52	0.000	16.47	.58	0.0	0.00	0.00	0.00
14-16	.37	0.000	11.97	.47	0.0	0.00	0.00	0.00
16-18	1.13	0.000	17.46	15.00	0.0	0.00	0.00	0.00
18-20	.71	0.000	9.50	27.14	0.0	0.00	0.00	0.00
20-22	.39	0.000	9.88	29.28	0.0	0.00	0.00	0.00
22-24	.15	0.000	4.78	23.75	0.0	0.00	0.00	0.00
24-26	.13	0.000	3.84	24.29	0.0	0.00	0.00	0.00
26-28	.26	0.000	6.37	29.76	0.0	0.00	0.00	0.00
28-30	.36	0.000	7.96	30.53	0.0	0.00	0.00	0.00
30-32	.35	0.000	7.90	32.21	0.0	0.00	0.00	0.00
32-34	.25	0.000	5.49	35.01	0.0	0.00	0.00	0.00
34-36	.23	0.000	5.65	35.17	0.0	0.00	0.00	0.00

DDH = 1200NE   LINE 500 NW   ELEV = 174 m

Depth (m)	Ni (%)	Co (%)	Fe (%)	MgO (%)	SiO_2 (%)	Al_2O_3 (%)	Cr_2O_3 (%)	LOI (%)
0-2	.25	0.000	27.80	.79	32.8	10.70	0.00	0.00
2-4	.51	0.000	33.80	1.04	27.8	7.30	0.00	0.00
4-6	.47	0.000	22.30	.81	49.3	3.61	0.00	0.00
6-8	.43	0.000	15.20	.60	64.5	2.14	0.00	0.00
8-10	.33	0.000	13.60	.63	68.1	1.82	0.00	0.00
10-12	.32	0.000	12.40	.61	68.9	1.56	0.00	0.00
12-14	.33	0.000	11.50	.65	74.7	1.72	0.00	0.00
14-16	.27	0.000	12.00	.85	76.4	1.78	0.00	0.00
16-18	.43	0.000	13.40	.78	69.6	2.32	0.00	0.00
18-20	.37	0.000	11.30	.65	76.2	1.14	0.00	0.00
20-22	.32	0.000	9.40	.60	81.5	.32	0.00	0.00
22-24	1.33	.159	35.10	2.25	26.2	6.50	0.00	9.31
24-26	.52	.085	13.10	.75	70.3	1.80	0.00	3.49
26-28	.37	.029	10.70	.66	73.2	.61	0.00	2.76
28-30	2.23	.047	12.90	18.20	50.5	.96	0.00	7.75
30-32	1.39	.085	21.80	3.15	54.5	1.51	0.00	5.90
32-34	2.36	.053	12.80	20.40	48.0	1.20	0.00	8.33
34-36	1.10	.026	8.80	24.20	51.7	1.10	0.00	9.08
36-38	1.16	.028	9.10	27.00	51.5	1.12	0.00	9.05
38-40	1.05	.022	7.80	25.50	51.3	1.12	0.00	9.19
40-42	.93	.013	7.80	28.50	48.5	1.15	0.00	8.26

DDH = 1418NE   LINE 500 NW   ELEV = 154 m

Depth (m)	Ni (%)	Co (%)	Fe (%)	MgO (%)	SiO_2 (%)	Al_2O_3 (%)	Cr_2O_3 (%)	LOI (%)
0-2	.71	0.000	33.42	.86	0.0	0.00	0.00	0.00
2-4	.92	0.000	26.36	6.22	0.0	0.00	0.00	0.00
4-6	.79	0.000	7.41	31.50	0.0	0.00	0.00	0.00
6-8	.71	0.000	7.63	33.51	0.0	0.00	0.00	0.00
8-10	.39	0.000	6.48	36.21	0.0	0.00	0.00	0.00
10-12	.36	0.000	6.86	34.20	0.0	0.00	0.00	0.00
12-14	.40	0.000	6.92	32.82	0.0	0.00	0.00	0.00
14-16	.38	0.000	7.41	32.45	0.0	0.00	0.00	0.00
16-18	.31	0.000	6.82	35.28	0.0	0.00	0.00	0.00

DDH = 1649   LINE 500 NW   ELEV = 154 m

Depth (m)	Ni (%)	Co (%)	Fe (%)	MgO (%)	SiO_2 (%)	Al_2O_3 (%)	Cr_2O_3 (%)	LOI (%)
0-2	.34	0.000	14.28	1.73	0.0	0.00	0.00	0.00
2-4	.54	0.000	16.75	.87	0.0	0.00	0.00	0.00
4-6	.87	0.000	11.91	9.02	0.0	0.00	0.00	0.00
6-8	1.47	0.000	9.06	18.77	0.0	0.00	0.00	0.00
8-10	1.39	0.000	13.73	14.98	0.0	0.00	0.00	0.00
10-12	1.29	0.000	7.85	22.70	0.0	0.00	0.00	0.00
12-14	1.38	0.000	8.13	25.06	0.0	0.00	0.00	0.00
14-16	.70	0.000	5.93	25.67	0.0	0.00	0.00	0.00
16-18	.53	0.000	6.86	32.40	0.0	0.00	0.00	0.00
18-20	.34	0.000	5.93	33.56	0.0	0.00	0.00	0.00
20-22	.21	0.000	5.33	28.75	0.0	0.00	0.00	0.00
22-24	.20	0.000	5.49	28.78	0.0	0.00	0.00	0.00
24-26	.18	0.000	5.49	32.52	0.0	0.00	0.00	0.00
26-28	.21	0.000	5.49	34.85	0.0	0.00	0.00	0.00
28-30	.21	0.000	5.60	35.00	0.0	0.00	0.00	0.00

DDH = 1806NE   LINE 500 NW   ELEV = 133 m

Depth (m)	Ni (%)	Co (%)	Fe (%)	MgO (%)	SiO_2 (%)	Al_2O_3 (%)	Cr_2O_3 (%)	LOI (%)
0–2	.28	0.000	20.00	.77	0.0	0.00	0.00	0.00
2–4	.24	0.000	11.81	.68	0.0	0.00	0.00	0.00
4–6	.45	0.000	11.85	8.06	0.0	0.00	0.00	0.00
6–8	0.00	0.000	0.00	0.00	0.0	0.00	0.00	0.00
8–10	.45	0.000	21.61	.97	0.0	0.00	0.00	0.00
10–12	.27	0.000	11.74	1.00	0.0	0.00	0.00	0.00
12–14	.58	0.000	15.05	1.82	0.0	0.00	0.00	0.00
14–16	.94	0.000	11.16	11.85	0.0	0.00	0.00	0.00
16–18	1.05	0.000	8.35	18.61	0.0	0.00	0.00	0.00
18–20	.62	0.000	8.34	26.70	0.0	0.00	0.00	0.00
20–22	.26	0.000	6.79	25.70	0.0	0.00	0.00	0.00
22–24	.30	0.000	8.13	23.01	0.0	0.00	0.00	0.00
24–26	.48	0.000	9.03	20.00	0.0	0.00	0.00	0.00
26–28	.30	0.000	7.88	28.46	0.0	0.00	0.00	0.00
28–30	.29	0.000	6.77	31.58	0.0	0.00	0.00	0.00
30–32	.31	0.000	7.31	29.31	0.0	0.00	0.00	0.00

DDH = 1921   LINE 500 NW   ELEV = 112 m

Depth (m)	Ni (%)	Co (%)	Fe (%)	MgO (%)	SiO_2 (%)	Al_2O_3 (%)	Cr_2O_3 (%)	LOI (%)
0–2	.22	0.000	20.50	1.00	0.0	0.00	0.00	0.00
2–4	.21	0.000	13.80	.80	0.0	0.00	0.00	0.00
4–6	.19	0.000	11.10	.60	0.0	0.00	0.00	0.00
6–8	.43	0.000	18.20	.80	0.0	0.00	0.00	0.00
8–10	.23	0.000	11.30	.80	0.0	0.00	0.00	0.00
10–12	.20	0.000	9.60	.80	0.0	0.00	0.00	0.00
12–14	.28	0.000	11.30	.80	0.0	0.00	0.00	0.00
14–16	.17	0.000	7.20	.70	0.0	0.00	0.00	0.00
16–18	.34	0.000	9.40	2.80	0.0	0.00	0.00	0.00
18–20	.64	0.000	7.40	15.50	0.0	0.00	0.00	0.00
20–22	.74	0.000	8.70	27.20	0.0	0.00	0.00	0.00
22–24	1.14	0.000	8.00	28.60	0.0	0.00	0.00	0.00
24–26	.87	0.000	7.40	33.80	0.0	0.00	0.00	0.00
26–28	.68	0.000	7.10	35.30	0.0	0.00	0.00	0.00

DDH = 2024NE   LINE 500 NW   ELEV = 96 m

Depth (m)	Ni (%)	Co (%)	Fe (%)	MgO (%)	SiO$_2$ (%)	Al$_2$O$_3$ (%)	Cr$_2$O$_3$ (%)	LOI (%)
0-2	.42	0.000	25.10	1.20	0.0	0.00	0.00	0.00
2-4	.61	0.000	21.50	2.30	0.0	0.00	0.00	0.00
4-6	1.04	0.000	14.60	10.00	0.0	0.00	0.00	0.00
6-8	.71	0.000	13.00	14.20	0.0	0.00	0.00	0.00
8-10	.94	0.000	11.10	12.50	0.0	0.00	0.00	0.00
10-12	.68	0.000	9.30	19.40	0.0	0.00	0.00	0.00
12-14	.29	0.000	6.60	20.00	0.0	0.00	0.00	0.00
14-16	.27	0.000	6.20	22.40	0.0	0.00	0.00	0.00
16-18	.27	0.000	6.20	25.10	0.0	0.00	0.00	0.00
18-20	.28	0.000	6.40	29.80	0.0	0.00	0.00	0.00
20-22	.21	0.000	5.60	33.50	0.0	0.00	0.00	0.00
22-24	.22	0.000	5.80	34.60	0.0	0.00	0.00	0.00

DDH = 700NE   LINE 1200 NW   ELEV = 95 m

Depth (m)	Ni (%)	Co (%)	Fe (%)	MgO (%)	SiO_2 (%)	Al_2O_3 (%)	Cr_2O_3 (%)	LOI (%)
0–2	.42	0.000	36.16	3.60	21.46	12.92	0.00	10.24
2–4	.48	0.000	35.12	3.35	21.16	14.18	0.00	10.92
4–6	1.56	.049	27.42	4.00	33.48	13.74	0.00	9.46
6–8	2.82	.057	32.71	4.20	26.92	9.90	0.00	9.64
8–10	2.66	.055	27.74	4.25	36.00	9.48	0.00	8.74
10–12	3.07	.040	25.72	2.15	39.80	7.04	0.00	7.84
12–14	2.70	.023	23.81	4.35	42.56	8.28	0.00	7.78
14–16	2.08	.124	16.84	4.85	55.08	8.60	0.00	6.60
16–18	1.82	.028	19.88	4.85	46.46	9.38	0.00	8.64
18–20	1.49	.034	17.80	5.40	49.76	8.78	0.00	9.36
20–22	1.65	.030	19.97	5.40	44.30	10.26	0.00	9.86
22–24	1.67	.034	21.17	5.40	42.94	9.08	0.00	10.32
24–26	1.70	.031	20.77	5.30	44.48	8.24	0.00	9.76
26–28	1.97	.052	16.60	5.65	48.80	9.92	0.00	10.74

DDH = 713   LINE 1200 NW   ELEV = 92 m

Depth (m)	Ni (%)	Co (%)	Fe (%)	MgO (%)	SiO_2 (%)	Al_2O_3 (%)	Cr_2O_3 (%)	LOI (%)
0–2	.44	.099	37.00	1.00	21.40	9.90	2.68	7.89
2–4	.47	.090	35.50	.90	24.20	9.70	2.63	10.23
4–6	.94	.095	33.20	1.20	29.60	8.32	2.43	8.57
6–8	2.13	.078	30.70	1.60	31.70	7.78	2.22	8.96
8–10	2.60	.088	29.60	1.70	32.50	7.47	2.00	9.05
10–12	2.55	.079	26.70	2.00	38.80	5.89	1.75	8.18
12–14	2.62	.096	30.10	2.60	38.10	4.52	1.54	7.40
14–16	2.28	.046	27.00	4.30	47.40	3.81	1.53	7.08
16–18	1.68	.041	12.00	6.30	61.30	1.78	.79	5.52
18–20	1.61	.051	16.80	6.20	50.40	2.91	1.10	9.02
20–22	1.65	.017	19.00	5.10	52.00	2.99	1.04	8.47
22–24	1.87	.038	21.50	5.00	46.50	3.90	1.33	9.52
24–26	1.88	.032	18.10	4.00	43.20	4.38	1.39	9.47
26–28	2.05	.058	18.80	5.50	48.70	3.88	1.41	8.56
28–30	1.94	.032	18.60	4.50	48.80	3.90	1.30	8.87
30–32	1.66	.046	20.10	5.70	45.10	3.81	1.40	11.05
32–34	1.63	.065	20.50	5.80	40.90	4.30	1.39	11.96
34–36	1.87	.034	21.10	6.00	42.10	4.33	1.36	11.33
36–38	1.95	.044	21.60	4.50	46.80	4.41	1.32	8.70
38–40	1.98	.070	21.00	5.10	41.10	4.87	1.62	8.13
40–42	1.99	.069	20.00	6.10	46.40	4.59	1.85	8.01
42–44	2.13	.065	18.30	11.90	42.10	3.87	1.54	8.47
44–46	2.02	.057	14.90	15.10	48.90	2.23	1.14	7.58

DDH = 769NE   LINE 1200 NW   ELEV = 98 m

Depth (m)	Ni (%)	Co (%)	Fe (%)	MgO (%)	SiO_2 (%)	Al_2O_3 (%)	Cr_2O_3 (%)	LOI (%)
0-2	2.25	.095	34.80	1.60	27.1	7.80	2.28	10.47
2-4	2.55	.118	39.30	2.10	20.2	5.00	2.33	10.47
4-6	4.20	.075	27.50	7.90	32.1	4.44	1.83	9.86
6-8	4.75	.056	18.20	12.90	45.1	2.35	1.18	8.12
8-10	3.30	.042	17.20	13.50	47.1	1.52	1.01	7.82
10-12	2.54	.037	11.40	13.90	57.8	.77	.90	7.13
12-14	1.54	.033	11.80	16.50	52.6	1.20	.91	8.36
14-16	1.23	.031	10.10	19.40	54.2	1.19	.67	8.79
16-18	2.10	.032	10.10	17.50	53.5	1.88	.70	8.48
18-20	1.45	.029	9.50	18.60	0.0	0.00	0.00	0.00
20-22	1.23	.028	8.90	21.40	0.0	0.00	0.00	0.00
22-24	.51	.025	7.40	29.70	0.0	0.00	0.00	0.00
24-26	.88	.027	7.90	27.70	0.0	0.00	0.00	0.00
26-28	.51	.028	7.30	34.20	0.0	0.00	0.00	0.00

DDH = 830NE   LINE 1200 NW   ELEV = 112 m

Depth (m)	Ni (%)	Co (%)	Fe (%)	MgO (%)	SiO_2 (%)	Al_2O_3 (%)	Cr_2O_3 (%)	LOI (%)
0-2	2.41	.076	27.86	2.58	36.9	5.36	2.17	7.89
2-4	2.72	.057	18.47	6.79	49.1	2.58	1.68	7.87
4-6	2.42	.032	12.39	15.35	51.5	1.31	.87	8.39
6-8	1.89	0.000	8.87	19.44	53.9	0.00	0.00	0.00
8-10	1.81	0.000	7.45	22.33	52.0	0.00	0.00	0.00
10-12	2.05	0.000	7.48	22.27	53.2	0.00	0.00	0.00
12-14	1.65	0.000	6.98	19.41	56.6	0.00	0.00	0.00
14-16	1.26	0.000	7.84	24.23	0.0	0.00	0.00	0.00
16-18	.79	0.000	7.16	33.06	0.0	0.00	0.00	0.00
18-20	.69	0.000	6.98	35.72	0.0	0.00	0.00	0.00

```
DDH = 880NE              LINE 1200 NW            ELEV = 133 m
```

Depth (m)	Ni (%)	Co (%)	Fe (%)	MgO (%)	SiO_2 (%)	Al_2O_3 (%)	Cr_2O_3 (%)	LOI (%)
0-2	.80	0.000	36.20	.82	0.0	0.00	0.00	0.00
2-4	.70	0.000	36.48	.90	0.0	0.00	0.00	0.00
4-6	1.55	.102	24.70	3.81	44.6	0.00	0.00	7.36
6-8	1.08	0.000	24.76	1.00	0.0	0.00	0.00	0.00
8-10	1.62	.062	21.93	3.06	51.5	0.00	0.00	6.35
10-12	2.18	.040	13.74	6.42	62.7	0.00	0.00	5.94
12-14	2.59	.028	10.61	17.39	52.8	0.00	0.00	9.20
14-16	2.20	.025	8.54	19.50	52.2	0.00	0.00	9.58
16-18	2.26	.018	9.10	26.96	43.7	0.00	0.00	11.38
18-20	1.72	.012	7.80	31.30	45.4	0.00	0.00	9.63
20-22	.89	0.000	7.45	34.34	0.0	0.00	0.00	0.00
22-24	.75	0.000	7.73	32.90	0.0	0.00	0.00	0.00
24-26	.34	0.000	7.10	34.22	0.0	0.00	0.00	0.00
26-28	.34	0.000	7.38	34.20	0.0	0.00	0.00	0.00
28-30	.33	0.000	7.70	33.82	0.0	0.00	0.00	0.00
30-32	.43	0.000	6.20	25.63	0.0	0.00	0.00	0.00
32-34	.32	0.000	6.92	36.53	0.0	0.00	0.00	0.00
34-36	.39	0.000	7.84	31.31	0.0	0.00	0.00	0.00

```
DDH = 929NE              LINE 1200 NW            ELEV = 145 m
```

Depth (m)	Ni (%)	Co (%)	Fe (%)	MgO (%)	SiO_2 (%)	Al_2O_3 (%)	Cr_2O_3 (%)	LOI (%)
0-2	.96	.096	27.90	.74	45.2	4.28	0.00	7.78
2-4	1.19	.092	20.10	1.91	58.0	2.25	0.00	5.75
4-6	2.15	.037	11.50	14.10	60.2	.78	0.00	7.43
6-8	2.29	.031	12.10	13.00	49.2	.65	0.00	7.00
8-10	2.22	.018	7.80	18.60	61.4	.45	0.00	8.21
10-12	2.01	.017	8.30	25.30	52.0	1.14	0.00	8.15
12-14	2.46	.017	8.40	17.50	62.4	.93	0.00	8.34
14-16	2.05	.016	7.50	22.10	52.6	1.44	0.00	7.57
16-18	1.77	.010	6.80	19.10	64.6	.48	0.00	7.62
18-20	1.53	.012	7.20	26.60	55.2	.47	0.00	7.79

DDH = 961   LINE 1200 NW   ELEV = 141 m

Depth (m)	Ni (%)	Co (%)	Fe (%)	MgO (%)	SiO_2 (%)	Al_2O_3 (%)	Cr_2O_3 (%)	LOI (%)
0-2	.91	0.000	25.20	2.50	0.0	0.00	0.00	0.00
2-4	1.03	0.000	14.20	5.10	0.0	0.00	0.00	0.00
4-6	1.69	.041	16.20	14.50	49.3	1.12	1.26	9.34
6-8	1.40	.045	9.20	20.50	52.8	1.40	.98	9.77
8-10	2.11	.021	8.30	20.60	52.0	1.48	.72	10.27
10-12	1.77	.019	9.90	18.70	52.9	1.73	.77	8.48
12-14	1.38	.017	10.50	17.10	50.6	1.82	.78	8.45
14-16	.92	.015	8.40	19.10	53.7	1.67	.63	9.18
16-18	.91	.017	8.50	20.60	51.5	1.48	.51	11.11
18-20	.87	.019	8.70	25.90	44.6	1.24	.56	8.12
20-22	.45	.014	7.50	31.90	42.1	.56	.54	10.55
22-24	.75	.018	6.70	26.60	48.7	.79	.53	10.43
24-26	.47	.016	7.70	32.10	42.3	1.23	.46	9.65
26-28	.26	.013	6.40	36.30	40.1	1.18	.35	9.47
28-30	.35	.015	7.10	35.00	40.1	1.22	.42	8.30
30-32	.77	.016	7.60	21.70	50.5	1.36	.42	9.11
32-34	.73	.019	8.60	22.70	48.2	1.75	.52	9.29
34-36	.76	.016	7.80	22.10	50.6	1.50	.47	8.88
36-38	.27	.015	6.30	35.70	39.8	1.15	.36	11.30
38-40	.39	.015	6.80	32.30	43.0	.92	.46	8.97
40-42	1.08	.016	7.20	22.40	50.6	1.32	.52	9.47
42-44	1.76	.018	7.16	22.80	54.2	1.24	.55	10.45
44-46	.94	0.000	6.30	24.10	0.0	0.00	0.00	0.00
46-48	.50	0.000	7.00	33.60	0.0	0.00	0.00	0.00
48-50	.26	0.000	6.20	37.90	0.0	0.00	0.00	0.00

DDH = 1042   LINE 1200 NW   ELEV = 154 m

Depth (m)	Ni (%)	Co (%)	Fe (%)	MgO (%)	SiO_2 (%)	Al_2O_3 (%)	Cr_2O_3 (%)	LOI (%)
0-2	1.26	0.000	36.84	7.48	0.0	0.00	0.00	0.00
2-4	1.95	.063	21.32	18.79	36.9	0.00	0.00	10.26
4-6	2.62	.077	22.06	19.61	32.5	0.00	0.00	11.12
6-8	2.92	.034	12.36	24.93	38.0	0.00	0.00	12.24
8-10	3.07	.026	10.61	28.26	39.4	0.00	0.00	12.49
10-12	1.88	.022	8.52	31.90	50.6	0.00	0.00	9.63
12-14	2.00	.026	10.54	26.24	40.6	0.00	0.00	9.92
14-16	2.48	.025	9.80	28.47	40.4	0.00	0.00	10.65
16-18	2.02	.014	8.55	27.35	39.9	0.00	0.00	11.14
18-20	1.82	.020	9.61	29.75	40.0	0.00	0.00	11.19
20-22	1.34	0.000	7.78	30.36	0.0	0.00	0.00	0.00
22-24	1.18	0.000	9.10	31.19	0.0	0.00	0.00	0.00
24-26	.74	0.000	8.00	33.90	0.0	0.00	0.00	0.00
26-28	.31	0.000	6.25	36.90	0.0	0.00	0.00	0.00
28-30	.30	0.000	6.53	34.81	0.0	0.00	0.00	0.00

DDH = 1065NE LINE 1200 NW ELEV = 159 m

Depth (m)	Ni (%)	Co (%)	Fe (%)	MgO (%)	SiO_2 (%)	Al_2O_3 (%)	Cr_2O_3 (%)	LOI (%)
0-2	.75	.052	30.50	1.20	0.0	0.00	0.00	0.00
2-4	.76	.071	26.10	.80	0.0	0.00	0.00	0.00
4-6	.65	.060	19.60	.80	0.0	0.00	0.00	0.00
6-8	2.07	.034	15.20	22.10	38.2	0.00	0.00	0.00
8-10	1.55	.020	11.30	10.50	61.6	0.00	0.00	0.00
10-12	1.54	.022	12.30	17.10	49.0	0.00	0.00	0.00
12-14	1.03	.016	9.30	12.30	0.0	0.00	0.00	0.00
14-16	.84	.015	7.90	11.60	0.0	0.00	0.00	0.00
16-18	.89	.018	9.20	16.40	0.0	0.00	0.00	0.00
18-20	.62	.016	7.90	20.40	0.0	0.00	0.00	0.00
20-22	.36	.010	7.50	23.40	0.0	0.00	0.00	0.00
22-24	.33	.012	8.30	27.00	0.0	0.00	0.00	0.00
24-26	.34	.010	10.80	25.90	0.0	0.00	0.00	0.00
26-28	.39	.020	12.90	23.80	0.0	0.00	0.00	0.00
28-30	.44	.080	8.00	22.60	0.0	0.00	0.00	0.00
30-32	.34	.014	8.20	29.80	0.0	0.00	0.00	0.00
32-34	.29	.013	15.20	34.90	0.0	0.00	0.00	0.00

DDH = 1095NE LINE 1200 NW ELEV = 165 m

Depth (m)	Ni (%)	Co (%)	Fe (%)	MgO (%)	SiO_2 (%)	Al_2O_3 (%)	Cr_2O_3 (%)	LOI (%)
0-2	.64	.061	27.60	.70	0.0	0.00	0.00	0.00
2-4	.65	.030	13.80	5.40	0.0	0.00	0.00	0.00
4-6	.92	.025	12.80	8.70	0.0	0.00	0.00	0.00
6-8	.98	.022	16.70	9.50	0.0	0.00	0.00	0.00
8-10	.78	.018	21.10	8.60	0.0	0.00	0.00	0.00
10-12	.61	.016	11.60	8.50	0.0	0.00	0.00	0.00
12-14	.68	.017	12.60	13.10	0.0	0.00	0.00	0.00
14-16	.24	.012	12.50	29.90	0.0	0.00	0.00	0.00
16-18	.26	.016	8.80	30.60	0.0	0.00	0.00	0.00
18-20	.27	.014	16.50	27.20	0.0	0.00	0.00	0.00
20-22	.28	.023	6.10	21.00	0.0	0.00	0.00	0.00
22-24	.30	.021	7.10	31.30	0.0	0.00	0.00	0.00
24-26	.29	.020	7.20	32.60	0.0	0.00	0.00	0.00
26-28	.27	.017	6.00	33.40	0.0	0.00	0.00	0.00
28-30	.26	.016	6.30	38.00	0.0	0.00	0.00	0.00
30-32	.24	.016	5.90	38.60	0.0	0.00	0.00	0.00

DDH = 1125NE   LINE 1200 NW   ELEV = 168 m

Depth (m)	Ni (%)	Co (%)	Fe (%)	MgO (%)	SiO$_2$ (%)	Al$_2$O$_3$ (%)	Cr$_2$O$_3$ (%)	LOI (%)
0-2	.35	.072	35.30	.90	0.0	0.00	0.00	0.00
2-4	.66	.149	45.90	.70	0.0	0.00	0.00	0.00
4-6	1.06	.051	24.70	16.70	0.0	0.00	0.00	0.00
6-8	.98	.037	13.40	23.50	0.0	0.00	0.00	0.00
8-10	1.05	.039	12.30	26.50	0.0	0.00	0.00	0.00
10-12	.83	.029	11.40	21.70	0.0	0.00	0.00	0.00
12-14	.29	.019	7.00	35.30	0.0	0.00	0.00	0.00
14-16	.18	.018	6.90	36.60	0.0	0.00	0.00	0.00
16-18	.21	.019	9.40	36.10	0.0	0.00	0.00	0.00

DDH = 1128 NE   LINE 1200 NW   ELEV = 168 m

Depth (m)	Ni (%)	Co (%)	Fe (%)	MgO (%)	SiO$_2$ (%)	Al$_2$O$_3$ (%)	Cr$_2$O$_3$ (%)	LOI (%)
0-2	.87	.093	33.10	.95	33.1	6.41	0.00	8.56
2-4	1.18	.069	35.60	.52	31.0	3.65	0.00	8.54
4-6	1.85	.141	22.90	13.30	38.1	1.30	0.00	9.48
6-8	1.74	.044	12.80	19.00	48.1	1.02	0.00	9.30
8-10	2.05	.030	10.20	24.70	40.8	1.33	0.00	11.55
10-12	2.12	.014	9.00	24.60	41.8	1.50	0.00	11.88
12-14	2.06	.027	8.40	27.90	43.1	1.37	0.00	10.32
14-16	2.05	.017	9.10	26.80	39.6	1.61	0.00	11.52
16-18	.48	.010	6.00	30.20	39.4	1.19	0.00	13.56
18-20	1.15	.016	7.40	29.60	41.9	1.44	0.00	11.24
20-22	1.20	.016	7.20	29.50	43.0	1.44	0.00	9.83
22-24	.43	.009	6.20	30.60	41.8	.98	0.00	10.53
24-26	.25	.009	5.70	32.10	41.9	1.02	0.00	10.21
26-28	.34	.013	6.50	28.10	45.0	1.26	0.00	9.96

DDH = 1157NE   LINE 1200 NW   ELEV = 175 m

Depth (m)	Ni (%)	Co (%)	Fe (%)	MgO (%)	SiO$_2$ (%)	Al$_2$O$_3$ (%)	Cr$_2$O$_3$ (%)	LOI (%)
0-2	.91	0.000	33.62	.81	0.0	0.00	0.00	0.00
2-4	2.56	.033	12.00	28.58	40.8	0.00	0.00	11.52
4-6	1.81	.023	7.48	31.60	41.3	0.00	0.00	10.19
6-8	2.10	.020	7.80	32.94	39.4	0.00	0.00	10.96
8-10	1.94	.016	6.90	28.08	44.3	0.00	0.00	9.95
10-12	.49	0.000	5.18	22.09	0.0	0.00	0.00	0.00
12-14	.58	0.000	6.04	23.21	0.0	0.00	0.00	0.00
14-16	.79	0.000	8.27	31.15	0.0	0.00	0.00	0.00

DDH = 1180NE   LINE 1200 NW   ELEV = 182 m

Depth (m)	Ni (%)	Co (%)	Fe (%)	MgO (%)	SiO$_2$ (%)	Al$_2$O$_3$ (%)	Cr$_2$O$_3$ (%)	LOI (%)
0-2	.96	.165	32.90	1.40	0.0	0.00	0.00	0.00
2-4	1.11	.054	23.50	4.20	0.0	0.00	0.00	0.00
4-6	2.12	.030	12.50	23.30	41.9	2.23	1.03	0.00
6-8	2.64	.024	9.40	30.20	39.0	2.14	.95	0.00
8-10	3.05	.018	8.20	31.90	38.0	1.11	.76	0.00
10-12	2.05	.010	7.00	35.20	38.8	.64	.64	0.00
12-14	3.67	.017	7.90	31.60	37.7	.58	.65	0.00
14-16	3.77	.023	8.50	29.30	38.9	.78	.52	0.00
16-18	3.05	.022	7.90	30.00	40.6	.85	.56	0.00
18-20	2.51	.021	7.90	28.30	42.5	.73	.62	0.00
20-22	1.99	.020	7.50	30.60	41.9	.51	.59	0.00
22-24	1.36	.019	7.40	33.10	0.0	0.00	0.00	0.00
24-26	.53	.015	6.30	35.20	0.0	0.00	0.00	0.00
26-28	.36	.018	6.00	30.70	0.0	0.00	0.00	0.00
28-30	.35	.017	6.40	36.80	0.0	0.00	0.00	0.00

DDH = 1209NE   LINE 1200 NW   ELEV = 189 m

Depth (m)	Ni (%)	Co (%)	Fe (%)	MgO (%)	SiO$_2$ (%)	Al$_2$O$_3$ (%)	Cr$_2$O$_3$ (%)	LOI (%)
0-2	.94	0.000	37.00	1.00	0.0	0.00	0.00	0.00
2-4	1.42	0.000	42.70	1.00	0.0	0.00	0.00	0.00
4-6	2.45	0.000	31.50	9.60	22.7	4.98	2.18	0.00
6-8	2.72	0.000	14.20	24.60	37.4	2.46	1.08	0.00
8-10	2.63	0.000	7.60	31.10	42.2	1.48	.64	0.00
10-12	2.41	0.000	7.20	31.10	42.2	1.20	.55	0.00
12-14	2.60	0.000	8.10	26.20	43.9	1.26	.63	0.00
14-16	2.02	0.000	6.50	27.00	48.1	.54	.56	0.00
16-18	.99	0.000	6.50	31.10	0.0	0.00	0.00	0.00
18-20	.27	0.000	6.50	36.20	0.0	0.00	0.00	0.00
20-22	.36	0.000	6.70	33.00	0.0	0.00	0.00	0.00
22-24	.28	0.000	6.20	37.40	0.0	0.00	0.00	0.00
24-26	.25	0.000	6.10	37.30	0.0	0.00	0.00	0.00
26-28	.43	0.000	6.40	33.40	0.0	0.00	0.00	0.00

DDH = 1228NE   LINE 1200 NW   ELEV = 196 m

Depth (m)	Ni (%)	Co (%)	Fe (%)	MgO (%)	SiO$_2$ (%)	Al$_2$O$_3$ (%)	Cr$_2$O$_3$ (%)	LOI (%)
0-2	1.04	.085	38.88	.65	22.6	0.00	0.00	9.45
2-4	1.97	.101	40.30	1.28	16.3	0.00	0.00	10.01
4-6	3.74	.034	13.65	24.78	35.7	0.00	0.00	12.44
6-8	4.37	.018	8.43	28.40	38.8	0.00	0.00	13.08
8-10	4.41	.038	16.55	21.38	33.2	0.00	0.00	11.97
10-12	3.74	.037	14.80	23.75	35.3	0.00	0.00	10.38
12-14	3.10	.023	10.70	27.80	38.9	0.00	0.00	10.38
14-16	2.36	.017	8.58	28.00	41.9	0.00	0.00	9.91
16-18	1.26	.016	7.91	29.71	43.6	0.00	0.00	10.54
18-20	1.81	.015	7.07	29.48	44.7	0.00	0.00	11.45

DDH = 1253NE   LINE 1200 NW   ELEV = 203 m

Depth (m)	Ni (%)	Co (%)	Fe (%)	MgO (%)	SiO$_2$ (%)	Al$_2$O$_3$ (%)	Cr$_2$O$_3$ (%)	LOI (%)
0-2	2.21	.038	15.30	7.60	56.7	2.86	1.16	6.80
2-4	.76	.059	15.10	.80	71.0	.90	1.32	3.83
4-6	2.30	.215	44.50	1.00	11.9	2.24	3.39	13.61
6-8	1.78	.113	27.20	1.30	47.6	1.40	2.22	6.76
8-10	2.07	.029	13.20	11.80	57.4	.63	1.09	6.76
10-12	2.44	.019	8.30	28.10	45.5	.44	.62	10.48
12-14	1.65	.013	7.50	34.40	43.7	.43	.57	8.61
14-16	2.54	.013	7.80	32.00	44.4	.68	.63	8.87
16-18	2.62	.012	6.80	32.80	42.5	.98	.53	10.84
18-20	1.70	.012	8.00	29.50	46.8	1.18	.56	8.05
20-22	.85	.010	6.90	32.80	46.6	1.37	.50	6.41
22-24	.97	.009	6.80	31.50	45.8	.69	.43	9.84
24-26	.95	.008	6.60	29.70	49.7	1.20	.46	8.21
26-28	1.51	.007	6.60	27.90	50.1	1.03	.45	8.80
28-30	.75	.010	6.60	33.70	44.0	1.06	.44	10.36
30-32	2.56	.014	7.20	26.20	46.2	1.38	.56	11.06
32-34	1.60	.013	6.20	31.20	46.3	.72	.46	10.81
34-36	1.19	0.000	7.20	33.10	0.0	0.00	0.00	0.00
36-38	.41	0.000	6.80	36.30	0.0	0.00	0.00	0.00

DDH = 1273NE   LINE 1200 NW   ELEV = 210 m

Depth (m)	Ni (%)	Co (%)	Fe (%)	MgO (%)	SiO_2 (%)	Al_2O_3 (%)	Cr_2O_3 (%)	LOI (%)
0-2	.89	0.000	30.50	0.00	0.0	0.00	0.00	0.00
2-4	1.36	0.000	31.00	0.00	0.0	0.00	0.00	0.00
4-6	1.47	0.000	27.00	.20	0.0	0.00	0.00	0.00
6-8	3.72	.101	30.60	8.10	23.0	4.70	2.20	9.25
8-10	2.26	.020	20.90	3.00	51.4	3.25	1.39	5.39
10-12	1.68	.026	14.60	.40	67.2	2.45	1.12	3.85
12-14	2.67	.027	12.60	10.70	57.5	2.00	.85	5.94
14-16	2.26	.014	7.30	10.80	68.6	1.47	.54	5.17
16-18	2.23	.017	7.80	16.30	62.5	1.42	.52	5.51
18-20	2.92	.010	9.70	17.40	52.9	1.78	.73	7.91
20-22	3.51	.018	9.70	16.40	55.7	1.45	.77	7.76
22-24	1.94	.015	8.30	7.50	73.0	.50	.63	4.62
24-26	2.06	.019	8.30	7.90	71.5	.53	.72	4.95
26-28	3.92	.011	8.50	10.80	64.0	1.08	.69	6.12
28-30	1.99	.020	12.00	7.30	66.0	1.16	.98	5.63
30-32	1.57	.020	7.90	8.00	68.6	.47	.64	5.02
32-34	1.43	.026	5.40	5.70	80.4	.40	.44	3.77
34-36	1.38	.017	8.70	8.00	70.7	.79	.70	5.24
36-38	.56	.011	7.90	13.90	65.0	.56	.67	6.67
38-40	.66	.027	7.60	23.40	55.7	.52	.59	8.98
40-42	2.08	.010	7.20	21.80	53.0	1.25	.70	9.13
42-44	2.12	.011	6.20	18.60	56.8	1.20	.49	9.15
44-46	2.45	.028	6.20	21.30	55.7	1.11	.51	9.40
46-48	2.43	.014	5.70	29.30	44.2	.74	.40	12.06
48-50	2.05	.017	5.60	29.10	46.2	.56	.35	11.68
50-52	1.59	.012	5.70	22.50	53.7	1.13	.53	9.09
52-54	.70	0.000	6.30	36.20	0.0	0.00	0.00	0.00
54-56	.68	0.000	7.00	27.20	0.0	0.00	0.00	0.00
56-58	.68	0.000	8.10	24.80	0.0	0.00	0.00	0.00
58-60	.85	0.000	8.10	26.90	0.0	0.00	0.00	0.00
60-62	.51	0.000	7.10	33.30	0.0	0.00	0.00	0.00

DDH = 1294NE   LINE 1200 NW   ELEV = 217 m

Depth (m)	Ni (%)	Co (%)	Fe (%)	MgO (%)	SiO_2 (%)	Al_2O_3 (%)	Cr_2O_3 (%)	LOI (%)
0-2	5.02	.040	15.00	11.09	47.5	0.00	0.00	8.19
2-4	2.94	.030	10.77	3.68	65.1	0.00	0.00	4.23
4-6	3.45	.082	40.00	2.13	14.8	0.00	0.00	9.34
6-8	4.16	.063	16.60	20.00	33.9	0.00	0.00	10.07
8-10	5.37	.039	9.62	21.80	43.1	0.00	0.00	9.54
10-12	3.42	.033	8.20	27.72	41.9	0.00	0.00	10.12
12-14	1.47	.017	6.82	34.40	42.9	0.00	0.00	7.57
14-16	3.33	.018	7.05	30.16	40.8	0.00	0.00	10.96
16-18	2.73	.015	6.56	33.15	41.4	0.00	0.00	11.09
18-20	3.43	.020	7.61	29.37	41.8	0.00	0.00	10.67
20-22	1.93	.014	6.42	33.90	40.6	0.00	0.00	9.71
22-24	.43	0.000	6.02	37.34	0.0	0.00	0.00	0.00

DDH = 1317NE   LINE 1200 NW   ELEV = 224 m

Depth (m)	Ni (%)	Co (%)	Fe (%)	MgO (%)	SiO_2 (%)	Al_2O_3 (%)	Cr_2O_3 (%)	LOI (%)
0-2	.76	0.000	30.30	.80	0.0	0.00	0.00	0.00
2-4	.73	0.000	24.20	.70	0.0	0.00	0.00	0.00
4-6	.59	0.000	15.90	.70	0.0	0.00	0.00	0.00
6-8	.83	0.000	17.20	1.00	0.0	0.00	0.00	0.00
8-10	1.01	.074	18.00	.80	63.9	0.00	0.00	0.00
10-12	.96	0.000	10.30	.70	0.0	0.00	0.00	0.00
12-14	.89	0.000	19.30	.70	0.0	0.00	0.00	0.00
14-16	1.77	.077	27.40	1.40	40.9	0.00	0.00	0.00
16-18	3.01	.076	18.70	19.90	32.2	0.00	0.00	0.00
18-20	2.25	.043	10.10	27.50	39.0	0.00	0.00	0.00
20-22	2.40	.094	24.80	15.30	25.5	0.00	0.00	0.00
22-24	1.49	.033	9.20	30.20	41.8	0.00	0.00	0.00
24-26	1.54	.035	9.80	22.80	49.5	0.00	0.00	0.00
26-28	1.89	.038	11.50	18.90	51.6	0.00	0.00	0.00
28-30	1.09	.026	7.50	9.90	69.1	0.00	0.00	0.00
30-32	1.73	.031	9.10	23.70	50.7	0.00	0.00	0.00
32-34	1.40	.055	9.40	26.20	49.5	0.00	0.00	0.00
34-36	1.05	.052	8.50	25.70	46.1	0.00	0.00	0.00
36-38	.42	0.000	5.10	24.90	0.0	0.00	0.00	0.00
38-40	1.03	.063	11.40	28.30	41.5	0.00	0.00	0.00
40-42	.42	0.000	6.80	34.80	0.0	0.00	0.00	0.00

DDH = 1353NE   LINE 1200 NW   ELEV = 231 m

Depth (m)	Ni (%)	Co (%)	Fe (%)	MgO (%)	SiO_2 (%)	Al_2O_3 (%)	Cr_2O_3 (%)	LOI (%)
0-2	.99	.113	40.10	1.10	0.0	0.00	0.00	0.00
2-4	1.29	.067	31.60	1.00	34.1	0.00	0.00	0.00
4-6	4.19	.066	20.40	3.80	48.5	4.09	1.71	6.69
6-8	4.43	.053	20.00	2.00	52.3	2.96	1.68	6.28
8-10	5.27	.052	23.20	2.80	41.0	4.34	1.86	7.84
10-12	7.16	.038	13.00	6.00	54.2	2.61	1.10	6.99
12-14	5.37	.018	10.90	3.50	68.6	1.47	.70	5.00
14-16	4.80	.020	6.10	8.90	69.1	1.10	.51	5.77
16-18	5.48	.027	9.70	9.80	59.0	1.47	.75	7.27
18-20	4.62	.031	9.80	10.80	60.9	1.08	.61	7.08
20-22	4.50	.019	10.20	9.40	61.7	1.35	.78	6.59
22-24	1.94	.019	7.50	1.30	79.8	1.22	.61	2.55
24-26	2.70	.014	5.70	3.60	79.0	.74	.45	3.32
26-28	3.89	.016	7.00	14.90	62.6	.58	.44	7.34
28-30	4.44	.014	5.70	13.80	63.9	.78	.45	7.31
30-32	4.88	.016	6.60	15.70	58.8	.84	.46	8.58
32-34	3.59	.023	8.90	17.40	52.7	1.47	.65	9.11
34-36	4.79	.019	8.30	16.70	53.1	1.34	.66	9.06
36-38	5.85	.014	7.90	16.70	51.0	1.50	.60	8.26
38-40	7.12	.014	7.10	13.60	56.6	1.38	.62	7.22
40-42	6.00	.014	7.80	19.40	50.5	1.81	.92	9.22
42-44	3.86	.020	9.90	20.90	45.6	2.13	.84	9.93
44-46	2.10	.018	10.80	23.80	42.5	.94	.62	9.35
46-48	.36	.009	6.00	35.10	41.6	0.00	0.00	0.00
48-50	1.10	.010	7.70	30.60	44.2	0.00	0.00	0.00
50-52	4.82	.015	8.50	18.70	51.0	1.14	.61	8.28
52-54	5.23	.015	8.10	17.40	51.4	1.10	.54	8.00
54-56	4.35	.013	7.50	20.10	50.8	1.50	.58	7.91
56-58	4.72	.011	7.10	18.00	52.5	1.13	.58	8.05
58-60	4.76	.012	6.80	21.00	48.4	1.56	.64	8.79
60-62	1.38	.023	7.00	29.90	47.8	0.00	0.00	0.00
62-64	.58	0.000	6.60	35.10	0.0	0.00	0.00	0.00
64-66	.51	0.000	6.80	36.70	0.0	0.00	0.00	0.00

DDH = 1375NE   LINE 1200 NW   ELEV. = 234 m

Depth (m)	Ni (%)	Co (%)	Fe (%)	MgO (%)	SiO_2 (%)	Al_2O_3 (%)	Cr_2O_3 (%)	LOI (%)
0-2	.80	.102	42.50	1.40	0.0	0.00	0.00	0.00
2-4	1.19	.151	36.60	1.10	0.0	0.00	0.00	0.00
4-6	1.50	.129	33.10	1.00	29.3	6.14	2.23	8.53
6-8	1.52	.135	31.10	1.00	32.6	5.59	2.31	8.41
8-10	1.68	.140	31.80	.90	29.3	6.46	2.63	8.61
10-12	1.41	.093	26.10	.60	41.9	4.94	2.27	6.99
12-14	1.18	.084	23.80	.80	45.9	4.44	1.75	6.48
14-16	1.13	.087	23.50	.90	47.3	3.73	1.72	5.96
16-18	1.61	.090	25.70	1.00	42.6	4.04	2.07	6.24
18-20	2.08	.061	21.00	1.10	50.9	2.43	1.83	5.47
20-22	2.78	.042	18.00	2.30	52.3	1.83	1.50	5.27
22-24	3.25	.041	14.40	7.60	53.0	1.92	1.32	6.19
24-26	4.25	.031	10.50	13.80	51.0	1.68	.94	7.63
26-28	5.48	.024	7.80	16.90	52.1	1.38	.51	7.99
28-30	4.45	.023	9.30	19.40	47.1	1.14	.59	9.28
30-32	2.75	.016	7.80	14.00	59.8	.90	.55	7.02
32-34	3.17	.015	7.70	13.90	57.9	1.02	.53	7.09
34-36	4.75	.016	8.90	16.30	51.7	.76	.81	8.37
36-38	1.36	.011	8.40	25.80	46.3	.74	.57	8.49
38-40	1.06	.013	8.00	28.50	44.8	.81	.53	8.55
40-42	1.70	.015	10.10	24.00	43.4	1.35	.74	9.47
42-44	1.75	.021	8.00	23.40	47.4	1.25	.62	8.81
44-46	.85	.016	7.50	29.80	0.0	0.00	0.00	0.00
46-48	.88	.020	7.10	27.30	0.0	0.00	0.00	0.00
48-50	.62	.023	7.10	30.10	0.0	0.00	0.00	0.00
50-52	.61	.018	7.30	28.20	0.0	0.00	0.00	0.00
52-54	.69	.016	7.10	28.10	0.0	0.00	0.00	0.00
54-56	.51	.016	7.20	29.10	0.0	0.00	0.00	0.00
56-58	.42	.010	6.70	29.30	0.0	0.00	0.00	0.00
58-60	.23	.016	5.80	36.00	0.0	0.00	0.00	0.00
60-62	.15	.016	6.40	35.60	0.0	0.00	0.00	0.00

DDH = 1400 LINE 1200 NW ELEV = 238 m

Depth (m)	Ni (%)	Co (%)	Fe (%)	MgO (%)	SiO_2 (%)	Al_2O_3 (%)	Cr_2O_3 (%)	LOI (%)
0-2	.45	0.000	46.41	.69	0.0	0.00	0.00	0.00
2-4	1.00	0.000	46.78	.72	0.0	0.00	0.00	0.00
4-6	1.30	0.000	48.21	.69	0.0	0.00	0.00	0.00
6-8	.95	0.000	39.87	.73	0.0	0.00	0.00	0.00
8-10	.81	0.000	37.19	.57	0.0	0.00	0.00	0.00
10-12	.75	0.000	25.60	.68	0.0	0.00	0.00	0.00
12-14	.63	0.000	21.79	.61	0.0	0.00	0.00	0.00
14-16	.50	0.000	15.45	.70	0.0	0.00	0.00	0.00
16-18	3.13	.039	13.10	8.48	54.0	0.00	0.00	6.22
18-20	4.06	.039	13.86	12.95	45.5	0.00	0.00	8.34
20-22	4.54	.028	10.27	18.27	48.1	0.00	0.00	8.55
22-24	4.85	.013	7.14	21.63	52.8	0.00	0.00	9.04
24-26	4.64	.013	8.34	23.65	47.2	0.00	0.00	10.52
26-28	5.50	.024	11.36	17.08	47.9	0.00	0.00	8.94
28-30	3.92	.038	8.60	23.20	43.6	.94	.10	10.16
30-32	5.06	.025	9.09	19.62	49.8	0.00	0.00	9.33
32-34	3.95	.035	10.16	19.82	48.6	0.00	0.00	9.42
34-36	2.84	.024	9.23	13.70	57.6	0.00	0.00	7.50
36-38	2.93	.024	8.86	13.63	62.0	0.00	0.00	6.50
38-40	3.70	.035	10.22	16.83	53.7	0.00	0.00	8.26
40-42	5.52	.036	11.17	16.94	48.5	0.00	0.00	8.82
42-44	.98	.016	9.14	26.62	47.2	0.00	0.00	8.84
44-46	2.13	.014	7.96	27.66	48.3	0.00	0.00	9.31
46-48	1.32	.014	7.26	29.58	49.5	0.00	0.00	7.49

DDH = 1454NE   LINE 1200 NW   ELEV = 238 m

Depth (m)	Ni (%)	Co (%)	Fe (%)	MgO (%)	SiO_2 (%)	Al_2O_3 (%)	Cr_2O_3 (%)	LOI (%)
0-2	.64	0.000	51.37	.68	0.0	0.00	0.00	0.00
2-4	.62	0.000	50.60	.67	0.0	0.00	0.00	0.00
4-6	.77	0.000	50.17	.67	0.0	0.00	0.00	0.00
6-8	.66	0.000	47.08	.66	0.0	0.00	0.00	0.00
8-10	.72	0.000	45.08	.82	0.0	0.00	0.00	0.00
10-12	.93	0.000	44.58	.73	0.0	0.00	0.00	0.00
12-14	.97	0.000	38.00	.77	0.0	0.00	0.00	0.00
14-16	.62	0.000	25.23	.59	0.0	0.00	0.00	0.00
16-18	.71	0.000	26.86	1.12	0.0	0.00	0.00	0.00
18-20	1.07	.186	32.01	1.00	35.8	0.00	0.00	8.31
20-22	1.00	.088	28.34	.95	40.0	0.00	0.00	2.37
22-24	1.91	.146	34.94	.97	25.2	0.00	0.00	8.48
24-26	2.57	.121	18.26	4.32	51.2	0.00	0.00	6.90
26-28	2.55	.087	19.01	2.70	54.5	0.00	0.00	5.87
28-30	6.30	.098	16.67	10.19	41.3	0.00	0.00	8.82
30-32	5.85	.095	24.60	5.32	35.9	0.00	0.00	8.29
32-34	2.77	.083	23.70	7.96	38.0	0.00	0.00	8.14
34-36	3.49	.077	23.70	7.30	32.0	0.00	0.00	8.23
36-38	2.32	.058	13.79	20.19	39.6	0.00	0.00	11.28
38-40	2.15	.017	14.10	8.59	59.4	0.00	0.00	6.96
40-42	2.32	.028	9.91	8.40	65.4	0.00	0.00	5.48
42-44	3.07	.027	8.97	15.90	54.3	0.00	0.00	9.18
44-46	3.67	.023	8.13	12.28	58.5	0.00	0.00	2.49
46-48	3.52	.031	10.58	13.56	53.0	0.00	0.00	8.08
48-50	3.00	0.000	10.63	15.45	54.2	0.00	0.00	0.00
50-52	2.56	0.000	10.38	18.88	52.3	0.00	0.00	0.00
52-54	1.46	0.000	10.03	22.78	51.0	0.00	0.00	0.00
54-56	1.71	0.000	8.76	20.77	51.4	0.00	0.00	0.00
56-58	3.29	0.000	9.45	18.30	51.3	0.00	0.00	0.00
58-60	2.39	0.000	8.22	20.27	52.6	0.00	0.00	0.00
60-62	2.07	0.000	9.33	23.66	47.9	0.00	0.00	0.00
62-64	1.40	0.000	11.36	20.56	0.0	0.00	0.00	0.00
64-66	1.11	0.000	8.86	21.56	0.0	0.00	0.00	0.00

DDH = 1487NE			LINE 1200 NW			ELEV = 230 m	
Depth (m)	Ni (%)	Co (%)	Fe (%)	MgO (%)	SiO_2 (%)	Al_2O_3 (%)	Cr_2O_3 (%)	LOI (%)
0-2	.60	0.000	45.80	.80	0.0	0.00	0.00	0.00
2-4	.80	0.000	50.70	.70	0.0	0.00	0.00	0.00
4-6	.80	0.000	53.50	.70	0.0	0.00	0.00	0.00
6-8	.74	0.000	51.90	.80	0.0	0.00	0.00	0.00
8-10	.72	0.000	53.20	.70	0.0	0.00	0.00	0.00
10-12	.99	0.000	51.30	.70	0.0	0.00	0.00	0.00
12-14	.69	0.000	49.00	.90	0.0	0.00	0.00	0.00
14-16	1.04	.385	47.70	.80	5.1	0.00	0.00	0.00
16-18	.69	0.000	29.70	.60	0.0	0.00	0.00	0.00
18-20	.56	0.000	26.40	.50	0.0	0.00	0.00	0.00
20-22	1.41	.223	24.90	1.00	49.4	0.00	0.00	0.00
22-24	4.30	.083	14.00	14.90	47.4	2.15	1.02	8.89
24-26	4.30	.057	12.20	14.00	52.4	1.61	.67	8.23
26-28	3.85	.062	15.40	9.70	51.7	2.30	.95	7.59
28-30	3.71	.049	16.80	6.20	54.0	2.04	.99	6.85
30-32	3.17	.046	19.90	3.20	55.0	1.78	1.30	6.05
32-34	3.92	.043	16.80	5.50	54.1	2.32	1.27	6.30
34-36	3.64	.040	11.40	12.40	50.2	1.28	.94	9.26
36-38	3.10	.050	10.90	21.80	44.1	1.65	.81	11.23
38-40	2.77	.065	13.30	20.30	41.9	1.33	.98	11.92
40-42	3.77	.081	13.80	15.30	44.7	2.54	1.38	10.32
42-44	4.55	.072	13.60	15.20	44.0	2.37	1.59	10.41
44-46	4.19	.068	12.80	18.60	43.2	2.06	1.20	10.96
46-48	4.37	.095	18.10	12.30	39.7	3.09	1.78	10.42
48-50	4.03	.094	15.80	9.80	49.8	2.38	1.51	8.08
50-52	2.57	.072	12.20	17.40	50.7	1.40	1.06	8.65
52-54	3.40	.054	9.40	13.60	46.3	.82	1.10	6.85
54-56	3.74	.077	9.30	18.60	54.2	.63	.95	9.16
56-58	4.00	.058	7.70	19.50	48.2	.55	.77	9.15
58-60	3.52	.060	7.70	21.80	49.6	1.02	.83	9.53
60-62	4.25	.050	7.10	20.90	48.0	1.55	.77	9.55
62-64	3.52	.046	9.10	20.30	49.6	1.60	1.32	9.01
64-66	5.14	.041	8.60	21.80	47.6	1.36	.91	9.60
66-68	1.50	.024	6.80	30.50	45.7	.68	.42	9.57
68-70	1.01	.032	7.10	32.90	43.9	0.00	0.00	0.00
70-72	3.02	.050	7.70	25.00	46.0	.99	.92	10.44
72-74	1.02	.031	6.80	32.00	46.0	0.00	0.00	0.00
74-76	.31	.017	6.90	28.70	50.4	0.00	0.00	0.00
76-78	3.45	.034	8.00	21.50	50.1	1.72	.89	8.52
78-80	4.02	.026	7.60	24.80	47.4	1.04	.58	8.30
80-82	2.03	.026	6.90	29.40	46.4	1.02	.56	8.51
82-84	1.30	.022	7.00	32.50	44.7	0.00	0.00	0.00
84-86	.50	0.000	6.70	36.30	0.0	0.00	0.00	0.00
86-88	.32	0.000	5.80	31.30	0.0	0.00	0.00	0.00

DDH = 1500NE			LINE 1200 NW			ELEV = 228 m	
Depth (m)	Ni (%)	Co (%)	Fe (%)	MgO (%)	SiO$_2$ (%)	Al$_2$O$_3$ (%)	Cr$_2$O$_3$ (%)	LOI (%)
0-2	.45	.009	40.51	.50	4.3	20.72	0.00	14.96
2-4	.76	.016	41.79	.25	5.5	20.88	0.00	13.58
4-6	.64	.009	49.51	.60	2.3	15.84	0.00	9.76
6-8	.74	.013	53.05	.30	2.0	13.66	0.00	7.54
8-10	.76	.017	54.17	.30	1.6	11.60	0.00	6.24
10-12	.64	.030	54.33	.25	1.6	11.36	0.00	6.58
12-14	.85	.081	54.98	.40	2.0	9.84	0.00	5.28
14-16	.90	.092	55.06	.35	1.7	8.82	0.00	5.56
16-18	.82	.048	54.49	.35	1.3	8.82	0.00	6.20
18-20	.82	.099	50.31	.40	3.9	10.64	0.00	7.20
20-22	1.17	.310	43.20	.50	6.0	10.64	0.00	11.64
22-24	1.28	.340	34.70	.60	23.7	6.78	0.00	8.86
24-26	1.54	.219	27.77	.85	37.9	4.62	0.00	8.60
26-28	1.28	.320	26.97	.65	35.3	5.40	0.00	8.88
28-30	1.23	.368	29.86	.40	30.3	5.78	0.00	8.94
30-32	1.40	.348	26.65	.40	35.3	6.64	0.00	8.08
32-34	1.66	.214	21.67	.70	49.1	3.52	0.00	6.76
34-36	1.63	.353	21.43	.70	44.4	5.06	0.00	7.14
36-38	1.36	.404	23.20	.70	40.8	5.40	0.00	7.90

DDH = 1511NE   LINE 1200 NW   ELEV = 224 m

Depth (m)	Ni (%)	Co (%)	Fe (%)	MgO (%)	SiO_2 (%)	Al_2O_3 (%)	Cr_2O_3 (%)	LOI (%)
0-2	.46	0.000	42.30	1.00	0.0	0.00	0.00	0.00
2-4	.65	0.000	13.50	1.00	0.0	0.00	0.00	0.00
4-6	.77	0.000	42.10	.90	0.0	0.00	0.00	0.00
6-8	.57	0.000	22.30	1.00	0.0	0.00	0.00	0.00
8-10	.58	0.000	57.60	.80	0.0	0.00	0.00	0.00
10-12	.68	0.000	54.30	.70	0.0	0.00	0.00	0.00
12-14	.72	0.000	52.50	.80	0.0	0.00	0.00	0.00
14-16	.94	0.000	55.10	.90	0.0	0.00	0.00	0.00
16-18	.72	0.000	55.90	.80	0.0	0.00	0.00	0.00
18-20	.86	0.000	50.50	.90	0.0	0.00	0.00	0.00
20-22	.94	0.000	54.70	.70	0.0	0.00	0.00	0.00
22-24	1.14	.107	51.00	.90	8.9	0.00	0.00	0.00
24-26	1.51	.123	37.10	1.20	21.0	0.00	0.00	0.00
26-28	1.48	.216	30.40	1.40	25.1	0.00	0.00	0.00
28-30	1.36	.217	22.30	1.80	43.0	0.00	0.00	0.00
30-32	1.85	.503	26.40	2.20	33.2	0.00	0.00	0.00
32-34	2.14	.179	22.50	3.10	38.9	0.00	0.00	0.00
34-36	1.58	.125	19.40	3.20	49.2	0.00	0.00	0.00
36-38	1.28	.099	23.20	2.10	45.4	0.00	0.00	0.00
38-40	2.73	.080	20.50	8.30	41.8	0.00	0.00	0.00
40-42	3.39	.072	15.70	15.70	46.9	0.00	0.00	0.00
42-44	3.21	.069	16.70	16.70	45.6	0.00	0.00	0.00
44-46	2.34	.151	22.60	3.70	42.9	0.00	0.00	0.00
46-48	2.86	.149	17.10	16.00	39.2	0.00	0.00	0.00
48-50	2.55	.102	12.30	21.80	40.1	0.00	0.00	0.00
50-52	2.28	.046	8.10	18.60	54.7	0.00	0.00	0.00
52-54	3.20	.046	8.70	24.60	45.4	0.00	0.00	0.00
54-56	2.29	.044	8.80	15.80	56.6	0.00	0.00	0.00
56-58	2.68	.071	13.90	10.30	52.5	0.00	0.00	0.00
58-60	2.47	.036	10.80	24.40	39.5	0.00	0.00	0.00
60-62	3.36	.034	7.80	25.80	45.3	0.00	0.00	0.00
62-64	2.66	.033	8.80	26.00	43.6	0.00	0.00	0.00
64-66	2.04	.022	8.00	28.50	44.2	0.00	0.00	0.00
66-68	1.42	.021	8.20	30.30	42.2	0.00	0.00	0.00
68-70	.75	0.000	6.90	29.50	0.0	0.00	0.00	0.00
70-72	.59	0.000	6.50	32.10	0.0	0.00	0.00	0.00
72-74	.40	0.000	6.40	34.00	0.0	0.00	0.00	0.00
74-76	1.04	.023	6.50	29.70	45.6	0.00	0.00	0.00
76-78	1.18	.023	6.60	29.60	45.8	0.00	0.00	0.00
78-80	.53	0.000	6.90	35.90	0.0	0.00	0.00	0.00

DDH = 1535NE   LINE 1200 NW   ELEV = 217 m

Depth (m)	Ni (%)	Co (%)	Fe (%)	MgO (%)	SiO_2 (%)	Al_2O_3 (%)	Cr_2O_3 (%)	LOI (%)
0-2	.39	0.000	36.75	.53	0.0	0.00	0.00	0.00
2-4	.49	0.000	35.56	.52	0.0	0.00	0.00	0.00
4-6	.59	0.000	40.93	.67	0.0	0.00	0.00	0.00
6-8	.57	0.000	41.62	.73	0.0	0.00	0.00	0.00
8-10	.66	0.000	44.82	.77	0.0	0.00	0.00	0.00
10-12	.88	0.000	44.58	.86	0.0	0.00	0.00	0.00
12-14	1.22	.091	47.84	.92	3.6	0.00	0.00	10.35
14-16	1.47	.090	47.67	.96	4.9	0.00	0.00	9.74
16-18	1.37	.092	48.34	.96	4.7	0.00	0.00	4.70
18-20	1.48	.154	45.71	1.25	5.4	0.00	0.00	8.44
20-22	1.73	.300	38.72	1.24	13.4	0.00	0.00	13.13
22-24	2.13	.276	28.66	1.15	30.5	0.00	0.00	3.13
24-26	1.71	.249	25.61	1.12	38.6	0.00	0.00	12.29
26-28	1.16	.172	23.85	2.96	40.6	0.00	0.00	12.87
28-30	1.13	.131	23.73	3.08	43.5	0.00	0.00	11.61
30-32	.99	.100	21.48	4.58	47.7	0.00	0.00	9.19
32-34	2.18	.059	18.21	10.75	49.3	0.00	0.00	9.60
34-36	3.56	.080	19.69	7.90	39.6	0.00	0.00	11.09
36-38	1.96	.085	22.83	2.40	40.1	0.00	0.00	10.57
38-40	1.61	.220	28.46	2.40	30.0	0.00	0.00	12.42
40-42	.90	.226	19.62	2.45	50.8	0.00	0.00	9.74
42-44	1.58	.264	23.39	4.14	39.8	0.00	0.00	12.16
44-46	1.14	.091	15.00	6.33	55.0	0.00	0.00	8.73
46-48	3.57	.046	11.71	19.09	46.4	0.00	0.00	11.18
48-50	2.70	.026	11.42	22.36	44.7	0.00	0.00	10.59
50-52	1.22	.025	13.84	20.17	43.7	0.00	0.00	9.55
52-54	.65	0.000	8.69	28.38	0.0	0.00	0.00	0.00
54-56	.40	0.000	8.90	30.81	0.0	0.00	0.00	0.00
56-58	.43	0.000	10.06	29.36	0.0	0.00	0.00	0.00
58-60	.56	0.000	11.96	26.29	0.0	0.00	0.00	0.00
60-62	.32	0.000	7.75	28.55	0.0	0.00	0.00	0.00
62-64	.39	0.000	9.66	27.19	0.0	0.00	0.00	0.00
64-66	.64	0.000	11.05	26.45	0.0	0.00	0.00	0.00
66-68	.27	0.000	7.08	36.28	0.0	0.00	0.00	0.00

267

DDH = 1554NE   LINE 1200 NW   ELEV = 213 m

Depth (m)	Ni (%)	Co (%)	Fe (%)	MgO (%)	SiO$_2$ (%)	Al$_2$O$_3$ (%)	Cr$_2$O$_3$ (%)	LOI (%)
0-2	.35	0.000	31.16	.27	0.0	0.00	0.00	0.00
2-4	.45	0.000	28.45	.41	0.0	0.00	0.00	0.00
4-6	.51	0.000	34.32	.45	0.0	0.00	0.00	0.00
6-8	.64	0.000	26.13	.48	0.0	0.00	0.00	0.00
8-10	.62	0.000	40.95	.69	0.0	0.00	0.00	0.00
10-12	.57	0.000	40.80	.79	0.0	0.00	0.00	0.00
12-14	.59	0.000	42.83	.66	0.0	0.00	0.00	0.00
14-16	.89	0.000	45.61	.74	0.0	0.00	0.00	0.00
16-18	1.31	0.000	47.12	.75	3.8	0.00	0.00	0.00
18-20	1.48	0.000	52.24	.64	4.2	0.00	0.00	0.00
20-22	1.59	0.000	50.43	.67	4.6	0.00	0.00	0.00
22-24	1.72	0.000	49.53	.67	3.2	0.00	0.00	0.00
24-26	1.44	0.000	48.17	1.13	4.8	0.00	0.00	0.00
26-28	1.44	0.000	48.48	.94	6.7	0.00	0.00	0.00
28-30	1.57	0.000	49.23	1.02	6.1	0.00	0.00	0.00
30-32	1.65	0.000	49.98	1.09	7.6	0.00	0.00	0.00
32-34	1.46	0.000	44.18	1.14	12.5	0.00	0.00	0.00
34-36	1.89	0.000	35.23	1.38	18.6	0.00	0.00	0.00
36-38	1.55	0.000	28.00	1.03	32.8	0.00	0.00	0.00
38-40	1.15	0.000	24.99	.88	43.2	0.00	0.00	0.00
40-42	1.21	0.000	28.45	1.11	30.6	0.00	0.00	0.00
42-44	.84	0.000	34.02	.95	39.5	0.00	0.00	0.00
44-46	.87	0.000	28.34	.93	39.5	0.00	0.00	0.00
46-48	.82	0.000	20.70	2.56	50.4	0.00	0.00	0.00
48-50	2.93	0.000	12.65	19.46	42.3	0.00	0.00	0.00
50-52	3.68	0.000	17.46	8.98	43.4	0.00	0.00	0.00
52-54	1.72	0.000	12.80	2.63	62.1	0.00	0.00	0.00
54-56	1.06	0.000	10.84	2.06	67.8	0.00	0.00	0.00
56-58	1.04	0.000	11.29	2.42	68.0	0.00	0.00	0.00
58-60	3.37	0.000	18.97	9.94	40.3	0.00	0.00	0.00
60-62	2.64	0.000	12.19	21.97	43.0	0.00	0.00	0.00
62-64	2.75	0.000	10.01	24.11	43.3	0.00	0.00	0.00
64-66	2.77	0.000	10.99	23.71	42.6	0.00	0.00	0.00
66-68	2.95	0.000	9.94	22.55	46.0	0.00	0.00	0.00
68-70	3.32	0.000	10.69	20.67	46.0	0.00	0.00	0.00
70-72	2.06	0.000	11.97	12.98	53.4	0.00	0.00	0.00
72-74	1.96	0.000	12.88	13.38	52.0	0.00	0.00	0.00
74-76	1.24	0.000	9.33	17.26	55.8	0.00	0.00	0.00
76-78	.68	0.000	8.43	27.31	0.0	0.00	0.00	0.00
78-80	1.07	0.000	7.23	26.51	0.0	0.00	0.00	0.00
80-82	1.19	0.000	7.68	29.33	0.0	0.00	0.00	0.00
82-84	.66	0.000	7.38	32.42	0.0	0.00	0.00	0.00
84-86	.66	0.000	7.60	31.93	0.0	0.00	0.00	0.00
86-88	1.04	0.000	8.88	31.76	0.0	0.00	0.00	0.00
88-90	1.13	0.000	9.63	27.80	0.0	0.00	0.00	0.00
90-92	.63	0.000	8.73	31.55	0.0	0.00	0.00	0.00
92-94	.29	0.000	6.93	37.62	0.0	0.00	0.00	0.00

DDH = 1572NE   LINE 1200 NW   ELEV = 210 m

Depth (m)	Ni (%)	Co (%)	Fe (%)	MgO (%)	SiO_2 (%)	Al_2O_3 (%)	Cr_2O_3 (%)	LOI (%)
0-2	.29	0.000	35.90	.70	0.0	0.00	0.00	0.00
2-4	.40	0.000	29.30	.70	0.0	0.00	0.00	0.00
4-6	.42	0.000	31.70	.60	0.0	0.00	0.00	0.00
6-8	.57	0.000	35.90	.70	0.0	0.00	0.00	0.00
8-10	.61	0.000	39.50	.70	0.0	0.00	0.00	0.00
10-12	.68	0.000	41.60	.80	0.0	0.00	0.00	0.00
12-14	.66	0.000	39.70	.90	0.0	0.00	0.00	0.00
14-16	.62	0.000	40.70	1.00	0.0	0.00	0.00	0.00
16-18	.66	0.000	41.30	1.00	0.0	0.00	0.00	0.00
18-20	.80	0.000	43.90	.80	0.0	0.00	0.00	0.00
20-22	1.08	0.000	46.80	.90	0.0	0.00	0.00	0.00
22-24	1.19	0.000	47.90	.90	0.0	0.00	0.00	0.00
24-26	1.22	0.000	51.40	1.10	0.0	0.00	0.00	0.00
26-28	1.05	0.000	48.40	1.10	0.0	0.00	0.00	0.00
28-30	1.27	0.000	49.80	1.30	0.0	0.00	0.00	0.00
30-32	1.46	0.000	51.40	1.30	0.0	0.00	0.00	0.00
32-34	1.60	0.000	48.10	1.40	7.8	9.03	3.45	0.00
34-36	1.57	0.000	48.30	1.40	8.2	8.32	3.60	0.00
36-38	1.36	0.000	43.00	1.20	16.2	6.97	3.75	0.00
38-40	1.35	0.000	37.00	1.30	23.7	6.14	3.03	0.00
40-42	1.40	0.000	33.00	1.90	28.7	3.73	3.22	0.00
42-44	1.13	0.000	27.50	1.70	40.5	2.65	2.22	0.00
44-46	1.23	0.000	25.30	2.00	40.8	3.40	3.17	0.00
46-48	1.83	0.000	30.50	2.60	28.2	5.65	2.45	0.00
48-50	2.06	0.000	30.00	2.20	26.7	5.95	3.25	0.00
50-52	3.17	0.000	19.20	15.80	34.4	3.08	1.63	0.00
52-54	2.97	0.000	9.30	22.80	47.4	.80	.67	0.00
54-56	2.85	0.000	11.70	23.10	42.0	1.45	.72	0.00
56-58	2.41	0.000	11.60	20.40	42.7	2.40	.73	0.00
58-60	1.96	0.000	13.10	16.20	46.5	2.06	.81	0.00
60-62	2.36	0.000	10.60	19.30	48.2	1.46	.82	0.00
62-64	2.69	0.000	9.70	22.40	46.2	1.49	.72	0.00
64-66	2.38	0.000	7.50	16.70	57.5	1.35	.60	0.00
66-68	3.54	0.000	8.30	26.00	43.0	1.36	.70	0.00
68-70	3.92	0.000	9.40	25.00	39.9	1.80	.84	0.00
70-72	2.77	0.000	7.60	28.90	42.0	1.32	.64	0.00
72-74	1.64	0.000	8.90	25.50	43.5	1.77	.86	0.00
74-76	1.86	0.000	9.00	21.40	47.1	1.34	.91	0.00
76-78	1.61	0.000	8.60	24.60	47.1	1.51	.79	0.00
78-80	1.42	0.000	9.30	25.60	43.9	1.61	.74	0.00
80-82	1.17	0.000	8.80	24.40	46.6	1.10	.66	0.00
82-84	2.36	0.000	7.70	19.40	52.3	1.53	.67	0.00
84-86	.80	0.000	8.70	26.60	43.1	2.05	.67	0.00
86-88	.33	0.000	6.40	30.30	44.8	1.00	.50	0.00
88-90	.40	0.000	6.80	30.20	44.2	1.00	.56	0.00
90-92	.71	0.000	7.50	23.50	52.2	1.16	.56	0.00
92-94	1.97	0.000	8.10	18.30	54.5	1.18	.72	0.00

DDH = 1572NE   LINE 1200 NW   ELEV = 210 m

(Cont.)

94–96	2.11	0.000	7.30	16.20	59.1	.66	.82	0.00
96–98	1.31	0.000	8.70	16.10	0.0	0.00	0.00	0.00
98–100	1.46	0.000	6.80	16.20	0.0	0.00	0.00	0.00
100–102	.77	0.000	8.60	16.50	0.0	0.00	0.00	0.00
102–104	.86	0.000	8.10	17.10	0.0	0.00	0.00	0.00
104–106	.87	0.000	8.30	15.40	0.0	0.00	0.00	0.00
106–108	1.37	0.000	6.40	12.70	0.0	0.00	0.00	0.00
108–110	1.49	0.000	7.40	20.60	0.0	0.00	0.00	0.00
110–112	.49	0.000	6.20	19.40	0.0	0.00	0.00	0.00
112–114	.50	0.000	6.10	30.20	0.0	0.00	0.00	0.00
114–116	.27	0.000	5.90	32.70	0.0	0.00	0.00	0.00

DDH = 1590NE   LINE 1200 NW   ELEV = 207 m

Depth (m)	Ni (%)	Co (%)	Fe (%)	MgO (%)	SiO_2 (%)	Al_2O_3 (%)	Cr_2O_3 (%)	LOI (%)
0-2	.21	0.000	32.82	.34	0.0	0.00	0.00	0.00
2-4	.19	0.000	24.09	.34	0.0	0.00	0.00	0.00
4-6	.30	0.000	21.38	.24	0.0	0.00	0.00	0.00
6-8	.41	0.000	29.51	1.04	0.0	0.00	0.00	0.00
8-10	.45	0.000	33.87	.76	0.0	0.00	0.00	0.00
10-12	.49	0.000	36.88	.56	0.0	0.00	0.00	0.00
12-14	.51	0.000	39.14	.62	0.0	0.00	0.00	0.00
14-16	.53	0.000	39.29	.84	0.0	0.00	0.00	0.00
16-18	.77	0.000	42.15	1.02	5.5	0.00	0.00	0.00
18-20	1.50	0.000	47.42	.76	6.1	0.00	0.00	0.00
20-22	1.71	0.000	50.58	.69	4.9	0.00	0.00	0.00
22-24	1.86	0.000	49.83	.88	5.2	0.00	0.00	0.00
24-26	1.71	0.000	49.68	.75	6.8	0.00	0.00	0.00
26-28	1.53	0.000	50.76	.73	6.4	0.00	0.00	0.00
28-30	1.56	0.000	49.83	.95	7.6	0.00	0.00	0.00
30-32	1.58	0.000	48.93	1.09	8.7	0.00	0.00	0.00
32-34	1.24	0.000	44.41	1.23	15.1	0.00	0.00	0.00
34-36	1.09	0.000	30.26	1.17	35.5	0.00	0.00	0.00
36-38	1.33	0.000	24.24	1.26	44.2	0.00	0.00	0.00
38-40	1.78	0.000	26.19	1.50	41.6	0.00	0.00	0.00
40-42	1.35	0.000	22.58	1.17	51.6	0.00	0.00	0.00
42-44	1.31	0.000	20.17	1.24	51.7	0.00	0.00	0.00
44-46	1.93	0.000	19.42	2.65	49.8	0.00	0.00	0.00
46-48	2.66	0.000	16.33	2.80	49.3	0.00	0.00	0.00
48-50	3.55	0.000	13.32	6.85	38.5	0.00	0.00	0.00
50-52	3.62	0.000	11.89	22.80	38.4	0.00	0.00	0.00
52-54	2.16	0.000	15.81	23.79	40.9	0.00	0.00	0.00
54-56	1.13	0.000	15.20	17.53	52.5	0.00	0.00	0.00
56-58	2.23	0.000	13.65	9.73	53.3	0.00	0.00	0.00
58-60	4.78	0.000	10.22	19.00	47.2	0.00	0.00	0.00
60-62	3.07	0.000	11.44	18.98	41.3	0.00	0.00	0.00
62-64	3.16	0.000	11.52	23.71	42.7	0.00	0.00	0.00
64-66	4.61	0.000	12.04	21.82	43.9	0.00	0.00	0.00
66-68	3.14	0.000	11.29	23.41	42.5	0.00	0.00	0.00
68-70	3.20	0.000	13.25	21.93	39.4	0.00	0.00	0.00
70-72	2.85	0.000	11.89	24.31	40.2	0.00	0.00	0.00
72-74	2.53	0.000	9.79	23.57	46.3	0.00	0.00	0.00
74-76	1.75	0.000	9.94	26.39	43.9	0.00	0.00	0.00
76-78	.53	0.000	7.53	32.82	42.3	0.00	0.00	0.00
78-80	.53	0.000	7.53	33.77	41.9	0.00	0.00	0.00
80-82	.34	0.000	7.53	37.33	0.0	0.00	0.00	0.00
82-84	.29	0.000	7.15	39.26	0.0	0.00	0.00	0.00
84-86	.25	0.000	6.32	38.64	0.0	0.00	0.00	0.00

DDH = 1607NE   LINE 1200 NW   ELEV = 206 m

Depth (m)	Ni (%)	Co (%)	Fe (%)	MgO (%)	SiO_2 (%)	Al_2O_3 (%)	Cr_2O_3 (%)	LOI (%)
0-2	.34	0.000	34.00	.80	0.0	0.00	0.00	0.00
2-4	.25	0.000	29.00	.70	0.0	0.00	0.00	0.00
4-6	.25	0.000	28.76	.60	0.0	0.00	0.00	0.00
6-8	.38	0.000	28.90	.60	0.0	0.00	0.00	0.00
8-10	.46	0.000	28.00	.90	0.0	0.00	0.00	0.00
10-12	.45	0.000	34.50	1.20	0.0	0.00	0.00	0.00
12-14	.56	0.000	36.40	.80	0.0	0.00	0.00	0.00
14-16	.62	0.000	41.50	.70	0.0	0.00	0.00	0.00
16-18	.68	0.000	40.90	.90	0.0	0.00	0.00	0.00
18-20	1.03	0.000	45.30	.90	0.0	0.00	0.00	0.00
20-22	1.35	0.000	50.70	.80	0.0	0.00	0.00	0.00
22-24	1.77	.047	48.60	.80	11.8	8.83	2.16	9.56
24-26	1.61	.071	48.00	1.10	9.3	8.47	2.22	10.54
26-28	1.62	.038	52.70	1.20	9.7	6.63	1.20	7.61
28-30	1.69	.050	51.10	1.30	6.2	8.50	2.32	6.54
30-32	1.63	.034	51.26	1.20	7.5	7.70	2.65	6.11
32-34	1.45	.058	48.00	1.40	8.1	9.64	2.16	7.47
34-36	1.37	.060	51.00	1.50	6.9	7.74	2.25	7.05
36-38	1.48	.067	47.60	1.60	8.1	8.13	3.89	7.91
38-40	1.26	.064	47.70	1.70	8.3	8.88	2.95	7.49
40-42	1.56	.062	48.70	1.10	9.3	8.51	3.95	5.54
42-44	1.45	.110	45.40	1.60	11.2	7.10	3.32	8.23
44-46	1.75	.292	36.41	1.70	18.4	8.04	2.31	11.64
46-48	1.70	.235	31.00	2.36	27.2	6.13	2.22	11.48
48-50	1.81	.381	33.90	2.20	20.9	6.08	2.32	12.31
50-52	1.84	.295	29.20	2.20	23.0	3.37	2.48	12.64
52-54	2.33	.219	24.50	2.80	41.1	3.39	1.60	11.76
54-56	3.45	.118	18.70	7.50	47.8	1.99	1.38	9.75
56-58	3.61	.132	18.30	15.40	34.6	2.33	1.32	13.41
58-60	1.65	.198	26.40	5.30	37.3	3.03	1.73	12.28
60-62	1.00	.279	21.80	2.78	46.0	3.44	1.36	11.98
62-64	.90	.182	21.00	3.20	49.5	2.06	1.15	12.69
64-66	2.03	.104	25.20	4.00	36.2	3.25	2.05	13.55
66-68	3.58	.075	18.00	17.80	35.5	2.54	1.14	12.17
68-70	3.20	.060	13.20	18.40	44.0	1.93	1.11	10.48
70-72	4.01	.058	14.36	22.36	36.8	2.41	.93	12.11
72-74	3.10	.039	13.00	24.86	38.0	1.98	1.00	12.76
74-76	2.68	.032	12.26	20.30	45.0	1.70	.93	11.99
76-78	2.93	.024	10.66	24.26	44.8	1.44	.91	11.26
78-80	1.85	.021	11.26	24.10	42.3	1.66	.95	11.34
80-82	.74	0.000	9.80	27.50	0.0	0.00	0.00	0.00
82-84	.43	0.000	8.66	35.00	0.0	0.00	0.00	0.00
84-86	.34	0.000	7.70	36.10	0.0	0.00	0.00	0.00
86-88	.74	0.000	8.10	30.30	0.0	0.00	0.00	0.00
88-90	.64	0.000	8.00	32.00	0.0	0.00	0.00	0.00
90-92	.60	0.000	11.20	32.30	0.0	0.00	0.00	0.00
92-94	1.49	0.000	8.30	31.30	0.0	0.00	0.00	0.00
94-96	1.11	0.000	7.46	33.20	0.0	0.00	0.00	0.00

DDH = 1636NE   LINE 1200 NW   ELEV = 203 m

Depth (m)	Ni (%)	Co (%)	Fe (%)	MgO (%)	SiO_2 (%)	Al_2O_3 (%)	Cr_2O_3 (%)	LOI (%)
0-2	.18	0.000	33.20	.80	0.0	0.00	0.00	0.00
2-4	.14	0.000	30.60	.60	0.0	0.00	0.00	0.00
4-6	.25	0.000	26.70	.70	0.0	0.00	0.00	0.00
6-8	.34	0.000	27.30	.90	0.0	0.00	0.00	0.00
8-10	.47	0.000	30.70	1.60	0.0	0.00	0.00	0.00
10-12	.59	0.000	35.00	.90	0.0	0.00	0.00	0.00
12-14	.83	0.000	46.00	.70	0.0	0.00	0.00	0.00
14-16	1.21	0.000	47.00	1.10	0.0	0.00	0.00	0.00
16-18	1.25	0.000	50.30	1.20	0.0	0.00	0.00	0.00
18-20	1.28	0.000	47.50	1.10	0.0	0.00	0.00	0.00
20-22	1.15	0.000	30.30	1.00	0.0	0.00	0.00	0.00
22-24	1.05	0.000	49.10	1.20	0.0	0.00	0.00	0.00
24-26	1.18	0.000	47.80	1.20	0.0	0.00	0.00	0.00
26-28	1.04	0.000	45.60	1.10	0.0	0.00	0.00	0.00
28-30	1.02	0.000	27.00	1.20	0.0	0.00	0.00	0.00
30-32	.55	0.000	17.10	1.20	0.0	0.00	0.00	0.00
32-34	.86	0.000	22.40	1.50	0.0	0.00	0.00	0.00
34-36	2.59	.068	18.30	8.90	48.7	2.80	1.24	7.88
36-38	3.95	.037	10.60	17.90	51.9	.65	.80	8.95
38-40	3.85	.043	11.70	15.60	51.3	.72	.82	10.13
40-42	4.41	.039	9.40	16.40	55.8	.77	.83	8.71
42-44	4.19	.042	13.30	14.60	50.1	1.15	1.08	10.28
44-46	4.71	.047	12.10	18.60	46.5	1.56	.87	9.61
46-48	4.15	.036	11.40	16.70	50.6	1.84	.80	9.40
48-50	4.28	.037	10.10	20.90	47.8	1.41	.75	9.70
50-52	4.41	.038	10.80	19.80	47.8	1.60	.81	9.79
52-54	4.33	.045	11.90	19.30	45.6	1.62	.84	9.80
54-56	4.10	.053	14.20	17.30	44.4	2.05	.95	9.68
56-58	2.26	.046	13.50	8.60	60.6	1.87	1.07	6.29
58-60	2.79	.040	12.20	19.30	48.4	1.73	.72	9.57
60-62	2.02	.025	8.10	13.20	62.5	1.05	.55	6.68
62-64	3.14	.024	9.60	24.80	45.3	1.68	.72	10.19
64-66	3.21	.023	9.20	21.50	51.6	.79	.71	9.94
66-68	2.17	.028	10.40	19.10	50.8	1.45	.88	10.89
68-70	2.06	.027	10.00	21.70	49.8	1.72	.64	11.18
70-72	1.19	0.000	11.00	21.50	0.0	0.00	0.00	0.00
72-74	.60	0.000	10.10	26.90	0.0	0.00	0.00	0.00
74-76	.31	0.000	7.10	33.50	0.0	0.00	0.00	0.00
76-78	.27	0.000	6.70	33.10	0.0	0.00	0.00	0.00
78-80	.28	0.000	6.50	34.60	0.0	0.00	0.00	0.00

DDH = 1660NE   LINE 1200 NW   ELEV = 201 m

Depth (m)	Ni (%)	Co (%)	Fe (%)	MgO (%)	SiO_2 (%)	Al_2O_3 (%)	Cr_2O_3 (%)	LOI (%)
0-2	.24	.013	31.50	1.20	0.0	0.00	0.00	0.00
2-4	.34	.014	33.70	1.30	0.0	0.00	0.00	0.00
4-6	.55	.011	40.60	.70	0.0	0.00	0.00	0.00
6-8	.56	.012	52.80	.70	0.0	0.00	0.00	0.00
8-10	.60	.010	50.10	1.30	0.0	0.00	0.00	0.00
10-12	.57	.018	43.70	.80	0.0	0.00	0.00	0.00
12-14	.44	.050	31.90	.80	0.0	0.00	0.00	0.00
14-16	.55	.040	42.00	.70	0.0	0.00	0.00	0.00
16-18	.90	.042	36.90	.70	0.0	0.00	0.00	0.00
18-20	1.05	.041	34.80	.80	0.0	0.00	0.00	0.00
20-22	1.00	.050	29.20	.90	0.0	0.00	0.00	0.00
22-24	1.92	.079	27.90	2.70	32.2	3.50	1.48	10.50
24-26	2.53	.047	16.60	13.10	38.6	2.09	.96	10.37
26-28	3.24	.051	17.00	15.70	37.1	2.22	.98	10.18
28-30	3.15	.057	19.40	17.70	35.3	2.41	.94	10.68
30-32	2.77	.054	15.80	12.90	40.8	2.07	.92	9.75
32-34	3.40	.036	13.30	20.40	36.5	1.82	.71	10.62
34-36	3.15	.034	11.90	18.00	43.5	1.14	.66	9.34
36-38	2.24	.034	12.50	12.10	50.3	.97	.71	7.61
38-40	2.25	.040	14.50	7.70	51.6	1.03	.96	6.87
40-42	2.73	.038	18.80	8.20	42.1	2.47	1.12	8.93
42-44	3.33	.034	15.70	15.20	38.0	2.59	.90	9.51
44-46	3.00	.039	17.10	13.30	36.5	2.87	1.15	10.10
46-48	3.29	.024	10.50	21.10	42.1	1.61	.66	9.97
48-50	3.01	.021	7.50	22.30	47.0	.91	.51	9.12
50-52	3.00	.020	8.80	24.60	41.5	.74	.47	10.81
52-54	3.63	.026	10.90	21.60	41.1	1.32	.61	10.97
54-56	3.83	.030	10.70	14.10	49.3	1.59	.66	9.33
56-58	3.35	.025	8.40	18.40	47.6	.84	.51	10.23
58-60	3.46	.024	9.10	20.40	51.3	.68	.50	10.87
60-62	3.45	.026	9.90	17.10	50.5	.82	.56	10.92
62-64	3.60	.024	8.80	18.50	51.4	.75	.63	10.55
64-66	3.79	.022	8.90	20.00	49.0	.79	.62	10.55
66-68	3.36	.029	10.90	18.20	44.2	1.30	.79	11.28
68-70	2.95	.020	8.90	23.70	48.4	.80	.51	10.44
70-72	3.58	.021	8.60	23.40	48.2	.91	.60	10.47
72-74	3.25	.027	8.70	15.20	51.5	.81	.56	10.37
74-76	3.50	.026	8.80	14.20	52.8	.86	.61	9.97
76-78	3.64	.031	10.30	15.00	49.4	1.00	.67	10.93
78-80	3.60	.025	8.00	15.20	54.3	.73	.59	9.64
80-82	2.90	.019	7.50	19.90	54.4	.58	.47	9.09
82-84	2.60	.017	6.90	22.60	53.8	.40	.37	9.31
84-86	2.69	.017	6.90	16.70	60.4	.43	.35	8.04
86-88	2.02	.014	5.80	16.60	62.2	.41	.53	7.33
88-90	2.84	.019	6.20	18.20	57.9	.53	.40	8.31
90-92	2.03	.011	4.80	14.40	66.7	.60	.38	6.20
92-94	2.35	.014	4.70	15.20	66.4	.65	.28	6.49

DDH = 1660NE   LINE 1200 NW   ELEV = 201 m

(Cont.)

94-96	3.60	.019	6.80	21.80	50.8	1.26	.48	9.71
96-98	2.44	.013	7.60	25.20	46.6	1.39	.56	10.38
98-100	3.31	.022	7.30	26.20	44.3	1.25	.50	11.12
100-102	2.80	.022	8.10	27.00	39.2	1.65	.56	12.18
102-104	2.58	.023	8.80	26.90	29.9	1.65	.61	12.39
104-106	2.35	.016	7.70	29.50	42.0	1.20	.51	11.72
106-108	1.58	.008	9.00	8.90	40.3	1.10	.67	12.55

DDH = 1678 NE   LINE 1200 NW   ELEV = 196 m

Depth (m)	Ni (%)	Co (%)	Fe (%)	MgO (%)	SiO_2 (%)	Al_2O_3 (%)	Cr_2O_3 (%)	LOI (%)
0-2	.26	0.000	31.63	.61	0.0	0.00	0.00	0.00
2-4	.41	0.000	32.89	.60	0.0	0.00	0.00	0.00
4-6	.63	0.000	41.12	.65	0.0	0.00	0.00	0.00
6-8	.70	0.000	47.00	.63	0.0	0.00	0.00	0.00
8-10	.92	0.000	48.64	.58	0.0	0.00	0.00	0.00
10-12	1.00	.099	45.60	.73	8.3	0.00	0.00	8.03
12-14	.92	0.000	47.21	.74	0.0	0.00	0.00	0.00
14-16	.73	0.000	43.03	.85	0.0	0.00	0.00	0.00
16-18	1.71	.048	24.00	6.93	45.0	0.00	0.00	8.01
18-20	2.67	.062	13.92	15.20	47.4	0.00	0.00	9.36
20-22	2.67	.049	13.92	15.20	42.9	0.00	0.00	12.31
22-24	2.44	.059	16.35	11.72	45.6	0.00	0.00	10.08
24-26	1.16	.068	20.32	2.14	39.9	0.00	0.00	9.48
26-28	1.78	.047	23.42	3.09	47.8	0.00	0.00	7.55
28-30	2.25	.071	25.57	4.78	33.8	0.00	0.00	9.53
30-32	3.46	.056	14.05	11.97	44.4	0.00	0.00	8.63
32-34	4.58	.034	12.06	15.85	44.7	0.00	0.00	9.68
34-36	4.06	.030	12.92	13.43	49.0	0.00	0.00	8.85
36-38	3.42	.025	11.10	16.20	48.6	0.00	0.00	9.17
38-40	3.34	.028	10.93	18.60	49.2	0.00	0.00	9.77
40-42	3.34	.036	15.86	7.79	47.9	0.00	0.00	9.68
42-44	3.58	.023	14.10	19.00	40.3	0.00	0.00	10.92
44-46	3.24	.019	10.70	21.24	43.2	0.00	0.00	11.23
46-48	3.30	.014	9.41	23.26	45.5	0.00	0.00	10.51
48-50	3.30	.016	8.93	23.43	45.2	0.00	0.00	10.72
50-52	2.58	.025	13.75	23.60	35.1	0.00	0.00	14.30
52-54	2.58	.020	11.64	25.34	39.8	0.00	0.00	12.58
54-56	3.36	.019	8.08	26.07	45.3	0.00	0.00	11.07
56-58	3.55	.017	8.19	28.60	44.3	0.00	0.00	11.11
58-60	3.44	.019	8.54	28.82	42.6	0.00	0.00	11.58
60-62	3.07	.019	9.44	26.06	43.7	0.00	0.00	12.22
62-64	3.07	.017	7.96	26.07	45.3	0.00	0.00	9.03
64-66	2.55	.022	9.14	23.00	47.6	0.00	0.00	10.93
66-68	2.95	.020	10.18	20.38	46.9	0.00	0.00	13.91
68-70	3.47	.026	10.32	17.91	48.9	0.00	0.00	11.98
70-72	4.18	.026	9.15	20.00	49.7	0.00	0.00	8.92
72-74	4.32	.022	9.48	20.69	46.3	0.00	0.00	12.22
74-76	3.49	.024	8.90	20.12	50.7	0.00	0.00	10.76
76-78	3.14	.016	7.39	24.50	51.9	0.00	0.00	10.14
78-80	4.02	.018	7.17	23.85	51.6	0.00	0.00	9.06
80-82	3.83	.015	6.70	25.76	49.0	0.00	0.00	10.43

DDH = 1700NE   LINE 1200 NW   ELEV = 191 m

Depth (m)	Ni (%)	Co (%)	Fe (%)	MgO (%)	SiO_2 (%)	Al_2O_3 (%)	Cr_2O_3 (%)	LOI (%)
0-2	.26	0.000	36.63	.20	11.1	20.84	0.00	14.90
2-4	.44	0.000	30.94	.35	17.6	24.82	0.00	12.76
4-6	.67	0.000	39.11	.45	8.7	20.65	0.00	14.04
6-8	.85	0.000	45.93	.35	4.0	17.06	0.00	9.36
8-10	1.17	.017	50.17	.50	6.4	13.22	0.00	7.14
10-12	1.59	.020	51.62	.40	4.3	11.36	0.00	7.16
12-14	1.57	.036	53.86	.55	3.7	9.04	0.00	7.70
14-16	1.66	.057	49.85	.40	3.4	12.48	0.00	8.30
16-18	1.66	.115	47.69	.70	3.9	12.46	0.00	8.86
18-20	1.48	.107	45.45	.60	7.5	13.12	0.00	7.45
20-22	1.40	.141	40.80	.85	14.2	10.68	0.00	11.04
22-24	1.95	.183	33.98	1.10	21.7	8.60	0.00	12.18
24-26	2.91	.094	25.73	6.00	33.9	5.82	0.00	10.98
26-28	2.99	.035	18.84	17.65	34.9	3.72	0.00	12.48
28-30	2.99	.023	16.83	21.30	35.9	3.08	0.00	12.12
30-32	3.47	.020	15.55	23.75	34.7	3.08	0.00	12.16
32-34	2.26	.050	24.69	6.65	38.3	3.96	0.00	10.00
34-36	1.76	.063	25.49	4.35	41.6	5.06	0.00	9.04
36-38	1.88	.052	26.53	4.70	38.0	5.14	0.00	9.34
38-40	1.95	.045	25.65	4.30	38.9	5.20	0.00	9.58
40-42	1.87	.041	24.37	4.10	40.5	5.40	0.00	9.66
42-44	3.73	.037	23.40	8.25	34.8	4.20	0.00	11.38
44-46	2.56	.023	18.11	19.70	34.0	3.52	0.00	11.86
46-48	2.17	.020	16.51	18.35	38.8	3.40	0.00	10.76
48-50	2.48	.025	18.92	19.50	34.2	3.96	0.00	11.96
50-52	2.58	.020	18.84	18.10	35.6	3.64	0.00	11.34
52-54	2.85	.030	19.24	16.40	35.8	4.52	0.00	11.84
54-56	2.48	.028	16.40	19.15	35.4	3.28	0.00	12.28
56-58	2.31	.031	21.16	16.90	33.1	5.15	0.00	12.40

DDH = 1707NE   LINE 1200 NW   ELEV = 189 m

Depth (m)	Ni (%)	Co (%)	Fe (%)	MgO (%)	SiO_2 (%)	Al_2O_3 (%)	Cr_2O_3 (%)	LOI (%)
0–2	.26	.011	33.50	1.40	0.0	0.00	0.00	0.00
2–4	.52	.011	32.30	1.00	0.0	0.00	0.00	0.00
4–6	.69	.009	43.60	.90	0.0	0.00	0.00	0.00
6–8	.92	.012	49.50	1.00	0.0	0.00	0.00	0.00
8–10	1.27	.016	50.00	1.00	0.0	0.00	0.00	0.00
10–12	1.50	.018	51.40	.70	5.6	7.24	3.38	0.00
12–14	1.67	.036	56.30	.70	4.0	5.29	1.80	0.00
14–16	1.57	.078	49.10	1.00	5.5	9.65	2.88	0.00
16–18	1.53	.157	47.80	1.00	4.7	10.75	3.15	0.00
18–20	1.33	.104	46.80	1.10	7.8	11.83	2.77	0.00
20–22	1.56	.180	46.00	1.30	9.2	9.98	1.90	0.00
22–24	1.36	.100	46.30	1.10	10.9	12.14	2.51	0.00
24–26	1.69	.263	34.30	1.60	20.1	7.94	2.25	0.00
26–28	1.28	.163	35.20	1.60	23.2	8.04	2.08	0.00
28–30	1.27	.172	33.00	1.70	27.8	6.33	2.26	0.00
30–32	1.91	.142	25.00	4.20	40.0	1.77	2.07	0.00
32–34	3.33	.053	16.50	9.00	50.7	1.05	1.28	0.00
34–36	2.35	.036	11.60	13.40	56.2	.81	.91	0.00
36–38	2.92	.036	12.80	18.20	46.2	.97	.98	0.00
38–40	2.04	.049	18.20	6.90	50.3	1.48	1.62	0.00
40–42	2.02	.056	20.30	4.80	46.3	3.59	1.84	0.00
42–44	3.58	.092	15.70	19.60	40.2	2.58	1.06	0.00
44–46	3.45	.092	13.80	15.00	45.3	1.91	1.10	0.00
46–48	3.50	.052	13.70	19.40	43.3	2.67	1.03	0.00
48–50	2.94	.044	13.30	23.20	40.0	2.37	1.00	0.00
50–52	2.48	.041	13.30	19.00	43.7	2.04	.98	0.00
52–54	2.54	.037	13.40	19.50	43.5	1.87	.97	0.00
54–56	2.14	.031	15.10	14.20	47.4	2.15	1.12	0.00
56–58	2.58	.019	10.90	22.10	46.7	1.53	.91	0.00
58–60	2.46	.024	10.80	24.50	43.5	1.66	.83	0.00
60–62	2.01	.023	10.00	14.90	57.2	1.05	.75	0.00
62–64	1.63	.028	13.10	11.00	56.3	.83	.88	0.00
64–66	1.32	.023	8.70	9.00	66.4	.68	.84	0.00
66–68	1.90	.032	10.80	13.60	54.9	1.11	.74	0.00
68–70	2.50	.030	11.30	20.90	45.0	1.76	.72	0.00
70–72	2.37	.019	9.30	24.40	44.8	1.81	.68	0.00
72–74	2.51	.018	10.50	22.10	46.9	1.14	.79	0.00
74–76	2.56	.020	10.10	18.20	52.3	.73	.84	0.00
76–78	2.56	.020	10.10	18.20	52.3	.73	.84	0.00
78–80	2.85	.016	6.80	25.20	50.2	.46	.53	0.00
80–82	2.48	.015	7.40	27.80	47.8	.44	.50	0.00
82–84	2.61	.017	8.50	23.70	48.4	.76	.61	0.00
84–86	2.81	.019	10.10	17.50	52.0	.42	.71	0.00
86–88	2.30	.016	8.50	23.60	49.7	.53	.69	0.00
88–90	2.09	.013	8.00	24.90	49.5	.48	.61	0.00
90–92	2.82	.017	7.70	20.30	54.0	.62	.68	0.00
92–94	2.90	.012	7.50	24.40	52.0	.36	.58	0.00

DDH = 1707NE   LINE 1200 NW   ELEV = 189 m

(Cont.)

94-96	2.57	.016	7.80	21.70	52.9	.46	.71	0.00
96-98	3.03	.017	8.50	19.70	52.1	.37	.76	0.00
98-100	2.58	.016	8.20	22.60	51.5	1.12	.92	0.00
100-102	1.45	.016	8.30	27.20	47.5	1.15	.64	0.00
102-104	3.77	.024	8.90	21.70	47.3	1.70	.75	0.00
104-106	4.46	.023	11.20	18.70	44.3	2.08	.87	0.00
106-108	5.18	.019	8.20	21.70	47.1	1.54	.72	0.00
108-110	4.77	.019	8.00	20.10	47.7	1.56	.75	0.00
110-112	5.31	.019	9.00	20.40	45.9	1.83	.77	0.00
112-114	4.38	.016	7.60	23.20	46.2	1.53	.78	0.00
114-116	3.72	.012	7.80	24.40	44.7	1.12	.62	0.00
116-118	4.11	.018	9.20	20.30	44.9	1.73	.77	0.00
118-120	4.27	.021	9.70	19.80	43.7	1.92	.79	0.00
120-122	3.91	.020	9.30	20.50	51.1	1.67	.71	0.00
122-124	3.69	.018	8.60	21.10	47.3	1.20	.63	0.00
124-126	3.43	.022	9.60	19.20	47.2	1.10	.73	0.00
126-128	3.16	.017	8.20	20.20	49.6	1.03	.64	0.00
128-130	3.35	.015	7.80	20.90	49.7	1.18	.68	0.00
130-132	2.68	.015	6.90	25.30	49.2	1.06	.62	0.00
132-134	1.74	.018	7.70	21.20	52.1	1.24	.57	0.00
134-136	1.16	.018	8.80	23.40	0.0	0.00	0.00	0.00

DDH = 1744NE			LINE 1200 NW			ELEV = 184 m	
Depth (m)	Ni (%)	Co (%)	Fe (%)	MgO (%)	SiO_2 (%)	Al_2O_3 (%)	Cr_2O_3 (%)	LOI (%)
0-2	.27	0.000	34.00	.90	0.0	0.00	0.00	0.00
2-4	.50	0.000	37.20	.90	0.0	0.00	0.00	0.00
4-6	.63	0.000	40.30	1.00	0.0	0.00	0.00	0.00
6-8	.81	0.000	42.40	.90	0.0	0.00	0.00	0.00
8-10	1.23	0.000	49.40	1.00	0.0	0.00	0.00	0.00
10-12	1.38	0.000	48.00	1.00	0.0	0.00	0.00	0.00
12-14	1.36	0.000	52.20	.90	0.0	0.00	0.00	0.00
14-16	1.30	0.000	51.80	1.00	0.0	0.00	0.00	0.00
16-18	1.11	0.000	49.60	.90	0.0	0.00	0.00	0.00
18-20	1.19	0.000	52.30	1.00	0.0	0.00	0.00	0.00
20-22	1.77	.138	51.10	1.10	15.4	8.09	2.87	2.53
22-24	1.71	.138	45.40	1.20	14.3	10.52	2.73	3.58
24-26	1.83	.441	40.10	1.40	19.9	10.54	3.45	5.02
26-28	1.35	.271	27.70	1.20	38.5	5.49	2.25	9.27
28-30	1.23	.238	26.00	1.50	42.1	3.35	2.13	9.03
30-32	1.95	.142	22.90	9.20	37.9	4.00	1.84	10.99
32-34	1.09	.108	18.90	13.00	41.6	3.70	1.36	9.33
34-36	1.94	.114	22.00	11.70	37.2	4.74	1.64	8.68
36-38	1.90	.159	24.80	10.90	37.5	5.02	1.56	8.18
38-40	2.22	.159	17.90	22.90	35.0	3.74	1.51	10.25
40-42	2.23	.109	16.70	17.50	45.3	2.39	1.45	8.96
42-44	2.73	.117	14.20	21.10	39.0	2.34	1.21	10.55
44-46	1.86	.118	14.30	21.20	44.1	1.60	1.54	9.53
46-48	1.31	.067	16.50	11.40	52.9	2.58	1.38	7.61
48-50	1.32	.075	13.70	23.40	43.7	2.10	1.19	9.64
50-52	.40	.017	8.20	30.42	45.6	.74	.63	11.42
52-54	.45	.011	7.80	30.80	42.7	.67	.56	11.62
54-56	.78	.013	8.00	33.70	44.5	.68	.62	11.27
56-58	1.13	.011	8.40	26.40	46.7	.70	.66	10.58
58-60	1.35	.015	9.50	24.20	46.4	1.13	.78	10.52
60-62	1.12	.013	8.50	28.30	48.7	.91	.66	10.10
62-64	1.33	.007	9.20	25.20	47.1	.85	.72	10.46
64-66	1.23	.005	9.30	23.50	50.8	1.03	.78	9.74
66-68	1.41	.009	9.00	28.00	46.1	1.20	.71	10.49
68-70	1.56	.009	8.80	32.00	44.7	1.12	.71	11.14
70-72	2.47	.007	8.30	29.50	44.6	1.10	.71	11.63
72-74	2.67	.005	7.50	30.70	45.3	.76	.65	11.71
74-76	1.63	.011	7.50	32.30	43.8	.72	.79	11.52
76-78	.94	.020	8.90	29.30	43.1	.90	.62	10.41
78-80	1.86	.016	8.60	24.30	48.7	.80	.59	10.38
80-82	1.34	.018	9.00	26.50	46.7	.65	.59	10.68
82-84	.66	.016	7.30	31.60	43.8	.62	.50	10.18
84-86	.31	.016	7.60	35.80	42.3	.47	.50	10.72
86-88	1.05	.016	7.40	30.90	46.2	.32	.51	10.87
88-90	2.56	.015	6.70	25.20	50.1	.37	.51	10.47
90-92	1.76	.125	14.50	18.40	46.0	2.55	1.21	9.19

DDH = 1744NE   LINE 1200 NW   ELEV = 184 m

(Cont.)

92–94	1.42	.140	13.50	20.00	43.0	2.74	1.17	9.75
94–96	1.07	.030	9.50	22.30	49.7	.75	.87	10.88
96–98	1.61	.075	10.90	21.50	45.3	2.20	1.22	10.64
98–100	1.21	.046	9.30	28.00	41.8	1.84	.76	10.90
100–102	1.63	.027	9.30	24.70	45.3	1.65	.73	10.81
102–104	1.73	.028	9.80	24.30	44.0	1.74	.73	11.38
104–106	.81	.024	7.70	30.90	44.6	1.29	.58	9.12
106–108	1.88	.064	11.00	23.40	44.5	2.39	.81	9.84
108–110	2.36	.033	8.90	23.30	46.4	1.63	.65	11.12
110–112	2.80	.026	10.00	23.50	45.1	1.56	.71	11.06
112–114	3.24	.027	7.80	23.40	45.6	1.48	.72	10.46
114–116	3.44	.024	10.30	22.10	45.6	1.52	.68	11.09
116–118	3.54	.022	8.50	25.50	44.1	1.42	.67	10.74
118–120	3.01	.023	15.90	23.60	44.8	1.68	.61	11.41

DDH = 1780NE   LINE 1200 NW   ELEV = 180 m

Depth (m)	Ni (%)	Co (%)	Fe (%)	MgO (%)	SiO_2 (%)	Al_2O_3 (%)	Cr_2O_3 (%)	LOI (%)
0-2	.16	.004	35.00	1.20	0.0	0.00	0.00	0.00
2-4	.28	.004	35.10	1.00	0.0	0.00	0.00	0.00
4-6	.48	.005	38.20	.90	0.0	0.00	0.00	0.00
6-8	.70	.012	43.40	1.20	0.0	0.00	0.00	0.00
8-10	1.05	.013	49.90	1.10	0.0	0.00	0.00	0.00
10-12	1.31	.009	49.40	1.20	0.0	0.00	0.00	0.00
12-14	1.12	.017	51.60	1.30	0.0	0.00	0.00	0.00
14-16	1.09	.027	50.20	1.20	0.0	0.00	0.00	0.00
16-18	1.17	.046	51.90	1.20	0.0	0.00	0.00	0.00
18-20	1.16	.052	50.80	1.30	0.0	0.00	0.00	0.00
20-22	1.21	.152	40.80	1.50	0.0	0.00	0.00	0.00
22-24	2.48	.082	19.00	19.50	31.1	2.12	1.01	11.78
24-26	2.66	.056	11.80	27.10	36.8	1.41	.60	11.28
26-28	2.28	.054	10.40	27.00	37.9	1.14	.71	11.54
28-30	1.96	.053	11.50	26.90	39.4	.99	.72	11.50
30-32	1.76	.054	12.80	24.70	39.0	1.14	.80	10.70
32-34	1.04	.053	11.50	27.10	40.6	1.56	.75	11.56
34-36	.62	.051	9.30	29.00	40.8	1.46	.61	11.53
36-38	.34	.052	9.00	26.20	46.3	.70	.63	10.54
38-40	.59	.051	8.90	25.70	46.6	.70	.63	10.67
40-42	.70	.051	8.10	25.10	49.7	.77	.69	10.09
42-44	.49	.052	8.50	24.10	52.5	.90	.73	9.43
44-46	.51	.052	9.20	23.40	50.5	1.44	.75	9.41
46-48	.62	.051	8.30	25.50	49.2	1.05	.62	10.18
48-50	.47	.051	7.10	30.60	46.2	.51	.49	11.29
50-52	.64	.052	9.20	18.80	57.6	.65	.76	9.14
52-54	.59	.051	7.50	9.30	68.8	.46	.72	5.84
54-56	.56	.053	9.30	18.00	55.9	.58	.82	9.47
56-58	.43	.040	8.60	19.70	55.6	.65	.70	9.55
58-60	.66	.039	8.80	27.10	48.9	.87	.64	10.06
60-62	1.38	.045	8.60	27.60	42.8	.80	.68	11.83
62-64	2.06	.060	10.80	23.60	42.9	1.72	1.15	11.70
64-66	1.58	.045	10.00	23.90	42.5	1.73	.95	11.72
66-68	.94	.039	8.70	27.80	0.0	0.00	0.00	0.00
68-70	.47	.035	6.60	30.00	0.0	0.00	0.00	0.00
70-72	.37	.034	6.40	32.70	0.0	0.00	0.00	0.00
72-74	.31	.035	6.30	31.00	0.0	0.00	0.00	0.00
74-76	.74	.033	6.40	30.30	0.0	0.00	0.00	0.00
76-78	1.09	.033	6.10	23.80	0.0	0.00	0.00	0.00
78-80	1.07	.038	6.80	28.60	0.0	0.00	0.00	0.00
80-82	.75	.038	7.00	29.00	0.0	0.00	0.00	0.00
82-84	.50	.034	6.50	24.80	0.0	0.00	0.00	0.00
84-86	.35	.035	6.90	34.00	0.0	0.00	0.00	0.00
86-88	.45	.032	7.90	32.80	0.0	0.00	0.00	0.00

DDH = 1810NE   LINE 1200 NW   ELEV = 179 m

Depth (m)	Ni (%)	Co (%)	Fe (%)	MgO (%)	SiO_2 (%)	Al_2O_3 (%)	Cr_2O_3 (%)	LOI (%)
0-2	.17	.042	42.30	1.00	0.0	0.00	0.00	0.00
2-4	.31	.043	40.00	.90	0.0	0.00	0.00	0.00
4-6	.67	.044	47.50	.60	4.0	11.62	2.99	9.40
6-8	.91	.045	50.90	.70	5.2	9.22	3.02	6.60
8-10	.85	.045	51.50	.50	5.0	9.27	3.06	6.61
10-12	.80	.049	52.20	.50	5.2	8.57	2.94	6.35
12-14	1.08	.081	52.80	.60	4.3	8.26	2.85	6.30
14-16	.96	.076	56.00	.70	3.2	8.67	3.10	5.67
16-18	.89	.071	54.80	.60	3.1	9.32	3.58	6.52
18-20	1.10	.079	51.90	.60	6.3	8.79	2.50	5.19
20-22	1.04	.067	50.30	.80	5.7	9.93	2.98	6.30
22-24	1.07	.130	41.40	1.10	16.6	8.36	2.65	8.77
24-26	.73	.079	20.30	1.50	50.8	1.66	1.31	10.42
26-28	1.69	.083	20.80	7.40	43.0	2.56	1.81	9.31
28-30	1.48	.055	17.00	12.30	47.9	2.20	1.04	6.86
30-32	.80	.047	12.50	18.10	49.2	1.83	.71	7.83
32-34	.49	.047	10.70	22.90	48.4	1.75	.69	9.00
34-36	.63	.047	11.30	23.80	44.9	1.67	.76	9.48
36-38	.57	.045	8.90	21.00	52.8	.84	.58	8.55
38-40	1.15	.046	8.30	21.90	51.0	.71	.62	9.07
40-42	1.07	.024	9.20	25.60	0.0	0.00	0.00	0.00
42-44	.43	.020	8.40	23.90	0.0	0.00	0.00	0.00
44-46	.33	.020	7.60	25.80	0.0	0.00	0.00	0.00
46-48	.64	.018	7.40	27.00	0.0	0.00	0.00	0.00
48-50	.98	.024	7.80	27.20	0.0	0.00	0.00	0.00
50-52	.83	.024	11.40	17.50	0.0	0.00	0.00	0.00
52-54	.72	.024	9.60	19.20	0.0	0.00	0.00	0.00
54-56	.72	.022	8.80	20.00	0.0	0.00	0.00	0.00
56-58	.55	.029	9.90	19.00	0.0	0.00	0.00	0.00
58-60	.41	.020	9.10	23.70	0.0	0.00	0.00	0.00
60-62	.35	.020	7.20	23.30	0.0	0.00	0.00	0.00
62-64	.36	.022	6.80	18.80	0.0	0.00	0.00	0.00
64-66	.37	.018	7.30	26.50	0.0	0.00	0.00	0.00
66-68	.32	.016	6.20	31.60	0.0	0.00	0.00	0.00
68-70	.28	.017	5.30	29.40	0.0	0.00	0.00	0.00
70-72	.31	.018	6.10	38.40	0.0	0.00	0.00	0.00
72-74	.34	.018	6.50	35.90	0.0	0.00	0.00	0.00

DDH = 1819NE   LINE 1200 NW   ELEV = 175 m

Depth (m)	Ni (%)	Co (%)	Fe (%)	MgO (%)	SiO_2 (%)	Al_2O_3 (%)	Cr_2O_3 (%)	LOI (%)
0-2	.32	0.000	40.31	.60	0.0	0.00	0.00	0.00
2-4	.61	0.000	47.71	.71	0.0	0.00	0.00	0.00
4-6	.68	0.000	48.34	.69	0.0	0.00	0.00	0.00
6-8	.76	0.000	46.29	.67	0.0	0.00	0.00	0.00
8-10	.91	0.000	49.21	.68	0.0	0.00	0.00	0.00
10-12	1.00	0.000	49.47	.70	0.0	0.00	0.00	0.00
12-14	1.08	0.000	47.79	.68	0.0	0.00	0.00	0.00
14-16	.77	0.000	48.83	.72	0.0	0.00	0.00	0.00
16-18	.87	0.000	49.28	.74	0.0	0.00	0.00	0.00
18-20	1.16	0.000	46.08	.84	0.0	0.00	0.00	0.00
20-22	.99	0.000	24.00	1.45	0.0	0.00	0.00	0.00
22-24	1.38	0.000	14.90	10.33	0.0	0.00	0.00	0.00
24-26	.88	0.000	11.12	17.71	0.0	0.00	0.00	0.00
26-28	.37	0.000	9.09	23.18	0.0	0.00	0.00	0.00
28-30	.29	0.000	7.89	25.25	0.0	0.00	0.00	0.00
30-32	.21	0.000	5.90	32.82	0.0	0.00	0.00	0.00
32-34	.54	0.000	5.62	23.02	0.0	0.00	0.00	0.00
34-36	.50	0.000	8.04	27.07	0.0	0.00	0.00	0.00
36-38	.78	0.000	9.13	23.71	0.0	0.00	0.00	0.00
38-40	.65	0.000	9.26	27.31	0.0	0.00	0.00	0.00
40-42	.48	0.000	9.76	27.20	0.0	0.00	0.00	0.00
42-44	.49	0.000	8.68	27.42	0.0	0.00	0.00	0.00
44-46	.44	0.000	9.30	27.22	0.0	0.00	0.00	0.00
46-48	.43	0.000	8.41	20.03	0.0	0.00	0.00	0.00
48-50	.38	0.000	8.05	24.00	0.0	0.00	0.00	0.00
50-52	.31	0.000	7.74	27.17	0.0	0.00	0.00	0.00
52-54	.31	0.000	8.08	26.88	0.0	0.00	0.00	0.00
54-56	.24	0.000	6.71	29.36	0.0	0.00	0.00	0.00
56-58	.26	0.000	6.84	29.33	0.0	0.00	0.00	0.00
58-60	.26	0.000	7.20	28.63	0.0	0.00	0.00	0.00
60-62	.24	0.000	6.54	33.06	0.0	0.00	0.00	0.00
62-64	.25	0.000	6.41	33.54	0.0	0.00	0.00	0.00

DDH = 1874NE   LINE 1200 NW   ELEV = 167 m

Depth (m)	Ni (%)	Co (%)	Fe (%)	MgO (%)	SiO_2 (%)	Al_2O_3 (%)	Cr_2O_3 (%)	LOI (%)
0-2	.58	.008	52.50	1.00	0.0	0.00	0.00	0.00
2-4	.64	.011	53.30	.80	0.0	0.00	0.00	0.00
4-6	.74	.017	50.90	.80	0.0	0.00	0.00	0.00
6-8	.59	.047	47.00	.80	0.0	0.00	0.00	0.00
8-10	.61	.098	47.20	.70	0.0	0.00	0.00	0.00
10-12	.77	.199	42.90	.60	0.0	0.00	0.00	0.00
12-14	.72	.155	34.30	.50	0.0	0.00	0.00	0.00
14-16	1.22	.354	32.30	.80	0.0	0.00	0.00	0.00
16-18	.86	.102	33.40	.80	0.0	0.00	0.00	0.00
18-20	.74	.158	26.10	.80	0.0	0.00	0.00	0.00
20-22	.69	.151	20.90	.80	0.0	0.00	0.00	0.00
22-24	.74	.249	22.30	.80	0.0	0.00	0.00	0.00
24-26	.62	.120	26.50	.80	0.0	0.00	0.00	0.00
26-28	.36	.075	17.90	.80	0.0	0.00	0.00	0.00
28-30	.51	.087	19.20	.80	0.0	0.00	0.00	0.00
30-32	.71	.074	13.10	6.50	0.0	0.00	0.00	0.00
32-34	.60	.018	8.90	20.80	0.0	0.00	0.00	0.00
34-36	.49	.017	8.90	21.90	0.0	0.00	0.00	0.00
36-38	.33	.020	7.80	23.80	0.0	0.00	0.00	0.00
38-40	.26	.015	6.00	23.50	0.0	0.00	0.00	0.00
40-42	.29	.019	7.00	20.40	0.0	0.00	0.00	0.00
42-44	.32	.022	7.80	30.40	0.0	0.00	0.00	0.00
44-46	.26	.017	6.00	34.30	0.0	0.00	0.00	0.00
46-48	.25	.016	5.90	28.40	0.0	0.00	0.00	0.00

DDH = 1900NE   LINE 1200 NW   ELEV = 158 m

Depth (m)	Ni (%)	Co (%)	Fe (%)	MgO (%)	SiO_2 (%)	Al_2O_3 (%)	Cr_2O_3 (%)	LOI (%)
0–2	.43	0.000	43.44	.40	8.0	13.94	0.00	13.28
2–4	.70	0.000	40.72	.25	5.8	13.76	0.00	14.18
4–6	.84	0.000	43.60	.30	5.3	11.48	0.00	13.80
6–8	.69	0.000	42.96	.30	14.2	8.66	0.00	11.24
8–10	.74	0.000	42.88	.30	14.6	6.76	0.00	11.14
10–12	.52	0.000	29.66	.20	41.4	4.30	0.00	8.16
12–14	.38	0.000	21.64	.20	56.6	3.96	0.00	5.83
14–16	.58	0.000	24.85	.20	49.8	3.84	0.00	6.80
16–18	.29	0.000	13.63	.20	71.5	2.52	0.00	4.56
18–20	.44	0.000	20.04	.25	59.8	3.32	0.00	5.68
20–22	.60	0.000	30.46	.25	38.5	5.12	0.00	7.98
22–24	.45	0.000	18.76	.25	62.7	2.14	0.00	5.34
24–26	.48	0.000	18.11	.25	63.4	1.50	0.00	5.30
26–28	.61	0.000	19.24	.25	61.9	1.98	0.00	5.68
28–30	.66	0.000	18.35	.70	60.7	3.08	0.00	5.30
30–32	.84	0.000	13.18	11.95	58.1	1.84	0.00	6.50
32–34	.61	0.000	11.54	16.85	47.9	2.76	0.00	10.66
34–36	.58	0.000	10.26	21.15	48.7	1.52	0.00	12.00
36–38	.56	0.000	12.02	17.55	51.7	1.56	0.00	11.04
38–40	.50	0.000	12.02	19.20	47.4	1.16	0.00	13.08
40–42	.55	0.000	13.14	16.00	50.5	1.52	0.00	10.66

DDH = 1907NE   LINE 1200 NW   ELEV = 154 m

Depth (m)	Ni (%)	Co (%)	Fe (%)	MgO (%)	SiO_2 (%)	Al_2O_3 (%)	Cr_2O_3 (%)	LOI (%)
0-2	.53	0.000	41.71	.86	0.0	0.00	0.00	0.00
2-4	.65	0.000	43.67	.74	0.0	0.00	0.00	0.00
4-6	.68	0.000	39.44	.83	0.0	0.00	0.00	0.00
6-8	.47	0.000	26.32	.49	0.0	0.00	0.00	0.00
8-10	.49	0.000	27.69	.57	0.0	0.00	0.00	0.00
10-12	.26	0.000	20.77	.56	0.0	0.00	0.00	0.00
12-14	.47	0.000	22.56	.55	0.0	0.00	0.00	0.00
14-16	.57	0.000	23.75	.59	0.0	0.00	0.00	0.00
16-18	.40	0.000	13.31	.42	0.0	0.00	0.00	0.00
18-20	.40	0.000	12.78	.39	0.0	0.00	0.00	0.00
20-22	.41	0.000	15.20	.85	0.0	0.00	0.00	0.00
22-24	.38	0.000	11.77	.84	0.0	0.00	0.00	0.00
24-26	.64	0.000	20.35	2.28	0.0	0.00	0.00	0.00
26-28	.29	0.000	9.46	.59	0.0	0.00	0.00	0.00
28-30	1.65	0.000	13.62	18.31	0.0	0.00	0.00	0.00
30-32	.29	0.000	6.47	31.98	0.0	0.00	0.00	0.00
32-34	.23	0.000	6.40	33.45	0.0	0.00	0.00	0.00
34-36	.21	0.000	5.63	36.89	0.0	0.00	0.00	0.00
36-38	.20	0.000	5.27	36.45	0.0	0.00	0.00	0.00
38-40	.18	0.000	5.32	36.60	0.0	0.00	0.00	0.00
40-42	.21	0.000	5.40	36.38	0.0	0.00	0.00	0.00
42-44	.22	0.000	5.85	38.18	0.0	0.00	0.00	0.00
44-46	.23	0.000	5.54	35.00	0.0	0.00	0.00	0.00
46-48	.22	0.000	5.96	38.80	0.0	0.00	0.00	0.00

	DDH = 1952NE		LINE 1200 NW			ELEV = 148 m	

Depth (m)	Ni (%)	Co (%)	Fe (%)	MgO (%)	SiO_2 (%)	Al_2O_3 (%)	Cr_2O_3 (%)	LOI (%)
0–2	.36	.043	32.20	1.20	0.0	0.00	0.00	0.00
2–4	.53	.023	18.20	2.10	0.0	0.00	0.00	0.00
4–6	.53	.068	33.10	1.30	0.0	0.00	0.00	0.00
6–8	.72	.073	26.10	1.90	0.0	0.00	0.00	0.00
8–10	1.49	.037	13.20	13.80	0.0	0.00	0.00	0.00
10–12	1.48	.031	13.40	13.50	0.0	0.00	0.00	0.00
12–14	1.43	.026	12.70	14.60	0.0	0.00	0.00	0.00
14–16	1.44	.024	12.90	16.00	0.0	0.00	0.00	0.00
16–18	1.24	.022	11.20	12.70	0.0	0.00	0.00	0.00
18–20	.66	.049	17.00	1.40	0.0	0.00	0.00	0.00
20–22	.78	.054	22.30	1.50	0.0	0.00	0.00	0.00
22–24	.63	.061	21.30	1.00	0.0	0.00	0.00	0.00
24–26	.34	.036	11.10	1.10	0.0	0.00	0.00	0.00
26–28	1.25	.026	13.30	8.80	0.0	0.00	0.00	0.00
28–30	.66	.015	8.50	15.00	0.0	0.00	0.00	0.00
30–32	.65	.018	10.00	20.80	0.0	0.00	0.00	0.00
32–34	.95	.025	12.90	15.10	0.0	0.00	0.00	0.00
34–36	.69	.023	12.20	16.50	0.0	0.00	0.00	0.00
36–38	.46	.020	9.60	22.80	0.0	0.00	0.00	0.00
38–40	.39	.020	9.70	24.30	0.0	0.00	0.00	0.00
40–42	.44	.019	8.80	24.00	0.0	0.00	0.00	0.00
42–44	.31	.017	10.00	28.70	0.0	0.00	0.00	0.00
44–46	.44	.019	8.40	17.60	0.0	0.00	0.00	0.00
46–48	.39	.021	10.00	24.40	0.0	0.00	0.00	0.00
48–50	.46	.022	8.90	23.30	0.0	0.00	0.00	0.00
50–52	.45	.020	8.00	25.00	0.0	0.00	0.00	0.00
52–54	.39	.021	9.60	27.80	0.0	0.00	0.00	0.00
54–56	.39	.019	8.60	25.90	0.0	0.00	0.00	0.00
56–58	.34	.020	8.30	24.30	0.0	0.00	0.00	0.00
58–60	.35	.020	8.00	27.20	0.0	0.00	0.00	0.00
60–62	.36	.019	5.90	26.70	0.0	0.00	0.00	0.00
62–64	.34	.017	9.90	28.20	0.0	0.00	0.00	0.00
64–66	.27	.017	8.50	37.20	0.0	0.00	0.00	0.00
66–68	.30	.018	7.70	33.60	0.0	0.00	0.00	0.00

DDH = 1975NE   LINE 1200 NW   ELEV = 141 m

Depth (m)	Ni (%)	Co (%)	Fe (%)	MgO (%)	SiO_2 (%)	Al_2O_3 (%)	Cr_2O_3 (%)	LOI (%)
0-2	.60	.049	37.50	.70	0.0	0.00	0.00	0.00
2-4	.59	.018	23.70	.50	0.0	0.00	0.00	0.00
4-6	.44	.017	16.60	.40	0.0	0.00	0.00	0.00
6-8	.74	.049	23.50	.50	0.0	0.00	0.00	0.00
8-10	.65	.085	26.60	.60	0.0	0.00	0.00	0.00
10-12	1.03	.302	34.00	.80	0.0	0.00	0.00	0.00
12-14	1.13	.281	35.50	.80	0.0	0.00	0.00	0.00
14-16	.80	.363	25.20	.80	0.0	0.00	0.00	0.00
16-18	1.15	.312	33.70	1.00	0.0	0.00	0.00	0.00
18-20	.80	.129	24.70	.90	0.0	0.00	0.00	0.00
20-22	1.18	.131	30.90	1.00	0.0	0.00	0.00	0.00
22-24	.48	.050	12.10	.80	0.0	0.00	0.00	0.00
24-26	.64	.029	9.70	6.70	0.0	0.00	0.00	0.00
26-28	.66	.024	8.30	13.30	0.0	0.00	0.00	0.00
28-30	.61	.021	7.60	26.50	0.0	0.00	0.00	0.00
30-32	1.14	.022	7.40	15.70	0.0	0.00	0.00	0.00
32-34	.38	.027	9.10	19.40	0.0	0.00	0.00	0.00
34-36	.34	.025	8.20	19.50	0.0	0.00	0.00	0.00
36-38	.40	.027	11.00	19.90	0.0	0.00	0.00	0.00
38-40	.43	.026	11.70	18.30	0.0	0.00	0.00	0.00
40-42	.30	.025	9.60	5.80	0.0	0.00	0.00	0.00
42-44	.60	.029	16.00	10.10	0.0	0.00	0.00	0.00
44-46	.66	.028	13.30	13.20	0.0	0.00	0.00	0.00
46-48	.73	.030	14.70	12.80	0.0	0.00	0.00	0.00
48-50	.68	.031	15.20	15.70	0.0	0.00	0.00	0.00
50-52	.75	.030	15.80	16.80	0.0	0.00	0.00	0.00
52-54	.66	.025	14.60	12.70	0.0	0.00	0.00	0.00
54-56	.75	.024	14.80	17.80	0.0	0.00	0.00	0.00
56-58	.90	.024	13.60	17.30	0.0	0.00	0.00	0.00
58-60	.52	.017	8.90	23.70	0.0	0.00	0.00	0.00
60-62	.32	.011	7.10	29.60	0.0	0.00	0.00	0.00
62-64	.37	.013	7.40	28.30	0.0	0.00	0.00	0.00
64-66	.44	.015	7.70	26.90	0.0	0.00	0.00	0.00
66-68	.28	.012	7.10	30.10	0.0	0.00	0.00	0.00
68-70	.55	.010	6.90	28.90	0.0	0.00	0.00	0.00

DDH = 2004NE   LINE 1200 NW   ELEV = 133 m

Depth (m)	Ni (%)	Co (%)	Fe (%)	MgO (%)	SiO_2 (%)	Al_2O_3 (%)	Cr_2O_3 (%)	LOI (%)
0-2	.69	.098	33.10	1.20	32.1	7.59	2.32	8.94
2-4	.82	.137	32.60	1.30	32.5	6.72	2.71	8.43
4-6	.34	.081	13.70	1.30	72.0	2.27	1.02	3.67
6-8	.37	.072	12.50	.90	73.3	2.95	.68	3.97
8-10	.46	.076	17.50	.90	64.5	1.65	1.50	5.18
10-12	.82	.054	10.20	3.40	52.9	11.27	.64	8.05
12-14	.83	.074	22.60	2.30	51.0	4.98	1.81	6.86
14-16	1.47	.061	18.10	5.90	52.2	3.48	1.68	7.28
16-18	1.62	.051	16.20	7.90	55.5	3.20	1.16	7.28
18-20	1.14	.045	11.70	6.60	57.5	3.60	1.17	7.03
20-22	1.13	.043	13.00	13.00	53.7	2.66	.99	8.22
22-24	.97	.036	10.80	18.60	49.9	2.08	.75	9.39
24-26	.44	.015	9.00	22.40	50.0	1.60	.58	9.24
26-28	.30	.014	7.70	25.00	51.7	1.50	.50	10.55
28-30	.29	.014	7.60	24.80	52.1	1.39	.53	9.65
30-32	.37	.015	8.70	23.80	53.1	.97	.55	9.21
32-34	.67	.016	8.00	20.20	55.6	.94	.54	8.34
34-36	.59	.017	8.20	21.10	54.2	1.06	.59	9.08
36-38	.40	.014	7.30	26.70	50.8	.64	.52	9.26
38-40	.77	.013	6.60	24.30	54.5	.54	.50	9.93
40-42	.86	.014	7.10	21.30	57.2	.58	.55	10.32
42-44	.33	.013	7.20	32.40	46.9	.62	.47	9.59
44-46	.35	.013	7.00	28.00	50.0	.54	.49	10.23
46-48	.29	.012	5.50	30.00	50.3	.50	.48	9.76

DDH = 2026NE   LINE 1200 NW   ELEV = 126 m

Depth (m)	Ni (%)	Co (%)	Fe (%)	MgO (%)	SiO_2 (%)	Al_2O_3 (%)	Cr_2O_3 (%)	LOI (%)
0–2	.50	.034	24.30	1.20	0.0	0.00	0.00	0.00
2–4	.70	.033	23.40	.80	0.0	0.00	0.00	0.00
4–6	.90	.094	27.00	1.00	0.0	0.00	0.00	0.00
6–8	1.22	.095	28.00	2.60	0.0	0.00	0.00	0.00
8–10	.87	.039	10.50	5.70	0.0	0.00	0.00	0.00
10–12	.95	.040	11.70	5.80	0.0	0.00	0.00	0.00
12–14	1.22	.040	8.10	14.50	0.0	0.00	0.00	0.00
14–16	1.18	.048	13.90	11.50	0.0	0.00	0.00	0.00
16–18	.86	.016	6.50	20.20	0.0	0.00	0.00	0.00
18–20	.45	.019	7.20	23.70	0.0	0.00	0.00	0.00
20–22	.21	.013	5.40	23.30	0.0	0.00	0.00	0.00
22–24	.24	.017	6.20	31.10	0.0	0.00	0.00	0.00
24–26	.21	.012	5.30	32.10	0.0	0.00	0.00	0.00
26–28	.21	.008	5.40	31.50	0.0	0.00	0.00	0.00
28–30	.22	.011	5.90	28.50	0.0	0.00	0.00	0.00
30–32	.54	.013	7.10	22.00	0.0	0.00	0.00	0.00
32–34	.60	.018	8.20	25.10	0.0	0.00	0.00	0.00
34–36	.57	.020	8.20	23.80	0.0	0.00	0.00	0.00
36–38	.63	.020	7.50	22.50	0.0	0.00	0.00	0.00
38–40	.31	.016	6.10	27.10	0.0	0.00	0.00	0.00
40–42	.24	.014	6.30	36.60	0.0	0.00	0.00	0.00
42–44	.29	.014	6.50	36.40	0.0	0.00	0.00	0.00
44–46	.21	.013	6.00	33.00	0.0	0.00	0.00	0.00

DDH = 2043NE   LINE 1200 NW   ELEV = 119 m

Depth (m)	Ni (%)	Co (%)	Fe (%)	MgO (%)	SiO_2 (%)	Al_2O_3 (%)	Cr_2O_3 (%)	LOI (%)
0–2	.25	.039	13.80	.90	0.0	0.00	0.00	0.00
2–4	.30	.015	14.60	.90	0.0	0.00	0.00	0.00
4–6	.44	.051	19.30	.70	0.0	0.00	0.00	0.00
6–8	.63	.089	20.70	.80	0.0	0.00	0.00	0.00
8–10	.62	.105	19.90	1.30	0.0	0.00	0.00	0.00
10–12	1.22	.035	11.50	15.30	0.0	0.00	0.00	0.00
12–14	1.09	.018	7.30	18.60	0.0	0.00	0.00	0.00
14–16	.28	.015	5.90	20.80	0.0	0.00	0.00	0.00
16–18	.25	.015	6.60	29.50	0.0	0.00	0.00	0.00
18–20	.26	.015	6.90	32.50	0.0	0.00	0.00	0.00
20–22	.36	.019	6.80	19.20	0.0	0.00	0.00	0.00
22–24	.45	.015	6.50	17.40	0.0	0.00	0.00	0.00
24–26	.63	.018	7.90	27.40	0.0	0.00	0.00	0.00
26–28	.32	.016	6.80	30.90	0.0	0.00	0.00	0.00
28–30	.31	.021	7.00	34.30	0.0	0.00	0.00	0.00

DDH = 2062NE   LINE 1200 NW   ELEV = 112 m

Depth (m)	Ni (%)	Co (%)	Fe (%)	MgO (%)	SiO_2 (%)	Al_2O_3 (%)	Cr_2O_3 (%)	LOI (%)
0-2	.56	0.000	30.40	.70	0.0	0.00	0.00	0.00
2-4	.52	0.000	22.80	.70	0.0	0.00	0.00	0.00
4-6	.63	0.000	23.80	.60	0.0	0.00	0.00	0.00
6-8	.69	0.000	25.70	.90	0.0	0.00	0.00	0.00
8-10	1.07	0.000	15.00	6.40	0.0	0.00	0.00	0.00
10-12	.64	0.000	8.30	4.50	0.0	0.00	0.00	0.00
12-14	.68	0.000	8.10	5.50	0.0	0.00	0.00	0.00
14-16	1.20	0.000	10.20	13.50	0.0	0.00	0.00	0.00
16-18	.66	0.000	9.20	21.50	0.0	0.00	0.00	0.00
18-20	.27	0.000	6.60	30.40	0.0	0.00	0.00	0.00
20-22	.32	0.000	6.90	30.80	0.0	0.00	0.00	0.00
22-24	.30	0.000	7.50	32.10	0.0	0.00	0.00	0.00
24-26	.22	0.000	7.70	32.90	0.0	0.00	0.00	0.00

DDH = 2085NE   LINE 1200 NW   ELEV = 104 m

Depth (m)	Ni (%)	Co (%)	Fe (%)	MgO (%)	SiO_2 (%)	Al_2O_3 (%)	Cr_2O_3 (%)	LOI (%)
0-2	.62	.043	35.00	.40	0.0	0.00	0.00	0.00
2-4	.31	.020	13.20	.60	0.0	0.00	0.00	0.00
4-6	.42	.040	18.20	.60	0.0	0.00	0.00	0.00
6-8	.95	.112	29.40	.80	0.0	0.00	0.00	0.00
8-10	1.11	.310	29.30	.50	0.0	0.00	0.00	0.00
10-12	1.21	.075	12.40	14.50	0.0	0.00	0.00	0.00
12-14	.83	.026	9.60	18.10	0.0	0.00	0.00	0.00
14-16	.35	.021	7.50	28.50	0.0	0.00	0.00	0.00
16-18	.27	.015	7.00	34.80	0.0	0.00	0.00	0.00
18-20	.25	.015	6.20	37.30	0.0	0.00	0.00	0.00
20-22	.24	.021	6.20	35.30	0.0	0.00	0.00	0.00

DDH = 2105NE   LINE 1200 NW   ELEV = 98 m

Depth (%)	Ni (%)	Co (%)	Fe (%)	MgO (%)	SiO_2 (%)	Al_2O_3 (%)	Cr_2O_3 (%)	LOI (%)
0-2	.88	.058	42.10	1.40	0.0	0.00	0.00	0.00
2-4	.73	.037	30.90	1.20	0.0	0.00	0.00	0.00
4-6	.75	.067	28.20	1.60	0.0	0.00	0.00	0.00
6-8	1.45	.062	19.80	2.50	0.0	0.00	0.00	0.00
8-10	1.35	.065	18.40	4.00	0.0	0.00	0.00	0.00
10-12	1.41	.034	12.40	34.00	0.0	0.00	0.00	0.00
12-14	.54	.021	8.10	23.70	0.0	0.00	0.00	0.00
14-16	.48	.019	6.70	29.50	0.0	0.00	0.00	0.00
16-18	.42	.020	6.60	30.80	0.0	0.00	0.00	0.00
18-20	1.10	.021	11.90	28.80	0.0	0.00	0.00	0.00
20-22	.60	.022	6.60	30.00	0.0	0.00	0.00	0.00
22-24	.54	.021	7.20	30.90	0.0	0.00	0.00	0.00
24-26	.56	.025	7.70	32.40	0.0	0.00	0.00	0.00
26-28	.46	.031	10.80	29.20	0.0	0.00	0.00	0.00

DDH = 2120NE   LINE 1200 NW   ELEV = 91 m

Depth (m)	Ni (%)	Co (%)	Fe (%)	MgO (%)	SiO_2 (%)	Al_2O_3 (%)	Cr_2O_3 (%)	LOI (%)
0-2	.64	.088	38.70	.60	24.7	5.36	2.09	9.92
2-4	1.26	.113	34.10	4.00	27.1	3.47	2.28	9.38
4-6	1.29	.110	38.60	2.60	23.8	3.10	2.49	9.22
6-8	2.07	.078	26.50	5.50	37.5	2.54	1.89	8.12
8-10	1.97	.047	23.70	8.20	39.0	2.15	1.54	7.96
10-12	1.52	.039	21.00	6.60	46.2	1.45	1.25	7.28
12-14	1.35	.017	13.10	16.60	49.0	1.05	.80	8.37
14-16	.68	.023	13.40	17.20	47.3	1.44	.81	8.42
16-18	.45	.019	8.80	20.10	49.8	1.35	.56	8.68
18-20	.35	.017	7.90	21.90	49.0	1.34	.51	8.19
20-22	.29	.017	10.20	28.10	44.8	1.28	.49	9.47
22-24	.25	.015	9.80	21.40	47.7	1.35	.54	10.71
24-26	.25	.015	9.10	22.20	44.8	1.31	.49	11.53

DDH = 2134NE   LINE 1200 NW   ELEV = 84 m

Depth (m)	Ni (%)	Co (%)	Fe (%)	MgO (%)	SiO_2 (%)	Al_2O_3 (%)	Cr_2O_3 (%)	LOI (%)
0-2	1.58	.099	22.30	9.80	41.6	2.14	1.58	7.76
2-4	1.87	.063	13.20	9.10	55.8	2.28	1.11	6.01
4-6	1.49	.047	13.30	13.20	0.0	0.00	0.00	0.00
6-8	1.42	.028	11.10	19.70	0.0	0.00	0.00	0.00
8-10	.52	.018	7.30	26.30	0.0	0.00	0.00	0.00
10-12	.61	.019	8.00	27.00	0.0	0.00	0.00	0.00
12-14	.42	.017	6.90	31.40	0.0	0.00	0.00	0.00
14-16	.37	.019	6.90	32.20	0.0	0.00	0.00	0.00
16-18	.33	.017	6.50	32.30	0.0	0.00	0.00	0.00
18-20	.32	.018	6.80	32.10	0.0	0.00	0.00	0.00

DDH = 2153NE   LINE 1200 NW   ELEV = 77 m

Depth (m)	Ni (%)	Co (%)	Fe (%)	MgO (%)	SiO_2 (%)	Al_2O_3 (%)	Cr_2O_3 (%)	LOI (%)
0-2	.96	.082	31.30	1.10	0.0	0.00	0.00	0.00
2-4	1.38	.092	25.90	1.80	0.0	0.00	0.00	0.00
4-6	2.24	.085	26.20	6.00	34.0	3.98	1.67	9.61
6-8	2.44	.049	10.90	15.60	50.0	1.47	.84	9.39
8-10	.85	.040	8.10	24.40	0.0	0.00	0.00	0.00
10-12	.52	.038	7.40	30.50	0.0	0.00	0.00	0.00
12-14	.48	.037	6.80	32.00	0.0	0.00	0.00	0.00
14-16	.49	.039	6.00	31.90	0.0	0.00	0.00	0.00
16-18	.48	.037	6.10	33.40	0.0	0.00	0.00	0.00
18-20	.31	.040	6.40	32.50	0.0	0.00	0.00	0.00
20-22	.36	.038	7.60	39.70	0.0	0.00	0.00	0.00
22-24	.30	.036	6.90	30.50	0.0	0.00	0.00	0.00
24-26	.45	.040	11.20	18.30	0.0	0.00	0.00	0.00
26-28	1.38	.039	8.90	25.40	0.0	0.00	0.00	0.00
28-30	1.09	.036	6.60	30.20	0.0	0.00	0.00	0.00
30-32	.65	.035	6.50	31.90	0.0	0.00	0.00	0.00
32-34	.51	.034	6.50	33.90	0.0	0.00	0.00	0.00

DDH = 2157NE   LINE 1200 NW   ELEV = 75 m

Depth (m)	Ni (%)	Co (%)	Fe (%)	MgO (%)	SiO_2 (%)	Al_2O_3 (%)	Cr_2O_3 (%)	LOI (%)
0-2	.45	.063	35.50	1.00	23.3	8.40	0.00	0.00
2-4	1.14	.097	30.80	.68	23.7	8.56	0.00	0.00
4-6	1.54	.161	31.40	1.90	28.6	6.14	0.00	0.00
6-8	2.32	.129	26.80	6.20	32.3	5.20	0.00	0.00
8-10	2.46	.058	16.40	16.20	33.5	3.26	0.00	0.00
10-12	1.29	.034	13.10	21.20	37.9	2.14	0.00	0.00
12-14	1.56	.036	10.20	25.40	40.2	1.28	0.00	0.00
14-16	.72	.027	10.60	25.40	39.1	.62	0.00	0.00
16-18	.55	.021	9.80	23.60	43.3	.51	0.00	0.00
18-20	.54	.023	10.90	19.40	44.3	.81	0.00	0.00
20-22	.45	.017	8.80	25.70	43.6	.27	0.00	0.00
22-24	.47	.019	10.20	19.10	47.5	.47	0.00	0.00
24-26	.93	.021	10.10	19.80	46.6	.13	0.00	0.00

DDH = 2221NE   LINE 1200 NW   ELEV = 63 m

Depth (m)	Ni (%)	Co (%)	Fe (%)	MgO (%)	SiO_2 (%)	Al_2O_3 (%)	Cr_2O_3 (%)	LOI (%)
0-2	.35	0.000	20.69	1.18	0.0	0.00	0.00	0.00
2-4	.06	0.000	7.40	2.88	0.0	0.00	0.00	0.00
4-6	.02	0.000	3.17	3.04	0.0	0.00	0.00	0.00
6-8	.07	0.000	5.21	3.11	0.0	0.00	0.00	0.00
8-10	.09	0.000	7.85	3.74	0.0	0.00	0.00	0.00
10-12	.11	0.000	8.46	4.51	0.0	0.00	0.00	0.00
12-14	.22	0.000	8.23	3.66	0.0	0.00	0.00	0.00
14-16	.10	0.000	8.00	4.90	0.0	0.00	0.00	0.00
16-18	.20	0.000	8.61	5.06	0.0	0.00	0.00	0.00
18-20	.59	0.000	20.33	5.29	0.0	0.00	0.00	0.00
20-22	.67	0.000	24.15	9.17	0.0	0.00	0.00	0.00
22-24	1.03	0.000	29.72	6.45	0.0	0.00	0.00	0.00
24-26	1.20	0.000	27.56	7.85	35.9	0.00	0.00	0.00
26-28	2.69	0.000	17.22	11.35	38.4	0.00	0.00	0.00
28-30	1.72	0.000	16.31	16.32	42.3	0.00	0.00	0.00

DDH = 2224NE   LINE 1200 NW   ELEV = 63 m

Depth (m)	Ni (%)	Co (%)	Fe (%)	MgO (%)	SiO_2 (%)	Al_2O_3 (%)	Cr_2O_3 (%)	LOI (%)
0-2	.44	0.000	25.27	1.25	0.0	0.00	0.00	0.00
2-4	.14	0.000	9.81	2.81	0.0	0.00	0.00	0.00
4-6	.05	0.000	6.19	3.38	0.0	0.00	0.00	0.00
6-8	.06	0.000	5.58	3.14	0.0	0.00	0.00	0.00
8-10	.06	0.000	5.88	3.87	0.0	0.00	0.00	0.00
10-12	.14	0.000	8.60	4.19	0.0	0.00	0.00	0.00
12-14	.20	0.000	7.69	3.05	0.0	0.00	0.00	0.00
14-16	.10	0.000	7.54	4.44	0.0	0.00	0.00	0.00
16-18	.13	0.000	9.82	5.37	0.0	0.00	0.00	0.00
18-20	.36	0.000	13.37	3.81	0.0	0.00	0.00	0.00
20-22	.88	0.000	25.15	4.98	0.0	0.00	0.00	0.00
22-24	.77	0.000	28.39	5.99	0.0	0.00	0.00	0.00
24-26	.94	0.000	30.74	6.69	0.0	0.00	0.00	0.00
26-28	1.21	0.000	24.32	9.87	28.2	0.00	0.00	0.00
28-30	1.83	0.000	12.08	20.62	40.9	0.00	0.00	0.00
30-32	1.55	0.000	10.41	24.43	43.4	0.00	0.00	0.00
32-34	.70	0.000	8.91	27.43	23.5	0.00	0.00	0.00
34-36	.29	0.000	7.48	29.13	0.0	0.00	0.00	0.00
36-38	.26	0.000	6.80	26.62	0.0	0.00	0.00	0.00
38-40	.28	0.000	6.34	31.65	0.0	0.00	0.00	0.00
40-42	.24	0.000	6.04	33.03	0.0	0.00	0.00	0.00
42-44	.24	0.000	6.19	33.59	0.0	0.00	0.00	0.00

DDH = 2247NE   LINE 1200 NW   ELEV = 62 m

Depth (m)	Ni (%)	Co (%)	Fe (%)	MgO (%)	SiO_2 (%)	Al_2O_3 (%)	Cr_2O_3 (%)	LOI (%)
0-2	.11	0.000	8.38	2.11	0.0	0.00	0.00	0.00
2-4	.25	0.000	14.03	2.03	0.0	0.00	0.00	0.00
4-6	.04	0.000	5.73	3.26	0.0	0.00	0.00	0.00
6-8	.03	0.000	6.03	4.88	0.0	0.00	0.00	0.00
8-10	.01	0.000	5.88	3.72	0.0	0.00	0.00	0.00
10-12	.06	0.000	6.04	3.03	0.0	0.00	0.00	0.00
12-14	.03	0.000	7.09	4.03	0.0	0.00	0.00	0.00
14-16	.06	0.000	6.79	4.80	0.0	0.00	0.00	0.00
16-18	.09	0.000	7.32	3.72	0.0	0.00	0.00	0.00
18-20	.09	0.000	8.83	5.11	0.0	0.00	0.00	0.00
20-22	.04	0.000	6.03	4.19	0.0	0.00	0.00	0.00
22-24	.11	0.000	6.86	4.11	0.0	0.00	0.00	0.00
24-26	.19	0.000	6.94	3.34	0.0	0.00	0.00	0.00
26-28	.92	0.000	21.27	4.65	0.0	0.00	0.00	0.00
28-30	.55	0.000	16.52	4.03	0.0	0.00	0.00	0.00

DDH = 2250NE   LINE 1200 NW   ELEV = 62 m

Depth (m)	Ni (%)	Co (%)	Fe (%)	MgO (%)	SiO_2 (%)	Al_2O_3 (%)	Cr_2O_3 (%)	LOI (%)
0-2	.10	0.000	7.69	1.64	0.0	0.00	0.00	0.00
2-4	.19	0.000	13.43	2.41	0.0	0.00	0.00	0.00
4-6	.03	0.000	5.28	3.57	0.0	0.00	0.00	0.00
6-8	.03	0.000	6.19	4.73	0.0	0.00	0.00	0.00
8-10	.03	0.000	5.43	3.65	0.0	0.00	0.00	0.00
10-12	.03	0.000	5.73	2.95	0.0	0.00	0.00	0.00
12-14	.04	0.000	6.49	3.80	0.0	0.00	0.00	0.00
14-16	.08	0.000	7.92	6.27	0.0	0.00	0.00	0.00
16-18	.14	0.000	9.28	3.65	0.0	0.00	0.00	0.00
18-20	.06	0.000	7.69	6.35	0.0	0.00	0.00	0.00
20-22	.03	0.000	6.56	4.57	0.0	0.00	0.00	0.00
22-24	.10	0.000	7.09	4.03	0.0	0.00	0.00	0.00
24-26	.05	0.000	2.87	3.42	0.0	0.00	0.00	0.00
26-28	.94	0.000	19.31	4.42	0.0	0.00	0.00	0.00
28-30	.40	0.000	12.82	4.42	0.0	0.00	0.00	0.00

DDH = 2270NE   LINE 1200 NW   ELEV = 60 m

Depth (m)	Ni (%)	Co (%)	Fe (%)	MgO (%)	SiO_2 (%)	Al_2O_3 (%)	Cr_2O_3 (%)	LOI (%)
0-2	.15	0.000	12.28	1.43	0.0	0.00	0.00	0.00
2-4	.10	0.000	7.54	7.33	0.0	0.00	0.00	0.00
4-6	.08	0.000	6.03	20.30	0.0	0.00	0.00	0.00
6-8	.04	0.000	6.33	4.63	0.0	0.00	0.00	0.00
8-10	.04	0.000	6.18	4.22	0.0	0.00	0.00	0.00
10-12	.08	0.000	6.33	2.91	0.0	0.00	0.00	0.00
12-14	.08	0.000	7.16	3.97	0.0	0.00	0.00	0.00
14-16	.07	0.000	6.93	7.82	0.0	0.00	0.00	0.00
16-18	.12	0.000	8.74	5.12	0.0	0.00	0.00	0.00
18-20	.04	0.000	6.33	4.71	0.0	0.00	0.00	0.00
20-22	.08	0.000	7.08	3.97	0.0	0.00	0.00	0.00
22-24	.11	0.000	6.18	3.32	0.0	0.00	0.00	0.00
24-26	.42	0.000	11.45	2.58	0.0	0.00	0.00	0.00
26-28	.20	0.000	9.19	3.40	0.0	0.00	0.00	0.00

DDH = 2273NE   LINE 1200 NW   ELEV = 59 m

Depth (m)	Ni (%)	Co (%)	Fe (%)	MgO (%)	SiO$_2$ (%)	Al$_2$O$_3$ (%)	Cr$_2$O$_3$ (%)	LOI (%)
0-2	.21	0.000	20.07	1.37	0.0	0.00	0.00	0.00
2-4	.09	0.000	8.89	5.45	0.0	0.00	0.00	0.00
4-6	.10	0.000	9.49	12.89	0.0	0.00	0.00	0.00
6-8	.09	0.000	11.30	5.61	0.0	0.00	0.00	0.00
8-10	.05	0.000	7.38	8.06	0.0	0.00	0.00	0.00
10-12	.05	0.000	7.01	5.61	0.0	0.00	0.00	0.00
12-14	.03	0.000	6.25	4.96	0.0	0.00	0.00	0.00
14-16	.05	0.000	5.95	3.32	0.0	0.00	0.00	0.00
16-18	.06	0.000	7.54	4.55	0.0	0.00	0.00	0.00
18-20	.08	0.000	7.38	6.26	0.0	0.00	0.00	0.00
20-22	.02	0.000	6.93	4.96	0.0	0.00	0.00	0.00
22-24	.09	0.000	6.86	3.48	0.0	0.00	0.00	0.00
24-26	.05	0.000	6.33	3.65	0.0	0.00	0.00	0.00
26-28	.28	0.000	7.99	2.91	0.0	0.00	0.00	0.00
28-30	.51	0.000	15.37	2.91	0.0	0.00	0.00	0.00

DDH = 659NE   LINE 1300 NW   ELEV = 77 m

Depth (m)	Ni (%)	Co (%)	Fe (%)	MgO (%)	SiO$_2$ (%)	Al$_2$O$_3$ (%)	Cr$_2$O$_3$ (%)	LOI (%)
0-2	.41	0.000	14.56	1.50	0.0	0.00	0.00	0.00
2-4	.92	0.000	17.10	2.50	0.0	0.00	0.00	0.00
4-6	.18	0.000	8.20	3.30	0.0	0.00	0.00	0.00
6-8	.18	0.000	8.20	3.30	0.0	0.00	0.00	0.00
8-10	.06	0.000	6.50	3.20	0.0	0.00	0.00	0.00
10-12	.18	0.000	5.90	3.30	0.0	0.00	0.00	0.00
12-14	.24	0.000	4.80	2.50	0.0	0.00	0.00	0.00

DDH = 754NE   LINE 1300 NW   ELEV = 91 m

Depth (m)	Ni (%)	Co (%)	Fe (%)	MgO (%)	SiO$_2$ (%)	Al$_2$O$_3$ (%)	Cr$_2$O$_3$ (%)	LOI (%)
0-2	.53	0.000	33.40	.92	0.0	0.00	0.00	0.00
2-4	.53	0.000	32.00	.66	0.0	0.00	0.00	0.00
4-6	1.43	0.000	32.90	.92	0.0	0.00	0.00	0.00

DDH = 800NE   LINE 1300 NW   ELEV = 100 m

Depth (m)	Ni (%)	Co (%)	Fe (%)	MgO (%)	SiO$_2$ (%)	Al$_2$O$_3$ (%)	Cr$_2$O$_3$ (%)	LOI (%)
0-2	.55	.070	31.10	.90	34.1	7.67	0.00	9.36
2-4	1.91	.099	27.90	1.20	36.3	6.92	0.00	8.18
4-6	2.85	.063	21.50	2.20	46.7	4.66	0.00	7.59
6-8	2.60	.047	19.60	2.90	48.1	4.18	0.00	6.91
8-10	2.65	.047	21.40	3.30	44.9	4.55	0.00	7.62
10-12	2.81	.044	21.80	4.70	43.4	4.37	0.00	8.24
12-14	2.01	.039	20.30	5.50	47.4	3.49	0.00	7.77
14-16	1.44	.037	19.30	4.70	48.5	4.54	0.00	7.68
16-18	1.52	.030	16.60	15.90	42.5	2.90	0.00	9.76
18-20	1.18	.025	12.40	24.00	41.1	2.28	0.00	10.79
20-22	.77	.017	11.10	23.60	44.1	2.19	0.00	9.95
22-24	.66	.020	9.90	37.00	44.2	1.64	0.00	11.12
24-26	.64	.021	9.60	26.20	46.3	1.06	0.00	10.70
26-28	.39	.010	7.40	32.20	43.4	1.32	0.00	8.34
28-30	.31	.012	6.60	35.10	42.7	1.22	0.00	6.80

DDH = 862NE   LINE 1300 NW   ELEV = 112 m

Depth (m)	Ni (%)	Co (%)	Fe (%)	MgO (%)	SiO_2 (%)	Al_2O_3 (%)	Cr_2O_3 (%)	LOI (%)
0-2	.73	0.000	32.76	.88	0.0	0.00	0.00	0.00
2-4	1.23	0.000	34.00	.90	0.0	0.00	0.00	0.00
4-6	1.58	.061	34.28	1.00	24.9	5.53	2.13	10.29
6-8	2.95	.051	30.52	5.61	31.4	4.43	1.61	10.52
8-10	3.20	.043	24.50	10.48	38.0	3.06	1.21	10.10
10-12	3.40	.031	19.53	12.85	53.2	1.59	.80	8.52
12-14	2.60	.049	13.34	13.11	58.5	2.09	1.53	8.53
14-16	1.21	0.000	7.78	12.15	0.0	0.00	0.00	0.00
16-18	1.21	0.000	6.47	13.69	0.0	0.00	0.00	0.00
18-20	1.22	0.000	5.69	16.63	0.0	0.00	0.00	0.00
20-22	.44	0.000	7.00	25.86	0.0	0.00	0.00	0.00
22-24	.57	0.000	7.20	34.55	0.0	0.00	0.00	0.00

DDH = 900NE   LINE 1300 NW   ELEV = 125 m

Depth (m)	Ni (%)	Co (%)	Fe (%)	MgO (%)	SiO_2 (%)	Al_2O_3 (%)	Cr_2O_3 (%)	LOI (%)
0-2	.85	0.000	30.57	.09	38.4	6.64	0.00	8.58
2-4	1.18	.137	39.07	.12	24.9	6.98	0.00	9.38
4-6	2.82	.051	17.65	9.35	48.1	3.00	0.00	8.76
6-8	4.24	.051	16.19	10.68	45.7	1.88	0.00	10.50
8-10	3.95	.069	19.88	9.60	40.7	2.56	0.00	11.00
10-12	3.16	.051	17.47	15.65	37.7	3.00	0.00	13.50
12-14	2.75	.038	13.14	19.40	40.8	2.30	0.00	12.74
14-16	2.81	.034	11.46	21.42	41.3	1.94	0.00	13.16
16-18	2.11	.038	11.78	20.10	39.3	1.72	0.00	10.58

DDH = 935NE   LINE 1300 NW   ELEV = 133 m

Depth (m)	Ni (%)	Co (%)	Fe (%)	MgO (%)	SiO_2 (%)	Al_2O_3 (%)	Cr_2O_3 (%)	LOI (%)
0-2	.74	0.000	22.36	.65	0.0	0.00	0.00	0.00
2-4	1.38	0.000	17.61	2.46	0.0	0.00	0.00	0.00
4-6	3.37	.035	9.52	29.21	41.9	0.00	0.00	12.25
6-8	2.00	.032	10.26	27.79	43.2	0.00	0.00	8.00
8-10	.24	0.000	6.09	39.02	0.0	0.00	0.00	0.00
10-12	.42	0.000	6.21	35.29	0.0	0.00	0.00	0.00
12-14	.25	0.000	6.09	36.22	0.0	0.00	0.00	0.00

DDH = 1005NE   LINE 1300 NW   ELEV = 154 m

Depth (m)	Ni (%)	Co (%)	Fe (%)	MgO (%)	SiO_2 (%)	Al_2O_3 (%)	Cr_2O_3 (%)	LOI (%)
0–2	.45	0.000	20.78	.48	0.0	0.00	0.00	0.00
2–4	.55	0.000	16.77	.55	0.0	0.00	0.00	0.00
4–6	1.82	.224	44.72	.72	9.0	0.00	0.00	11.19
6–8	3.00	.033	41.90	2.84	14.5	0.00	0.00	9.22
8–10	2.88	.051	14.35	21.35	42.3	0.00	0.00	9.23
10–12	2.32	.030	8.98	28.16	43.1	0.00	0.00	10.69
12–14	1.85	.021	6.96	30.83	42.5	0.00	0.00	11.92
14–16	1.93	.020	7.57	25.87	49.4	0.00	0.00	10.32
16–18	1.88	.021	6.95	24.08	52.6	0.00	0.00	9.50
18–20	2.14	.018	6.83	31.30	45.2	0.00	0.00	11.54
20–22	1.71	.019	7.35	32.83	43.4	0.00	0.00	11.83
22–24	.53	0.000	6.04	33.02	0.0	0.00	0.00	0.00
24–26	.34	0.000	5.70	36.00	0.0	0.00	0.00	0.00
26–28	.22	0.000	5.28	33.82	0.0	0.00	0.00	0.00

DDH = 1080NE   LINE 1300 NW   ELEV = 169 m

Depth (m)	Ni (%)	Co (%)	Fe (%)	MgO (%)	SiO_2 (%)	Al_2O_3 (%)	Cr_2O_3 (%)	LOI (%)
0–2	.84	.049	25.90	2.70	0.0	0.00	0.00	0.00
2–4	.73	.139	19.30	.80	0.0	0.00	0.00	0.00
4–6	1.82	.229	38.10	1.30	23.4	0.00	0.00	0.00
6–8	.69	.090	16.10	1.00	59.3	0.00	0.00	0.00
8–10	2.23	.058	17.00	20.20	40.3	0.00	0.00	0.00
10–12	2.97	.041	11.20	27.20	40.7	0.00	0.00	0.00
12–14	2.47	.026	8.70	27.90	43.4	0.00	0.00	0.00
14–16	2.55	.023	7.90	21.40	51.8	0.00	0.00	0.00
16–18	2.41	.019	7.10	23.30	53.4	0.00	0.00	0.00
18–20	1.80	.018	6.60	33.20	42.3	0.00	0.00	0.00
20–22	1.14	.017	6.20	34.60	0.0	0.00	0.00	0.00
22–24	.45	.015	5.70	36.90	0.0	0.00	0.00	0.00
24–26	.39	.017	5.60	36.50	0.0	0.00	0.00	0.00

DDH = 1105NE			LINE 1300 NW			ELEV = 175 m	
Depth (m)	Ni (%)	Co (%)	Fe (%)	MgO (%)	SiO$_2$ (%)	Al$_2$O$_3$ (%)	Cr$_2$O$_3$ (%)	LOI (%)
0–2	.92	0.000	31.45	.70	0.0	0.00	0.00	0.00
2–4	1.50	.200	39.29	.70	13.7	0.00	0.00	10.56
4–6	1.37	0.000	34.70	.74	0.0	0.00	0.00	0.00
6–8	1.60	.100	21.62	2.09	51.6	0.00	0.00	8.60
8–10	1.93	.080	14.72	9.67	53.4	0.00	0.00	6.84
10–12	2.43	.059	12.00	9.15	61.1	0.00	0.00	5.80
12–14	2.51	.075	7.38	14.38	61.0	0.00	0.00	6.76
14–16	2.76	.024	7.86	18.56	54.5	0.00	0.00	7.55
16–18	2.42	.015	7.20	24.57	51.7	0.00	0.00	9.57
18–20	2.23	.014	6.18	20.11	57.6	0.00	0.00	7.98
20–22	1.45	0.000	7.00	28.53	0.0	0.00	0.00	0.00
22–24	1.79	.013	8.34	29.50	41.6	0.00	0.00	12.88
24–26	.95	0.000	6.45	30.80	0.0	0.00	0.00	0.00
26–28	.53	0.000	6.10	36.66	0.0	0.00	0.00	0.00
28–30	.46	0.000	6.48	36.39	0.0	0.00	0.00	0.00

DDH = 1126NE			LINE 1300 NW			ELEV = 182 m	
Depth (m)	Ni (%)	Co (%)	Fe (%)	MgO (%)	SiO$_2$ (%)	Al$_2$O$_3$ (%)	Cr$_2$O$_3$ (%)	LOI (%)
0–2	.92	.088	24.10	1.50	0.0	0.00	0.00	0.00
2–4	.59	.029	8.20	2.00	0.0	0.00	0.00	0.00
4–6	1.02	.079	23.50	1.30	0.0	0.00	0.00	0.00
6–8	.86	.060	15.70	1.50	0.0	0.00	0.00	0.00
8–10	3.30	.047	13.70	15.00	46.0	1.32	1.21	0.00
10–12	3.70	.028	9.20	26.10	40.8	.89	.73	0.00
12–14	2.81	.022	8.00	30.30	41.8	1.31	.68	0.00
14–16	2.41	.020	7.80	25.50	47.6	1.30	.62	0.00
16–18	2.96	.018	7.80	28.70	43.4	1.40	.63	0.00
18–20	3.07	.022	9.00	25.80	42.9	1.76	.71	0.00
20–22	2.12	.020	7.60	30.00	42.0	1.46	.71	0.00
22–24	1.41	.021	8.40	28.50	43.1	1.59	.65	0.00
24–26	.46	.018	7.30	36.10	40.9	1.34	.52	0.00
26–28	.41	.019	6.20	36.30	39.5	1.07	.51	0.00
28–30	1.62	.016	7.00	31.70	43.4	1.41	.58	0.00
30–32	.80	.021	7.50	32.40	0.0	0.00	0.00	0.00

DDH = 1150NE   LINE 1300 NW   ELEV = 189 m

Depth (m)	Ni (%)	Co (%)	Fe (%)	MgO (%)	SiO$_2$ (%)	Al$_2$O$_3$ (%)	Cr$_2$O$_3$ (%)	LOI (%)
0-2	2.60	0.000	14.60	19.10	42.1	3.03	1.12	0.00
2-4	2.52	0.000	22.20	14.40	34.5	4.58	1.57	0.00
4-6	2.61	0.000	14.10	20.90	39.0	3.10	1.06	0.00
6-8	2.97	0.000	13.60	20.30	41.1	3.19	1.14	0.00
8-10	2.72	0.000	12.30	20.60	44.7	2.36	.94	0.00
10-12	2.35	0.000	9.60	16.10	56.3	1.01	.94	0.00
12-14	3.41	0.000	4.50	17.90	61.6	.39	.49	0.00
14-16	2.90	0.000	5.40	18.40	57.0	1.23	.55	0.00
16-18	2.98	0.000	7.10	21.40	52.8	1.22	.65	0.00
18-20	2.41	0.000	7.60	27.40	44.9	.94	.69	0.00
20-22	2.45	0.000	7.10	23.50	51.0	.52	.56	0.00
22-24	2.77	0.000	6.30	23.10	53.1	.44	.50	0.00
24-26	1.47	0.000	6.30	28.80	49.2	.43	.57	0.00
26-28	.43	0.000	6.40	37.60	40.3	.47	.51	0.00
28-30	.33	0.000	6.00	36.70	40.0	.53	.49	0.00
30-32	.85	0.000	6.30	34.10	43.1	.51	.50	0.00
32-34	1.77	0.000	6.50	24.50	53.1	.65	.56	0.00
34-36	1.40	0.000	6.20	25.30	52.6	.96	.54	0.00
36-38	1.76	0.000	6.40	29.60	43.7	1.48	.59	0.00
38-40	1.20	0.000	6.20	30.80	0.0	0.00	0.00	0.00
40-42	.36	0.000	6.00	33.70	0.0	0.00	0.00	0.00
42-44	.46	0.000	6.00	22.40	0.0	0.00	0.00	0.00

DDH = 1171NE   LINE 1300 NW   ELEV = 196 m

Depth (m)	Ni (%)	Co (%)	Fe (%)	MgO (%)	SiO$_2$ (%)	Al$_2$O$_3$ (%)	Cr$_2$O$_3$ (%)	LOI (%)
0-2	.66	0.000	25.85	.58	0.0	0.00	0.00	0.00
2-4	.77	0.000	22.70	.59	0.0	0.00	0.00	0.00
4-6	.92	0.000	24.70	.67	0.0	0.00	0.00	0.00
6-8	.93	0.000	22.62	.70	0.0	0.00	0.00	0.00
8-10	2.05	.056	18.60	10.54	46.5	0.00	0.00	8.73
10-12	2.62	.052	14.34	15.03	48.4	0.00	0.00	8.70
12-14	3.38	.028	10.86	17.52	50.1	0.00	0.00	8.88
14-16	3.27	.022	10.23	20.01	47.9	0.00	0.00	9.38
16-18	2.89	.019	9.43	17.52	50.9	0.00	0.00	8.57
18-20	3.10	.014	7.09	22.36	51.7	0.00	0.00	9.65
20-22	3.43	.014	6.63	22.92	50.1	0.00	0.00	10.24
22-24	1.82	.017	7.06	23.90	50.2	0.00	0.00	9.99
24-26	1.86	.018	7.41	22.15	53.4	0.00	0.00	9.42
26-28	2.66	.011	6.81	21.78	52.6	0.00	0.00	9.68
28-30	2.10	.013	6.92	26.06	43.3	0.00	0.00	11.12
30-32	1.67	.015	7.50	25.60	48.9	0.00	0.00	11.20
32-34	2.64	.013	6.90	22.58	49.3	0.00	0.00	10.43
34-36	1.46	.015	7.71	21.94	49.7	0.00	0.00	4.18
36-38	1.60	.012	7.21	22.77	51.0	0.00	0.00	10.36

DDH = 1173NE   LINE 1300 NW   ELEV = 196 m

Depth (m)	Ni (%)	Co (%)	Fe (%)	MgO (%)	SiO_2 (%)	Al_2O_3 (%)	Cr_2O_3 (%)	LOI (%)
0-2	.66	0.000	19.45	.61	0.0	0.00	0.00	0.00
2-4	2.46	.054	15.25	15.00	54.3	0.00	0.00	8.04
4-6	2.50	.043	15.80	8.75	45.1	0.00	0.00	7.53
6-8	2.58	.033	12.38	14.80	50.9	0.00	0.00	8.44
8-10	2.68	.020	8.37	22.87	48.1	0.00	0.00	10.07
10-12	2.86	.022	8.00	21.02	51.7	0.00	0.00	10.05
12-14	3.16	.010	7.85	22.00	52.3	0.00	0.00	9.67
14-16	2.80	.015	8.80	21.68	49.8	0.00	0.00	9.58
16-18	2.91	.013	8.47	20.39	49.7	0.00	0.00	9.59
18-20	1.95	.012	7.84	27.00	44.5	0.00	0.00	10.03
20-22	1.86	.010	7.79	26.10	47.6	0.00	0.00	10.04
22-24	1.29	0.000	7.37	27.48	0.0	0.00	0.00	0.00
24-26	2.74	.013	6.84	20.80	54.0	0.00	0.00	8.84
26-28	1.95	.012	7.47	21.84	52.6	0.00	0.00	8.52
28-30	2.73	.006	6.20	26.02	49.9	0.00	0.00	10.49
30-32	.97	0.000	7.41	26.80	0.0	0.00	0.00	0.00
32-34	.53	0.000	8.06	28.90	0.0	0.00	0.00	0.00
34-36	1.46	0.000	7.20	25.27	0.0	0.00	0.00	0.00
36-38	1.39	0.000	7.07	24.86	0.0	0.00	0.00	0.00
38-40	1.77	0.000	7.44	23.12	0.0	0.00	0.00	0.00
40-42	.48	0.000	6.70	29.27	0.0	0.00	0.00	0.00
42-44	2.31	.006	7.38	22.70	53.6	0.00	0.00	9.38
44-46	1.48	0.000	6.97	27.78	0.0	0.00	0.00	0.00
46-48	.76	0.000	7.53	29.61	0.0	0.00	0.00	0.00
48-50	2.55	.010	7.36	23.40	50.2	0.00	0.00	9.83
50-52	2.40	.010	6.64	27.84	49.8	0.00	0.00	9.70
52-54	3.57	.007	7.07	24.60	48.1	0.00	0.00	9.94
54-56	2.69	.012	6.98	26.40	48.4	0.00	0.00	9.99
56-58	3.28	.010	6.92	23.43	45.9	0.00	0.00	9.78
58-60	3.11	.011	7.65	24.60	45.9	0.00	0.00	10.19
60-62	3.21	.011	7.71	25.36	46.3	0.00	0.00	10.18
62-64	2.71	.009	7.37	25.60	45.6	0.00	0.00	10.36
64-66	2.06	.009	7.56	25.88	45.8	0.00	0.00	10.54
66-68	2.79	.005	4.63	23.41	53.1	0.00	0.00	9.95
68-70	1.41	0.000	6.80	22.50	0.0	0.00	0.00	0.00
70-72	.89	0.000	8.63	21.93	0.0	0.00	0.00	0.00
72-74	.79	0.000	8.03	26.79	0.0	0.00	0.00	0.00

DDH = 1203NE   LINE 1300 NW   ELEV = 203 m

Depth (m)	Ni (%)	Co (%)	Fe (%)	MgO (%)	SiO_2 (%)	Al_2O_3 (%)	Cr_2O_3 (%)	LOI (%)
0-2	1.06	0.000	35.90	.90	0.0	0.00	0.00	0.00
2-4	3.33	.048	18.00	3.30	57.9	2.40	1.48	5.50
4-6	3.91	.044	14.80	2.70	63.5	2.17	1.40	5.31
6-8	3.99	.074	22.80	14.10	29.5	3.80	2.11	10.60
8-10	3.74	.051	12.30	23.20	37.7	2.37	1.10	10.98
10-12	3.53	.019	7.70	27.70	42.4	.91	.65	11.20
12-14	3.54	.040	11.30	20.40	39.4	1.44	.93	11.11
14-16	3.02	.023	8.80	23.80	39.3	1.28	.65	10.51
16-18	2.74	.022	8.50	25.40	42.7	1.45	.72	10.01
18-20	2.91	.024	8.10	27.70	40.6	1.31	.68	12.80
20-22	2.83	.022	7.40	29.90	39.3	.70	.53	13.59
22-24	1.02	.014	6.40	34.10	39.4	.45	.41	13.88
24-26	.83	.012	6.30	34.20	40.7	.64	.48	13.80
26-28	2.16	.015	6.70	32.20	40.7	1.00	.48	13.84
28-30	1.37	.013	6.30	33.60	39.4	.88	.47	14.06
30-32	.78	.015	6.30	33.90	39.3	1.06	.43	14.52
32-34	1.36	.014	6.70	33.00	39.8	1.05	.46	13.82
34-36	1.75	.015	7.00	31.70	39.7	1.02	.47	13.78
36-38	1.21	0.000	6.90	31.80	0.0	0.00	0.00	0.00
38-40	1.03	0.000	6.70	32.70	0.0	0.00	0.00	0.00
40-42	.68	0.000	7.50	31.50	0.0	0.00	0.00	0.00
42-44	1.02	0.000	6.50	26.60	0.0	0.00	0.00	0.00
44-46	1.10	0.000	7.40	22.50	0.0	0.00	0.00	0.00
46-48	.50	0.000	5.30	20.10	0.0	0.00	0.00	0.00
48-50	.33	0.000	5.30	23.50	0.0	0.00	0.00	0.00
50-52	.37	0.000	6.30	30.30	0.0	0.00	0.00	0.00
52-54	.47	0.000	6.70	30.00	0.0	0.00	0.00	0.00
54-56	.73	0.000	6.70	28.80	0.0	0.00	0.00	0.00
56-58	.55	0.000	6.80	31.10	0.0	0.00	0.00	0.00
58-60	.49	0.000	6.50	31.90	0.0	0.00	0.00	0.00

DDH = 1230NE   LINE 1300 NW   ELEV = 208 m

Depth (m)	Ni (%)	Co (%)	Fe (%)	MgO (%)	SiO_2 (%)	Al_2O_3 (%)	Cr_2O_3 (%)	LOI (%)
0–2	.93	0.000	40.20	.90	0.0	0.00	0.00	0.00
2–4	3.13	.041	15.20	20.80	37.4	2.47	1.08	10.10
4–6	2.90	.030	13.90	18.00	40.4	2.76	1.35	9.16
6–8	2.57	.019	9.90	24.30	44.0	1.37	.82	9.24
8–10	2.40	.018	10.20	26.60	44.6	1.30	.87	8.65
10–12	2.81	.023	10.90	23.00	44.7	1.70	1.02	9.54
12–14	2.91	.016	8.90	25.90	44.0	1.01	.66	10.07
14–16	2.08	.021	10.70	25.10	43.8	1.30	.79	8.70
16–18	.50	.012	8.10	34.10	44.0	.90	.54	7.36
18–20	.72	.012	7.10	30.90	46.5	.78	.52	8.56
20–22	.60	.013	5.80	30.60	50.0	.81	.90	6.00
22–24	2.06	.016	7.00	27.00	48.2	.47	.72	8.35
24–26	3.80	.019	7.90	24.00	45.5	.90	.71	8.80
26–28	2.99	.020	8.20	28.00	43.9	1.15	.73	8.79
28–30	2.60	.016	6.50	31.40	43.1	.85	.45	10.31
30–32	1.17	.016	6.50	34.50	0.0	0.00	0.00	0.00
32–34	.30	.012	5.70	36.80	0.0	0.00	0.00	0.00
34–36	.38	.012	6.00	36.80	0.0	0.00	0.00	0.00

DDH = 1249NE   LINE 1300 NW   ELEV = 210 m

Depth (m)	Ni (%)	Co (%)	Fe (%)	MgO (%)	SiO$_2$ (%)	Al$_2$O$_3$ (%)	Cr$_2$O$_3$ (%)	LOI (%)
0-2	.73	0.000	36.80	1.00	0.0	0.00	0.00	0.00
2-4	.89	0.000	29.40	.90	0.0	0.00	0.00	0.00
4-6	.57	0.000	17.20	.80	0.0	0.00	0.00	0.00
6-8	.56	0.000	15.20	.80	0.0	0.00	0.00	0.00
8-10	.38	0.000	8.30	1.10	0.0	0.00	0.00	0.00
10-12	.30	0.000	7.30	.70	0.0	0.00	0.00	0.00
12-14	1.04	0.000	27.60	1.10	0.0	0.00	0.00	0.00
14-16	1.48	0.000	19.10	5.50	0.0	0.00	0.00	0.00
16-18	2.14	.050	11.60	19.20	46.4	2.45	.90	9.15
18-20	1.75	.026	10.80	23.20	40.4	2.22	.91	10.11
20-22	1.47	.019	9.70	25.10	41.4	1.72	.75	10.23
22-24	1.72	.025	8.40	28.90	42.1	1.57	.70	9.81
24-26	.35	.015	6.40	35.40	44.0	1.28	.42	8.73
26-28	1.99	.018	6.70	28.30	46.5	.87	.54	10.21
28-30	.92	.016	6.50	33.90	43.8	1.10	.53	10.20
30-32	1.20	.016	6.90	35.10	40.2	.86	.50	10.26
32-34	3.75	.047	14.60	20.40	36.4	2.21	1.14	10.55
34-36	4.18	.077	17.80	17.10	32.6	2.55	1.49	10.93
36-38	3.46	.042	13.10	22.50	35.5	1.98	1.13	11.69
38-40	2.99	.024	9.00	29.70	38.6	1.25	.70	12.41
40-42	2.98	.038	13.40	23.40	36.5	2.23	1.14	11.03
42-44	.86	.017	6.50	34.50	42.8	1.13	.55	11.30
44-46	2.28	.018	8.00	25.40	46.6	.93	.59	10.12
46-48	1.94	.019	7.00	26.90	45.3	.84	.84	11.04
48-50	4.36	.012	5.00	18.80	57.0	1.31	.37	8.16
50-52	2.17	.065	7.90	24.60	51.6	1.12	.61	9.92
52-54	1.67	.065	7.70	24.90	50.2	1.36	.54	9.37
54-56	1.20	.066	8.20	27.10	49.5	1.24	.60	8.66
56-58	.97	.066	7.80	30.20	40.7	.85	.58	10.48
58-60	2.20	.061	6.80	27.80	47.1	.77	.50	10.78
60-62	2.19	.058	7.20	24.20	50.7	.67	.47	9.92
62-64	1.79	.064	8.40	27.90	45.5	1.17	.53	10.66
64-66	2.10	.062	8.80	24.10	41.1	1.53	.62	10.02
66-68	3.03	.060	8.10	22.10	49.3	1.44	.53	10.04
68-70	3.28	.057	8.80	21.80	48.8	1.37	.56	10.04
70-72	2.40	.058	9.30	22.60	47.4	1.33	.64	10.42
72-74	.67	.062	8.10	32.10	42.4	.88	.56	9.81
74-76	.70	.059	7.60	31.20	43.5	.92	.72	11.21
76-78	1.19	.066	9.90	23.70	47.4	1.09	.77	10.69
78-80	.83	.060	9.50	19.50	52.2	.90	.64	11.05
80-82	.60	.057	7.60	23.70	51.9	.71	.47	10.43
82-84	1.82	.059	8.40	18.30	57.8	1.02	.56	9.15

DDH = 1292NE LINE 1300 NW ELEV = 217 m

Depth (m)	Ni (%)	Co (%)	Fe (%)	MgO (%)	SiO_2 (%)	Al_2O_3 (%)	Cr_2O_3 (%)	LOI (%)
0-2	.94	0.000	42.00	.75	0.0	0.00	0.00	0.00
2-4	.82	0.000	32.00	.68	0.0	0.00	0.00	0.00
4-6	.92	0.000	30.50	.96	0.0	0.00	0.00	0.00
6-8	1.33	.109	35.43	.77	29.5	0.00	0.00	8.80
8-10	1.59	.225	39.53	.71	15.7	0.00	0.00	10.52
10-12	1.31	.126	33.25	.75	34.1	0.00	0.00	8.46
12-14	1.65	.182	42.20	.73	12.8	0.00	0.00	10.73
14-16	3.45	.104	14.00	23.80	38.2	0.00	0.00	11.08
16-18	3.09	.039	7.70	28.75	41.8	0.00	0.00	10.83
18-20	2.35	.032	10.00	26.58	40.6	0.00	0.00	11.74
20-22	1.25	.027	9.00	32.61	39.5	0.00	0.00	12.40
22-24	.29	0.000	6.49	36.10	0.0	0.00	0.00	0.00
24-26	.26	0.000	5.92	38.16	0.0	0.00	0.00	0.00

DDH = 1334NE   LINE 1300 NW   ELEV = 224 m

Depth (m)	Ni (%)	Co (%)	Fe (%)	MgO (%)	SiO_2 (%)	Al_2O_3 (%)	Cr_2O_3 (%)	LOI (%)
0–2	.57	0.000	40.50	.90	0.0	0.00	0.00	0.00
2–4	.64	0.000	32.30	.80	0.0	0.00	0.00	0.00
4–6	.25	0.000	10.50	.70	0.0	0.00	0.00	0.00
6–8	.41	0.000	14.60	.60	0.0	0.00	0.00	0.00
8–10	.42	0.000	15.10	.60	0.0	0.00	0.00	0.00
10–12	.80	0.000	12.80	6.40	0.0	0.00	0.00	0.00
12–14	1.48	.018	7.70	15.90	58.0	0.00	0.00	0.00
14–16	.89	0.000	6.60	9.30	0.0	0.00	0.00	0.00
16–18	.93	0.000	8.60	13.60	0.0	0.00	0.00	0.00
18–20	1.27	.017	8.00	24.80	48.7	0.00	0.00	0.00
20–22	.98	0.000	7.70	11.00	0.0	0.00	0.00	0.00
22–24	1.47	.035	13.90	13.80	54.2	0.00	0.00	0.00
24–26	.99	.028	9.30	8.80	67.9	0.00	0.00	0.00
26–28	2.35	.030	11.20	25.90	42.5	0.00	0.00	0.00
28–30	1.44	.024	9.60	29.20	41.9	0.00	0.00	0.00
30–32	.42	.018	7.20	36.20	43.6	0.00	0.00	0.00
32–34	.34	.016	6.50	28.00	51.4	0.00	0.00	0.00
34–36	.38	.014	6.30	27.10	48.6	0.00	0.00	0.00
36–38	.46	.019	8.30	26.70	48.3	0.00	0.00	0.00
38–40	.63	.024	9.30	20.50	51.5	0.00	0.00	0.00
40–42	.80	.023	8.60	21.60	51.9	0.00	0.00	0.00
42–44	.76	.020	8.20	23.10	51.8	0.00	0.00	0.00
44–46	.91	.019	8.30	23.30	51.6	0.00	0.00	0.00
46–48	1.07	.024	9.20	23.00	50.6	0.00	0.00	0.00
48–50	.70	.020	8.40	27.20	46.1	0.00	0.00	0.00
50–52	.51	.018	8.10	31.30	43.3	0.00	0.00	0.00
52–54	.82	.019	8.10	27.50	45.4	0.00	0.00	0.00
54–56	1.38	.020	8.90	23.20	48.9	0.00	0.00	0.00
56–58	1.67	.019	8.70	21.70	49.8	0.00	0.00	0.00
58–60	.84	0.000	8.50	25.50	0.0	0.00	0.00	0.00
60–62	.62	0.000	9.80	21.90	0.0	0.00	0.00	0.00
62–64	.68	0.000	9.10	21.00	0.0	0.00	0.00	0.00
64–66	.81	0.000	9.50	23.20	0.0	0.00	0.00	0.00
66–68	.72	0.000	9.30	23.70	0.0	0.00	0.00	0.00
68–70	.73	0.000	8.70	30.10	0.0	0.00	0.00	0.00
70–72	.69	0.000	8.50	28.10	0.0	0.00	0.00	0.00
72–74	.53	0.000	6.70	17.70	0.0	0.00	0.00	0.00
74–76	.48	0.000	6.60	25.70	0.0	0.00	0.00	0.00
76–78	.43	0.000	6.20	26.20	0.0	0.00	0.00	0.00
78–80	.35	0.000	6.00	27.50	0.0	0.00	0.00	0.00
80–82	.49	0.000	7.00	25.40	0.0	0.00	0.00	0.00
82–84	.38	0.000	6.40	22.10	0.0	0.00	0.00	0.00

DDH = 1369NE LINE 1300 NW ELEV = 232 m

Depth (m)	Ni (%)	Co (%)	Fe (%)	MgO (%)	SiO_2 (%)	Al_2O_3 (%)	Cr_2O_3 (%)	LOI (%)
0–2	.56	0.000	46.20	.90	0.0	0.00	0.00	0.00
2–4	.62	0.000	45.90	1.10	0.0	0.00	0.00	0.00
4–6	.86	0.000	39.30	.90	0.0	0.00	0.00	0.00
6–8	.69	0.000	25.20	.80	0.0	0.00	0.00	0.00
8–10	1.49	0.000	33.90	1.00	0.0	0.00	0.00	0.00
10–12	.88	0.000	27.10	.80	0.0	0.00	0.00	0.00
12–14	.87	0.000	28.90	.90	0.0	0.00	0.00	0.00
14–16	1.34	0.000	25.70	3.40	0.0	0.00	0.00	0.00
16–18	2.94	.049	22.10	4.00	43.5	3.93	1.47	7.27
18–20	4.19	.035	14.20	7.70	50.6	2.44	.95	6.67
20–22	2.50	.034	17.80	9.10	47.4	1.66	.85	7.25
22–24	2.81	.043	18.00	9.10	46.1	2.07	.94	7.55
24–26	2.42	.028	8.80	5.10	66.3	1.85	.70	4.34
26–28	1.41	.033	8.90	2.60	71.3	.84	.75	3.21
28–30	1.91	.030	12.80	5.30	61.2	.94	.90	5.01
30–32	2.13	.026	11.70	12.60	53.2	.80	.68	7.67
32–34	1.45	.035	15.30	6.80	55.7	1.32	1.14	6.23
34–36	1.01	.033	17.50	13.10	45.3	1.40	1.04	8.15
36–38	.94	.036	14.00	16.40	46.2	1.76	.94	8.28
38–40	.73	.024	10.60	16.10	50.1	1.66	.68	8.31
40–42	.64	.021	10.46	20.50	50.6	1.55	.65	7.98
42–44	.72	.023	10.30	20.60	51.0	1.56	.74	7.61
44–46	.82	.021	10.10	22.00	51.3	1.14	.71	8.84
46–48	.60	.022	10.90	20.10	51.0	1.60	.71	7.36
48–50	.55	.021	9.90	21.80	50.6	1.45	.67	9.88
50–52	.43	.020	9.60	27.20	43.9	1.44	.58	9.23
52–54	.35	.022	7.70	31.30	43.7	1.21	.55	8.67
54–56	.83	.023	9.90	24.80	40.1	1.63	.68	9.15
56–58	1.17	.021	9.70	21.60	49.2	1.58	.73	9.00
58–60	.97	.020	8.50	23.10	48.0	1.37	.58	9.57
60–62	1.52	.021	9.20	20.50	50.9	1.56	.80	8.75
62–64	1.76	.022	10.30	20.50	49.1	1.48	.64	9.26
64–66	2.30	.023	9.30	22.30	48.7	1.44	.65	9.44
66–68	2.13	.021	9.60	20.10	51.9	1.24	.65	8.64
68–70	.62	.018	9.90	28.50	44.7	1.21	.54	9.74
70–72	.74	.016	8.10	30.40	43.8	.84	.51	10.47
72–74	1.31	.016	6.10	22.40	54.4	.81	1.00	8.64
74–76	.67	.022	9.40	22.90	48.1	1.56	.64	8.86
76–78	.33	.019	8.20	27.90	45.1	1.07	.50	9.47
78–80	.59	.019	9.20	21.50	52.0	.99	.58	8.49
80–82	1.50	.018	7.80	19.50	54.6	.82	.65	8.80
82–84	1.43	.017	9.10	15.30	59.2	.98	.63	7.56
84–86	1.41	.014	6.80	14.10	64.4	.62	.46	6.48
86–88	.96	.013	6.60	18.20	59.3	.65	.51	7.34
88–90	.69	.014	7.00	27.20	48.3	.63	.51	8.42
90–92	1.72	.015	8.80	19.30	54.0	.70	.54	8.99
92–94	2.13	.017	8.70	19.00	52.2	.70	.65	9.29
94–96	2.06	.017	9.40	20.00	50.6	.75	.70	10.00
96–98	1.64	.020	9.00	21.20	49.9	.84	.65	9.97

DDH = 1410NE   LINE 1300 NW   ELEV = 237 m

Depth (m)	Ni (%)	Co (%)	Fe (%)	MgO (%)	SiO_2 (%)	Al_2O_3 (%)	Cr_2O_3 (%)	LOI (%)
0-2	.68	.021	50.00	1.30	0.0	0.00	0.00	0.00
2-4	.70	.023	49.50	.90	0.0	0.00	0.00	0.00
4-6	.70	.025	49.10	1.30	0.0	0.00	0.00	0.00
6-8	.67	.044	45.10	1.10	0.0	0.00	0.00	0.00
8-10	.71	.089	46.10	1.00	0.0	0.00	0.00	0.00
10-12	.89	.221	42.70	1.00	0.0	0.00	0.00	0.00
12-14	.99	.294	35.60	.80	0.0	0.00	0.00	0.00
14-16	1.22	.207	33.20	.90	0.0	0.00	0.00	0.00
16-18	1.01	.101	41.80	.90	0.0	0.00	0.00	0.00
18-20	2.25	.080	25.10	4.50	39.7	3.12	1.21	8.15
20-22	3.46	.032	9.70	11.00	56.7	.65	.47	7.09
22-24	3.75	.029	11.00	13.10	51.5	.64	.50	8.27
24-26	.92	.035	8.00	3.50	69.9	.33	.54	3.35
26-28	1.56	.056	14.90	3.20	59.0	.80	.89	5.32
28-30	2.29	.028	15.90	14.30	44.6	1.13	.64	8.94
30-32	2.20	.020	10.40	13.80	54.8	.62	.55	7.76
32-34	1.24	.017	8.80	13.90	58.2	.57	.55	7.27
34-36	.61	.020	9.10	21.10	49.3	.61	.48	9.47
36-38	.39	.016	7.70	18.70	42.3	.57	.47	15.29
38-40	.76	.018	7.90	18.70	54.4	.54	.54	8.80
40-42	.75	.027	10.50	14.40	52.6	.69	.54	8.78
42-44	1.50	.026	11.30	16.60	50.5	.84	.56	9.15
44-46	3.68	.032	10.60	10.00	55.9	.88	.58	7.23
46-48	4.11	.038	12.00	14.50	47.4	1.26	.65	9.49
48-50	2.85	.034	12.00	11.80	52.7	.97	.78	8.92
50-52	2.51	.034	11.50	11.00	54.7	1.45	.83	8.03
52-54	2.30	.032	11.20	9.50	58.3	1.31	.73	7.15
54-56	3.20	.035	12.10	12.30	44.9	2.19	1.12	9.70
56-58	2.51	.030	12.40	12.40	50.4	1.97	.73	8.83
58-60	1.95	.037	15.30	13.40	44.5	2.81	1.07	9.89
60-62	1.22	.031	13.40	15.40	49.0	2.32	1.06	7.70
62-64	.60	.025	9.30	16.90	52.7	1.23	.74	8.16
64-66	.57	.018	8.20	27.60	46.2	.54	.48	9.62
66-68	.48	.020	9.10	27.70	45.2	.49	.47	8.49
68-70	2.28	.023	8.70	19.70	50.3	.52	.50	8.98
70-72	2.78	.028	9.30	19.00	49.0	.65	.54	9.06
72-74	2.57	.028	10.00	16.90	51.6	.55	.63	8.57
74-76	2.58	.028	12.90	14.50	50.0	.83	.74	9.11
76-78	4.03	.022	8.80	21.60	45.5	1.10	.61	9.27
78-80	3.15	.025	7.70	25.80	45.3	.85	.52	9.91
80-82	.66	.018	6.10	21.20	0.0	0.00	0.00	0.00
82-84	.49	.022	6.60	22.60	0.0	0.00	0.00	0.00
84-86	.39	.018	7.10	33.60	0.0	0.00	0.00	0.00
86-88	.31	.019	7.20	37.70	0.0	0.00	0.00	0.00

DDH = 1447NE   LINE 1300 NW   ELEV = 235 m

Depth (m)	Ni (%)	Co (%)	Fe (%)	MgO (%)	SiO$_2$ (%)	Al$_2$O$_3$ (%)	Cr$_2$O$_3$ (%)	LOI (%)
0–2	.55	0.000	50.30	1.20	0.0	0.00	0.00	0.00
2–4	.55	0.000	50.80	.90	0.0	0.00	0.00	0.00
4–6	1.65	.092	43.20	1.10	10.6	8.03	2.40	12.35
6–8	1.11	.071	20.30	3.20	53.6	3.32	1.50	6.38
8–10	.87	.181	30.10	1.20	38.8	3.40	1.71	8.09
10–12	1.16	.246	33.66	1.30	30.9	4.70	2.17	9.01
12–14	1.28	.224	25.40	1.00	45.9	3.72	1.50	7.46
14–16	1.91	.456	32.60	1.30	28.0	5.43	2.04	9.73
16–18	1.22	.120	17.30	1.00	59.7	2.08	1.71	5.73
18–20	1.98	.068	24.20	1.70	45.7	3.72	2.19	7.36
20–22	1.80	.067	26.40	1.40	41.7	4.33	2.83	7.78
22–24	2.51	.055	19.90	2.20	53.6	2.80	1.72	4.61
24–26	3.89	.034	10.40	11.90	55.8	1.32	.80	8.11
26–28	4.50	.022	10.10	14.80	53.1	1.15	.74	8.77
28–30	5.36	.021	10.30	18.20	46.9	1.66	.75	9.68
30–32	5.19	.021	10.30	19.50	44.3	1.89	.78	11.38
32–34	4.29	.020	9.70	17.30	50.5	1.29	.77	9.07
34–36	4.14	.021	8.90	15.60	54.6	1.33	.70	7.89
36–38	4.42	.017	9.40	14.60	55.2	1.45	.69	7.80
38–40	4.43	.018	7.60	15.20	55.8	1.15	.66	8.73
40–42	4.16	.017	8.80	13.96	55.6	1.28	.86	8.38
42–44	5.26	.038	10.40	9.50	56.6	1.36	1.05	7.38
44–46	2.31	.014	8.30	5.40	70.6	.68	.58	3.43
46–48	1.22	.015	6.80	2.00	83.8	.59	.57	1.95
48–50	4.51	.048	8.90	8.70	63.5	2.75	1.04	5.89
50–52	2.92	.023	9.90	11.00	64.5	1.63	.75	6.46
52–54	2.94	.023	8.90	19.10	52.0	2.03	.80	8.97
54–56	2.20	.019	7.30	12.90	65.2	1.58	.69	6.14
56–58	1.63	.020	8.90	16.70	58.5	1.60	.57	7.36
58–60	1.07	.015	7.80	15.60	62.5	1.47	.66	6.96
60–62	1.30	.020	9.00	21.10	52.1	2.14	.81	9.12
62–64	2.11	.021	9.80	20.26	50.8	1.77	.83	8.93
64–66	2.12	.015	8.30	18.20	57.7	1.07	.80	8.22
66–68	2.21	.017	9.40	19.10	53.6	1.00	.73	9.02
68–70	2.36	.018	9.20	17.10	55.8	1.15	.75	8.82
70–72	2.56	.019	10.60	16.60	52.5	1.45	.85	9.69
72–74	2.58	.025	10.70	14.40	56.0	1.48	.91	7.62
74–76	2.76	.022	10.50	21.00	45.9	1.80	.77	10.53
76–78	3.80	.022	9.40	22.60	45.3	1.75	.71	9.67
78–80	4.17	.019	8.70	21.10	49.0	1.53	.67	9.37
80–82	4.27	.020	8.10	23.60	46.3	1.61	.66	10.04

DDH = 1481NE			LINE 1300 NW			ELEV = 230 m	
Depth	Ni	Co	Fe	MgO	SiO_2	Al_2O_3	Cr_2O_3	LOI
(m)	(%)	(%)	(%)	(%)	(%)	(%)	(%)	(%)

Depth (m)	Ni (%)	Co (%)	Fe (%)	MgO (%)	SiO_2 (%)	Al_2O_3 (%)	Cr_2O_3 (%)	LOI (%)
0–2	.54	0.000	52.20	.70	0.0	0.00	0.00	0.00
2–4	.66	0.000	52.30	.80	0.0	0.00	0.00	0.00
4–6	.83	0.000	50.70	.70	0.0	0.00	0.00	0.00
6–8	.90	0.000	54.30	.80	0.0	0.00	0.00	0.00
8–10	.56	0.000	48.80	.90	0.0	0.00	0.00	0.00
10–12	.68	0.000	47.10	1.10	0.0	0.00	0.00	0.00
12–14	1.27	.694	41.90	1.00	4.8	0.00	0.00	0.00
14–16	1.13	.366	46.80	.80	8.4	0.00	0.00	0.00
16–18	1.12	.360	47.00	.70	6.3	0.00	0.00	0.00
18–20	1.02	.480	35.70	.90	25.2	0.00	0.00	0.00
20–22	1.22	.263	35.50	1.10	29.0	0.00	0.00	0.00
22–24	4.77	.097	20.00	11.80	37.2	3.04	1.18	9.99
24–26	5.25	.040	13.00	17.40	43.2	2.36	.98	9.76
26–28	4.00	.030	11.60	14.80	51.6	1.77	.92	9.07
28–30	3.85	.027	10.80	18.80	48.0	1.98	.81	9.71
30–32	2.85	.022	8.40	16.60	57.1	1.52	.73	8.59
32–34	2.22	.020	8.30	14.40	60.2	1.07	.89	7.35
34–36	2.27	.029	8.80	12.70	61.6	1.24	.67	6.64
36–38	1.81	.033	11.40	9.90	61.3	1.38	.99	6.66
38–40	1.63	.032	13.00	16.20	52.1	.94	.87	8.79
40–42	1.52	.023	8.60	18.50	56.9	.97	.63	8.31
42–44	.86	0.000	10.30	20.70	0.0	0.00	0.00	0.00
44–46	.39	0.000	8.00	22.40	0.0	0.00	0.00	0.00
46–48	.30	0.000	7.10	22.00	0.0	0.00	0.00	0.00
48–50	.25	0.000	6.70	22.40	0.0	0.00	0.00	0.00
50–52	.32	0.000	7.50	24.80	0.0	0.00	0.00	0.00
52–54	.32	0.000	7.10	27.30	0.0	0.00	0.00	0.00
54–56	.39	0.000	8.10	29.90	0.0	0.00	0.00	0.00

DDH = 1500NE   LINE 1300 NW   ELEV = 225 m

Depth (m)	Ni (%)	Co (%)	Fe (%)	MgO (%)	SiO_2 (%)	Al_2O_3 (%)	Cr_2O_3 (%)	LOI (%)
0-2	.63	.011	43.48	.02	6.0	19.60	0.00	12.60
2-4	.77	.009	51.98	.02	2.2	13.62	0.00	8.38
4-6	.94	.008	56.11	.03	1.4	10.40	0.00	6.56
6-8	.81	.017	53.71	.03	1.4	10.60	0.00	7.38
8-10	.82	.028	52.12	.02	1.6	11.86	0.00	7.26
10-12	.68	.040	51.96	.04	2.1	10.60	0.00	6.64
12-14	.70	.059	50.36	.04	1.9	11.74	0.00	8.30
14-16	.83	.250	46.36	.04	3.6	13.40	0.00	11.54
16-18	1.14	.350	40.92	.04	9.2	8.72	0.00	13.58
18-20	.96	.116	36.77	.05	26.0	5.52	0.00	10.86
20-22	.86	.031	31.97	.08	29.3	8.40	0.00	10.64
22-24	3.34	.107	22.22	2.70	41.8	5.25	0.00	10.44
24-26	6.05	.075	21.58	3.20	40.6	3.68	0.00	11.76
26-28	8.00	.069	20.14	4.58	36.8	4.12	0.00	12.24
28-30	5.35	.073	17.15	4.16	48.1	3.90	0.00	9.46
30-32	6.05	.051	19.32	3.97	43.4	4.38	0.00	11.06
32-34	4.05	.042	21.16	2.40	46.6	3.56	0.00	9.40
34-36	2.96	.046	30.62	3.18	32.7	3.76	0.00	10.98
36-38	3.22	.049	21.00	11.00	39.1	3.24	0.00	10.74
38-40	3.58	.051	19.00	13.70	38.2	3.38	0.00	10.76

DDH = 1502NE   LINE 1300 NW   ELEV = 224 m

Depth (m)	Ni (%)	Co (%)	Fe (%)	MgO (%)	SiO_2 (%)	Al_2O_3 (%)	Cr_2O_3 (%)	LOI (%)
0-2	.64	0.000	42.60	1.00	0.0	0.00	0.00	0.00
2-4	.95	0.000	52.30	.80	0.0	0.00	0.00	0.00
4-6	.94	0.000	55.40	.70	0.0	0.00	0.00	0.00
6-8	.87	0.000	55.80	.70	0.0	0.00	0.00	0.00
8-10	.95	0.000	52.10	1.10	0.0	0.00	0.00	0.00
10-12	.76	0.000	50.70	1.10	0.0	0.00	0.00	0.00
12-14	.72	0.000	48.10	1.00	0.0	0.00	0.00	0.00
14-16	1.31	.432	42.00	.90	6.9	0.00	0.00	0.00
16-18	1.41	.380	38.50	.80	14.2	0.00	0.00	0.00
18-20	.94	0.000	31.70	.70	0.0	0.00	0.00	0.00
20-22	1.24	.230	27.40	.70	34.6	0.00	0.00	0.00
22-24	4.85	.174	14.40	15.80	41.3	0.00	0.00	0.00
24-26	6.08	.055	12.60	16.20	43.7	0.00	0.00	0.00
26-28	5.31	.046	10.40	14.10	51.9	0.00	0.00	0.00
28-30	6.06	.042	11.60	12.20	52.1	0.00	0.00	0.00
30-32	5.42	.047	10.50	15.70	49.3	0.00	0.00	0.00
32-34	2.80	.053	10.80	16.50	46.9	0.00	0.00	0.00
34-36	2.58	.050	8.90	13.20	57.4	0.00	0.00	0.00
36-38	2.99	.060	16.10	9.20	47.4	0.00	0.00	0.00
38-40	3.23	.060	12.20	19.30	40.2	0.00	0.00	0.00
40-42	2.48	.053	10.60	26.20	39.7	0.00	0.00	0.00
42-44	2.34	.047	10.00	26.30	40.1	0.00	0.00	0.00
44-46	2.04	.048	10.50	18.40	50.8	0.00	0.00	0.00
46-48	1.80	.048	11.60	13.70	54.4	0.00	0.00	0.00
48-50	1.91	.047	10.60	20.50	46.7	0.00	0.00	0.00
50-52	1.65	.046	8.90	26.80	43.0	0.00	0.00	0.00
52-54	1.50	.044	7.20	28.80	45.2	0.00	0.00	0.00
54-56	1.59	.046	8.00	22.60	48.0	0.00	0.00	0.00
56-58	1.57	.046	8.20	20.30	52.5	0.00	0.00	0.00
58-60	1.61	.045	9.10	25.20	45.5	0.00	0.00	0.00
60-62	1.59	.045	9.00	25.30	45.3	0.00	0.00	0.00
62-64	1.63	.046	9.90	21.10	48.2	0.00	0.00	0.00
64-66	1.65	.047	10.40	20.50	46.8	0.00	0.00	0.00
66-68	1.70	.045	10.20	21.90	45.0	0.00	0.00	0.00
68-70	1.92	.048	11.90	22.20	42.3	0.00	0.00	0.00
70-72	1.65	.046	10.60	26.40	41.8	0.00	0.00	0.00
72-74	1.59	.045	10.90	21.90	44.4	0.00	0.00	0.00
74-76	1.09	.044	7.90	25.70	47.8	0.00	0.00	0.00
76-78	.68	.042	7.60	31.30	45.7	0.00	0.00	0.00
78-80	.50	.043	7.80	34.80	41.2	0.00	0.00	0.00
80-82	.97	.043	8.10	29.20	46.3	0.00	0.00	0.00
82-84	.78	.045	9.90	25.30	47.8	0.00	0.00	0.00
84-86	.66	.046	10.30	24.90	45.2	0.00	0.00	0.00
86-88	.53	.046	10.00	24.80	45.9	0.00	0.00	0.00
88-90	.77	.025	9.60	20.30	52.5	0.00	0.00	0.00
90-92	.71	.021	11.50	14.60	61.8	0.00	0.00	0.00
92-94	.97	.023	8.10	16.00	60.4	0.00	0.00	0.00

DDH = 1502NE   LINE 1300 NW   ELEV = 224 m

(Cont.)

94–96	1.70	.016	6.90	10.20	68.3	0.00	0.00	0.00
96–98	1.00	.023	10.10	17.70	54.1	0.00	0.00	0.00
98–100	1.53	.021	9.40	18.80	52.8	0.00	0.00	0.00
100–102	1.90	.021	8.90	22.70	48.7	0.00	0.00	0.00
102–104	1.77	.019	8.90	21.70	48.6	0.00	0.00	0.00
104–106	1.76	.019	8.40	21.40	50.1	0.00	0.00	0.00
106–108	1.89	.019	7.20	24.40	50.0	0.00	0.00	0.00
108–110	1.36	.016	8.30	26.40	46.0	0.00	0.00	0.00
110–112	1.34	.014	6.90	23.80	51.1	0.00	0.00	0.00
112–114	1.71	.013	6.00	18.10	60.7	0.00	0.00	0.00
114–116	1.36	.019	8.90	20.70	53.6	0.00	0.00	0.00
116–118	.92	.018	7.70	27.70	46.0	0.00	0.00	0.00
118–120	1.94	.013	7.70	23.10	52.3	0.00	0.00	0.00
120–122	1.68	.017	7.70	19.80	56.4	0.00	0.00	0.00
122–124	1.01	0.000	7.40	27.80	47.5	0.00	0.00	0.00

DDH = 1524NE   LINE 1300 NW   ELEV = 217 m

Depth (m)	Ni (%)	Co (%)	Fe (%)	MgO (%)	SiO_2 (%)	Al_2O_3 (%)	Cr_2O_3 (%)	LOI (%)
0-2	.58	0.000	40.00	.64	0.0	0.00	0.00	0.00
2-4	.58	0.000	50.00	.66	0.0	0.00	0.00	0.00
4-6	.59	0.000	51.45	.66	0.0	0.00	0.00	0.00
6-8	.91	0.000	51.31	.54	0.0	0.00	0.00	0.00
8-10	.68	0.000	51.36	.66	0.0	0.00	0.00	0.00
10-12	.78	0.000	43.53	.71	0.0	0.00	0.00	0.00
12-14	.94	0.000	51.56	.56	0.0	0.00	0.00	0.00
14-16	1.02	0.000	48.68	.68	0.0	0.00	0.00	0.00
16-18	.80	0.000	46.72	.82	0.0	0.00	0.00	0.00
18-20	.82	0.000	52.00	.65	0.0	0.00	0.00	0.00
20-22	1.32	.173	28.25	3.26	35.5	0.00	0.00	9.00
22-24	5.15	.040	13.58	7.65	53.6	0.00	0.00	7.96
24-26	3.82	.036	17.78	5.40	43.5	0.00	0.00	7.81
26-28	4.59	.030	13.18	12.67	35.3	0.00	0.00	9.27
28-30	4.65	.040	15.10	12.60	41.2	1.60	0.00	8.96
30-32	3.55	.018	10.20	17.30	49.5	0.00	0.00	9.71
32-34	3.72	.021	10.75	17.39	50.4	0.00	0.00	9.39
34-36	4.08	.017	11.48	18.99	45.5	0.00	0.00	10.77
36-38	4.05	.031	13.30	16.15	50.9	0.00	0.00	10.54
38-40	4.30	.043	16.80	17.70	36.0	0.00	0.00	10.68
40-42	3.64	.020	10.79	26.80	42.4	0.00	0.00	11.63
42-44	3.14	.015	9.15	22.70	48.8	0.00	0.00	10.41
44-46	3.11	.020	9.87	18.70	53.1	0.00	0.00	9.99
46-48	2.75	.015	7.75	21.90	53.5	0.00	0.00	9.85
48-50	1.90	.010	7.22	23.87	53.8	0.00	0.00	9.35
50-52	1.53	.010	6.87	22.19	58.7	0.00	0.00	8.56
52-54	1.42	.011	6.65	24.61	57.9	0.00	0.00	8.77
54-56	1.90	.011	8.50	20.00	56.0	0.00	0.00	9.08
56-58	1.45	.018	11.80	21.00	47.9	0.00	0.00	9.63
58-60	1.55	.015	8.91	22.66	53.0	0.00	0.00	9.60

DDH = 1549NE   LINE 1300 NW   ELEV = 210 m

Depth (m)	Ni (%)	Co (%)	Fe (%)	MgO (%)	SiO_2 (%)	Al_2O_3 (%)	Cr_2O_3 (%)	LOI (%)
0-2	.43	0.000	44.70	.90	0.0	0.00	0.00	0.00
2-4	.52	0.000	43.80	.80	0.0	0.00	0.00	0.00
4-6	.72	0.000	51.20	.90	0.0	0.00	0.00	0.00
6-8	.78	0.000	52.50	.70	0.0	0.00	0.00	0.00
8-10	.87	0.000	56.20	.60	0.0	0.00	0.00	0.00
10-12	.68	0.000	54.40	.70	0.0	0.00	0.00	0.00
12-14	.96	0.000	52.90	.70	0.0	0.00	0.00	0.00
14-16	.97	0.000	55.80	.80	0.0	0.00	0.00	0.00
16-18	.87	0.000	52.40	.90	0.0	0.00	0.00	0.00
18-20	.88	0.000	53.50	.70	0.0	0.00	0.00	0.00
20-22	.71	0.000	47.20	.90	0.0	0.00	0.00	0.00
22-24	.72	0.000	49.40	.80	0.0	0.00	0.00	0.00
24-26	1.62	0.000	38.80	1.30	12.2	9.14	4.15	0.00
26-28	1.55	0.000	31.50	.70	34.5	4.87	2.27	0.00
28-30	1.85	0.000	29.00	.90	35.7	5.45	2.50	0.00
30-32	2.88	0.000	19.00	9.70	47.8	2.40	1.41	0.00
32-34	4.53	0.000	15.50	16.70	48.9	1.62	.85	0.00
34-36	4.85	0.000	13.80	19.80	44.4	2.02	.96	0.00
36-38	5.10	0.000	24.00	7.20	32.6	5.00	1.95	0.00
38-40	4.13	0.000	29.90	3.60	26.4	6.00	2.53	0.00
40-42	2.18	0.000	31.20	3.00	30.5	4.50	2.55	0.00
42-44	5.46	0.000	19.10	11.60	47.1	3.10	1.38	0.00
44-46	5.42	0.000	14.40	15.20	46.3	1.97	1.04	0.00
46-48	4.64	0.000	13.50	14.80	0.0	0.00	0.00	0.00
48-50	6.09	0.000	9.60	18.20	46.4	1.80	.88	0.00
50-52	5.00	0.000	10.20	14.40	50.0	1.99	.82	0.00
52-54	4.78	0.000	10.80	15.20	48.8	2.07	1.06	0.00
54-56	4.60	0.000	10.00	15.70	50.2	1.23	.88	0.00
56-58	3.36	0.000	8.30	16.00	55.1	.68	.78	0.00
58-60	3.09	0.000	8.40	16.90	56.0	.65	.72	0.00
60-62	3.43	0.000	8.20	16.80	56.0	.85	.75	0.00
62-64	2.48	0.000	11.10	12.40	56.6	.66	.68	0.00
64-66	2.44	0.000	11.00	15.50	52.1	.90	.76	0.00
66-68	2.52	0.000	15.00	18.20	49.6	1.97	.90	0.00
68-70	2.82	0.000	10.70	15.70	51.4	1.98	.78	0.00
70-72	2.81	0.000	11.70	18.70	46.0	2.52	.98	0.00
72-74	2.73	0.000	10.70	17.90	48.9	1.96	.78	0.00
74-76	2.34	0.000	11.30	17.70	48.5	2.20	.88	0.00
76-78	2.71	0.000	10.70	19.60	45.7	2.35	.86	0.00
78-80	2.70	0.000	10.50	22.40	45.4	2.40	.89	0.00
80-82	3.01	0.000	10.10	20.20	47.2	2.17	.82	0.00
82-84	6.82	0.000	7.90	18.30	49.7	1.73	.65	0.00
84-86	6.27	0.000	6.30	17.90	53.6	1.23	.54	0.00
86-88	1.91	0.000	7.50	20.70	0.0	0.00	0.00	0.00
88-90	1.91	0.000	7.50	20.70	0.0	0.00	0.00	0.00
90-92	2.36	0.000	7.70	18.20	54.5	1.36	.53	0.00
92-94	.38	0.000	7.00	32.30	0.0	0.00	0.00	0.00
94-96	.28	0.000	6.10	32.90	0.0	0.00	0.00	0.00
96-98	.27	0.000	5.60	34.80	0.0	0.00	0.00	0.00

DDH = 1594NE   LINE 1300 NW   ELEV = 196 m

Depth (m)	Ni (%)	Co (%)	Fe (%)	MgO (%)	SiO_2 (%)	Al_2O_3 (%)	Cr_2O_3 (%)	LOI (%)
0-2	.31	0.000	35.42	.64	0.0	0.00	0.00	0.00
2-4	.51	0.000	39.24	.62	0.0	0.00	0.00	0.00
4-6	.68	0.000	44.53	.75	0.0	0.00	0.00	0.00
6-8	.72	0.000	48.27	.69	0.0	0.00	0.00	0.00
8-10	.84	0.000	49.76	.63	0.0	0.00	0.00	0.00
10-12	.74	0.000	48.39	.61	0.0	0.00	0.00	0.00
12-14	.89	0.000	51.00	.66	0.0	0.00	0.00	0.00
14-16	.83	0.000	51.50	.66	0.0	0.00	0.00	0.00
16-18	.91	0.000	50.66	.69	0.0	0.00	0.00	0.00
18-20	1.00	0.000	43.31	.72	0.0	0.00	0.00	0.00
20-22	.74	0.000	36.82	.63	0.0	0.00	0.00	0.00
22-24	.43	0.000	24.80	.57	0.0	0.00	0.00	0.00
24-26	.51	0.000	27.49	.57	0.0	0.00	0.00	0.00
26-28	.57	0.000	28.04	.63	0.0	0.00	0.00	0.00
28-30	.57	0.000	24.16	.57	0.0	0.00	0.00	0.00
30-32	1.21	0.000	18.29	.81	0.0	0.00	0.00	0.00
32-34	2.20	.086	23.22	1.21	47.5	0.00	0.00	7.97
34-36	.85	0.000	15.33	2.81	0.0	0.00	0.00	0.00
36-38	1.93	.043	15.91	3.92	56.7	0.00	0.00	7.22
38-40	4.03	.065	19.30	3.31	46.1	0.00	0.00	8.75
40-42	4.09	.056	18.06	6.15	45.8	0.00	0.00	8.75
42-44	4.00	.065	14.77	14.75	45.1	0.00	0.00	10.22
44-46	3.92	.068	15.17	11.50	44.6	0.00	0.00	10.53
46-48	4.23	.066	14.68	11.71	46.4	0.00	0.00	10.00
48-50	4.43	.067	17.38	10.73	40.4	0.00	0.00	11.94
50-52	2.48	.085	23.84	2.60	41.0	0.00	0.00	13.57
52-54	3.26	.045	13.31	3.00	60.0	0.00	0.00	8.99
54-56	2.88	.040	8.60	10.80	63.6	0.00	0.00	7.94
56-58	4.00	.053	9.35	17.30	54.5	0.00	0.00	9.94
58-60	3.77	.035	8.33	16.48	59.5	0.00	0.00	9.16
60-62	3.27	.034	7.22	12.18	66.7	0.00	0.00	7.46
62-64	3.13	.025	7.40	13.27	65.8	0.00	0.00	8.04
64-66	2.71	.019	6.52	14.24	65.9	0.00	0.00	6.86
66-68	2.86	.017	7.00	15.80	55.8	0.00	0.00	7.23
68-70	1.95	.012	5.77	17.60	51.6	0.00	0.00	6.49
70-72	2.94	.016	7.68	22.22	52.8	0.00	0.00	8.52
72-74	3.21	.015	8.34	24.78	46.2	0.00	0.00	9.74
74-76	1.81	.017	6.98	30.85	42.2	0.00	0.00	9.10
76-78	2.09	.014	7.07	29.51	39.0	0.00	0.00	11.70
78-80	.32	0.000	5.60	33.50	0.0	0.00	0.00	0.00
80-82	.23	0.000	5.84	36.00	0.0	0.00	0.00	0.00
82-84	.25	0.000	6.30	34.47	0.0	0.00	0.00	0.00

DDH = 1624NE   LINE 1300 NW   ELEV = 189 m

Depth (m)	Ni (%)	Co (%)	Fe (%)	MgO (%)	SiO_2 (%)	Al_2O_3 (%)	Cr_2O_3 (%)	LOI (%)
0–2	.32	.006	34.80	1.00	0.0	0.00	0.00	0.00
2–4	.44	.007	34.00	.80	0.0	0.00	0.00	0.00
4–6	.71	.009	41.30	.90	0.0	0.00	0.00	0.00
6–8	.84	.013	53.20	.90	0.0	0.00	0.00	0.00
8–10	.99	.012	57.00	.80	0.0	0.00	0.00	0.00
10–12	.92	.033	53.70	.90	0.0	0.00	0.00	0.00
12–14	1.02	.051	53.00	.90	0.0	0.00	0.00	0.00
14–16	.95	.093	52.10	1.10	0.0	0.00	0.00	0.00
16–18	.77	.037	53.40	1.10	0.0	0.00	0.00	0.00
18–20	.92	.064	41.90	1.30	0.0	0.00	0.00	0.00
20–22	1.12	.120	49.00	1.10	0.0	0.00	0.00	0.00
22–24	.82	.076	46.40	1.30	0.0	0.00	0.00	0.00
24–26	.81	.128	43.90	1.10	0.0	0.00	0.00	0.00
26–28	1.10	.337	42.30	1.00	0.0	0.00	0.00	0.00
28–30	.86	.189	42.30	1.00	0.0	0.00	0.00	0.00
30–32	1.03	.271	40.90	1.10	0.0	0.00	0.00	0.00
32–34	1.84	.212	37.10	1.40	22.2	5.60	2.49	0.00
34–36	1.68	.112	18.90	1.40	56.5	2.54	1.85	0.00
36–38	4.81	.131	18.50	3.40	51.7	1.47	1.47	0.00
38–40	2.57	.062	16.50	1.60	59.8	1.29	1.26	0.00
40–42	4.31	.063	17.00	2.10	54.9	1.67	1.31	0.00
42–44	4.56	.074	19.00	3.40	46.4	2.84	1.29	0.00
44–46	3.77	.047	15.00	3.50	56.5	2.42	1.21	0.00
46–48	4.81	.052	23.40	3.70	38.9	2.66	1.87	0.00
48–50	2.58	.051	17.40	2.20	54.3	1.50	1.57	0.00
50–52	1.50	.085	17.10	2.50	54.7	1.99	1.35	0.00
52–54	1.06	.058	11.50	1.50	66.9	1.16	1.36	0.00
54–56	2.14	.079	19.00	3.10	49.5	1.75	1.84	0.00
56–58	4.58	.096	17.50	10.10	41.5	3.06	1.67	0.00
58–60	1.92	.087	15.00	13.00	58.3	1.91	1.06	0.00
60–62	1.85	.107	15.00	7.00	53.8	1.12	1.15	0.00
62–64	2.10	.084	12.70	11.90	53.9	1.05	.77	0.00
64–66	2.67	.065	11.00	16.90	52.2	.97	.75	0.00
66–68	3.23	.046	10.60	15.40	52.1	1.85	1.04	0.00
68–70	3.75	.044	11.40	13.70	52.4	2.17	.96	0.00
70–72	3.86	.019	7.60	19.80	52.5	1.43	.70	0.00
72–74	2.22	.037	10.50	21.20	48.0	1.71	.85	0.00
74–76	2.30	.035	11.10	20.30	47.8	1.81	.86	0.00
76–78	.50	.017	6.90	29.80	0.0	0.00	0.00	0.00
78–80	.32	.017	8.40	30.90	0.0	0.00	0.00	0.00
80–82	.29	.018	8.20	33.50	0.0	0.00	0.00	0.00
82–84	.19	.008	6.30	36.20	0.0	0.00	0.00	0.00

DDH = 1639NE   LINE 1300 NW   ELEV = 185 m

Depth (m)	Ni (%)	Co (%)	Fe (%)	MgO (%)	SiO_2 (%)	Al_2O_3 (%)	Cr_2O_3 (%)	LOI (%)
0-2	.26	0.000	35.75	.26	0.0	0.00	0.00	0.00
2-4	.41	0.000	32.30	.33	0.0	0.00	0.00	0.00
4-6	.52	0.000	37.78	.41	0.0	0.00	0.00	0.00
6-8	.61	0.000	46.12	.51	0.0	0.00	0.00	0.00
8-10	.72	0.000	48.29	.72	0.0	0.00	0.00	0.00
10-12	.80	0.000	53.48	.48	0.0	0.00	0.00	0.00
12-14	.76	0.000	51.90	.72	0.0	0.00	0.00	0.00
14-16	.98	0.000	54.53	.49	0.0	0.00	0.00	0.00
16-18	1.17	0.000	51.15	.67	0.0	0.00	0.00	0.00
18-20	.90	0.000	49.05	.69	0.0	0.00	0.00	0.00
20-22	.87	0.000	48.82	.54	0.0	0.00	0.00	0.00
22-24	.87	0.000	48.82	.54	0.0	0.00	0.00	0.00
24-26	.59	0.000	26.96	.30	0.0	0.00	0.00	0.00
26-28	.50	0.000	26.89	.36	0.0	0.00	0.00	0.00
28-30	.76	0.000	34.85	.60	28.7	0.00	0.00	0.00
30-32	1.40	0.000	31.17	.64	35.5	0.00	0.00	0.00
32-34	4.60	0.000	20.20	7.54	41.6	0.00	0.00	0.00
34-36	4.94	0.000	15.32	12.92	43.2	0.00	0.00	0.00
36-38	5.86	0.000	14.12	10.29	47.4	0.00	0.00	0.00
38-40	5.79	0.000	14.05	9.79	48.2	0.00	0.00	0.00
40-42	3.01	0.000	12.99	4.74	56.6	0.00	0.00	0.00
42-44	2.31	0.000	14.87	2.48	60.2	0.00	0.00	0.00
44-46	1.86	0.000	26.06	2.56	58.5	0.00	0.00	0.00
46-48	3.31	0.000	22.08	2.56	36.1	0.00	0.00	0.00
48-50	2.17	0.000	20.73	1.99	45.5	0.00	0.00	0.00
50-52	1.71	0.000	20.28	2.07	48.0	0.00	0.00	0.00
52-54	1.60	0.000	18.85	3.85	48.1	0.00	0.00	0.00
54-56	1.42	0.000	9.01	1.74	48.6	0.00	0.00	0.00
56-58	1.14	0.000	8.78	.60	70.8	0.00	0.00	0.00
58-60	1.03	0.000	11.91	.96	67.2	0.00	0.00	0.00
60-62	1.69	0.000	12.24	2.37	62.7	0.00	0.00	0.00
62-64	3.99	0.000	8.94	9.47	56.2	0.00	0.00	0.00
64-66	3.60	0.000	9.39	13.10	57.8	0.00	0.00	0.00
66-68	4.31	0.000	10.74	15.60	52.8	0.00	0.00	0.00
68-70	3.74	0.000	11.27	19.18	47.9	0.00	0.00	0.00
70-72	2.48	0.000	12.62	14.13	54.0	0.00	0.00	0.00
72-74	1.34	0.000	10.36	13.10	53.2	0.00	0.00	0.00
74-76	.50	0.000	8.94	24.64	48.6	0.00	0.00	0.00
76-78	.37	0.000	8.23	29.89	0.0	0.00	0.00	0.00
78-80	.40	0.000	9.03	25.32	0.0	0.00	0.00	0.00
80-82	.45	0.000	9.93	24.19	0.0	0.00	0.00	0.00

DDH = 1655NE   LINE 1300 NW   ELEV = 182 m

Depth (m)	Ni (%)	Co (%)	Fe (%)	MgO (%)	SiO_2 (%)	Al_2O_3 (%)	Cr_2O_3 (%)	LOI (%)
0-2	.37	.011	35.30	.90	0.0	0.00	0.00	0.00
2-4	.73	.016	35.00	.80	0.0	0.00	0.00	0.00
4-6	.90	.028	48.30	.80	0.0	0.00	0.00	0.00
6-8	.92	.028	51.10	.80	0.0	0.00	0.00	0.00
8-10	.80	.025	53.40	.80	0.0	0.00	0.00	0.00
10-12	.94	.058	53.00	.80	0.0	0.00	0.00	0.00
12-14	.89	.052	51.70	.80	0.0	0.00	0.00	0.00
14-16	.90	.038	50.60	.80	0.0	0.00	0.00	0.00
16-18	.59	.040	50.40	.80	0.0	0.00	0.00	0.00
18-20	.70	.270	40.50	.70	0.0	0.00	0.00	0.00
20-22	.65	.112	27.50	.60	0.0	0.00	0.00	0.00
22-24	.60	.174	24.80	1.50	0.0	0.00	0.00	0.00
24-26	.47	.197	22.10	.90	0.0	0.00	0.00	0.00
26-28	.69	.202	31.30	1.00	0.0	0.00	0.00	0.00
28-30	.71	.081	26.00	1.20	0.0	0.00	0.00	0.00
30-32	6.47	.089	18.50	4.70	42.2	3.81	1.53	0.00
32-34	5.07	.052	14.10	7.90	48.6	2.44	1.01	0.00
34-36	4.93	.027	11.50	10.50	52.0	1.67	.82	0.00
36-38	5.67	.021	10.60	10.50	53.4	1.52	.69	0.00
38-40	4.58	.025	11.80	13.20	47.5	1.75	.90	0.00
40-42	3.45	.035	13.70	7.10	52.3	1.66	1.06	0.00
42-44	3.78	.024	12.10	8.80	54.1	1.10	1.02	0.00
44-46	4.52	.031	12.80	6.80	53.5	1.03	.96	0.00
46-48	4.64	.023	10.40	7.20	57.6	1.22	.87	0.00
48-50	4.20	.029	12.10	6.70	55.3	1.00	.95	0.00
50-52	2.81	.041	15.60	12.00	48.2	2.24	1.55	0.00
52-54	3.79	.038	14.10	10.60	54.0	1.58	1.45	0.00
54-56	4.02	.048	11.80	7.40	57.2	1.34	1.26	0.00
56-58	2.26	.059	10.30	4.70	67.5	1.10	1.10	0.00
58-60	1.09	.059	6.20	1.60	76.9	.54	.67	0.00
60-62	1.25	.028	9.00	2.10	75.4	.67	1.03	0.00
62-64	1.51	.016	2.80	1.70	85.5	.34	.92	0.00
64-66	2.77	.032	3.80	3.00	78.4	.66	1.14	0.00
66-68	3.88	.046	8.50	19.90	51.9	1.25	.86	0.00
68-70	3.77	.022	6.60	20.60	56.8	.75	.59	0.00
70-72	3.79	.019	7.70	22.50	50.2	1.21	.62	0.00
72-74	.85	.013	7.30	25.90	0.0	0.00	0.00	0.00
74-76	.39	.015	5.60	30.00	0.0	0.00	0.00	0.00
76-78	.43	.011	6.10	32.70	0.0	0.00	0.00	0.00
78-80	.66	.022	6.90	34.60	0.0	0.00	0.00	0.00

DDH = 1670NE   LINE 1300 NW   ELEV = 180 m

Depth (m)	Ni (%)	Co (%)	Fe (%)	MgO (%)	SiO_2 (%)	Al_2O_3 (%)	Cr_2O_3 (%)	LOI (%)
0-2	.44	0.000	33.70	1.00	0.0	0.00	0.00	0.00
2-4	.61	0.000	32.80	.80	0.0	0.00	0.00	0.00
4-6	.91	0.000	42.70	1.00	0.0	0.00	0.00	0.00
6-8	.86	0.000	49.50	.90	0.0	0.00	0.00	0.00
8-10	.91	0.000	45.50	1.00	0.0	0.00	0.00	0.00
10-12	.89	0.000	51.60	.80	0.0	0.00	0.00	0.00
12-14	.83	0.000	49.50	1.10	0.0	0.00	0.00	0.00
14-16	.89	0.000	48.10	1.10	0.0	0.00	0.00	0.00
16-18	.69	0.000	44.30	1.00	0.0	0.00	0.00	0.00
18-20	.60	0.000	35.40	.90	0.0	0.00	0.00	0.00
20-22	.69	0.000	32.90	1.00	0.0	0.00	0.00	0.00
22-24	.47	0.000	24.20	.90	0.0	0.00	0.00	0.00
24-26	.53	0.000	27.10	.70	0.0	0.00	0.00	0.00
26-28	.56	0.000	25.80	.80	0.0	0.00	0.00	0.00
28-30	.68	0.000	32.80	.80	0.0	0.00	0.00	0.00
30-32	.50	0.000	18.90	.90	0.0	0.00	0.00	0.00
32-34	1.42	.186	11.00	1.00	0.0	0.00	0.00	0.00
34-36	2.79	.061	11.80	1.50	69.1	.90	.83	5.02
36-38	6.19	.053	13.00	7.30	55.9	1.80	1.05	6.79
38-40	5.12	.057	13.80	13.00	46.6	2.33	1.14	10.45
40-42	4.51	.055	16.00	11.40	46.8	2.25	1.92	10.91
42-44	3.44	.069	24.90	4.40	38.8	2.40	3.35	10.72
44-46	4.00	.064	16.30	5.00	57.5	1.12	1.36	8.09
46-48	4.00	.042	12.30	5.80	63.3	.85	1.02	7.35
48-50	3.56	.040	13.20	2.70	65.0	1.26	1.35	5.50
50-52	5.49	.057	13.60	9.10	52.1	1.44	1.54	8.61
52-54	7.61	.048	11.80	10.20	51.4	2.06	1.20	8.05
54-56	7.38	.047	12.90	13.40	46.0	1.65	1.11	9.80
56-58	5.33	.055	12.70	15.00	46.7	1.96	1.40	8.85
58-60	2.63	.046	12.30	23.50	45.2	1.14	.85	10.87
60-62	5.72	.047	10.70	14.70	53.6	.86	.97	8.92
62-64	2.40	.030	10.30	23.90	50.5	.54	.65	10.43
64-66	.43	.023	6.80	29.20	51.2	.38	.47	10.34
66-68	.34	.029	6.90	33.30	44.5	.51	.64	10.74
68-70	2.18	.023	5.80	31.10	43.5	.60	.49	11.62
70-72	.35	0.000	7.20	31.40	0.0	0.00	0.00	0.00
72-74	.28	0.000	5.80	33.80	0.0	0.00	0.00	0.00
74-76	.35	0.000	8.10	28.00	0.0	0.00	0.00	0.00
76-78	.40	0.000	10.80	25.00	0.0	0.00	0.00	0.00
78-80	.44	0.000	9.90	17.60	0.0	0.00	0.00	0.00

DDH = 1690NE   LINE 1300 NW   ELEV = 180 m

Depth (m)	Ni (%)	Co (%)	Fe (%)	MgO (%)	SiO_2 (%)	Al_2O_3 (%)	Cr_2O_3 (%)	LOI (%)
0–2	.49	0.000	33.46	.52	0.0	0.00	0.00	0.00
2–4	.49	0.000	35.64	.49	0.0	0.00	0.00	0.00
4–6	.80	0.000	50.60	.62	0.0	0.00	0.00	0.00
6–8	.81	0.000	51.13	.62	0.0	0.00	0.00	0.00
8–10	.84	0.000	49.02	.62	0.0	0.00	0.00	0.00
10–12	.41	0.000	45.41	.63	0.0	0.00	0.00	0.00
12–14	.93	0.000	33.31	.60	0.0	0.00	0.00	0.00
14–16	.71	0.000	28.50	.93	0.0	0.00	0.00	0.00
16–18	.95	0.000	21.50	1.12	0.0	0.00	0.00	0.00
18–20	1.27	0.000	24.06	.57	0.0	0.00	0.00	0.00
20–22	.99	0.000	21.35	.61	0.0	0.00	0.00	0.00
22–24	2.14	0.000	17.90	5.12	50.7	0.00	0.00	0.00
24–26	4.13	0.000	13.04	13.56	47.7	0.00	0.00	0.00
26–28	3.59	0.000	15.19	12.90	46.6	0.00	0.00	0.00
28–30	3.15	0.000	13.07	8.88	53.2	0.00	0.00	0.00
30–32	2.74	0.000	16.45	13.34	44.0	0.00	0.00	0.00
32–34	3.28	0.000	16.37	13.41	44.5	0.00	0.00	0.00
34–36	2.96	0.000	14.57	13.10	48.7	0.00	0.00	0.00
36–38	3.84	0.000	12.69	9.96	53.9	0.00	0.00	0.00
38–40	4.01	0.000	10.52	14.45	52.7	0.00	0.00	0.00
40–42	2.18	0.000	13.74	8.57	54.4	0.00	0.00	0.00
42–44	3.17	0.000	9.69	9.03	63.4	0.00	0.00	0.00
44–46	4.74	0.000	9.61	9.89	59.5	0.00	0.00	0.00
46–48	5.39	0.000	8.56	10.12	59.4	0.00	0.00	0.00
48–50	5.98	0.000	10.06	11.62	53.4	0.00	0.00	0.00
50–52	5.67	0.000	10.82	15.15	49.5	0.00	0.00	0.00
52–54	4.48	0.000	10.52	17.06	50.2	0.00	0.00	0.00
54–56	4.31	0.000	7.36	13.57	59.1	0.00	0.00	0.00
56–58	4.01	0.000	6.76	9.61	68.7	0.00	0.00	0.00
58–60	4.31	0.000	6.53	9.61	69.3	0.00	0.00	0.00
60–62	4.55	0.000	7.10	13.97	58.2	0.00	0.00	0.00
62–64	5.98	0.000	10.21	14.36	50.0	0.00	0.00	0.00
64–66	8.03	0.000	9.31	13.34	50.6	0.00	0.00	0.00
66–68	6.42	0.000	10.44	13.10	54.0	0.00	0.00	0.00
68–70	4.07	0.000	13.22	7.84	54.7	0.00	0.00	0.00

DDH = 1710NE   LINE 1300 NW   ELEV = 178 m

Depth (m)	Ni (%)	Co (%)	Fe (%)	MgO (%)	SiO_2 (%)	Al_2O_3 (%)	Cr_2O_3 (%)	LOI (%)
0-2	.33	.011	33.60	.80	0.0	0.00	0.00	0.00
2-4	.57	.014	43.70	.90	0.0	0.00	0.00	0.00
4-6	.84	.013	52.10	.90	0.0	0.00	0.00	0.00
6-8	.80	.019	52.90	.90	0.0	0.00	0.00	0.00
8-10	.56	.042	49.30	1.10	0.0	0.00	0.00	0.00
10-12	.26	.043	49.30	.70	0.0	0.00	0.00	0.00
12-14	.40	.097	34.70	.70	0.0	0.00	0.00	0.00
14-16	.42	.087	27.20	.70	0.0	0.00	0.00	0.00
16-18	.60	.064	31.60	.80	0.0	0.00	0.00	0.00
18-20	.63	.197	33.20	.70	0.0	0.00	0.00	0.00
20-22	.68	.206	23.50	.90	0.0	0.00	0.00	0.00
22-24	.93	.186	28.70	1.90	0.0	0.00	0.00	0.00
24-26	1.51	.079	19.00	3.10	54.9	1.51	1.38	5.33
26-28	2.11	.051	13.80	6.40	57.8	1.60	1.39	5.82
28-30	4.27	.052	16.20	14.40	39.0	2.97	1.30	10.34
30-32	3.42	.034	14.70	15.90	43.5	2.52	1.01	9.59
32-34	3.08	.032	14.50	16.40	43.8	2.68	.95	9.62
34-36	4.67	.032	12.30	13.70	48.2	1.83	.92	7.60
36-38	3.61	.030	13.20	11.40	51.4	1.49	1.03	7.61
38-40	3.00	.036	11.50	9.80	55.9	1.11	.95	6.34
40-42	2.78	.036	11.30	8.60	59.6	.78	.87	5.97
42-44	2.02	.028	15.50	7.70	62.2	.65	.92	5.57
44-46	2.69	.034	15.80	8.70	54.6	1.21	.97	7.82
46-48	3.94	.020	9.70	8.70	62.8	.85	.83	5.55
48-50	4.06	.024	10.20	14.50	54.5	.86	.73	6.73
50-52	2.95	.021	8.60	20.70	51.9	.69	.66	8.24
52-54	1.40	.019	10.30	27.10	46.3	.79	.62	7.74
54-56	1.51	.022	10.80	24.10	47.4	1.49	.71	8.09
56-58	1.99	.018	9.80	16.40	60.4	.92	.55	6.05
58-60	.91	.017	5.80	16.20	63.0	.77	.45	6.72
60-62	.84	.017	7.00	22.20	54.3	.94	.54	7.94
62-64	.49	.017	6.00	25.20	53.0	.43	.44	9.13
64-66	1.31	.018	6.80	27.00	48.4	.45	.44	9.26
66-68	1.41	.016	6.10	25.60	51.7	.66	.46	8.60
68-70	3.86	.018	6.70	18.70	54.3	1.17	.53	8.08
70-72	1.02	.029	8.00	29.20	45.2	1.43	.62	8.12
72-74	2.22	.017	7.20	27.70	46.8	1.28	.56	7.94
74-76	2.63	.020	7.70	27.70	47.0	1.00	.51	7.25
76-78	2.43	.017	6.50	28.80	46.8	.84	.49	7.68

DDH = 1738NE   LINE 1300 NW   ELEV = 175 m

Depth (m)	Ni (%)	Co (%)	Fe (%)	MgO (%)	SiO_2 (%)	Al_2O_3 (%)	Cr_2O_3 (%)	LOI (%)
0-2	.61	.008	46.64	.68	0.0	0.00	0.00	0.00
2-4	.79	0.000	51.58	.66	0.0	0.00	0.00	0.00
4-6	.53	.025	46.22	.72	0.0	0.00	0.00	0.00
6-8	.54	.078	46.49	.66	0.0	0.00	0.00	0.00
8-10	1.09	.325	42.34	.72	0.0	0.00	0.00	0.00
10-12	1.29	0.000	37.06	.67	0.0	0.00	0.00	0.00
12-14	1.18	.158	38.39	.69	0.0	0.00	0.00	0.00
14-16	.78	.065	22.26	.59	0.0	0.00	0.00	0.00
16-18	1.39	.275	22.63	.66	0.0	0.00	0.00	0.00
18-20	4.84	.069	21.04	9.73	38.7	0.00	0.00	9.03
20-22	5.34	.049	13.78	6.00	58.4	0.00	0.00	6.08
22-24	3.43	.045	14.63	14.42	46.6	0.00	0.00	10.46
24-26	4.19	.053	15.36	13.71	43.0	0.00	0.00	11.96
26-28	2.50	.062	9.57	5.73	68.9	0.00	0.00	6.01
28-30	3.37	.085	13.60	6.70	55.4	0.00	0.00	7.10
30-32	4.95	.043	11.51	7.52	57.8	0.00	0.00	6.34
32-34	4.14	.032	8.23	6.16	72.8	0.00	0.00	4.90
34-36	3.87	.035	10.02	6.89	67.7	0.00	0.00	5.40
36-38	3.72	.030	8.31	9.72	67.6	0.00	0.00	6.06
38-40	2.60	.032	10.14	12.55	58.7	0.00	0.00	6.62
40-42	3.65	.022	6.76	9.27	71.5	0.00	0.00	5.34
42-44	3.93	.027	10.00	15.31	57.8	0.00	0.00	7.09
44-46	1.33	.015	9.20	25.71	0.0	0.00	0.00	0.00
46-48	.31	.011	6.60	32.90	0.0	0.00	0.00	0.00
48-50	.68	.011	7.22	33.19	0.0	0.00	0.00	0.00

DDH = 1767NE   LINE 1300 NW   ELEV = 167 m

Depth (m)	Ni (%)	Co (%)	Fe (%)	MgO (%)	SiO_2 (%)	Al_2O_3 (%)	Cr_2O_3 (%)	LOI (%)
0-2	.38	.012	31.30	1.10	0.0	0.00	0.00	0.00
2-4	.69	.016	35.00	.80	0.0	0.00	0.00	0.00
4-6	.74	.010	41.20	1.00	0.0	0.00	0.00	0.00
6-8	.81	.015	47.40	.90	0.0	0.00	0.00	0.00
8-10	1.00	.027	52.20	.90	0.0	0.00	0.00	0.00
10-12	1.20	.056	52.00	.90	0.0	0.00	0.00	0.00
12-14	1.15	.068	51.00	.90	0.0	0.00	0.00	0.00
14-16	1.41	.097	50.50	1.10	0.0	0.00	0.00	0.00
16-18	1.46	.130	50.30	1.30	0.0	0.00	0.00	0.00
18-20	1.35	.158	51.40	1.40	0.0	0.00	0.00	0.00
20-22	1.28	.062	49.90	1.30	0.0	0.00	0.00	0.00
22-24	1.75	.198	51.00	1.30	7.3	7.72	3.14	0.00
24-26	1.81	.317	41.00	1.50	12.9	7.59	3.28	0.00
26-28	1.41	.166	23.10	1.30	41.7	3.93	1.90	0.00
28-30	.65	.063	11.20	1.00	65.4	1.57	1.39	0.00
30-32	2.40	.070	15.30	2.60	56.3	1.22	1.36	0.00
32-34	2.95	.049	12.40	5.00	60.5	1.00	1.12	0.00
34-36	4.37	.041	11.50	6.60	59.2	1.08	.99	0.00
36-38	4.35	.041	11.90	7.60	57.6	1.14	1.04	0.00
38-40	4.36	.032	9.30	9.40	60.7	1.33	.72	0.00
40-42	4.87	.037	11.50	13.70	49.9	2.01	1.36	0.00
42-44	4.82	.037	11.10	14.40	51.1	1.99	1.11	0.00
44-46	3.14	.028	8.00	14.60	59.7	1.23	.73	0.00
46-48	3.29	.037	10.10	17.00	51.8	1.64	1.03	0.00
48-50	4.75	.033	8.70	16.50	52.8	2.14	.96	0.00
50-52	2.37	.022	8.70	21.70	50.4	1.76	.76	0.00
52-54	.58	.027	8.90	29.40	0.0	0.00	0.00	0.00
54-56	.38	.018	7.40	32.50	0.0	0.00	0.00	0.00
56-58	.28	.015	6.80	34.60	0.0	0.00	0.00	0.00

DDH = 1813NE   LINE 1300 NW   ELEV = 158 m

Depth (m)	Ni (%)	Co (%)	Fe (%)	MgO (%)	SiO_2 (%)	Al_2O_3 (%)	Cr_2O_3 (%)	LOI (%)
0-2	.30	0.000	30.30	.80	0.0	0.00	0.00	0.00
2-4	.49	0.000	34.30	.40	0.0	0.00	0.00	0.00
4-6	.69	0.000	38.90	.50	0.0	0.00	0.00	0.00
6-8	.72	0.000	41.70	.50	0.0	0.00	0.00	0.00
8-10	1.01	0.000	48.10	.60	0.0	0.00	0.00	0.00
10-12	1.38	0.000	50.90	.40	0.0	0.00	0.00	0.00
12-14	1.52	.099	52.60	.60	4.6	8.21	2.44	6.07
14-16	1.56	.076	53.30	.70	4.3	7.24	2.47	6.85
16-18	1.86	.132	49.90	.60	4.0	9.02	2.69	8.51
18-20	1.70	.107	53.50	.50	4.0	6.66	2.71	6.72
20-22	1.75	.066	54.2	.50	4.1	6.49	2.75	5.27
22-24	1.50	.104	49.70	.70	5.6	7.75	2.74	8.02
24-26	1.43	.110	48.70	.60	6.6	6.87	3.33	8.45
26-28	1.59	.090	51.70	.60	6.9	7.43	3.32	4.45
28-30	1.70	.154	45.50	.70	9.6	7.03	4.28	8.82
30-32	1.49	.222	37.50	.90	18.0	6.80	3.11	11.08
32-34	1.42	0.000	29.80	1.30	33.5	5.29	2.19	9.59
34-36	1.52	.171	29.60	1.40	31.4	5.74	2.30	9.63
36-38	1.43	.123	28.90	1.50	33.5	5.19	2.45	9.24
38-40	2.02	.298	30.40	1.80	29.8	5.54	2.34	10.28
40-42	1.92	.291	27.70	1.80	37.4	4.45	1.92	9.29
42-44	1.53	.144	22.50	1.50	49.7	2.05	1.82	8.31
44-46	1.21	.106	18.20	1.40	59.1	1.46	1.32	7.17
46-48	1.28	.081	18.20	1.80	59.2	1.56	1.28	6.47
48-50	4.06	.046	14.50	7.90	53.8	2.33	1.11	7.14
50-52	4.66	.041	15.00	10.80	48.5	2.31	1.02	8.25
52-54	4.60	.037	14.30	10.90	51.7	1.17	1.02	8.43
54-56	3.96	.030	11.20	12.20	55.4	.87	.88	8.22
56-58	5.12	.031	9.50	17.80	50.0	.92	1.03	8.88
58-60	5.16	.056	8.50	19.30	47.7	.77	.83	9.36
60-62	4.88	.057	9.00	19.60	48.8	1.00	.76	9.67
62-64	5.11	.054	9.10	18.80	48.9	1.66	.76	9.30
64-66	4.95	.020	8.80	20.00	49.0	1.42	.82	9.61
66-68	4.29	.021	8.90	23.30	46.7	1.27	.70	9.68
68-70	2.03	.019	8.40	26.00	48.0	.90	.61	9.80
70-72	5.10	.027	8.40	22.10	50.0	.70	.73	9.51
72-74	4.40	.025	7.90	21.40	52.3	.70	.79	9.47
74-76	3.46	.028	9.70	19.00	54.0	.94	.75	8.90
76-78	2.28	.026	9.80	28.30	46.0	1.08	.67	9.01
78-80	4.39	.021	8.40	20.80	52.0	.83	.68	9.65
80-82	6.00	.024	8.29	23.30	47.0	1.47	.70	10.04
82-84	.59	0.000	7.10	35.40	43.4	1.30	.52	11.90
84-86	.31	0.000	6.10	37.80	0.0	0.00	0.00	0.00

DDH = 1850NE			LINE 1300 NW			ELEV = 155 m		
Depth	Ni	Co	Fe	MgO	SiO_2	Al_2O_3	Cr_2O_3	LOI
(m)	(%)	(%)	(%)	(%)	(%)	(%)	(%)	(%)
0–2	.27	.011	36.00	.90	0.0	0.00	0.00	0.00
2–4	.47	.017	38.10	.80	0.0	0.00	0.00	0.00
4–6	.64	.018	41.10	.70	0.0	0.00	0.00	0.00
6–8	.64	.018	42.70	1.00	0.0	0.00	0.00	0.00
8–10	.83	.019	48.00	.80	0.0	0.00	0.00	0.00
10–12	1.20	.020	47.40	.90	0.0	0.00	0.00	0.00
12–14	1.30	.030	50.90	.90	0.0	0.00	0.00	0.00
14–16	1.11	.045	51.80	.20	0.0	0.00	0.00	0.00
16–18	1.48	.099	50.40	.60	0.0	0.00	0.00	0.00
18–20	1.32	.104	51.00	.80	0.0	0.00	0.00	0.00
20–22	1.63	.088	49.90	.70	3.2	8.90	2.71	9.02
22–24	1.61	.128	46.90	.90	4.0	10.40	3.45	9.42
24–26	1.48	.078	51.70	.90	4.4	8.02	2.68	6.90
26–28	1.49	.109	49.20	.30	6.6	9.92	2.59	6.51
28–30	1.25	.125	46.60	.70	12.3	7.87	2.85	6.48
30–32	1.28	.162	28.20	1.00	36.1	3.93	1.83	9.31
32–34	1.88	.258	22.50	1.20	44.3	2.88	1.63	7.83
34–36	3.10	.133	17.70	5.60	47.7	1.80	1.28	7.70
36–38	4.33	.053	15.60	13.40	47.5	1.92	.89	8.43
38–40	4.70	.036	12.70	14.80	47.2	1.91	.86	9.00
40–42	5.79	.035	10.60	17.40	46.0	1.85	1.03	9.36
42–44	5.60	.049	10.00	18.20	45.4	1.84	1.15	10.06
44–46	6.00	.047	9.70	18.10	47.0	1.71	.82	9.47
46–48	4.63	.028	9.20	16.80	52.0	.95	.66	8.65
48–50	4.83	.035	9.00	15.20	52.4	.74	.70	8.24
50–52	4.65	.027	8.80	16.70	53.1	.74	.68	8.23
52–54	4.49	.026	8.70	18.50	50.6	.68	.65	9.04
54–56	3.99	.032	10.00	16.70	50.5	.91	.97	8.50
56–58	3.35	.028	9.40	12.70	54.5	.76	.68	7.93
58–60	4.21	.033	9.40	16.70	51.7	.87	.79	9.17
60–62	4.43	.033	10.00	15.80	49.4	.86	.75	9.57
62–64	3.84	.022	8.70	14.80	55.8	.84	.67	8.32
64–66	4.33	.029	9.80	16.30	51.1	.82	.83	9.01
66–68	4.22	.023	10.40	17.20	48.5	1.07	.74	9.39
68–70	4.35	.029	9.80	18.60	49.2	1.74	.77	9.49
70–72	4.41	.032	9.50	20.10	47.7	2.12	.80	9.25
72–74	4.49	.030	10.00	18.40	45.6	2.13	.82	10.37
74–76	3.82	.025	10.30	19.90	45.4	2.23	.79	10.25
76–78	2.20	.020	9.90	25.10	45.1	1.82	.63	9.56
78–80	2.06	.030	10.60	20.30	48.1	2.12	.75	9.90
80–82	1.36	.026	8.80	24.30	48.3	1.07	.56	8.95
82–84	1.97	.027	9.10	17.90	53.2	.83	.65	8.79
84–86	2.35	.022	9.10	17.50	53.3	.72	.58	8.69
86–88	2.43	.024	9.30	20.70	49.9	.73	.65	9.26
88–90	2.33	.025	9.50	16.80	52.7	.79	.81	9.35
90–92	1.86	.030	9.00	17.80	53.3	1.14	.69	9.45
92–94	1.75	.024	7.70	20.60	53.7	1.34	.63	8.48
94–96	.70	.023	7.00	35.20	0.0	0.00	0.00	0.00
96–98	.28	.020	6.40	35.30	0.0	0.00	0.00	0.00

DDH = 1884NE   LINE 1300 NW   ELEV = 154 m

Depth (m)	Ni (%)	Co (%)	Fe (%)	MgO (%)	SiO$_2$ (%)	Al$_2$O$_3$ (%)	Cr$_2$O$_3$ (%)	LOI (%)
0-2	.29	0.000	35.73	.38	0.0	0.00	0.00	0.00
2-4	.64	0.000	41.40	.49	0.0	0.00	0.00	0.00
4-6	.81	0.000	53.52	.47	0.0	0.00	0.00	0.00
6-8	.84	0.000	55.11	.47	0.0	0.00	0.00	0.00
8-10	.92	0.000	53.82	.51	0.0	0.00	0.00	0.00
10-12	.88	0.000	54.11	.49	0.0	0.00	0.00	0.00
12-14	.86	0.000	53.09	.43	0.0	0.00	0.00	0.00
14-16	.97	0.000	51.17	.50	0.0	0.00	0.00	0.00
16-18	.88	0.000	47.14	.68	0.0	0.00	0.00	0.00
18-20	.88	0.000	36.35	.64	0.0	0.00	0.00	0.00
20-22	3.71	.116	17.97	10.26	44.1	0.00	0.00	13.08
22-24	4.67	.080	16.03	13.63	43.3	0.00	0.00	12.96
24-26	4.83	.061	14.56	13.61	42.4	0.00	0.00	11.85
26-28	5.23	.055	14.70	14.72	40.8	0.00	0.00	11.79
28-30	5.33	.053	13.84	14.14	43.6	0.00	0.00	10.59
30-32	4.34	.052	13.69	11.47	52.1	0.00	0.00	9.42
32-34	4.37	.053	14.46	13.72	41.6	0.00	0.00	10.15
34-36	4.47	.051	16.54	12.46	41.9	0.00	0.00	10.16
36-38	3.67	.063	17.57	11.68	43.1	0.00	0.00	10.38
38-40	4.66	.058	17.11	12.55	41.6	0.00	0.00	9.79
40-42	4.71	.078	18.53	8.52	42.5	0.00	0.00	9.49
42-44	4.81	.066	17.07	9.11	44.9	0.00	0.00	8.63
44-46	3.62	.040	12.13	9.84	58.5	0.00	0.00	7.43
46-48	3.83	.056	14.60	8.44	53.9	0.00	0.00	8.27
48-50	4.19	.042	14.08	11.52	48.7	0.00	0.00	9.24
50-52	4.48	.040	14.04	12.72	49.1	0.00	0.00	8.87
52-54	4.07	.028	13.27	17.36	43.9	0.00	0.00	10.29
54-56	4.04	.025	12.10	18.40	42.3	0.00	0.00	9.72
56-58	3.71	.022	13.20	15.50	49.1	0.00	0.00	9.33
58-60	3.77	.030	12.98	14.76	48.4	0.00	0.00	9.95
60-62	4.87	.026	9.66	19.11	46.4	0.00	0.00	9.55
62-64	3.94	.024	12.05	20.80	43.2	0.00	0.00	10.42
64-66	4.38	.031	12.00	20.45	42.2	0.00	0.00	10.33
66-68	4.25	.024	9.85	21.31	45.9	0.00	0.00	10.07
68-70	4.37	.022	9.34	21.98	45.5	0.00	0.00	9.93
70-72	3.89	.029	11.24	22.50	42.9	0.00	0.00	10.66
72-74	2.68	.023	10.74	23.29	40.1	0.00	0.00	11.12
74-76	3.32	.017	9.40	21.52	41.5	0.00	0.00	11.21
76-78	3.94	.014	8.52	22.15	44.3	0.00	0.00	10.18

DDH = 1884NE   LINE 1300 NW   ELEV = 154 m

(Cont.)

78–80	3.97	.016	9.15	24.43	44.1	0.00	0.00	11.14
80–82	3.64	.022	12.03	18.24	41.1	0.00	0.00	10.44
82–84	3.78	.019	9.22	21.51	43.2	0.00	0.00	10.69
84–86	4.46	.035	9.23	22.02	43.7	0.00	0.00	10.52
86–88	3.52	.036	12.99	20.69	41.4	0.00	0.00	11.01
88–90	2.55	.039	13.48	21.15	42.4	0.00	0.00	10.32
90–92	2.38	.036	12.06	22.15	43.4	0.00	0.00	11.46
92–94	2.97	.035	12.33	18.75	45.8	0.00	0.00	10.69
94–96	3.68	.035	12.68	16.49	48.5	0.00	0.00	10.11
96–98	2.90	.034	11.44	19.78	48.7	0.00	0.00	9.40
98–100	3.78	.036	9.60	18.08	52.8	0.00	0.00	9.53
100–102	2.61	.029	7.87	18.14	57.6	0.00	0.00	7.71

DDH = 1900NE			LINE 1300 NW			ELEV = 152 m		
Depth (m)	Ni (%)	Co (%)	Fe (%)	MgO (%)	SiO_2 (%)	Al_2O_3 (%)	Cr_2O_3 (%)	LOI (%)
0–2	.20	0.000	39.01	.03	5.0	22.14	0.00	15.90
2–4	.82	0.000	48.92	.04	2.0	13.50	0.00	9.98
4–6	.73	0.000	53.23	.12	1.6	11.08	0.00	6.40
6–8	.84	0.000	53.71	.05	1.8	9.64	0.00	6.48
8–10	.84	0.000	53.15	.04	1.8	9.44	0.00	7.12
10–12	.84	0.000	53.71	.03	3.0	9.44	0.00	6.16
12–14	.82	0.000	52.28	.02	2.2	8.88	0.00	7.32
14–16	1.09	.121	48.76	.04	2.6	7.56	0.00	12.78
16–18	.71	0.000	39.97	.03	22.5	4.38	0.00	10.86
18–20	1.30	.124	35.01	.07	26.8	5.96	0.00	10.90
20–22	1.53	.151	33.09	.11	31.3	5.10	0.00	11.08
22–24	1.48	.159	30.45	.39	33.6	4.04	0.00	12.48
24–26	1.23	.096	31.18	.65	30.6	5.18	0.00	13.88
26–28	2.68	.066	23.24	6.18	37.9	4.60	0.00	12.30
28–30	3.51	.055	20.60	7.57	39.1	3.60	0.00	11.96
30–32	3.85	.064	19.24	11.52	38.4	3.96	0.00	11.60
32–34	3.85	.060	19.40	15.10	33.6	4.28	0.00	12.74
34–36	3.67	.053	16.91	17.50	35.4	4.10	0.00	12.54
36–38	4.01	.060	16.99	13.25	41.0	3.30	0.00	11.44
38–40	3.91	.060	16.91	14.21	40.9	2.72	1.42	11.18
40–42	3.75	.055	16.83	12.88	43.2	2.36	1.30	10.98
42–44	4.11	.046	17.27	12.00	44.4	2.72	1.17	10.40
44–46	4.59	.049	17.37	14.50	37.7	3.30	1.40	11.36
46–48	5.42	.042	15.63	13.22	42.8	2.78	1.10	11.14
48–50	4.47	.034	15.07	15.05	43.9	2.72	1.16	10.44

DDH = 1934NE   LINE 1300 NW   ELEV = 148 m

Depth (m)	Ni (%)	Co (%)	Fe (%)	MgO (%)	SiO_2 (%)	Al_2O_3 (%)	Cr_2O_3 (%)	LOI (%)
0-2	.47	.014	46.40	1.00	0.0	0.00	0.00	0.00
2-4	.42	.014	46.20	.80	0.0	0.00	0.00	0.00
4-6	.46	.044	45.90	.80	0.0	0.00	0.00	0.00
6-8	.58	.122	50.50	.70	0.0	0.00	0.00	0.00
8-10	.77	.091	45.50	.70	0.0	0.00	0.00	0.00
10-12	.98	.189	41.10	.60	0.0	0.00	0.00	0.00
12-14	.97	.085	27.70	.70	0.0	0.00	0.00	0.00
14-16	1.44	.109	32.20	.80	0.0	0.00	0.00	0.00
16-18	1.08	.109	28.20	.70	0.0	0.00	0.00	0.00
18-20	4.08	.052	16.10	14.60	43.7	1.76	.99	0.00
20-22	4.63	.027	11.80	19.60	42.8	1.77	.67	0.00
22-24	4.52	.026	10.20	21.50	43.7	1.34	.66	0.00
24-26	3.57	.025	12.70	20.50	44.7	2.03	.83	0.00
26-28	4.23	.024	11.90	23.90	41.7	1.84	.66	0.00
28-30	3.56	.026	11.80	20.70	43.5	1.71	.72	0.00
30-32	3.59	.029	12.60	16.90	46.2	1.77	.79	0.00
32-34	2.87	.028	13.60	17.70	44.2	2.34	.85	0.00
34-36	3.06	.032	15.40	19.30	40.9	2.56	1.07	0.00
36-38	3.19	.023	12.80	19.30	43.5	2.17	.81	0.00
38-40	3.09	.027	13.60	20.80	39.7	2.10	.95	0.00
40-42	2.62	.028	12.60	20.50	43.7	1.46	1.07	0.00
42-44	3.66	.026	13.90	15.40	46.9	1.06	1.04	0.00
44-46	3.90	.026	13.20	18.40	44.7	1.22	.92	0.00
46-48	4.52	.022	12.60	23.70	42.5	1.54	.71	0.00
48-50	3.42	.020	9.90	23.90	42.9	1.34	.66	0.00
50-52	4.08	.021	11.20	23.60	42.7	1.67	.76	0.00
52-54	4.01	.025	10.90	23.10	41.7	1.90	.73	0.00
54-56	3.64	.025	10.80	22.40	43.9	1.43	.74	0.00
56-58	3.69	.025	10.90	20.50	48.2	.73	.71	0.00
58-60	4.23	.026	11.60	17.80	44.5	.76	.84	0.00
60-62	3.24	.023	12.20	20.70	43.8	1.09	.69	0.00
62-64	2.61	.027	12.60	22.20	41.6	2.07	.82	0.00
64-66	2.64	.023	12.10	22.50	41.6	1.79	.77	0.00
66-68	2.76	.019	9.50	22.00	46.7	.76	.69	0.00
68-70	2.18	.022	10.80	15.80	48.5	1.09	.80	0.00
70-72	2.80	.022	10.70	19.90	43.0	1.92	.85	0.00
72-74	2.74	.025	13.00	22.40	40.4	1.78	.86	0.00
74-76	3.37	.021	10.20	24.40	40.1	1.70	.98	0.00
76-78	2.37	.017	9.70	22.10	52.2	.67	.60	0.00
78-80	2.61	.013	7.90	24.80	49.6	.33	.52	0.00
80-82	2.79	.016	10.80	28.00	43.1	.59	.52	0.00
82-84	2.01	.016	9.20	32.60	39.5	.52	.49	0.00
84-86	1.78	.029	9.60	20.10	51.5	1.03	.69	0.00
86-88	1.74	.025	9.00	22.50	48.7	.94	.59	0.00
88-90	.42	.021	8.90	34.50	0.0	0.00	0.00	0.00
90-92	.92	.019	7.90	31.20	0.0	0.00	0.00	0.00
92-94	.58	.019	8.70	30.50	0.0	0.00	0.00	0.00

DDH = 1955NE   LINE 1300 NW   ELEV = 140 m

Depth (m)	Ni (%)	Co (%)	Fe (%)	MgO (%)	SiO$_2$ (%)	Al$_2$O$_3$ (%)	Cr$_2$O$_3$ (%)	LOI (%)
0-2	.72	.181	44.60	.90	0.0	0.00	0.00	0.00
2-4	1.18	.180	42.60	.80	0.0	0.00	0.00	0.00
4-6	1.10	.104	26.10	.70	0.0	0.00	0.00	0.00
6-8	1.02	.163	25.60	.80	0.0	0.00	0.00	0.00
8-10	1.07	.216	24.50	.70	0.0	0.00	0.00	0.00
10-12	3.77	.068	18.10	10.80	41.0	3.25	1.38	0.00
12-14	1.70	.206	18.90	2.10	52.5	2.14	1.55	0.00
14-16	4.55	.048	14.40	11.50	47.0	2.01	1.11	0.00
16-18	4.64	.060	20.40	9.40	34.3	3.78	1.28	0.00
18-20	3.79	.049	17.10	16.60	34.6	3.23	1.08	0.00
20-22	3.87	.036	13.60	18.60	39.4	2.54	.89	0.00
22-24	4.22	.044	15.50	16.10	39.0	3.06	1.07	0.00
24-26	7.60	.045	13.40	14.50	39.7	2.69	.95	0.00
26-28	9.93	.057	16.90	7.70	36.8	3.64	1.29	0.00
28-30	7.80	.053	15.70	11.30	35.4	3.09	1.16	0.00
30-32	4.11	.033	9.70	11.60	57.6	1.00	.79	0.00
32-34	4.61	.052	18.80	13.50	36.7	1.81	1.09	0.00
34-36	3.54	.049	18.40	7.20	45.6	1.80	1.24	0.00
36-38	3.25	.056	16.70	11.10	46.0	1.60	1.32	0.00
38-40	2.56	.060	20.50	13.10	36.5	1.79	1.46	0.00
40-42	2.10	.075	25.00	8.90	33.7	2.28	1.60	0.00
42-44	1.34	.047	19.60	3.60	49.8	2.06	1.56	0.00
44-46	2.14	.061	23.00	4.40	40.3	3.20	1.59	0.00
46-48	2.67	.068	21.20	6.00	41.2	3.60	1.62	0.00
48-50	2.15	.045	16.60	12.20	46.6	1.78	1.09	0.00
50-52	2.49	.047	16.40	16.60	41.8	1.10	1.06	0.00
52-54	2.50	.034	11.20	18.00	50.4	.83	.86	0.00
54-56	2.90	.032	12.10	18.30	47.1	.82	.80	0.00
56-58	3.71	.024	10.80	21.80	43.6	1.60	.87	0.00
58-60	3.38	.024	9.90	23.70	43.3	1.93	.75	0.00
60-62	2.31	.021	9.10	17.70	54.2	1.03	.64	0.00
62-64	2.68	.021	9.60	16.70	54.7	.75	.68	0.00
64-66	2.66	.025	11.40	18.60	48.0	.98	.75	0.00
66-68	2.72	.022	10.10	25.20	42.8	1.54	.73	0.00
68-70	2.82	.016	7.60	27.60	45.0	.72	.54	0.00
70-72	2.51	.016	7.70	29.00	43.8	.76	.55	0.00
72-74	1.43	.016	6.60	24.40	51.8	.72	.53	0.00
74-76	.52	.014	6.20	34.20	42.1	.56	.49	0.00
76-78	.46	.017	7.40	31.70	44.0	.37	.66	0.00
78-80	.51	.019	8.70	28.70	44.3	.40	.64	0.00
80-82	.37	.017	7.70	28.80	47.4	.40	.62	0.00
82-84	.52	.015	7.50	24.80	51.8	.41	.66	0.00

334

DDH = 1955NE   LINE 1300 NW   ELEV = 140 m

(Cont.)

```
 84-86    1.49   .014   8.00   28.30   44.0   1.19   .64   0.00
 86-88     .85   .014   7.60   28.40   46.1   1.36   .60   0.00
 88-90     .40   .016   7.00   32.20   43.4   1.38   .56   0.00
 90-92     .72   .017   7.40   29.80   43.8   1.20   .67   0.00
 92-94     .55   .018   7.10   33.40   42.6    .68   .59   0.00
 94-96    1.70   .018   7.00   25.80   49.5    .42   .61   0.00
 96-98    1.95   .019   7.20   27.50   47.8    .52   .79   0.00
 98-100   2.52   .019   7.00   23.40   51.4    .37   .81   0.00
100-102   2.56   .019   7.40   26.70   47.7    .41   .82   0.00
102-104   1.79   .020   7.20   30.00   45.2    .42   .70   0.00
104-106    .54   .017   6.10   33.80    0.0   0.00  0.00   0.00
```

DDH = 1973NE			LINE 1300 NW			ELEV = 133 m	
Depth (m)	Ni (%)	Co (%)	Fe (%)	MgO (%)	SiO_2 (%)	Al_2O_3 (%)	Cr_2O_3 (%)	LOI (%)
0-2	.76	.081	43.30	1.00	16.0	6.73	2.77	9.82
2-4	1.02	.050	33.00	.90	36.3	3.21	2.59	7.82
4-6	1.00	.109	27.50	1.00	46.9	4.60	2.05	5.93
6-8	2.08	.090	30.80	1.80	36.0	5.46	2.20	8.05
8-10	2.64	.081	27.90	3.30	37.2	3.88	2.13	7.81
10-12	6.34	.060	19.80	9.40	37.0	4.34	1.75	9.19
12-14	3.00	.116	23.00	5.70	42.9	3.98	1.75	7.46
14-16	3.60	.028	9.60	25.30	42.1	1.11	.67	11.41
16-18	2.82	.021	7.10	24.20	48.7	.73	.52	10.22
18-20	2.64	.018	7.20	24.40	49.4	.69	.55	10.19
20-22	2.50	.019	8.60	28.20	43.2	.76	.54	11.81
22-24	3.14	.019	7.70	23.10	48.7	.89	.57	10.07
24-26	3.06	.020	7.50	18.10	55.5	.93	.67	8.57
26-28	4.46	.021	8.60	24.30	41.4	1.74	.71	11.29
28-30	3.72	.024	9.10	23.00	42.8	1.63	.75	11.28
30-32	2.54	.024	10.00	23.70	41.4	1.78	.65	12.06
32-34	3.51	.026	13.50	20.80	44.0	1.77	.84	11.45
34-36	4.08	.021	10.30	21.30	45.8	1.29	.71	9.58
36-38	2.50	.021	9.90	20.40	45.5	1.09	.67	11.23
38-40	2.61	.025	11.30	17.70	50.3	.86	.68	10.23
40-42	3.09	.027	12.50	18.80	46.0	.73	.82	10.68
42-44	2.21	.025	12.20	16.90	49.6	.68	.81	10.57
44-46	2.27	.026	13.00	17.60	45.3	.87	.92	11.26
46-48	2.34	.022	11.50	18.50	47.6	.66	.71	11.05
48-50	2.32	.017	7.80	19.00	52.5	1.00	.52	9.43
50-52	3.10	.021	9.70	23.90	41.6	1.89	.66	12.78
52-54	3.23	.020	11.30	21.30	43.6	2.10	.76	12.16
54-56	2.57	.017	8.40	22.10	47.1	1.25	.54	10.97
56-58	2.26	.017	8.00	22.60	47.6	.88	.53	10.60
58-60	2.17	.016	7.60	20.40	51.1	.57	.46	9.59
60-62	2.48	.016	7.00	22.70	54.2	.65	.52	9.17
62-64	1.68	.019	9.60	15.50	58.0	.51	.77	9.46
64-66	1.51	.021	10.00	17.70	54.5	.59	.84	10.57
66-68	1.44	.019	9.10	15.50	59.0	.96	.89	9.56
68-70	1.07	.016	8.30	10.70	69.0	1.05	.65	6.60
70-72	1.15	.013	7.20	12.70	66.5	.87	.50	7.97
72-74	1.07	.017	5.90	9.20	73.5	.82	.43	5.13

DDH = 1992NE   LINE 1300 NW   ELEV = 126 m

Depth (m)	Ni (%)	Co (%)	Fe (%)	MgO (%)	SiO$_2$ (%)	Al$_2$O$_3$ (%)	Cr$_2$O$_3$ (%)	LOI (%)
0-2	3.02	.076	26.30	6.60	33.6	3.79	1.65	0.00
2-4	5.95	.041	11.50	17.30	42.4	1.66	.90	0.00
4-6	6.23	.043	10.10	19.20	40.9	1.94	.80	0.00
6-8	4.82	.042	12.20	18.70	42.0	1.25	.90	0.00
8-10	4.39	.040	11.20	18.60	44.4	1.26	.87	0.00
10-12	4.27	.059	18.70	14.70	35.3	2.58	1.02	0.00
12-14	3.50	.051	18.00	11.00	42.3	3.17	1.13	0.00
14-16	3.16	.028	12.20	14.30	48.8	1.69	.83	0.00
16-18	2.51	.027	11.50	24.30	38.6	1.72	.68	0.00
18-20	2.34	.024	10.30	27.10	38.1	1.87	.55	0.00
20-22	2.84	.025	11.40	23.20	39.8	1.89	.80	0.00
22-24	3.19	.023	10.90	22.50	39.9	2.10	.74	0.00
24-26	2.33	.024	10.30	24.60	40.8	2.07	.56	0.00
26-28	2.14	.022	9.70	23.70	43.5	2.05	.60	0.00
28-30	2.26	.025	10.00	25.50	41.7	1.87	.63	0.00
30-32	2.16	.023	10.50	21.60	46.4	1.07	.71	0.00
32-34	3.18	.023	9.60	20.70	49.7	.86	.67	0.00
34-36	2.74	.017	7.80	19.00	53.6	.69	.58	0.00
36-38	2.21	.017	8.30	18.50	54.2	.60	.51	0.00
38-40	2.54	.018	7.40	23.60	49.7	1.79	.47	0.00
40-42	2.96	.022	9.60	23.50	43.3	2.14	.66	0.00
42-44	4.04	.019	9.90	22.80	43.2	2.18	.80	0.00
44-46	2.43	.018	8.00	21.40	49.3	1.37	.54	0.00
46-48	2.56	.020	9.70	25.40	42.4	1.57	.68	0.00
48-50	2.19	.014	7.70	30.00	41.7	1.05	.54	0.00
50-52	.66	.013	7.00	31.60	0.0	0.00	0.00	0.00
52-54	.37	.012	6.20	32.20	0.0	0.00	0.00	0.00

DDH = 2010NE   LINE 1300 NW   ELEV = 119 m

Depth (m)	Ni (%)	Co (%)	Fe (%)	MgO (%)	SiO_2 (%)	Al_2O_3 (%)	Cr_2O_3 (%)	LOI (%)
0-2	.80	.065	36.20	1.00	0.0	0.00	0.00	0.00
2-4	1.43	.103	36.60	1.90	0.0	0.00	0.00	0.00
4-6	3.31	.053	20.60	11.20	39.9	2.75	1.16	0.00
6-8	1.58	.028	12.80	5.00	61.5	1.34	.76	0.00
8-10	4.90	.049	18.10	13.10	37.8	3.71	1.25	0.00
10-12	2.59	.066	26.70	4.70	34.9	5.42	1.67	0.00
12-14	3.03	.032	13.00	22.00	40.5	2.67	.83	0.00
14-16	4.44	.048	20.80	8.60	38.9	3.89	1.72	0.00
16-18	3.27	.047	20.10	8.00	43.6	3.22	1.32	0.00
18-20	3.64	.013	10.60	23.90	41.3	2.02	.68	0.00
20-22	3.29	.010	11.80	22.70	39.5	1.67	.71	0.00
22-24	3.36	.012	11.60	22.40	41.6	1.98	.74	0.00
24-26	3.26	.016	12.70	17.90	45.1	2.10	.83	0.00
26-28	2.23	.008	11.10	17.20	49.1	1.10	.64	0.00
28-30	2.25	.008	10.50	25.90	42.2	1.58	.57	0.00
30-32	2.42	.010	12.00	24.60	42.4	1.93	.58	0.00
32-34	2.66	.013	12.30	21.30	42.2	2.24	.76	0.00
34-36	2.62	.009	12.20	26.40	40.7	1.27	.62	0.00
36-38	3.10	.010	10.70	28.00	39.3	.89	.67	0.00
38-40	3.57	.012	9.10	26.60	43.5	.96	.54	0.00
40-42	3.78	.006	5.90	18.10	54.4	.89	.48	0.00
42-44	2.62	.006	7.70	27.30	43.5	1.23	.62	0.00
44-46	1.56	.008	7.70	30.50	44.0	.88	.62	0.00
46-48	.37	.005	7.20	35.40	0.0	0.00	0.00	0.00
48-50	.44	.004	6.00	35.70	0.0	0.00	0.00	0.00

DDH = 2030NE   LINE 1300 NW   ELEV = 112 m

Depth (m)	Ni (%)	Co (%)	Fe (%)	MgO (%)	SiO_2 (%)	Al_2O_3 (%)	Cr_2O_3 (%)	LOI (%)
0-2	1.01	0.000	23.40	1.50	0.0	0.00	0.00	0.00
2-4	1.74	0.000	28.60	2.70	36.6	5.07	1.76	7.64
4-6	3.54	0.000	15.10	15.10	41.5	3.02	1.05	10.23
6-8	3.68	0.000	14.90	12.40	44.9	3.06	1.01	8.89
8-10	2.96	0.000	13.80	15.40	46.7	2.22	.84	9.56
10-12	3.49	0.000	13.90	16.70	42.3	2.43	.92	10.59
12-14	3.53	0.000	11.70	17.00	45.5	2.08	.77	10.20
14-16	3.61	0.000	8.70	24.60	42.3	1.20	.62	11.53
16-18	2.73	0.000	8.90	25.00	42.4	.82	.65	11.57
18-20	.72	0.000	7.30	32.10	0.0	0.00	0.00	0.00
20-22	.24	0.000	5.70	34.20	0.0	0.00	0.00	0.00
22-24	.86	0.000	6.50	30.90	0.0	0.00	0.00	0.00
24-26	.77	0.000	6.60	32.00	0.0	0.00	0.00	0.00

DDH = 2046NE   LINE 1300 NW   ELEV = 105 m

Depth (m)	Ni (%)	Co (%)	Fe (%)	MgO (%)	SiO_2 (%)	Al_2O_3 (%)	Cr_2O_3 (%)	LOI (%)
0-2	.94	.069	29.00	1.20	0.0	0.00	0.00	0.00
2-4	.94	.052	24.40	1.10	0.0	0.00	0.00	0.00
4-6	1.36	.057	26.30	1.60	0.0	0.00	0.00	0.00
6-8	3.50	.043	17.70	19.60	33.6	2.05	1.10	0.00
8-10	2.83	.051	20.20	12.40	37.1	2.53	1.27	0.00
10-12	1.99	.030	13.00	19.50	41.8	2.25	.91	0.00
12-14	1.85	.017	12.50	24.70	41.5	1.79	.62	0.00
14-16	.82	.014	8.40	27.20	0.0	0.00	0.00	0.00
16-18	.43	.013	7.50	29.70	0.0	0.00	0.00	0.00
18-20	.35	.011	6.30	32.30	0.0	0.00	0.00	0.00
20-22	.33	.012	6.40	34.80	0.0	0.00	0.00	0.00

DDH = 2064NE   LINE 1300 NW   ELEV = 98 m

Depth (m)	Ni (%)	Co (%)	Fe (%)	MgO (%)	SiO_2 (%)	Al_2O_3 (%)	Cr_2O_3 (%)	LOI (%)
0-2	1.55	.057	23.50	3.30	49.5	1.70	1.84	7.35
2-4	3.27	.032	11.90	21.80	44.3	.90	.93	11.30
4-6	1.89	.044	17.70	10.60	48.9	2.13	1.28	8.54
6-8	1.13	.054	21.20	1.10	54.7	2.00	1.81	6.26
8-10	1.50	.049	20.10	2.20	55.1	1.33	1.89	6.10
10-12	3.44	.035	12.30	14.30	51.0	.99	1.20	9.20
12-14	3.31	.034	13.70	13.00	51.0	.88	1.15	8.77
14-16	3.55	.028	12.10	14.70	50.4	.91	1.16	9.15
16-18	1.69	.018	8.40	25.90	45.2	.89	.69	11.44
18-20	.80	.018	7.40	30.50	42.1	1.37	.59	11.86
20-22	1.15	.016	7.10	27.90	45.8	1.16	.58	10.65
22-24	3.30	.018	7.90	25.20	45.6	.74	.79	8.72
24-26	1.03	.020	8.30	28.50	43.2	1.04	.69	12.08
26-28	.80	.018	8.40	28.80	44.4	1.25	.62	11.67
28-30	1.59	.014	7.70	30.10	41.4	1.07	.67	14.11
30-32	2.76	.015	7.10	29.80	41.2	1.28	.63	12.63
32-34	1.56	.017	7.20	30.70	41.8	.81	.65	12.50
34-36	1.53	.018	7.00	31.20	41.6	.63	.59	12.48
36-38	.73	.018	7.00	32.10	0.0	0.00	0.00	0.00
38-40	.68	.017	6.60	34.50	0.0	0.00	0.00	0.00
40-42	.90	.016	7.10	33.50	0.0	0.00	0.00	0.00
42-44	.65	.020	8.00	33.20	0.0	0.00	0.00	0.00
44-46	.38	.012	6.20	35.10	0.0	0.00	0.00	0.00
46-48	.25	.015	6.00	37.20	0.0	0.00	0.00	0.00
48-50	.21	.013	5.00	36.50	0.0	0.00	0.00	0.00

DDH = 2080NE   LINE 1300 NW   ELEV = 92 m

Depth (m)	Ni (%)	Co (%)	Fe (%)	MgO (%)	SiO$_2$ (%)	Al$_2$O$_3$ (%)	Cr$_2$O$_3$ (%)	LOI (%)
0-2	.69	0.000	31.00	4.70	0.0	0.00	0.00	0.00
2-4	.84	0.000	29.00	11.00	0.0	0.00	0.00	0.00
4-6	1.17	0.000	36.60	2.30	0.0	0.00	0.00	0.00
6-8	1.22	0.000	33.80	2.50	0.0	0.00	0.00	0.00
8-10	1.51	0.000	26.80	1.60	47.0	1.76	2.23	7.10
10-12	2.02	0.000	27.60	9.00	34.0	1.58	2.60	9.51
12-14	2.24	0.000	10.80	26.90	39.4	1.17	.86	12.14
14-16	2.40	0.000	15.00	26.40	37.1	1.23	1.01	12.12
16-18	1.97	0.000	10.40	27.00	40.4	1.22	.82	11.60
18-20	1.24	0.000	11.30	28.30	39.4	1.44	.79	12.42
20-22	.49	0.000	7.90	32.40	39.4	1.21	.62	12.51
22-24	.56	0.000	8.10	32.20	38.4	1.22	.67	11.96
24-26	1.19	0.000	7.40	35.80	39.0	.79	.65	12.79
26-28	2.04	0.000	6.80	36.90	38.4	.56	.54	13.34

DDH = 2105NE   LINE 1300 NW   ELEV = 85 m

Depth (m)	Ni (%)	Co (%)	Fe (%)	MgO (%)	SiO$_2$ (%)	Al$_2$O$_3$ (%)	Cr$_2$O$_3$ (%)	LOI (%)
0-2	1.23	.125	35.80	.80	0.0	0.00	0.00	0.00
2-4	1.09	.064	41.60	.80	0.0	0.00	0.00	0.00
4-6	1.51	.110	36.20	.70	29.8	2.59	2.36	7.15
6-8	2.28	.101	31.30	4.10	32.0	2.34	2.21	7.96
8-10	2.75	.068	20.80	19.50	31.2	1.40	1.62	10.87
10-12	.94	.026	9.70	28.80	0.0	0.00	0.00	0.00
12-14	.37	.019	7.00	31.40	0.0	0.00	0.00	0.00
14-16	.40	.024	7.20	32.10	0.0	0.00	0.00	0.00
16-18	.38	.023	7.40	33.90	0.0	0.00	0.00	0.00
18-20	.31	.019	7.00	34.50	0.0	0.00	0.00	0.00
20-22	.27	.019	6.30	35.80	0.0	0.00	0.00	0.00
22-24	.26	.019	6.10	36.40	0.0	0.00	0.00	0.00

DDH = 2129NE   LINE 1300 NW   ELEV = 77 m

Depth (m)	Ni (%)	Co (%)	Fe (%)	MgO (%)	SiO_2 (%)	Al_2O_3 (%)	Cr_2O_3 (%)	LOI (%)
0-2	.80	.083	42.50	1.00	0.0	0.00	0.00	0.00
2-4	2.16	.112	41.20	1.60	17.4	3.62	2.69	10.43
4-6	3.49	.081	23.10	10.90	36.9	1.72	2.00	9.70
6-8	4.88	.050	22.00	12.90	33.3	1.56	1.75	10.04
8-10	3.42	.036	14.90	18.30	41.2	1.22	1.20	10.25
10-12	1.74	.032	14.30	20.00	42.0	1.02	1.16	11.19
12-14	.57	.028	14.40	12.30	0.0	0.00	0.00	0.00
14-16	.54	.026	10.10	21.90	0.0	0.00	0.00	0.00
16-18	.38	.023	8.70	32.30	0.0	0.00	0.00	0.00
18-20	.54	.019	8.00	32.80	0.0	0.00	0.00	0.00
20-22	.38	.018	8.00	33.80	0.0	0.00	0.00	0.00
22-24	.38	.016	7.90	34.30	0.0	0.00	0.00	0.00
24-26	.37	.017	7.20	34.30	0.0	0.00	0.00	0.00
26-28	.37	.016	7.20	34.30	0.0	0.00	0.00	0.00
28-30	.41	.016	7.20	33.70	0.0	0.00	0.00	0.00

DDH = 2148NE   LINE 1300 NW   ELEV = 70 m

Depth (m)	Ni (%)	Co (%)	Fe (%)	MgO (%)	SiO_2 (%)	Al_2O_3 (%)	Cr_2O_3 (%)	LOI (%)
0-2	.94	0.000	37.00	1.20	0.0	0.00	0.00	0.00
2-4	2.95	.125	33.60	1.20	20.3	10.70	2.17	12.26
4-6	2.25	.102	32.90	2.70	22.1	9.15	2.30	13.28
6-8	2.15	.050	25.70	11.20	25.7	3.80	1.87	17.04
8-10	2.55	.035	20.00	14.00	33.1	1.21	1.60	16.61
10-12	1.87	.022	12.00	23.10	41.0	.70	.87	13.41
12-14	.39	0.000	8.80	29.60	0.0	0.00	0.00	0.00
14-16	.36	0.000	9.00	28.70	0.0	0.00	0.00	0.00
16-18	.34	0.000	7.80	27.10	0.0	0.00	0.00	0.00
18-20	.39	0.000	7.40	31.90	0.0	0.00	0.00	0.00
20-22	.57	0.000	8.00	30.70	0.0	0.00	0.00	0.00
22-24	.36	0.000	7.00	33.50	0.0	0.00	0.00	0.00
24-26	.33	0.000	7.00	32.70	0.0	0.00	0.00	0.00
26-28	.34	0.000	6.70	34.70	0.0	0.00	0.00	0.00
28-30	.46	0.000	7.10	34.80	0.0	0.00	0.00	0.00
30-32	.40	0.000	6.80	35.00	0.0	0.00	0.00	0.00
32-34	.31	0.000	6.20	35.50	0.0	0.00	0.00	0.00
34-36	.29	0.000	6.80	35.60	0.0	0.00	0.00	0.00
36-38	.35	0.000	6.10	35.70	0.0	0.00	0.00	0.00
38-40	.29	0.000	6.00	35.90	0.0	0.00	0.00	0.00
40-42	.25	0.000	5.80	35.10	0.0	0.00	0.00	0.00

DDH = 774NE   LINE 2000 NW   ELEV = 57 m

Depth (m)	Ni (%)	Co (%)	Fe (%)	MgO (%)	SiO_2 (%)	Al_2O_3 (%)	Cr_2O_3 (%)	LOI (%)
0-2	.42	0.000	21.20	.10	0.0	0.00	0.00	0.00
2-4	.81	0.000	13.60	9.30	0.0	0.00	0.00	0.00
4-6	.60	0.000	9.80	19.80	0.0	0.00	0.00	0.00
6-8	.44	0.000	7.20	19.30	0.0	0.00	0.00	0.00
8-10	.39	0.000	7.50	28.90	0.0	0.00	0.00	0.00
10-12	.41	0.000	7.40	32.90	0.0	0.00	0.00	0.00
12-14	.25	0.000	6.40	33.50	0.0	0.00	0.00	0.00
14-16	.20	0.000	5.70	36.80	0.0	0.00	0.00	0.00

DDH = 852NE   LINE 2000 NW   ELEV = 70 m

Depth (m)	Ni (%)	Co (%)	Fe (%)	MgO (%)	SiO_2 (%)	Al_2O_3 (%)	Cr_2O_3 (%)	LOI (%)
0-2	.53	0.000	32.10	.70	0.0	0.00	0.00	0.00
2-4	.51	0.000	32.70	4.00	0.0	0.00	0.00	0.00
4-6	.47	0.000	29.30	3.30	0.0	0.00	0.00	0.00
6-8	.76	0.000	19.70	4.70	0.0	0.00	0.00	0.00
8-10	.49	0.000	9.60	17.80	0.0	0.00	0.00	0.00
10-12	.40	0.000	8.30	18.60	0.0	0.00	0.00	0.00
12-14	.24	0.000	6.20	19.40	0.0	0.00	0.00	0.00
14-16	.26	0.000	6.30	25.60	0.0	0.00	0.00	0.00
16-18	.20	0.000	6.00	27.40	0.0	0.00	0.00	0.00
18-20	.20	0.000	5.80	29.10	0.0	0.00	0.00	0.00

DDH = 930NE   LINE 2000 NW   ELEV = 81 m

Depth (m)	Ni (%)	Co (%)	Fe (%)	MgO (%)	SiO_2 (%)	Al_2O_3 (%)	Cr_2O_3 (%)	LOI (%)
0-2	.40	0.000	25.70	.80	0.0	0.00	0.00	0.00
2-4	.44	0.000	20.20	.60	0.0	0.00	0.00	0.00
4-6	.32	0.000	11.60	.70	0.0	0.00	0.00	0.00
6-8	.34	0.000	10.00	2.00	0.0	0.00	0.00	0.00
8-10	.34	0.000	6.00	24.40	0.0	0.00	0.00	0.00
10-12	.28	0.000	7.70	28.60	0.0	0.00	0.00	0.00
12-14	.28	0.000	7.20	30.40	0.0	0.00	0.00	0.00
14-16	.25	0.000	6.20	35.20	0.0	0.00	0.00	0.00
16-18	.23	0.000	6.00	36.20	0.0	0.00	0.00	0.00

DDH = 953NE   LINE 2000 NW   ELEV = 84 m

Depth (m)	Ni (%)	Co (%)	Fe (%)	MgO (%)	SiO_2 (%)	Al_2O_3 (%)	Cr_2O_3 (%)	LOI (%)
0-2	.23	0.000	20.50	.90	0.0	0.00	0.00	0.00
2-4	.22	0.000	16.30	.80	0.0	0.00	0.00	0.00
4-6	.10	0.000	9.70	.90	0.0	0.00	0.00	0.00
6-8	.29	0.000	9.00	2.90	0.0	0.00	0.00	0.00
8-10	.93	0.000	13.20	15.00	0.0	0.00	0.00	0.00
10-12	.77	0.000	9.90	27.40	0.0	0.00	0.00	0.00
12-14	.39	0.000	7.10	31.10	0.0	0.00	0.00	0.00

DDH = 975NE   LINE 2000 NW   ELEV = 87 m

Depth (m)	Ni (%)	Co (%)	Fe (%)	MgO (%)	SiO_2 (%)	Al_2O_3 (%)	Cr_2O_3 (%)	LOI (%)
0-2	.49	0.000	31.00	1.20	0.0	0.00	0.00	0.00
2-4	.43	0.000	25.40	.70	0.0	0.00	0.00	0.00
4-6	.37	0.000	15.20	.50	0.0	0.00	0.00	0.00
6-8	.66	0.000	14.00	20.20	0.0	0.00	0.00	0.00
8-10	.53	0.000	8.00	26.40	0.0	0.00	0.00	0.00
10-12	.27	0.000	6.00	32.90	0.0	0.00	0.00	0.00
12-14	.23	0.000	5.60	35.90	0.0	0.00	0.00	0.00
14-16	.22	0.000	5.80	35.70	0.0	0.00	0.00	0.00
16-18	.26	0.000	5.80	35.40	0.0	0.00	0.00	0.00
18-20	.21	0.000	5.60	35.20	0.0	0.00	0.00	0.00

DDH = 995NE   LINE 2000 NW   ELEV = 89 m

Depth (m)	Ni (%)	Co (%)	Fe (%)	MgO (%)	SiO_2 (%)	Al_2O_3 (%)	Cr_2O_3 (%)	LOI (%)
0-2	.46	0.000	29.50	.60	0.0	0.00	0.00	0.00
2-4	.43	0.000	24.40	.30	0.0	0.00	0.00	0.00
4-6	.87	0.000	27.20	3.50	0.0	0.00	0.00	0.00
6-8	.89	0.000	11.20	22.90	0.0	0.00	0.00	0.00
8-10	.90	0.000	10.60	25.30	0.0	0.00	0.00	0.00
10-12	.28	0.000	6.30	35.20	0.0	0.00	0.00	0.00
12-14	.27	0.000	6.40	35.30	0.0	0.00	0.00	0.00
14-16	.27	0.000	6.10	36.00	0.0	0.00	0.00	0.00
16-18	.31	0.000	6.30	35.30	0.0	0.00	0.00	0.00
18-20	.30	0.000	6.20	34.80	0.0	0.00	0.00	0.00

DDH = 1013NE   LINE 2000 NW   ELEV = 91 m

Depth (m)	Ni (%)	Co (%)	Fe (%)	MgO (%)	SiO_2 (%)	Al_2O_3 (%)	Cr_2O_3 (%)	LOI (%)
0-2	.46	.051	31.70	.60	33.9	9.13	2.21	8.55
2-4	.54	.068	32.20	.70	31.9	9.69	2.37	8.76
4-6	.95	.054	24.00	9.70	35.8	6.06	1.67	8.83
6-8	1.29	.036	17.30	16.30	38.5	3.77	1.37	9.47
8-10	1.39	.037	17.00	18.00	38.5	3.40	1.19	9.55
10-12	1.41	.030	13.90	22.10	39.7	2.80	1.00	10.45
12-14	.85	.023	10.40	27.80	39.6	2.10	.75	11.11

DDH = 1040NE   LINE 2000 NW   ELEV = 94 m

Depth (m)	Ni (%)	Co (%)	Fe (%)	MgO (%)	SiO_2 (%)	Al_2O_3 (%)	Cr_2O_3 (%)	LOI (%)
0-2	.28	0.000	17.50	.90	0.0	0.00	0.00	0.00
2-4	.77	0.000	18.60	18.50	0.0	0.00	0.00	0.00
4-6	1.28	0.000	8.40	28.70	0.0	0.00	0.00	0.00
6-8	1.27	0.000	9.30	27.30	0.0	0.00	0.00	0.00
8-10	.28	0.000	6.20	32.50	0.0	0.00	0.00	0.00
10-12	.35	0.000	7.40	29.80	0.0	0.00	0.00	0.00
12-14	.25	0.000	8.80	31.60	0.0	0.00	0.00	0.00

DDH = 1065NE   LINE 2000 NW   ELEV = 97 m

Depth (m)	Ni (%)	Co (%)	Fe (%)	MgO (%)	SiO_2 (%)	Al_2O_3 (%)	Cr_2O_3 (%)	LOI (%)
0-2	.45	0.000	34.50	.90	0.0	0.00	0.00	0.00
2-4	.92	0.000	45.40	.50	0.0	0.00	0.00	0.00
4-6	1.76	0.000	30.80	12.90	30.2	0.00	0.00	0.00
6-8	1.66	0.000	36.90	7.60	16.5	0.00	0.00	0.00
8-10	1.15	0.000	10.40	27.20	0.0	0.00	0.00	0.00
10-12	.35	0.000	6.60	33.20	0.0	0.00	0.00	0.00
12-14	.35	0.000	6.70	33.70	0.0	0.00	0.00	0.00
14-16	.25	0.000	6.40	33.60	0.0	0.00	0.00	0.00

DDH = 1090NE   LINE 2000 NW   ELEV = 99 m

Depth (m)	Ni (%)	Co (%)	Fe (%)	MgO (%)	SiO_2 (%)	Al_2O_3 (%)	Cr_2O_3 (%)	LOI (%)
0-2	.46	0.000	35.20	.80	0.0	0.00	0.00	0.00
2-4	.81	0.000	44.60	.60	0.0	0.00	0.00	0.00
4-6	1.36	0.000	48.50	.60	0.0	0.00	0.00	0.00
6-8	1.60	0.000	33.30	7.60	22.1	0.00	0.00	0.00
8-10	1.74	0.000	23.30	15.70	31.1	0.00	0.00	0.00
10-12	1.20	0.000	11.90	26.20	0.0	0.00	0.00	0.00
12-14	.80	0.000	7.90	32.70	0.0	0.00	0.00	0.00
14-16	.27	0.000	6.20	34.70	0.0	0.00	0.00	0.00
16-18	.22	0.000	5.50	34.80	0.0	0.00	0.00	0.00

DDH = 1113NE   LINE 2000 NW   ELEV = 100 m

Depth (m)	Ni (%)	Co (%)	Fe (%)	MgO (%)	SiO_2 (%)	Al_2O_3 (%)	Cr_2O_3 (%)	LOI (%)
0-2	.54	0.000	37.70	.80	0.0	0.00	0.00	0.00
2-4	.82	0.000	47.50	.60	0.0	0.00	0.00	0.00
4-6	1.12	.119	48.50	2.10	0.0	0.00	0.00	0.00
6-8	1.66	.048	15.80	25.70	31.4	1.04	1.13	12.12
8-10	.60	0.000	9.20	32.80	0.0	0.00	0.00	0.00
10-12	.42	0.000	9.00	32.60	0.0	0.00	0.00	0.00
12-14	.36	0.000	8.30	34.70	0.0	0.00	0.00	0.00

DDH = 1212NE   LINE 2000 NW   ELEV = 98 m

Depth (m)	Ni (%)	Co (%)	Fe (%)	MgO (%)	SiO_2 (%)	Al_2O_3 (%)	Cr_2O_3 (%)	LOI (%)
0-2	1.45	.075	32.25	6.87	2.2	0.00	0.00	10.49
2-4	1.92	.107	26.88	10.01	2.8	0.00	0.00	9.12
4-6	.41	0.000	6.43	34.15	0.0	0.00	0.00	0.00
6-8	.29	0.000	5.61	37.15	0.0	0.00	0.00	0.00
8-10	.22	0.000	5.32	37.88	0.0	0.00	0.00	0.00

DDH = 1232NE   LINE 2000 NW   ELEV = 105 m

Depth (m)	Ni (%)	Co (%)	Fe (%)	MgO (%)	SiO_2 (%)	Al_2O_3 (%)	Cr_2O_3 (%)	LOI (%)
0-2	.91	0.000	37.52	1.45	0.0	0.00	0.00	0.00
2-4	.49	0.000	14.76	3.02	0.0	0.00	0.00	0.00
4-6	1.02	0.000	9.04	22.25	0.0	0.00	0.00	0.00
6-8	.68	0.000	6.31	27.95	0.0	0.00	0.00	0.00
8-10	.79	0.000	7.84	27.20	0.0	0.00	0.00	0.00
10-12	.40	0.000	7.34	29.30	0.0	0.00	0.00	0.00
12-14	.30	0.000	6.28	30.36	0.0	0.00	0.00	0.00
14-16	.32	0.000	7.50	27.67	0.0	0.00	0.00	0.00
16-18	.30	0.000	7.26	29.20	0.0	0.00	0.00	0.00
18-20	.27	0.000	6.21	31.19	0.0	0.00	0.00	0.00
20-22	.25	0.000	6.00	32.91	0.0	0.00	0.00	0.00
22-24	.25	0.000	6.25	33.91	0.0	0.00	0.00	0.00
24-26	.24	0.000	6.00	35.00	0.0	0.00	0.00	0.00
26-28	.33	0.000	6.66	29.07	0.0	0.00	0.00	0.00
28-30	.30	0.000	6.56	29.37	0.0	0.00	0.00	0.00
30-32	.31	0.000	6.16	30.61	0.0	0.00	0.00	0.00
32-34	.31	0.000	7.00	32.13	0.0	0.00	0.00	0.00
34-36	.46	0.000	7.92	31.10	0.0	0.00	0.00	0.00
36-38	.38	0.000	7.51	32.15	0.0	0.00	0.00	0.00

DDH = 1267NE   LINE 2000 NW   ELEV = 112 m

Depth (m)	Ni (%)	Co (%)	Fe (%)	MgO (%)	SiO_2 (%)	Al_2O_3 (%)	Cr_2O_3 (%)	LOI (%)
0-2	1.08	.092	44.50	1.03	8.9	0.00	0.00	10.74
2-4	1.37	.087	36.25	9.70	19.3	0.00	0.00	10.77
4-6	1.43	.029	11.97	28.00	41.8	0.00	0.00	9.88
6-8	.40	0.000	7.04	37.63	0.0	0.00	0.00	0.00
8-10	.27	0.000	6.70	38.00	0.0	0.00	0.00	0.00
10-12	.27	0.000	7.03	37.68	0.0	0.00	0.00	0.00
12-14	.27	0.000	6.84	34.00	0.0	0.00	0.00	0.00
14-16	.26	0.000	6.59	37.81	0.0	0.00	0.00	0.00

DDH = 1320NE   LINE 2000 NW   ELEV = 119 m

Depth (m)	Ni (%)	Co (%)	Fe (%)	MgO (%)	SiO$_2$ (%)	Al$_2$O$_3$ (%)	Cr$_2$O$_3$ (%)	LOI (%)
0-2	.90	0.000	42.49	.91	8.6	0.00	0.00	11.51
2-4	1.07	0.000	43.10	.65	8.0	0.00	0.00	11.33
4-6	1.39	.134	46.13	.75	8.5	0.00	0.00	11.17
6-8	2.03	.050	15.07	22.53	32.6	0.00	0.00	12.18
8-10	1.27	.023	9.72	31.11	38.5	0.00	0.00	9.58
10-12	.36	.025	6.37	35.88	39.6	0.00	0.00	13.85
12-14	.43	.026	6.47	36.71	38.6	0.00	0.00	13.77
14-16	.25	.027	6.32	38.90	42.6	0.00	0.00	8.41
16-18	.42	.030	6.78	39.27	41.4	0.00	0.00	8.62
18-20	.61	.031	8.27	35.14	39.8	0.00	0.00	10.11
20-22	.62	.033	8.23	35.62	40.2	0.00	0.00	10.59
22-24	.72	.020	7.83	36.50	40.4	0.00	0.00	11.65
24-26	.37	.025	6.93	38.82	40.1	0.00	0.00	9.93
26-28	.49	.021	7.43	36.30	40.3	0.00	0.00	12.52
28-30	.35	.030	6.54	37.07	40.5	0.00	0.00	12.55

DDH = 1378NE   LINE 2000 NW   ELEV = 126 m

Depth (m)	Ni (%)	Co (%)	Fe (%)	MgO (%)	SiO$_2$ (%)	Al$_2$O$_3$ (%)	Cr$_2$O$_3$ (%)	LOI (%)
0-2	.80	.130	41.29	.75	12.5	9.02	0.00	10.68
2-4	1.02	.160	42.70	.68	9.9	7.95	0.00	11.40
4-6	1.70	.090	31.53	12.41	22.9	2.74	0.00	10.54
6-8	2.13	.030	10.21	26.00	40.2	1.08	0.00	10.58
8-10	1.87	.030	10.00	25.81	39.6	1.33	0.00	9.59
10-12	1.54	.020	6.90	31.37	40.4	1.08	0.00	11.12
12-14	1.35	.020	7.84	31.70	41.4	1.05	0.00	8.98
14-16	2.63	.020	7.60	24.85	40.3	1.05	0.00	12.24
16-18	1.15	.020	7.20	31.54	43.0	.93	0.00	10.38
18-20	.28	.010	6.38	35.00	44.4	.75	0.00	10.73
20-22	.30	.010	6.20	35.71	42.9	.71	0.00	10.63

DDH = 1427NE   LINE 2000 NW   ELEV = 133 m

Depth (m)	Ni (%)	Co (%)	Fe (%)	MgO (%)	SiO_2 (%)	Al_2O_3 (%)	Cr_2O_3 (%)	LOI (%)
0-2	.77	.111	44.00	1.50	12.6	7.45	2.94	11.44
2-4	.58	.148	40.50	1.90	12.1	11.68	2.64	12.11
4-6	1.07	.051	45.30	1.20	9.5	7.18	3.40	12.08
6-8	1.10	.041	41.80	1.10	15.4	7.25	3.60	10.26
8-10	.76	.044	27.30	.90	45.3	4.06	2.75	6.92
10-12	1.58	.099	20.50	4.10	51.4	3.25	1.97	6.71
12-14	1.75	.226	29.50	9.30	25.1	6.57	2.90	10.03
14-16	1.81	.246	41.30	1.90	9.9	8.60	3.96	11.18
16-18	1.73	.248	41.80	1.90	10.3	8.15	3.70	11.19
18-20	1.90	.114	28.30	11.40	26.2	4.63	2.30	11.19
20-22	.92	.020	8.90	30.10	40.3	1.74	.66	13.24
22-24	.46	.015	6.60	33.70	40.5	1.12	.52	13.84
24-26	1.10	.019	8.70	30.00	42.1	1.38	.73	10.55
26-28	.49	.017	6.90	36.00	41.5	.92	.60	10.68
28-30	.29	.015	6.10	36.10	38.7	1.10	.46	14.73
30-32	.30	.016	6.50	35.70	38.9	1.30	.45	14.60

DDH = 1500NE   LINE 2000 NW   ELEV = 146 m

Depth (m)	Ni (%)	Co (%)	Fe (%)	MgO (%)	SiO_2 (%)	Al_2O_3 (%)	Cr_2O_3 (%)	LOI (%)
0-2	.67	0.000	40.89	.02	5.7	20.00	0.00	14.64
2-4	.67	0.000	44.35	.02	4.1	18.56	0.00	11.88
4-6	.65	0.000	49.58	.02	2.3	16.43	0.00	8.90
6-8	.71	0.000	49.34	.02	4.9	14.50	0.00	7.66
8-10	.76	0.000	50.70	.02	4.9	13.74	0.00	6.76
10-12	1.03	.050	53.68	.01	4.2	10.48	0.00	6.44
12-14	.79	0.000	47.57	.01	5.6	12.84	0.00	10.34
14-16	.77	0.000	50.62	.01	2.8	10.54	0.00	12.92
16-18	.74	0.000	52.34	.01	3.1	6.52	0.00	12.66
18-20	1.22	.145	44.43	.01	10.8	7.24	0.00	12.74
20-22	1.05	.244	22.63	.01	50.5	3.80	0.00	7.18
22-24	.71	0.000	19.48	.31	58.2	4.16	0.00	6.10
24-26	1.16	.082	21.17	1.35	50.4	4.32	0.00	7.56
26-28	2.20	.044	16.10	4.72	53.5	4.72	0.00	8.66
28-30	2.06	.025	12.07	10.79	55.1	2.20	0.00	8.58
30-32	1.77	.030	12.15	2.47	58.8	2.24	0.00	7.92
32-34	1.77	.034	15.94	6.00	58.9	2.44	0.00	8.98
34-36	1.80	.042	18.03	7.04	45.9	1.36	0.00	11.36
36-38	2.11	.024	11.14	14.35	51.5	1.28	0.00	9.24
38-40	3.45	.028	10.58	18.75	47.3	1.18	0.00	10.26
40-42	2.01	.031	11.38	10.24	56.5	1.38	0.00	7.00
42-44	1.19	.028	11.14	5.76	67.3	.96	0.00	5.16
44-46	1.06	.040	12.50	3.94	67.3	1.77	0.00	5.20
46-48	.91	0.000	15.87	3.00	60.7	2.38	0.00	5.52
48-50	1.04	.049	15.07	2.44	63.6	2.34	0.00	5.96
50-52	.89	0.000	14.11	2.14	65.3	1.92	0.00	6.06
52-54	1.10	.042	16.51	3.12	58.0	2.24	0.00	7.66
54-56	1.27	.046	16.35	4.60	54.5	2.56	0.00	8.56
56-58	1.49	.037	13.87	9.24	53.4	2.04	0.00	9.12
58-60	1.00	.036	13.77	5.32	61.7	1.40	0.00	6.80

DDH = 1502NE   LINE 2000 NW   ELEV = 144 m

Depth (m)	Ni (%)	Co (%)	Fe (%)	MgO (%)	SiO$_2$ (%)	Al$_2$O$_3$ (%)	Cr$_2$O$_3$ (%)	LOI (%)
0-2	.46	0.000	41.80	.50	0.0	0.00	0.00	0.00
2-4	.61	0.000	47.30	.50	0.0	0.00	0.00	0.00
4-6	.70	0.000	53.20	.50	0.0	0.00	0.00	0.00
6-8	.77	0.000	53.30	.50	0.0	0.00	0.00	0.00
8-10	.90	0.000	56.10	.40	0.0	0.00	0.00	0.00
10-12	.92	0.000	49.70	.50	0.0	0.00	0.00	0.00
12-14	.89	0.000	54.40	.40	0.0	0.00	0.00	0.00
14-16	1.05	0.000	48.60	.40	0.0	0.00	0.00	0.00
16-18	1.23	0.000	32.20	.70	0.0	0.00	0.00	0.00
18-20	1.65	.099	22.00	3.20	51.6	1.89	1.57	6.38
20-22	2.08	.189	27.70	3.70	39.3	3.24	1.75	6.91
22-24	.73	.126	15.10	1.30	69.5	1.59	.89	3.76
24-26	.83	.090	19.30	1.40	62.1	1.64	1.12	4.71
26-28	1.11	.053	18.50	4.30	56.8	1.64	1.20	6.84
28-30	2.09	.028	10.50	15.10	59.0	.81	.79	7.55
30-32	2.07	.026	10.70	17.50	55.1	.91	.72	8.33
32-34	1.78	.049	22.30	6.20	46.2	3.49	1.48	7.26
34-36	1.18	.033	14.80	8.90	54.9	2.78	1.04	6.46
36-38	.91	.024	11.40	20.70	47.1	1.54	.72	10.70
38-40	1.79	.021	8.50	19.80	54.5	1.20	.66	8.70
40-42	1.51	.018	7.50	22.80	52.9	.84	.59	9.39
42-44	2.34	.018	9.90	23.30	50.0	.73	.49	9.26
44-46	2.79	.025	9.80	21.80	47.7	1.19	.63	10.09
46-48	1.56	.025	9.90	12.80	61.6	1.62	.65	6.47
48-50	.76	.028	9.50	4.10	74.3	1.16	.76	3.27
50-52	1.72	.084	19.20	4.20	54.3	2.29	1.08	5.52
52-54	1.83	.081	17.30	9.80	48.8	2.50	1.02	8.21
54-56	1.87	.068	14.20	13.00	49.9	2.22	.92	8.55
56-58	1.74	.061	11.40	16.00	51.7	1.73	.73	8.79
58-60	1.49	0.000	10.00	13.50	59.0	1.12	.69	7.10
60-62	1.31	0.000	10.30	16.70	54.6	1.31	.84	8.64
62-64	1.38	0.000	11.40	17.80	49.2	1.37	.88	9.46
64-66	1.37	0.000	10.80	20.60	49.0	1.21	.71	9.76
66-68	1.32	0.000	10.10	19.80	52.1	1.12	.81	9.76
68-70	1.26	0.000	10.00	19.10	52.2	1.12	.67	9.33
70-72	1.62	.058	10.30	19.60	51.2	1.07	.77	9.67
72-74	1.21	0.000	9.60	18.00	54.8	1.35	.68	8.97
74-76	1.51	.055	8.00	21.90	51.9	1.27	.60	9.13
76-78	.90	0.000	7.20	25.10	0.0	0.00	0.00	0.00
78-80	.80	0.000	7.00	24.90	0.0	0.00	0.00	0.00
80-82	1.00	0.000	7.70	20.20	0.0	0.00	0.00	0.00
82-84	.53	0.000	7.50	33.40	0.0	0.00	0.00	0.00
84-86	1.34	0.000	6.90	25.80	0.0	0.00	0.00	0.00
86-88	.70	0.000	7.10	31.10	0.0	0.00	0.00	0.00
88-90	.47	0.000	7.80	29.20	0.0	0.00	0.00	0.00
90-92	.43	0.000	7.80	28.60	0.0	0.00	0.00	0.00
92-94	.52	0.000	7.40	28.10	0.0	0.00	0.00	0.00
94-96	.37	0.000	7.00	33.70	0.0	0.00	0.00	0.00

DDH = 1574NE   LINE 2000 NW   ELEV = 134 m

Depth (m)	Ni (%)	Co (%)	Fe (%)	MgO (%)	SiO_2 (%)	Al_2O_3 (%)	Cr_2O_3 (%)	LOI (%)
0-2	.75	.027	50.90	1.40	6.0	10.15	2.67	10.15
2-4	.62	.026	49.30	1.10	5.6	10.69	3.14	9.07
4-6	.45	.059	44.80	1.40	13.0	8.00	2.76	11.45
6-8	.60	.076	36.70	1.00	30.8	4.50	1.84	9.61
8-10	1.11	.113	36.70	.90	26.0	5.60	2.64	10.45
10-12	.71	.085	37.60	.70	26.8	4.36	2.75	10.15
12-14	1.24	.115	31.10	2.90	34.4	4.35	2.76	9.61
14-16	3.51	.052	16.00	13.80	42.1	2.58	1.16	10.86
16-18	2.02	.032	15.90	9.40	30.4	1.26	.75	10.48
18-20	1.69	.025	10.20	9.20	61.9	.97	.78	6.43
20-22	2.14	.034	16.50	12.60	44.8	1.95	1.12	10.26
22-24	3.58	.025	9.20	20.80	47.9	1.20	.72	10.67
24-26	2.90	.029	11.00	14.20	54.7	1.26	.95	9.01
26-28	3.43	.020	8.00	19.70	51.4	.94	.70	9.43
28-30	2.54	.026	9.90	23.30	51.0	1.07	.91	9.92
30-32	1.81	.023	8.80	22.30	50.0	.96	.74	10.47
32-34	1.20	.023	7.90	26.00	49.7	.78	.69	11.15
34-36	.43	.019	7.20	31.00	44.6	.68	.59	10.94
36-38	.44	.016	6.80	29.00	46.6	.60	.53	10.67
38-40	.74	.021	8.60	26.40	46.9	.90	.71	10.65
40-42	.53	.019	7.50	28.50	45.5	.79	.64	11.11
42-44	.36	.018	7.30	28.70	43.8	1.37	.62	11.11
44-46	.38	.016	6.30	34.80	40.6	.60	.50	11.52
46-48	.32	.016	6.00	35.00	43.2	.56	.66	11.46
48-50	.36	.015	6.10	33.80	43.4	1.24	.51	8.39

DDH = 1600NE   LINE 2000 NW   ELEV = 131 m

Depth (m)	Ni (%)	Co (%)	Fe (%)	MgO (%)	SiO$_2$ (%)	Al$_2$O$_3$ (%)	Cr$_2$O$_3$ (%)	LOI (%)
0-2	.34	0.000	36.84	.29	5.6	25.84	1.76	15.32
2-4	.58	0.000	46.31	.33	4.4	18.12	1.76	0.00
4-6	.82	0.000	49.92	.61	2.3	12.16	1.76	0.00
6-8	.68	0.000	47.03	.50	7.8	7.74	1.76	0.00
8-10	.71	0.000	38.85	.37	24.7	5.60	1.62	0.00
10-12	.67	0.000	46.75	.26	6.8	7.28	0.00	0.00
12-14	.48	0.000	36.59	.26	26.1	5.04	0.00	10.64
14-16	.58	0.000	27.89	.43	39.9	7.18	0.00	8.38
16-18	.83	0.000	30.47	.55	38.5	5.36	0.00	8.54
18-20	.77	0.000	26.44	.48	44.7	4.60	0.00	7.64
20-22	.90	0.000	29.85	.34	40.4	5.10	0.00	8.08
22-24	2.76	.046	20.47	7.80	37.9	4.04	0.00	11.08
24-26	2.36	.048	16.16	10.62	41.0	3.52	0.00	11.52
26-28	1.29	.048	21.44	2.18	43.4	4.28	0.00	10.10
28-30	1.63	.039	15.96	7.40	37.9	4.12	0.00	14.08

DDH = 1657NE   LINE 2000 NW   ELEV = 112 m

Depth (m)	Ni (%)	Co (%)	Fe (%)	MgO (%)	SiO$_2$ (%)	Al$_2$O$_3$ (%)	Cr$_2$O$_3$ (%)	LOI (%)
0-2	.78	.028	41.30	.90	7.7	13.43	2.73	12.10
2-4	1.27	.035	41.30	.80	10.0	11.36	3.19	12.01
4-6	1.08	.025	50.90	.70	5.6	7.96	3.42	7.38
6-8	1.17	.050	51.30	.80	6.2	8.38	3.21	6.87
8-10	1.67	.112	51.00	.90	8.4	7.58	3.66	4.69
10-12	1.65	.103	53.90	.70	7.9	6.07	3.16	4.50
12-14	1.97	.258	49.40	.70	7.5	5.85	5.01	7.96
14-16	0.00	0.000	0.00	0.00	0.0	0.00	0.00	0.00
16-18	0.00	0.000	0.00	0.00	0.0	0.00	0.00	0.00
18-20	0.00	0.000	0.00	0.00	0.0	0.00	0.00	0.00
20-22	0.00	0.000	0.00	0.00	0.0	0.00	0.00	0.00
22-24	3.59	.066	17.10	15.30	41.2	1.96	1.74	10.65
24-26	2.15	.026	12.20	19.20	50.4	1.77	.95	8.73
26-28	.67	.017	7.20	23.50	42.2	1.21	.50	15.12
28-30	.27	.013	5.00	22.50	34.0	.82	.37	20.90
30-32	.26	.013	5.10	23.40	34.0	1.00	.35	20.34
32-34	.39	.013	6.10	29.00	40.7	.95	.45	15.33
34-36	.29	.012	5.70	35.70	39.1	1.02	.46	14.62
36-38	.30	.013	6.20	37.00	40.8	1.22	.41	10.32

DDH = 1753NE   LINE 2000 NW   ELEV = 92 m

Depth (m)	Ni (%)	Co (%)	Fe (%)	MgO (%)	SiO_2 (%)	Al_2O_3 (%)	Cr_2O_3 (%)	LOI (%)
0-2	.31	0.000	27.90	1.00	0.0	0.00	0.00	0.00
2-4	.60	0.000	29.20	.80	0.0	0.00	0.00	0.00
4-6	.58	0.000	31.50	.90	0.0	0.00	0.00	0.00
6-8	.58	0.000	37.80	1.00	0.0	0.00	0.00	0.00
8-10	.65	0.000	41.00	.80	0.0	0.00	0.00	0.00
10-12	.67	0.000	43.10	.90	0.0	0.00	0.00	0.00
12-14	.68	0.000	43.00	1.00	0.0	0.00	0.00	0.00
14-16	.69	0.000	43.40	.80	0.0	0.00	0.00	0.00
16-18	.84	0.000	43.20	.70	0.0	0.00	0.00	0.00
18-20	.81	0.000	53.70	.70	0.0	0.00	0.00	0.00
20-22	.77	0.000	45.50	.80	0.0	0.00	0.00	0.00
22-24	1.22	0.000	52.10	.90	0.0	0.00	0.00	0.00
24-26	1.58	0.000	48.50	.90	5.0	9.09	2.90	9.55
26-28	1.55	0.000	49.80	.90	6.3	8.65	3.08	7.28
28-30	1.53	0.000	45.70	1.20	12.7	7.69	2.36	7.47
30-32	1.90	0.000	24.00	4.70	43.5	2.98	2.67	8.40
32-34	1.67	0.000	16.10	17.50	45.2	2.71	1.07	9.27
34-36	1.28	0.000	9.50	24.90	48.5	1.73	.71	10.45
36-38	2.74	0.000	9.00	24.20	47.6	1.96	.73	10.76
38-40	2.94	0.000	9.20	25.60	44.9	1.93	.70	11.53
40-42	3.47	0.000	8.50	25.50	45.2	1.66	.67	11.73
42-44	3.54	0.000	8.40	25.30	46.7	1.59	.78	11.40
44-46	1.35	0.000	6.70	31.70	0.0	0.00	0.00	0.00
46-48	.30	0.000	6.50	33.30	0.0	0.00	0.00	0.00
48-50	.24	0.000	6.00	35.20	0.0	0.00	0.00	0.00
50-52	.28	0.000	6.00	32.70	0.0	0.00	0.00	0.00

DDH = 1800NE   LINE 2000 NW   ELEV = 91 m

Depth (m)	Ni (%)	Co (%)	Fe (%)	MgO (%)	SiO$_2$ (%)	Al$_2$O$_3$ (%)	Cr$_2$O$_3$ (%)	LOI (%)
0-2	.10	0.000	19.18	.14	44.0	18.68	0.00	10.48
2-4	.24	0.000	27.40	.11	21.2	25.74	0.00	13.20
4-6	.40	0.000	29.82	.23	16.5	26.48	0.00	13.36
6-8	.49	0.000	29.05	1.16	22.2	21.26	0.00	11.94
8-10	.57	0.000	35.62	.19	16.4	22.06	0.00	9.28
10-12	.77	0.000	41.78	.07	7.7	17.46	0.00	12.40
12-14	.90	0.000	44.66	.10	5.9	16.46	0.00	10.86
14-16	1.21	.086	49.79	.17	5.3	10.52	0.00	8.44
16-18	1.45	.117	50.67	.13	5.4	8.50	0.00	8.16
18-20	1.51	.171	51.07	.22	5.4	9.12	0.00	7.56
20-22	1.51	.137	51.47	.23	5.4	8.28	0.00	6.28
22-24	1.35	.132	50.34	.23	6.6	9.64	0.00	5.86
24-26	1.54	.184	46.01	.24	9.3	9.36	0.00	8.28
26-28	1.60	.184	37.51	1.01	16.7	8.34	0.00	12.06
28-30	1.86	.190	32.06	1.89	22.0	5.72	0.00	15.34
30-32	1.31	.096	28.05	1.40	36.6	5.80	0.00	10.96
32-34	2.38	.096	25.33	6.99	33.6	4.44	0.00	11.76
34-36	2.57	.064	18.76	10.88	42.5	3.80	0.00	10.60
36-38	2.92	.060	18.60	14.61	38.6	3.76	0.00	11.28
38-40	2.22	.042	15.47	17.14	42.4	4.54	0.00	10.92
40-42	1.98	.034	13.31	19.92	41.7	3.81	0.00	11.32
42-44	2.68	.046	16.30	16.75	40.7	4.01	0.00	11.40
44-46	2.49	.038	14.99	16.54	42.3	4.11	0.00	11.28
46-48	1.88	.034	14.11	17.63	43.9	4.40	0.00	11.18
48-50	2.22	.029	13.71	20.39	41.4	4.60	0.00	11.58
50-52	1.63	.034	15.55	20.01	39.7	4.60	0.00	11.20
52-54	1.61	.042	15.23	20.79	38.6	4.44	0.00	11.30
54-56	1.26	.038	16.51	18.90	38.0	4.70	0.00	10.72
56-58	.99	0.000	14.43	23.21	38.6	3.01	0.00	11.40

DDH = 1859NE   LINE 2000 NW   ELEV = 84 m

Depth (m)	Ni (%)	Co (%)	Fe (%)	MgO (%)	SiO$_2$ (%)	Al$_2$O$_3$ (%)	Cr$_2$O$_3$ (%)	LOI (%)
0-2	.28	0.000	31.50	.60	0.0	0.00	0.00	0.00
2-4	.41	0.000	34.90	.60	0.0	0.00	0.00	0.00
4-6	.76	0.000	41.30	.60	0.0	0.00	0.00	0.00
6-8	1.38	.029	51.40	.80	0.0	0.00	0.00	0.00
8-10	1.43	.022	51.20	.70	0.0	0.00	0.00	0.00
10-12	1.39	.071	49.50	.90	0.0	0.00	0.00	0.00
12-14	2.81	.182	35.90	2.10	18.9	9.17	3.42	9.64
14-16	1.80	.090	39.00	1.40	13.7	9.16	3.53	10.50
16-18	1.14	.056	31.50	1.20	26.6	10.19	4.93	9.49
18-20	1.24	.069	25.50	1.20	42.8	7.48	3.66	8.46
20-22	1.71	.097	25.90	2.40	41.1	4.80	2.43	10.07
22-24	2.56	.070	21.20	11.20	39.0	4.96	2.34	10.68
24-26	3.10	.088	25.00	7.40	34.4	5.86	2.51	9.70
26-28	2.65	.083	22.90	7.50	40.0	4.27	2.60	9.32
28-30	2.55	.056	19.30	14.90	37.6	4.39	1.96	11.16
30-32	2.59	.053	19.40	12.20	42.0	4.68	2.12	10.35
32-34	3.80	.052	16.30	14.40	40.9	4.48	.22	10.32
34-36	3.57	.041	11.70	21.80	44.1	2.67	1.27	10.81
36-38	1.88	.032	8.20	27.10	46.6	1.80	.70	11.84
38-40	.36	0.000	6.20	30.20	0.0	0.00	0.00	0.00
40-42	.34	0.000	5.70	31.40	0.0	0.00	0.00	0.00
42-44	.30	0.000	5.60	32.00	0.0	0.00	0.00	0.00
44-46	.30	0.000	5.30	31.30	0.0	0.00	0.00	0.00
46-48	.29	0.000	6.50	32.30	0.0	0.00	0.00	0.00
48-50	.47	0.000	8.60	29.00	0.0	0.00	0.00	0.00
50-52	.47	0.000	8.80	27.40	0.0	0.00	0.00	0.00
52-54	.67	0.000	11.50	22.90	0.0	0.00	0.00	0.00
54-56	.94	0.000	13.80	20.80	0.0	0.00	0.00	0.00
56-58	.77	0.000	10.80	23.80	0.0	0.00	0.00	0.00
58-60	1.09	.032	15.10	19.20	0.0	0.00	0.00	0.00
60-62	.96	0.000	17.30	15.70	0.0	0.00	0.00	0.00
62-64	.54	0.000	10.00	26.40	0.0	0.00	0.00	0.00

DDH = 1955NE   LINE 2000 NW   ELEV = 75 m

Depth (m)	Ni (%)	Co (%)	Fe (%)	MgO (%)	SiO$_2$ (%)	Al$_2$O$_3$ (%)	Cr$_2$O$_3$ (%)	LOI (%)
0-2	.26	0.000	24.30	.80	0.0	0.00	0.00	0.00
2-4	.92	0.000	35.80	.60	0.0	0.00	0.00	0.00
4-6	.47	0.000	12.40	.90	0.0	0.00	0.00	0.00
6-8	.51	0.000	8.30	2.60	0.0	0.00	0.00	0.00
8-10	.69	0.000	10.60	2.70	0.0	0.00	0.00	0.00
10-12	.96	0.000	21.00	1.90	0.0	0.00	0.00	0.00
12-14	1.14	.034	41.50	1.60	0.0	0.00	0.00	0.00
14-16	1.39	.109	34.30	1.90	0.0	0.00	0.00	0.00
16-18	1.28	.167	22.70	3.40	0.0	0.00	0.00	0.00
18-20	2.47	.096	21.30	12.60	32.0	2.42	1.00	15.05
20-22	1.55	.040	12.90	4.80	59.4	1.86	.91	7.58
22-24	2.24	.022	11.50	7.80	0.0	0.00	0.00	0.00
24-26	2.00	.020	10.20	17.40	53.6	1.23	.71	8.51
26-28	1.18	.024	9.00	25.50	54.7	1.11	.51	8.27
28-30	.99	.024	8.80	22.20	48.6	1.30	.53	10.16
30-32	1.80	0.000	9.20	20.10	47.1	1.41	.56	10.30
32-34	2.19	0.000	10.10	25.20	47.8	1.34	.62	9.43
34-36	1.03	.048	18.10	16.70	0.0	0.00	0.00	0.00
36-38	.40	0.000	8.00	28.00	0.0	0.00	0.00	0.00
38-40	.51	0.000	8.70	25.60	0.0	0.00	0.00	0.00
40-42	.69	0.000	6.90	25.90	0.0	0.00	0.00	0.00
42-44	.70	0.000	7.40	29.80	0.0	0.00	0.00	0.00
44-46	.32	0.000	6.70	30.90	0.0	0.00	0.00	0.00
46-48	.33	0.000	6.50	32.40	0.0	0.00	0.00	0.00

DDH = 2000NE   LINE 2000 NW   ELEV = 79 m

Depth (m)	Ni (%)	Co (%)	Fe (%)	MgO (%)	SiO$_2$ (%)	Al$_2$O$_3$ (%)	Cr$_2$O$_3$ (%)	LOI (%)
0-2	.32	0.000	33.04	.37	28.0	9.96	0.00	0.00
2-4	.43	0.000	19.29	.36	55.0	6.64	0.00	0.00
4-6	.47	0.000	17.36	.43	61.4	4.66	0.00	0.00
6-8	1.45	.520	31.27	.87	28.0	6.42	0.00	9.73
8-10	3.14	.330	25.72	1.81	34.2	6.64	0.00	9.71
10-12	4.21	.332	22.47	6.00	31.7	3.44	0.00	15.58
12-14	4.64	.222	14.71	12.05	42.1	2.68	0.00	12.34
14-16	3.95	.127	11.15	13.85	49.4	2.84	0.00	10.80
16-18	2.40	.049	9.46	17.10	51.1	1.88	0.00	10.71
18-20	1.60	.027	6.38	20.00	54.9	1.72	0.00	8.30
20-22	.33	0.000	6.01	31.44	35.3	1.00	0.00	0.00
22-24	.28	0.000	5.61	28.60	38.2	.92	0.00	0.00
24-26	.67	0.000	5.57	27.82	39.8	1.34	0.00	0.00
26-28	1.64	.079	0.00	0.00	0.0	0.00	0.00	0.00
28-30	1.17	.065	0.00	0.00	0.0	0.00	0.00	0.00
30-32	1.00	.047	0.00	0.00	0.0	0.00	0.00	0.00

DDH = 2047NE   LINE 2000 NW   ELEV = 72 m

Depth (m)	Ni (%)	Co (%)	Fe (%)	MgO (%)	SiO_2 (%)	Al_2O_3 (%)	Cr_2O_3 (%)	LOI (%)
0-2	.67	0.000	10.90	.80	0.0	0.00	0.00	0.00
2-4	.74	0.000	13.30	1.20	0.0	0.00	0.00	0.00
4-6	1.40	.083	16.70	2.30	0.0	0.00	0.00	0.00
6-8	1.09	.064	14.90	2.30	0.0	0.00	0.00	0.00
8-10	.66	0.000	17.00	.90	0.0	0.00	0.00	0.00
10-12	1.60	.037	13.20	12.60	56.6	.82	1.01	7.40
12-14	.75	0.000	8.50	24.50	0.0	0.00	0.00	0.00
14-16	.24	0.000	5.90	32.30	0.0	0.00	0.00	0.00
16-18	.25	0.000	5.20	33.30	0.0	0.00	0.00	0.00
18-20	.23	0.000	4.90	33.80	0.0	0.00	0.00	0.00
20-22	.25	0.000	5.20	34.10	0.0	0.00	0.00	0.00
22-24	.25	0.000	5.60	35.00	0.0	0.00	0.00	0.00
24-26	.23	0.000	5.40	33.60	0.0	0.00	0.00	0.00
26-28	.44	0.000	6.30	30.80	0.0	0.00	0.00	0.00
28-30	.30	0.000	6.00	32.30	0.0	0.00	0.00	0.00
30-32	.48	0.000	6.10	33.80	0.0	0.00	0.00	0.00
32-34	.29	0.000	5.80	36.30	0.0	0.00	0.00	0.00
34-36	.29	0.000	6.20	35.50	0.0	0.00	0.00	0.00

DDH = 2100NE   LINE 2000 NW   ELEV = 69 m

Depth (m)	Ni (%)	Co (%)	Fe (%)	MgO (%)	SiO_2 (%)	Al_2O_3 (%)	Cr_2O_3 (%)	LOI (%)
0-2	.32	0.000	22.42	.12	40.9	16.50	0.00	10.36
2-4	.69	0.000	24.11	.29	39.6	13.40	0.00	9.70
4-6	2.67	.088	21.44	4.10	44.1	4.74	0.00	9.08
6-8	3.55	.046	15.25	11.16	47.2	2.92	0.00	9.72
8-10	4.21	.040	12.20	14.85	48.9	2.64	0.00	9.56
10-12	3.72	.031	13.16	20.00	39.8	2.60	0.00	12.46
12-14	4.04	.028	10.11	20.00	45.2	2.20	0.00	11.70
14-16	2.90	.025	11.88	20.00	43.7	2.32	0.00	11.36
16-18	3.71	.025	8.83	24.30	45.4	1.44	0.00	10.94
18-20	3.12	.046	10.59	18.85	47.5	1.52	0.00	10.84
20-22	2.74	.037	8.68	19.70	53.9	1.66	0.00	8.88
22-24	1.56	.023	9.32	14.10	59.3	1.20	0.00	9.68
24-26	1.49	.025	9.79	15.20	55.3	1.80	0.00	8.60
26-28	4.27	.044	8.51	23.20	46.1	2.00	0.00	10.32
28-30	4.63	.037	7.06	20.35	52.6	1.20	0.00	8.84

DDH = 2155NE   LINE 2000 NW   ELEV = 61 m

Depth (m)	Ni (%)	Co (%)	Fe (%)	MgO (%)	SiO$_2$ (%)	Al$_2$O$_3$ (%)	Cr$_2$O$_3$ (%)	LOI (%)
0-2	1.34	.047	24.70	1.90	0.0	0.00	0.00	0.00
2-4	.24	.025	16.00	.80	0.0	0.00	0.00	0.00
4-6	.12	0.000	12.00	.70	0.0	0.00	0.00	0.00
6-8	.72	0.000	20.70	1.40	0.0	0.00	0.00	0.00
8-10	1.14	.048	29.60	3.00	0.0	0.00	0.00	0.00
10-12	1.34	.064	28.70	3.30	0.0	0.00	0.00	0.00
12-14	2.92	.048	16.70	17.70	35.4	4.19	1.18	12.96
14-16	3.14	.034	11.60	25.60	37.8	1.94	.81	13.06
16-18	3.18	.023	10.40	24.20	42.3	1.66	.92	12.15
18-20	2.43	.024	13.30	16.70	45.1	1.53	1.10	13.19
20-22	3.27	.024	11.00	21.50	43.8	1.03	1.09	12.65
22-24	2.80	.018	10.50	18.70	45.8	.92	1.24	11.85
24-26	2.60	.014	8.50	24.10	46.2	.93	.70	11.58
26-28	2.22	.013	8.80	23.20	43.9	.89	.68	12.14
28-30	1.57	.015	10.10	23.70	38.0	1.68	.73	11.91
30-32	.36	0.000	8.00	25.40	0.0	0.00	0.00	0.00
32-34	.25	0.000	6.40	30.30	0.0	0.00	0.00	0.00

Toco

Qal

Toco

P

50

X

Toco

200

X'

100

125

Toco

100

URE RIVER

75

50

Qal

Toco
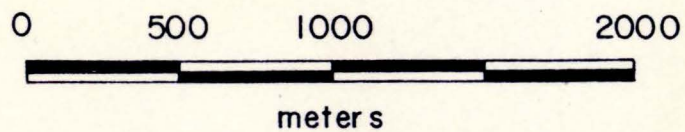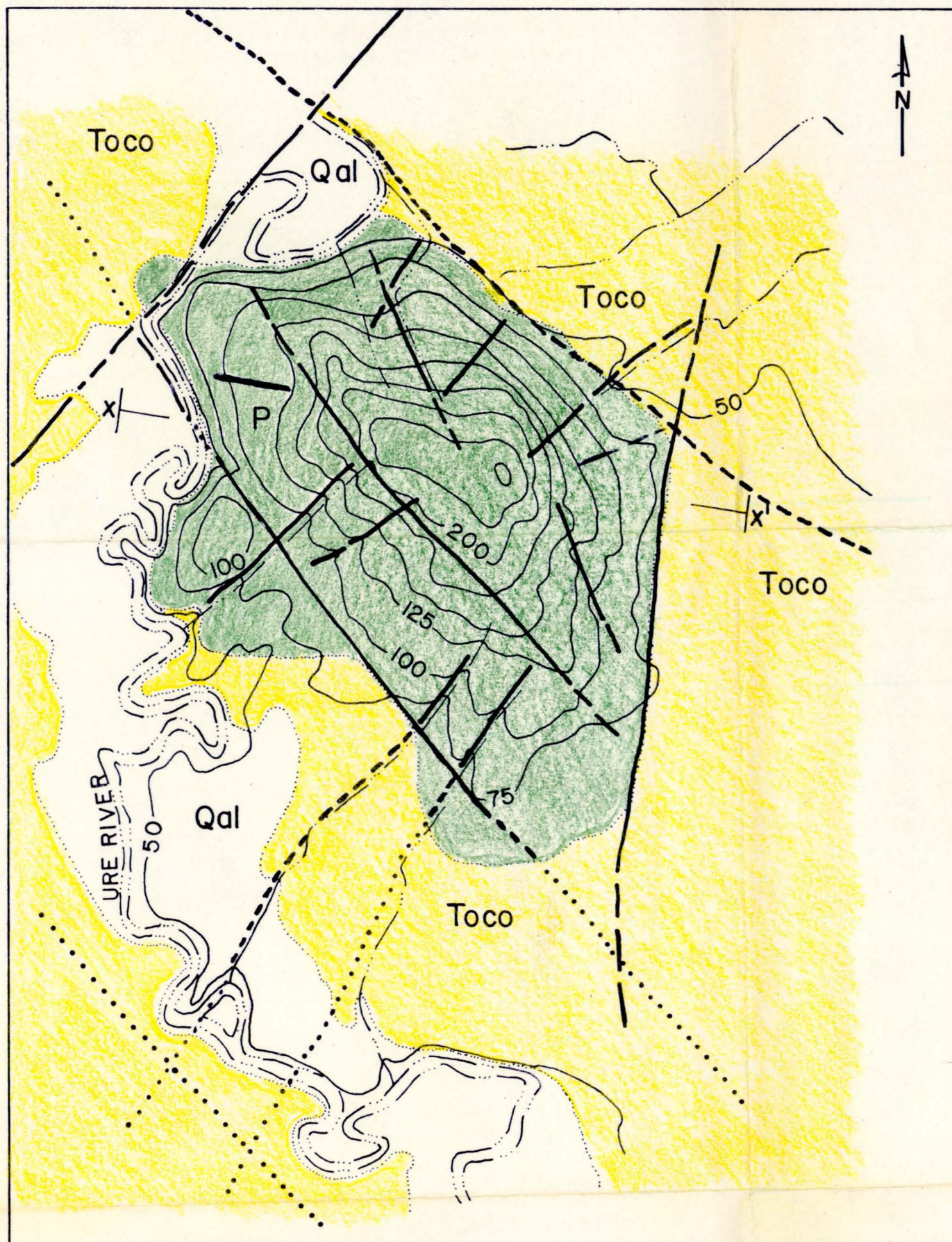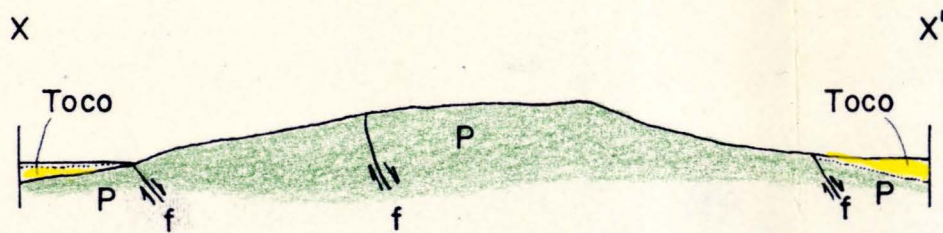
PLATE I

General Geology, Cerro Matoso Area,

Montelibano, Colombia

EXPLANATION

UNITS

| Qal | Alluvium |

| Toco | Lower Oligocene – Lower Miocene Cienaga de Oro Formation. Reddish-brown ferruginous sandstone, gray sandy and calcareous shale, black carbonaceous shale; coal beds near top and at base. |

| P | Pre-Upper Cretaceous Peridotite |

SYMBOLS

Approximate contact

Fault; long dashes where approximately located, short dashes where inferred, dots where covered

River

Stream

125 — Contour line, meters above sea level

f   Fault

Topographic base from Plate 82-III-D, Montelibano Area, Instituto Geografico Agustin Codazzi, scale 1:25,000

Geology by J.E. López-Rendón (1984)

0   500   1000   2000

meters

Contour interval 25 m.

X   X'

Toco   Toco

P   P

P   f   f   f   P

REFERENCE LINE 2400 NE

2000 NW

URE RIVER

Toco

300 NW

1200 NW

500 NW

REFERENCE LINE 000 NE

2000 NW

Toco

Toco

Toco

1300 NW

1200 NW

500 NW
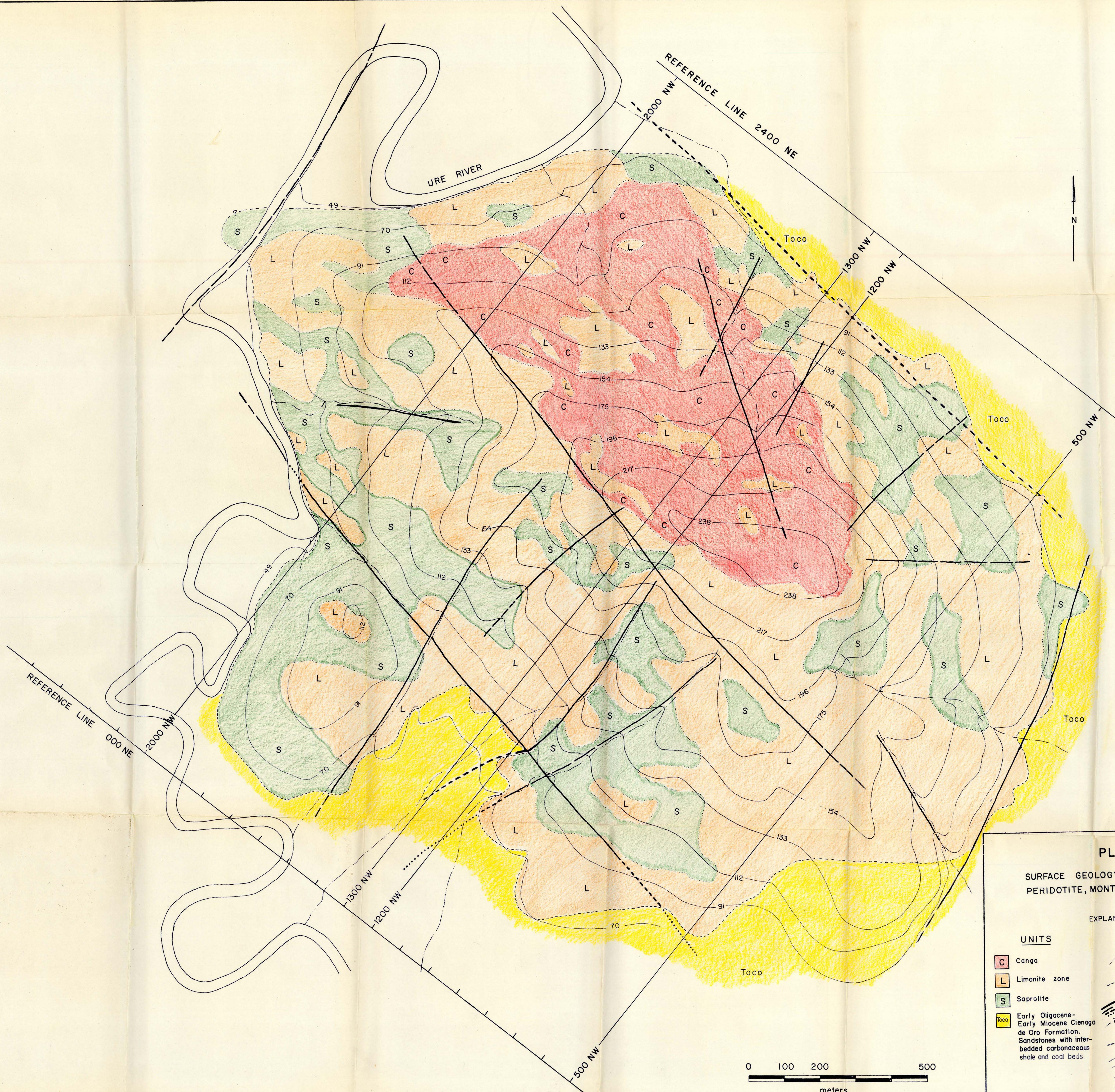
PLATE 2

SURFACE GEOLOGY, CERRO MATOSO
PERIDOTITE, MONTELIBANO, COLOMBIA

EXPLANATION

UNITS

C Canga

L Limonite zone

S Saprolite

Toco Early Oligocene–
Early Miocene Cienaga
de Oro Formation.
Sandstones with inter-
bedded carbonaceous
shale and coal beds.

SYMBOLS

Approximate contact between
weathered peridotite units

Contact between peridotite
and sediments

Fault; long dashes where approximately located,
short dashes where inferred, dots where
covered

70 Contour line, meters above sea level

Stream

River
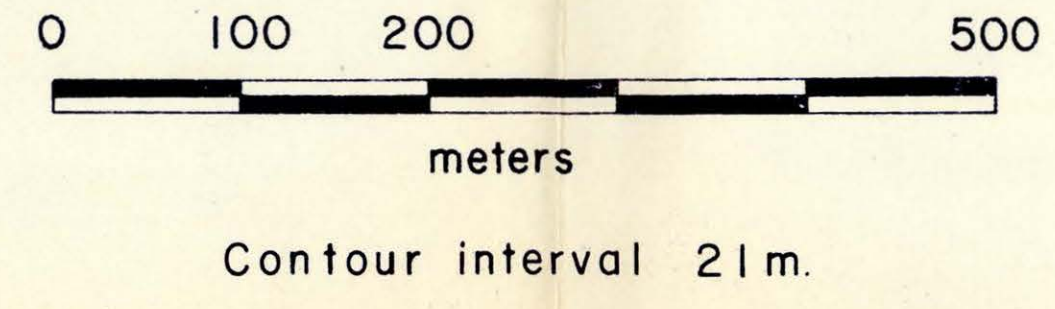
Topographic base after Cia. de Niquel
Colombiano S.A.; surface geology modified after
V.M. Mejia and J. Durango of Cerro Matoso S.A.

0 100 200 500

meters

Contour interval 21 m.
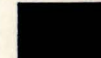
PLATE 3
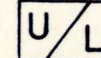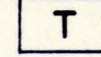
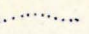Vertical section, line 1200 NW, showing the distribution of the laterite profile at Cerro Matoso

1200 NW SECTION

0   100   300
meters
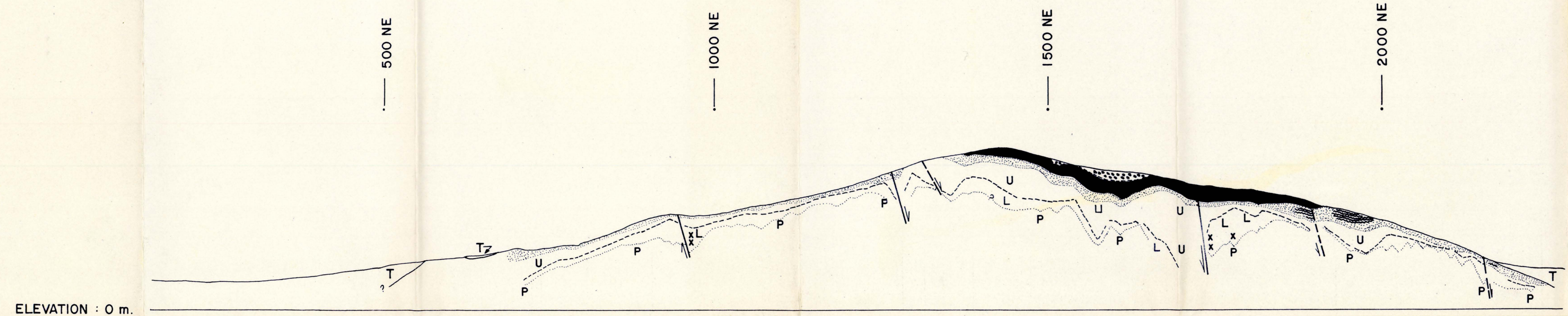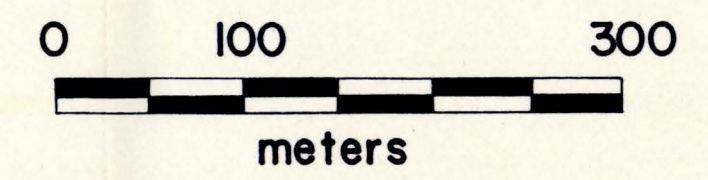
Earthy canga with iron concretions

Canga

Limonite

"Laminated" limonite

U/L Saprolite (U: Upper; L: Lower)

P Peridotite

T Tertiary sediments

Contact

.... Approximate transition from Lower saprolite to peridotite bedrock

Approximate transition from Upper to Lower saprolite

x Peridotite blocks

Fault; dashes where inferred

ELEVATION : 0 m.